MORPHOLOGICAL AND PHOTOMETRIC STUDIES OF GALAXIES BY ELECTRONOGRAPHY

by

David Paul Youll, B.Sc. (Phys.), A.R.C.S.

October, 1978

A thesis submitted for the degree of Doctor of Philosophy of the University of London and for the Diploma of Imperial College

Physics Department
Imperial College
London, S.W.7.

ERRATA

Page 10	Insert "4.9 Principal elements of handscans of 1ZW166 121"
Page 15, line 10	Change "light levels in" to "light levels which exist in"
Page 24	The title to figure 1.5 should read: "THE TRANSMISSION CHARACTERISTICS OF U,B,V FILTERS AND THE ATMOSPHERE, AND THE RESPONSES OF S11 AND S20 TYPE PHOTOCATHODES"
Page 46, line 24	Change "measured signal to the" to "measured signal to noise ratio to the"
Page 54	Add to the note: "The graphs are drawn for a gaussian profile of maximum density equal to 1" In the note change "squares" to "circles" and change "circles" to "squares".
Page 105, line 9	Change "step-length" to "step-length and".
Page 113, line 20	Change "The profiles" to "The profiles of".
Page 162, line 13	Delete "A photograph of the electronograph is also given."
Page 259	Change the comments to read: "BINTEG=AVERAGE TRANSMISSION DENSITY" "DINTEG=AVERAGE DENSITY"

ABSTRACT

Astronomical sources of low surface brightness, or sources with high luminosity gradients can be difficult to observe with photographic techniques. However, developments in electronographic techniques over recent years have made them suitable for precise observations of such objects. The use of these techniques for morphological and photometric studies of galaxies is discussed. Where appropriate, improvements in the methods for recovering information from electronographs, and analysing the data with computers are suggested.

These techniques were used to study eight galaxy systems which have compact parts where the luminosity gradients are relatively high. Morphological studies of these systems are presented, together with measurements of some of their photometric parameters. The galaxy NGC 4881 was also studied so that the photometric calibration could be checked against previous studies, and so that the parameters of compact galaxies could be compared against this elliptical galaxy.

ACKNOWLEDGEMENTS

Although this thesis bears a single name as author, it would not have been completed without the assistance of a large number of people. To all these people, I would like to say a very sincere "THANKYOU" for the information, help, guidance and comfort that you have given to me.

I must give a special mention and many thanks to my supervisor, Dr. Brian Morgan, who always had time and patience whenever I needed guidance.

My thanks also go to Mrs. Isobel Smith for being able to convert my handwritten notes into a polished typescript with the ease of a true expert.

This thesis is dedicated to my parents, Joyce and Austin Youll, for their continuous help, guidance and support. They could not have given more; I am very gratefull.

CONTENTS LIST

Page

Page

Page

FIGURES

TABLES

CHAPTER 1

TECHNIQUES FOR THE STUDY OF GALAXIES

1.1. Morphological and Photometric Studies of Galaxies

A morphological study of a galaxy is a study of the distribution of its surface luminosity. A photometric study is possible when the measured luminosity has been calibrated, usually against previously calibrated stars, to give the absolute luminosity. By studying the morphology of a galaxy in several different colours (e.g. U, B and V) and colour indices (e.g. B-V) then aspects of the structure may be derived e.g. the distribution of stars and stellar types. Many such studies will yield information about the process of the formation and evolution of galaxies, enabling more accurate cosmological studies to be made.

The first attempts to measure the distribution of luminosity in galaxies were made by Reynolds (1913, 1920) using photography. Soon afterwards Hubble began a study of elliptical galaxies and by 1930 he was able to formulate a luminosity law for these systems (Hubble, 1930).

Much progress has been made since this initial work, but the measurement of the distribution of luminosity in a galaxy is still very difficult because the luminosity of galaxies is very low. Often measurements of the outer regions of a galaxy have to be made at a luminosity which is less than 1% of the

sky background luminosity, which is itself only about 21 mag.arcsec^{-2} at a good site. Hence, a small error in the measurement of the value of the sky background luminosity can have a great effect on the measured luminosity distribution. Due to these problems, studies of faint and distant galaxies have to be restricted to their central brighter regions.

The photographic plate has long been used to record the luminosity distribution in galaxies because it is easy to use and it detects light across an area, i.e. the surface luminosity at all points on the galaxy are recorded simultaneously. However, photography has several drawbacks which are outlined below:

a) The detective quantum efficiency of the photographic process is low, only a few percent for the better emulsions so the luminosity distribution of only the nearer, brighter galaxies can be studied.

b) The D.Q.E. varies with photon flux. Hence, only galaxies which have a small luminosity range which is within certain limits can be studied without complications.

c) The density-exposure relationship is non-linear. Hence, measurements of luminosity have to be corrected for this variation before they can be studied.

Figure 1.1 shows the density-exposure and DQE-flux relationships for some photographic emulsions. The corrections that have to be made to measurements from a photographic plate to correct for non-linearity of

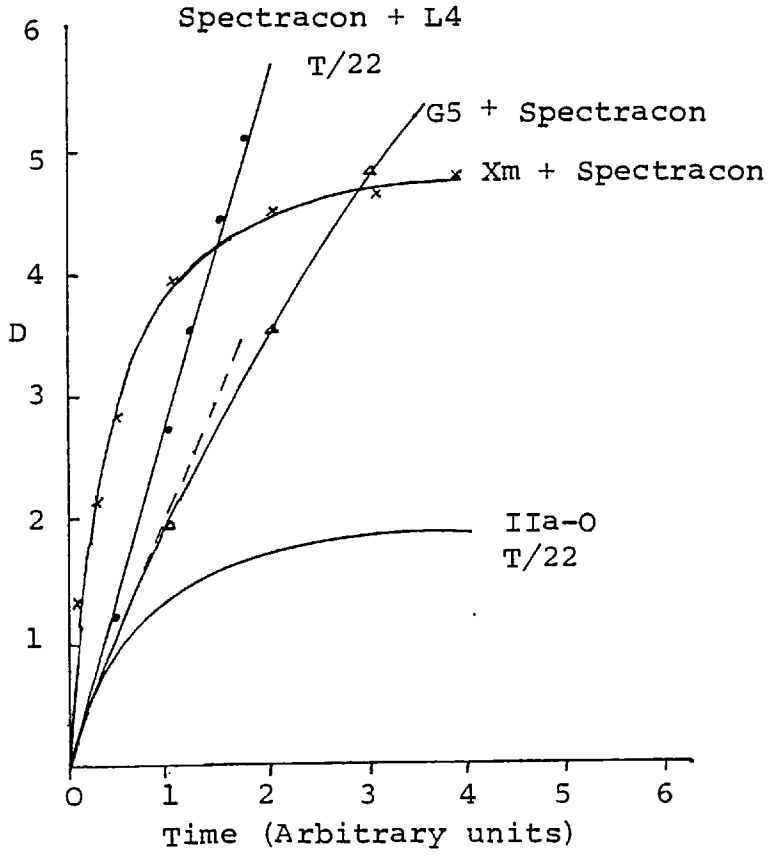

Figure 1.1a Optical Density - Exposure Characteristics

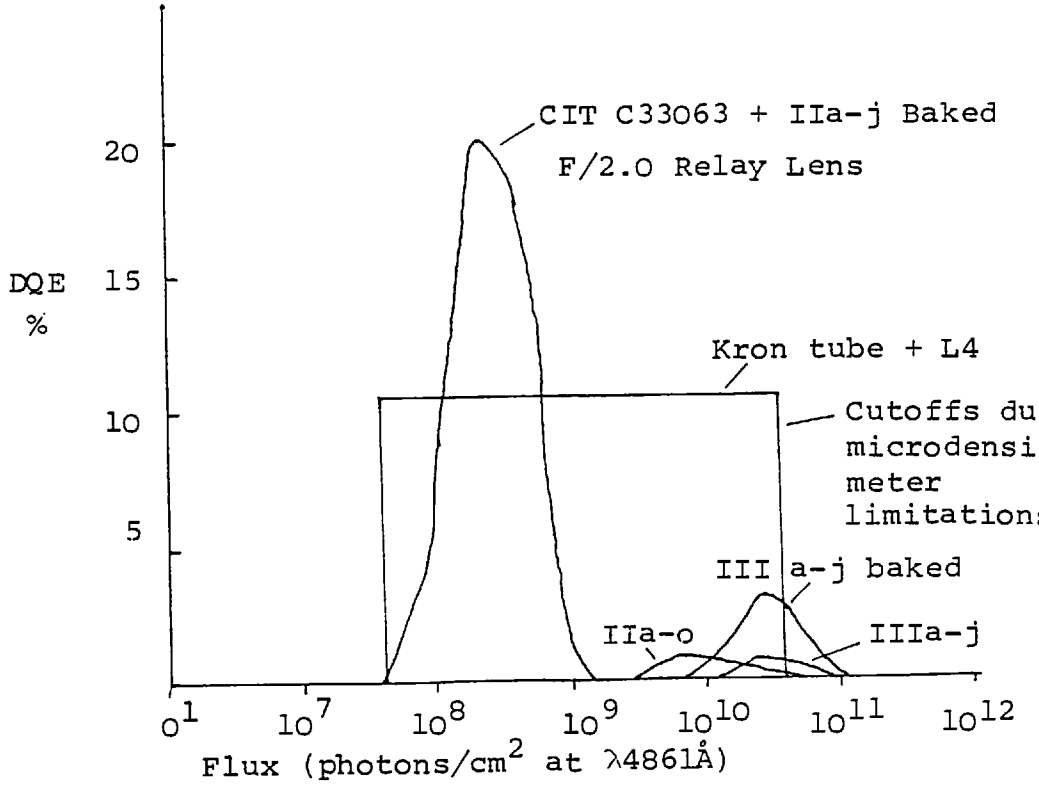

Figure 1.1b D.Q.E. - Flux

FIGURE 1.1 CHARACTERISTICS OF PHOTOGRAPHIC AND ELECTRONOGRAPHIC EMULSIONS

detection and the variation in D.Q.E. may introduce errors and additional noise into the results. The discrepancies in the results of some observers (Van Houter, 1961; Miller and Prendergast, 1962; Ables and Ables, 1972a) can be traced to difficulties in trying to make accurate measurements of the surface luminosity when strong luminosity gradients are present, as in the nuclei of galaxies, and to the inherent inaccuracy of photographic methods at the very low light levels in the outer regions of galaxies (Bird et al, 1969).

In order to overcome some of the problems of the photographic process, photo-electric devices are now frequently used for observations. These employ photocathodes which emit electrons when photons are incident. The electrons emitted by the photocathode are difficult to detect directly, but their energy can be increased to a detectable level by accelerating them through an electric field. Some devices further amplify the signal by directing accelerated electrons onto a phosphor screen which emits a large number of photons for each incident electron. By repeating this process several times a large number of electrons or photons can be produced for detection. Thus, the output due to each single electron emitted by the photocathode may be large enough to be easily detected. Hence, the D.Q.E. of the detecting system is close to the photocathode responsive quantum efficiency (RQE) which is usually greater than 10% in the visible wavelengths, i.e. much greater than the D.Q.E. of photography. The number of electrons emitted by the photocathode is directly proportional to the photon flux,

except when the flux is very high, i.e. much greater than that produced by stellar and galactic sources. Hence, if the detector has a linear detection-exposure relationship, the system will have a linear density exposure relationship and its D.Q.E. will be independent of photon flux, unlike photography.

Some photo-electric devices are not imaging devices and can only measure the number of photons passing through an aperture. These devices can be used to study the morphology of a galaxy, either by using a small aperture to measure the surface luminosity at many points over the galaxy (e.g. Miller and Prendergast, 1962), or by measuring the integrated luminosity through several larger apertures which are centred on the galaxy (e.g. de Vaucouleurs, 1961). Each of these methods, though accurate, is very time consuming because many, sometimes hundreds, of readings have to be taken for each galaxy.

Photo-electric devices which can record the distribution of light over an area have been under development for some years. Examples of this type of device are the T.V. camera, two-dimensional diode arays, electronographic recording systems and image intensifiers. These devices have higher quantum efficiencies than a photographic plate, but some are limited to about 500 by 500 pixels. The technique of electronography has the advantages of image detection with a large number of pixels and high and constant D.Q.E.

1.2 Electronography

Kiepenheur (1934), knowing that the

photographic process was very inefficient, suggested a more sensitive system using silver halide emulsion to record electrons accelerated from a photocathode. This process is now known as electronography.

In an electronographic recording system, the image to be recorded is focused onto a photocathode which emits photo-electrons. These photo-electrons are accelerated and focussed onto an electronographic emulsion by means of a suitable combination of magnetic and electric fields. Each photo-electron has a high probability of leaving a track of developable grains in the emulsion. In principle, this recording system does not suffer from reciprocity failure because

(a) the number of photo-electrons emitted by the photocathode is proportional to the number of incident photons,

and (b) each photo-electron has a constant probability of being detected, except when the emulsion is nearing saturation density, which is much higher in electronographic emulsions than photographic emulsions (see below).

In these circumstances, the D.Q.E. is therefore independent of photon flux and only slightly less than the R.Q.E. of the photocathode (see section 1.3.1).

Electronographic emulsions are characterised by, with examples for L4 emulsion,

(1) low fog levels (0.02D)

(2) small grain sizes (0.14 μm)

(3) linear relationship between optical density and exposure (to D = 6)

The units of optical density (D) are a convenient indicator to the number of recorded tracks in the emulsion (see next chapter). Figures 1.1a and 1.1b show some characteristics of electronographic recording systems, compared with photographic emulsions (Gull, 1974; Kahan and Cohen, 1969).

The small grain sizes and low fog levels of electronographic emulsions enable them to store a large amount of information with a high signal to noise ratio. The information content of electronographic emulsions is typically ten times that of unaided photography in the visible wavelengths (Bird et al, 1969).

The practical realisation of an electronographic recording system took many years because photocathodes are very reactive and require a high vacuum environment, whilst emulsions desorb vapours which are harmful to the photocathode. This problem was reduced by Lallemand (1936, 1966 - see figure 1.2) by cooling the emulsion to liquid nitrogen temperature; thus lowering the desorption rate. This enabled the photocathode to last for a period of several months in the presence of the emulsion. However, when appropriate exposures have been made on the emulsion, the tube has to be broken in order to recover the emulsion. This exposes the photocathode to the atmosphere and destroys it. In the U.S. Navy electronic camera (Kron et al, 1969 - see figure 1.3), the photocathode is protected from the atmosphere by a valve when the emulsion is changed. This makes it a more practicable device because the same tube can be used to expose many plates of

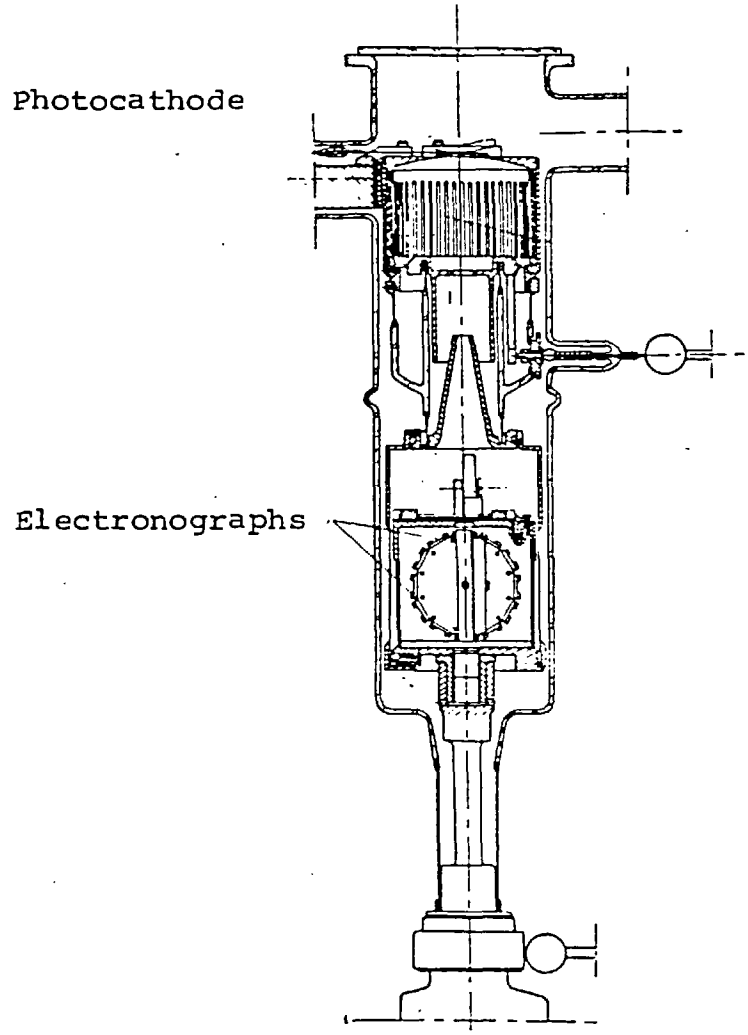

FIGURE 1.2 THE LALLEMAND ELECTRONIC CAMERA

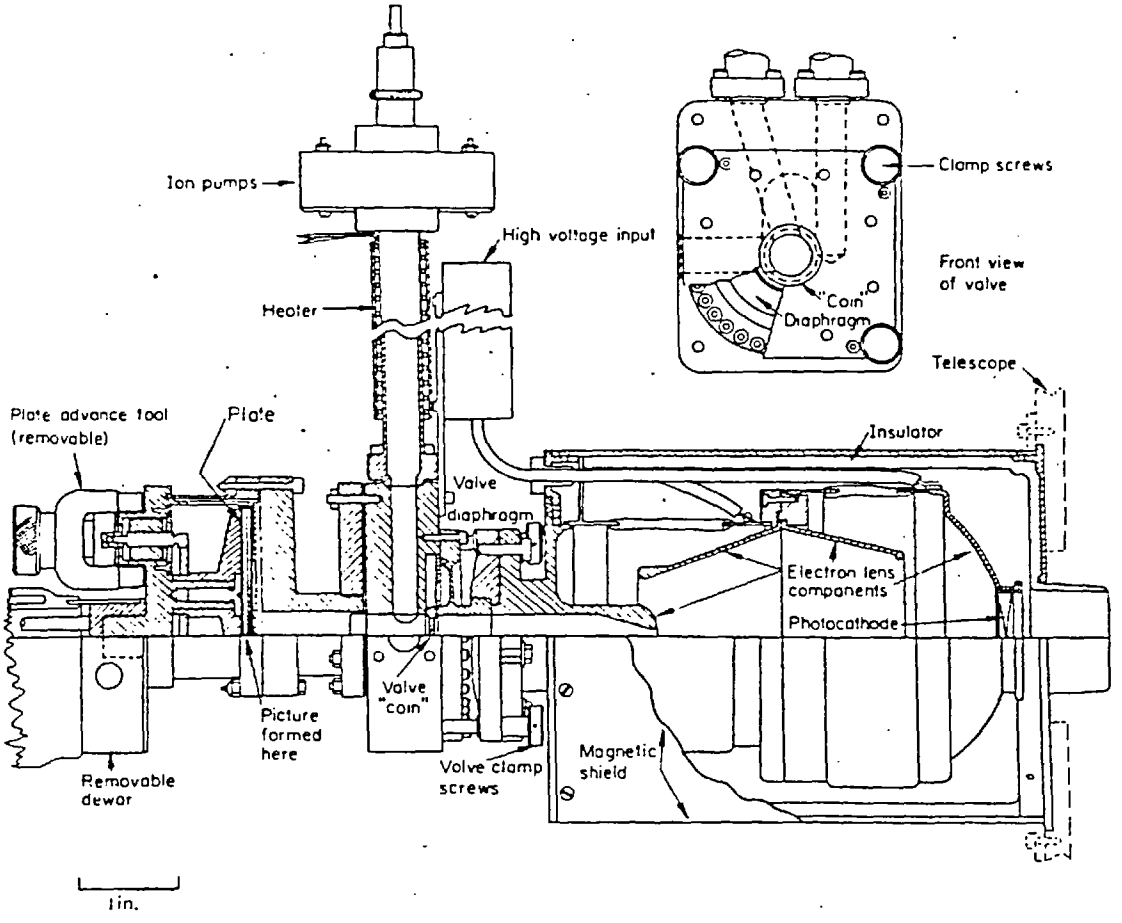

FIGURE 1.3 THE KRON ELECTRONIC CAMERA

emulsion. A disadvantage of this tube is that pumps are required to reduce the pressure around the emulsion to that of the photocathode after plates have been changed. The time taken to change plates limits the number of exposures that can be made during a night to about 2 sets of 6 exposures.

A simpler approach has been to provide a thin barrier membrane of mica between the photocathode and the emulsion, as in the spectracon (McGee et al, 1969 - see figure 1.4). The membrane permits the photocathode to be kept in a vacuum and the emulsion to be easily changed. The spectracon is a sealed unit requiring no vacuum pumps or special cooling of the emulsion. It is therefore a simple and convenient image tube for use in astronomical observations. The size of electronographs produced by the spectracon is only about 1 cm by 3 cm, but work is being undertaken at the Royal Greenwich Observatory to develop a system which will permit circular electronographs of 8 cm diameter (McMullen et al, 1972).

1.3 The Spectracon

Figure 1.4 shows a cross-section of a spectracon. The photocathode (A) is enclosed in a vacuum-tight lime soda glass envelope. Photons imaged onto the photocathode liberate electrons which are accelerated to the mica window (B) by an axial electric field. The electrons are focused onto the mica window by a combination of the electric field with an axial magnetic field from the solenoid (c). Electronographic emulsion is placed directly against the mica by an applicator (D) to ensure that the electrons

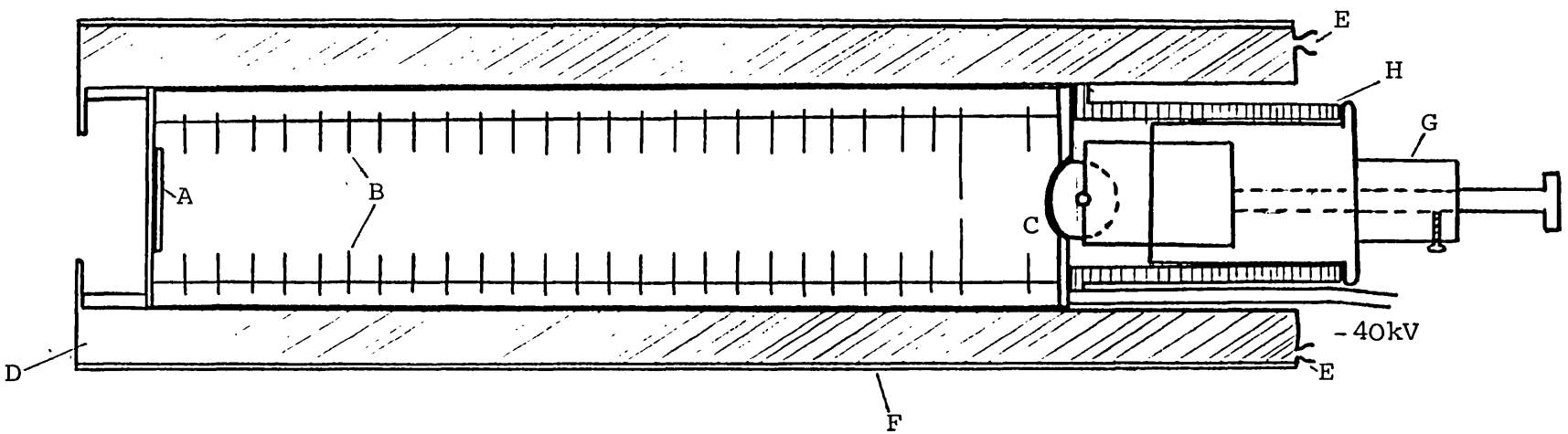

A	Photocathode	D	Solenoid	G	Applicator
B	Annular Electrodes	E	Cooling Inlet/Outlet	H	Applicator Holder
C	Mica window	F	Mu-metal Screens		

FIGURE 1.4 THE SPECTRACON AND SOLENOID

emerging from the mica do not lose energy in the atmosphere and to reduce the loss of resolution by scattering.

The principal components of the spectracon assembly are summarised below; detailed studies can be found elsewhere (e.g. McGee et al, 1969; McGee et al, 1972, Bacik et al, 1972; Bacik, 1973; McGee, 1973; Coleman, 1974).

The spectracon assembly, including the solenoid is relatively small (40 cm by 15 cm) and light (12 kgm) so it can be used on both large and small telescopes. Since the spectracon is a permanently sealed device, requiring no vacuum pumps, it is easy to use and needs only the electric and magnetic fields to be set at the correct levels (see section 1.3.2) before operation. The solenoid is normally water cooled, except at the prime focus of telescopes where accidental failure might result in the spillage of water onto the telescope mirror. In these situations, solid state (Peltier) electrical heat pumps are used to remove the 15W of heat generated by the solenoid.

1.3.1 The Photocathode

Photocathodes can be made with various wavelengths responses, but spectracons normally employ the S11 or S20 types for astronomical observations. The S11 type is used for observations with U, B and V filters because it has a response which is similar to that of the S4 cathode used to define the U, B, V system (Johnson and Morgan, 1953 - see figure 1.5). In this wavelength range this type of photocathode can

FIGURE 1.5 RELATIVE RESPONSES OF U, B, V FILTERS,
S11, S20 PHOTOCATHODE AND THE ATMOSPHERE

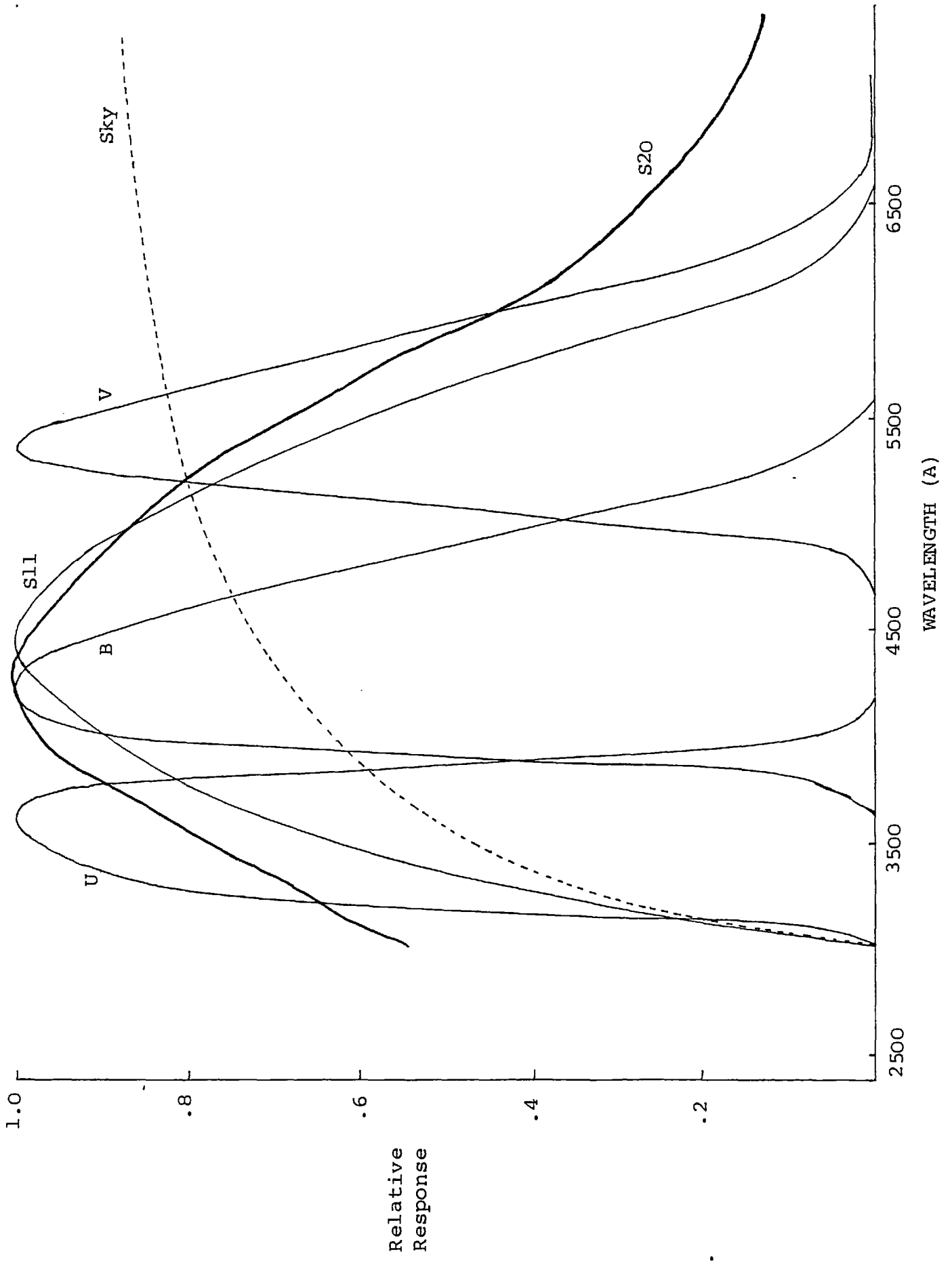

have an RQE which is greater than 10%, with a typical sensitivity of 70 μAL. The S20 type photocathodes have an extended red response (see figure 1.5) so they are generally used for studies of objects with interesting features in the red region of the spectrum.

The thermal background emission rate of an S11 photocathode is about 5.10^{-7} electrons $\mu m^{-2} sec^{-1}$ at $0^{o}C$ (McGee et al, 1969). At the I.N.T. (2.5 m) prime focus, the sky background can be about 21 mag. per square arcsecond, through a blue filter. This sky background gives a count of 2.10^{-3} electrons $\mu m^{-2} sec^{-1}$, which is much larger than that from the photocathode background.

1.3.2 Electric and Magnetic Fields

The electrons emitted by the photocathode are accelerated along the tube by a strong axial electric field which must enable the electrons to emerge from the mica with enough energy to leave a detectable track in the emulsion (see figure 1.6). However, the field must be low enough to avoid serious internal electric breakdown (arcing). The operating voltage of the spectracon is chosen as 40 kV, with the cathode at a potential of - 40kV so that the mica window and the film applicator can be earthed for safety. To enable safe handling of the tube, and to reduce arcing, the tube is encapsulated in a highly insulating silicone rubber with a pyrosil window at the "live" end.

The electrons are focussed onto the mica window by a combination of the electric field with the magnetic field from a solenoid. For a particular

FIGURE 1.6 THE ENERGY DISTRIBUTION OF ELECTRONS EMERGING FROM A SPECTRACON OPERATED AT 40 kV

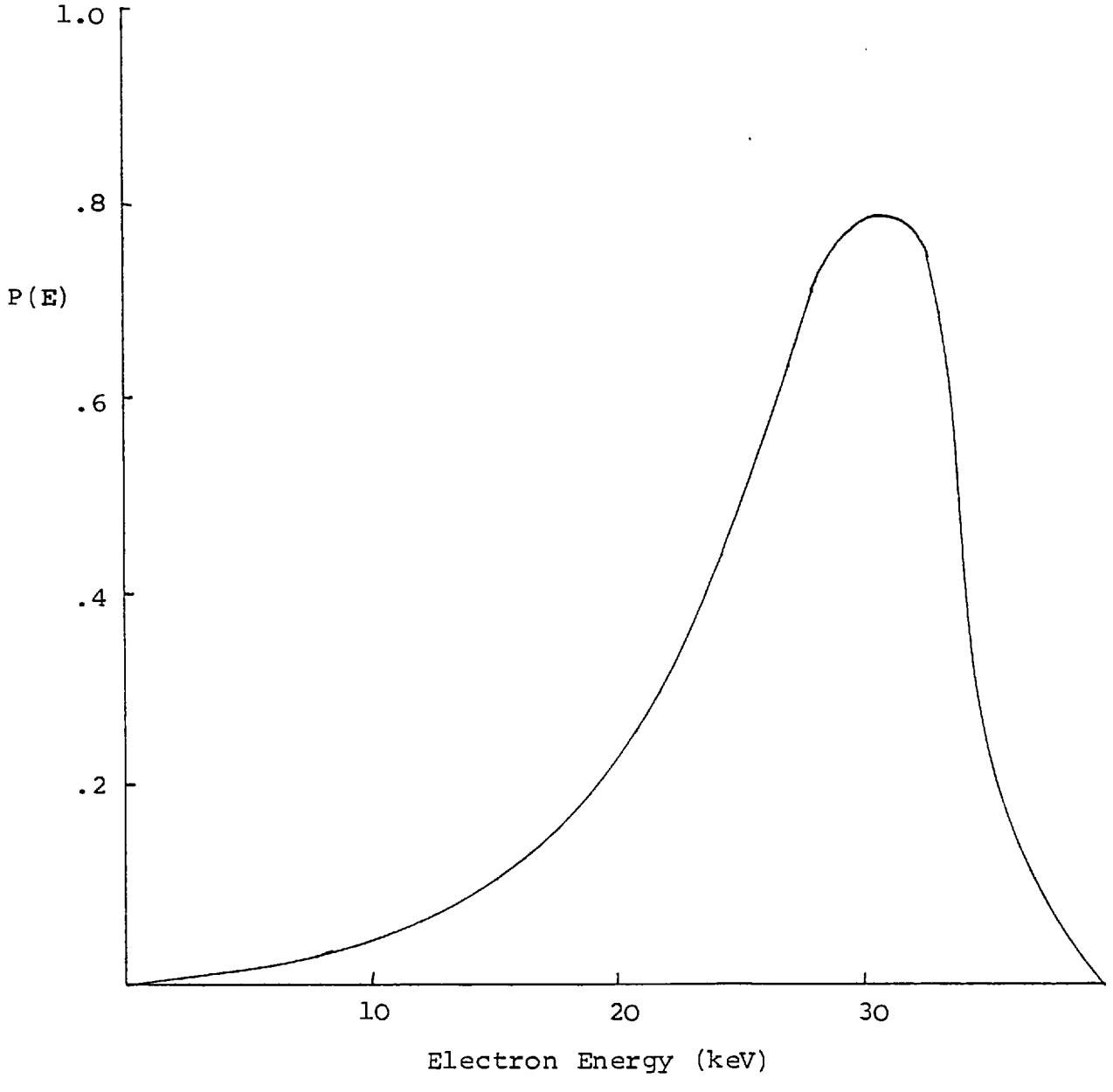

electric field, which is usually defined by the constraints mentioned above, focus conditions can be found with several specific values of the magnetic field. In practice, the lowest magnetic field which permits a focus condition with a 40 kV electric field in the spectracon, gives a resolution of 70 $lp.mm^{-1}$ at the outside face of the mica. This resolution is adequate for most studies. For example, the plate-scales used for most observations do not exceed $27\hat{''}\ mm^{-1}$, so that star images of $1\hat{''}$ diameter are imaged to about 0.04 mm on an electronograph.

When the magnetic field is increased to twice the value of the lowest field a second focus condition is obtained. This value of magnetic field increases the resolution of the image, but a higher electric current is required in the solenoid increasing the amount of heat dissipated. This focus condition gives a resolution of 120 $lp.mm^{-1}$ at the outside face of the mica, but this is rarely needed and causes increased heat dissipation so it is not often used. This resolution is limited by the scattering of the electrons by the mica window. Hence increasing the magnetic field will not increase the resolution of a spectracon.

1.3.3 The Mica Window

The mica window allows electrons to emerge from the spectracon and leave tracks in the emulsion, whilst keeping the photocathode in a high vacuum environment of 10^{-8} torr. Mica is used for this purpose because it has a relatively low density and is therefore permeable to high energy electrons, but not

gas molecules. It can also be cleaved into strong, thin and uniform sheets. It is preferred that the window be uniformly thin because this permits the energy distribution of emerging electrons to be constant at all points on the window, which simplifies the analysis of electronographs (see next chapter).

The dimensions of the window are normally 30 mm by 10 mm, though larger windows of 20 mm by 30 mm have been tested in the laboratory (McGee, 1974). The internal surface of the window has to be covered with an electrically conducting, and optically opaque layer of aluminium to prevent the window from being charged by the electron beam and to shield the emulsion from light transmitted by the photocathode. This layer is about 100 nm thick and has little effect on the electron beam.

The mica window is curved across its width in order to reduce the stresses at the junction with the end-plate, but this causes the electron image recorded on the emulsion to be distorted (see figure 1.7). The amount of distortion can be calculated if it is assumed that the mica window has a constant radius of curvature (R) and that the electrons are focussed onto a plane which touches the mica window at the centre of the window (Point P on figure 1.7). At a distance x from the centre of the window, an element of length δx is imaged onto a length δl of the film pressed against the window. Thus, assuming that there are no out-of-focus effects:

$$\delta l = \frac{\delta x}{\cos\theta} \qquad \text{and} \qquad \sin\theta = \frac{x}{R}$$

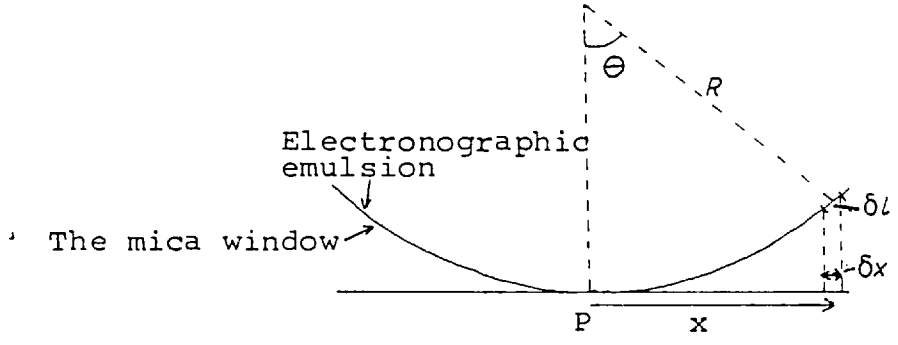

FIGURE 1.7 EFFECTS OF CURVATURE OF THE MICA WINDOW

$$\therefore \quad \delta l = \frac{\delta x}{\sqrt{1-\frac{x^2}{R^2}}} \qquad \text{I-1}$$

The percentage error in a measurement of distance at x is therefore,

$$\frac{\delta l - \delta x}{\delta x} \times 100\% \doteq \left(\frac{1}{\sqrt{1-\frac{x^2}{R^2}}} - 1 \right) \%$$

$$= 50\frac{x^2}{R^2} \% \text{ for } \frac{x^2}{R^2} \ll 1 \qquad \text{I-2}$$

A typical radius of curvature for a 10 mm wide window is 15 mm (Bacik, 1973). This implies that an image at the edge of the mica window is distorted by about 5% due to the curvature of the window. The distortion is less than 1% within the central 4 mm width of the window. If necessary, the distortion of an image can be calculated and corrected. The resolution at the edge of the window is only slightly reduced from that at the centre of the window as the depth of focus in the electron image is relatively high (Coleman, 1974).

The thickness of a mica window is about 4 μm. Since electrons lose energy whilst passing through the mica, some of the electrons do not retain enough energy to leave a track in the emulsion. McGee et al (1966) found that 75% of the electrons which have passed through a mica window of the spectracon leave a detectable track in the emulsion, whilst 90% of the electrons leave a detectable track when the emulsion

is contained in the vacuum with the cathode. The D.Q.E. of a spectracon is therefore slightly less than that of other electronographic recording systems which do not employ a barrier membrane and are operated at the same voltage.

The resolution of the spectracon is limited by the scattering of electrons in the mica window to 120 $lp.mm^{-1}$ (Coleman, 1974). However, this does not constrain most observations (see section 1.3.2).

1.3.4 The Emulsion Applicator

The applicator holds a strip of film coated with emulsion of length 10 cm by 3 cm on a soft rubber roller. The curvature of the roller is slightly greater than that of the mica window. When an exposure is made, the applicator presses the emulsion directly against the mica window to reduce loss of resolution caused by electron scattering in the mica and to stop absorption by the atmosphere. By rotating the roller, up to 6 exposures can be made on one strip of film. The film can be quickly and easily changed, enabling a large number of exposures to be made in a single observing session.

1.4 Electronographic Emulsions

Several emulsions have been used with a spectracon, the most common type being Ilford L4 and G5. These emulsions have been shown to have a linear density-exposure relationship, to within 2%, up to optical densities of 6 and 2 respectively

(Kahan and Cohen, 1969; Cohen, 1972, Gull, 1974). Figure 1.1 showed some characteristics of nuclear track emulsions compared with photographic emulsions (see also section 1.2). G5 emulsion darkens faster than L4 emulsion because its grain size is about two times larger than that of L4. L4 has a larger range over which the density-exposure relationship is linear, and its smaller grain size permits it to store more information.

Studies by Cohen and Kahan (1972) showed that using L4 emulsion the D.Q.E. of electronography is independant of exposure level up to optical densities greater than 4. The procedure used to develop emulsions to obtain an optimum D.Q.E. is critical and has been studied by Coleman (1975). His suggested development procedure has been used for all electronographs studied in this thesis (see Appendix A).

In the next chapter, it is shown that the analysis of electronographs is made easier if the relationship between optical density and the number of tracks per unit area is the same at all points on an electronograph, i.e. the average number of grains per track must be constant. This relationship will hold when the thickness of emulsion is greater than the maximum track length of electrons. Electrons emerging from the mica window of a spectracon operated at 40 kV have an energy distribution (see figure 1.6) which gives the electrons an average track length of 7 μm (Coleman, 1974). Therefore, the thickness of emulsions for astronomical studies should be greater than 10 μm. The standard emulsion thickness which is

supplied by manufacturers is 10 μm.

Emulsion defects may occur, causing the emulsion to be thinner than the average track length, so emulsions are checked by eye before they are used in order to ensure that electronographs are free from defects. Such checks also ensure that the emulsion is free from dirt. In addition, due to variations in thickness and composition, small variations in sensitivity of about $\pm$ 2% occur between batches of emulsion (Wlerick et al, 1974). This indicates a need for the calibration of each electronograph on an area of emulsion which is near to that used for the electronograph of an object. This is discussed in more detail in section 3.3.

CHAPTER 2

DATA ANALYSIS

As has been stated in the previous chapter, electronographs can store a great deal of information in the form of electron tracks. The information can be recovered by counting the number of tracks per unit area at every point on the electronograph (McGee et al, 1966). This method of access must have the highest detective quantum efficiency (D.Q.E.) because all the available information is accessed. However, track counting is very tedious and time consuming because there can be several tracks within a square micron (Coleman, 1974), and an electronograph taken by a spectracon covers an area of 3.10^{11} μm^2. In addition, track counting soon becomes impossible in areas where the track density is high and individual tracks cannot be distinguished.

Alternative techniques using automated machines can be used to access the information stored in an electronograph, but with reduced D.Q.E. A microdensitometer is commonly used for this work.

2.1. The Principle of the Microdensitometer

A microdensitometer can be used to measure the optical density at a point on an electronograph by passing a beam of light through the electronograph and measuring the transmitted intensity. The following argument shows that the optical density is proportional to the number of tracks per unit area in the electronograph, and that the microdensitometer can therefore be used to

recover the information stored in electronographs.

By definition, the optical density (D) and the transmission (T) of an electronograph are related by:

$$D = -\log_{10} T \qquad \text{II-1}$$

Let S be the total fraction of the area covered by the blackened grains on the emulsion. Some grains will have a shielding effect on others, so the effective fraction of the projected area is S'. Silverstein and Trivelli (1938) showed that these parameters can be related by equation II-2, assuming that

(1) each grain is sensitised by only one photon

(2) the grains are randomly distributed

(3) the density is much less than the saturation density

$$S' = 1 - e^{-S} \qquad \text{II-2}$$

The quantity S' can be related to the transmission by

$$T = 1 - S' \qquad \text{II-3}$$

therefore, by substitution,

$$D = S \log_{10} e \qquad \text{II-4}$$

S is the product of the number of tracks per unit area (N) and the average projected area of grains per track ($\bar{a}$), therefore,

$$D = 0.434\ N\bar{a} \qquad \text{II-5}$$

Hence,

$$D \propto N \qquad \text{II-6}$$

The number of tracks is proportional to the number of photons per unit area (n) striking the photocathode

(see section 1.2), therefore

$$D \propto n \qquad \text{II-7}$$

Thus, an ideal nuclear track emulsion will have a linear density-exposure relationship. Several assumptions were made in this derivation, but the relationship has been found to be linear, to within $\pm$ 2%, up to an optical density of 6 for L4 emulsion, and to an optical density of 2 for G5 emulsion (see figure 1.1 in previous chapter). The D.Q.E. of microdensitometry is less than that for track counting because of the variance in developed track areas, but this problem can be reduced by using a good development procedure (Coleman, 1974; see also section 1.4 and Appendix A).

The microdensitometer can be used to measure the average density on an electronograph within an area defined by a square shaped aperture. When this aperture is small compared to the size of an image, the measured density is proportional to the surface luminosity at that point on the image (see equation II-7). However, when a galaxy is to be studied, the luminosity at all points on its surface must be measured. The microdensitometer can move the electronograph across the aperture so that a two-dimensional array of measurements can be obtained which covers the area of the galaxy. Such a series of movements is termed a scan.

The accuracy of a density measurement from an electronograph should be limited by the characteristics of the emulsion, not by the properties of the microdensitometer. Hence, a microdensitometer should have the following features:

(1) the reading from a microdensitometer

should be proportional to the density on an electronograph,

(2) the noise contributed to the system by the microdensitometer must be very small compared to that due to other sources (e.g. emulsion, photocathode).

(3) the position of the analysing aperture must be known accurately for all the readings made over an extended image.

NOTE: The first feature is not as important as the others because the relationship between a reading and the measured density can normally be found. However, when this relationship is linear, the analysis of measurements is easier and there is one less step in the data analysis where an error could occur.

2.2. The Joyce-Loebl Mk III Cs Microdensitometer

This machine has been in use by the Astronomy group at Imperial College for some years now and it was used to obtain data from all of the electronographs studied in this thesis. Its operation and characteristics have been studied in some detail (Kahan and Cohen, 1969; Cullum, 1973; Worswick, 1975), so only the principle features are given here (see figure 2.1).

A lamp (a) is used to produce two beams of light; one beam (the measuring beam) passes through the electronograph, whilst the other (the reference beam) passes through a calibrated grey wedge. The transmitted intensities of the two beams are alternately measured by a photomultiplier (h) and the results are compared by an electronic system. The wedge (j) is then moved to

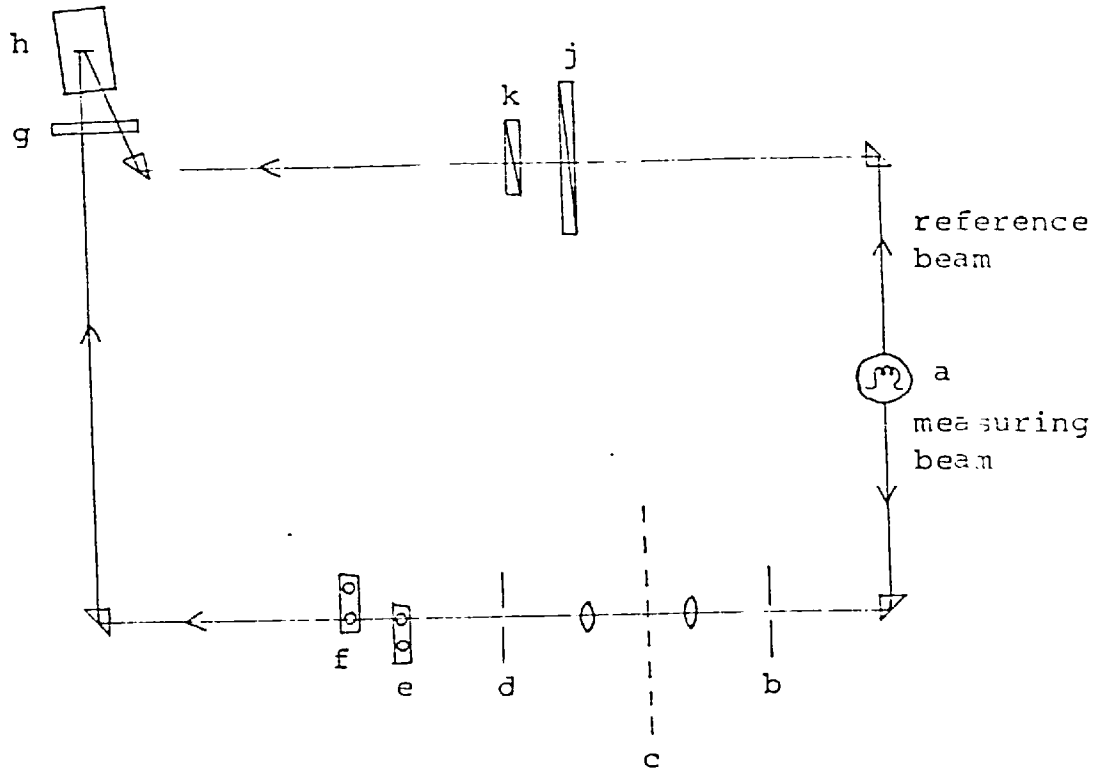

a.	lamp	g.	synchronous motor and chopper
b.	pre-slit	h.	photomultiplier
c.	sample plane	j.	density wedge
d.	post-slit	k.	zero correction wedge
e.	neutral density filter		
f.	filter to prevent light from red glass jaws of pre-slit reaching the photometer		

FIGURE 2.1. Schematic diagram of a Joyce-Loebl MkIII Cs Microdensitometer

a position where the two intensities are equal. Thus, the position of the wedge corresponds to a particular density reading. By using different wedges the resolution and range of the instrument can be varied (see table 2.1).

The optical system uses a pre-slit (b) and a post-slit (d) which serve both to reduce scattered light and to define the area to be measured on the electronograph. Objectives with up to 20x magnification can be used to magnify the measuring area. This permits the size of the post-slit to be accurately set to 5 μm by 5 μm, or larger, with an error of less than 10%.

There is a facility for one dimensional scanning; the electronograph being positioned on a sample table which is moved through the measuring beam. The sample table is coupled to a recording table by a ratio arm so that sample travels of between 125 μm and 25 cm can be made. This technique is called "handscanning" due to its manual nature; it is generally used to obtain profiles of an object as a preliminary to two-dimensional automated scanning.

In order to achieve two dimensional scans, stepping motors and lead screws have been added so that the table can be moved in multiples of 5 μm steps in the X and Y directions. Cullum (1973) showed that, using this system, the error in the position of the table is only 6 μm in 25 cm of travel. The motion of the table is controlled by an electronic system (Cullum and Stephens, 1972) to move in an automatic raster scan, the backlash of the motor being automatically corrected. At each point in the scan, when the wedge servo-system

TABLE 2.1

DENSITY RANGES AND RESOLUTION OF WEDGES

Wedge	Range	Density Resolution of Digital Output
A	0.39	0.00022
B	0.79	0.00048
D	1.67	0.001
F	2.50	0.0015
J	3.90	0.0022

is ready, a reading of the density is taken and written onto a 7-track magnetic tape. The scans are slow, typically 10 readings are made per second; thus a scan of an area of 10 mm by 25 mm, with 25 μm between readings, would take over 10 hours.

On completion of the scan, the data is read from the tape and translated into computer-readable form by a program developed by Stephens (1974). This translated data is stored on an archive tape which is available for processing by the large computers which are necessary for the analysis of the large arrays of data produced.

2.2.1. Linearity of the Microdensitometer

In section 2.1 it was stated that a microdensitometer reading must be directly proportional to the density being measured over the range of density on an electronograph. Primary sources of non-linearity in the Joyce-Loebl Mk III Cs microdensitometer are non-linearity of the grey wedge and a transmission averaging effect which arises whenever there is a density gradient across the measuring aperture.

Cohen (1972) showed that defects in the wedges can produce small scale departures from linearity of up to 2%. The effect can be removed by calibrating the wedge (Ables and Ables, 1972b), but in practice the error is normally too small to warrant correction.

The microdensitometer reading is proportional to the density within a measuring aperture only when the density is constant across the aperture. When there is a density gradient across the aperture, the measured density (D*) will not equal the true

average density ($\bar{D}$) because of a transmission averaging effect. The amplitude of this effect is calculated below for small measuring apertures. It is assumed that the gradient is constant over the aperture (i.e. second-order density effects are negligible).

If the aperture is small, the density (D) across a square aperture (of side a) can be represented by

$$D = G_x x + G_y y + Do \qquad \text{II-8}$$

where Gx and Gy are the density gradients in the x and y directions, and Do is the central density within the aperture (see figure 2.2)

The density (D) and the transmission (T) at each point on an electronograph can be related by equation II-1, which can be re-written

$$T = 10^{-D} = e^{-KD} \qquad \text{II-9}$$

where $K = \ln 10 = 2.30$

The microdensitometer determines the average density within an aperture from the average transmission ($\bar{T}$) through the aperture. The average transmission within the aperture is

$$\bar{T} = \frac{1}{a^2} \int_{y=-a/2}^{y=a/2} \int_{x=-a/2}^{x=a/2} e^{-K(G_x x + G_y y + Do)}\, dx\, dy$$

$$= \frac{e^{-KDo}}{a^2} \frac{1}{-KG_x} \left[e^{-KG_x x} \right]_{-a/2}^{a/2} \frac{1}{-KG_y} \left[e^{-KG_y y} \right]_{-a/2}^{a/2}$$

$$= \frac{e^{-KDo}}{a^2 K^2 G_x G_y} \left(e^{-KG_x a/2} - e^{-KG_x a/2} \right) \left(e^{-KG_y a/2} - e^{KG_y a/2} \right)$$

$$= e^{-KDo} \frac{\sinh U \sinh V}{U \quad V} \qquad \text{II-10}$$

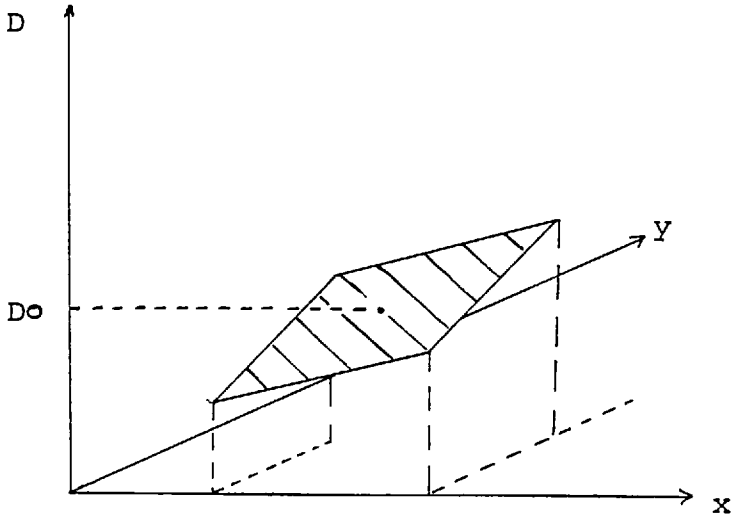

FIGURE 2.2 VARIATION OF DENSITY ACROSS A SQUARE APERTURE

where $U = KG_x a/2$ and $V = KG_y a/2$

The measured density can be calculated, using equation II-1:

$$D^* = -\log_{10}\bar{T} = \frac{1}{K}\ln\left(\frac{1}{\bar{T}}\right)$$

$$= \frac{1}{K}\ln\left(\frac{UVe^{KDo}}{\text{Sinh U Sinh V}}\right)$$

$$= Do + \frac{1}{K}\ln\left(\frac{UV}{\text{Sinh U Sinh V}}\right) \qquad \text{II-12}$$

The average density $\bar{D}$ is just Do; therefore the percentage error in the measurement caused by this effect is

$$\triangle_G = \frac{D^* - \bar{D}}{\bar{D}} \times 100$$

$$= \frac{100}{DoK}\ln\left(\frac{UV}{\text{Sinh U Sinh V}}\right) \qquad \text{II-12}$$

It will be shown below that U and V are normally less than 1 so the following expansions can be made

$$\frac{\text{Sinh U}}{U} = 1 + \frac{U^2}{3!} + \frac{U^4}{5!} + \frac{U^6}{7!} + \cdots$$

$$(1+U)^{-1} = 1 - U + \frac{U^2}{2} - \frac{U^3}{3} + \cdots \qquad \text{II-13}$$

$$\ln(1+U) = U - \frac{U^2}{2} + \frac{U^3}{3} - \cdots$$

Equation II-12 can then be reduced using the equations specified in II-13 to the following

$$\triangle_G = \frac{+100}{DoK}\left[\left(\frac{-U^2}{3!}\right) + \left(\frac{-V^2}{3!}\right)\right]$$

$$= \frac{-100a^2K^2(G^2_x+G_y^2)}{DoK.24} \qquad \text{II-14}$$

where terms of order higher than the second are ignored. The percentage error $\triangle_G$ will be a maximum when G_x and G_y equal the maximum gradient G within an image; then

$$\triangle_G = \frac{-19.2a^2G^2}{Do} \qquad \text{II-15}$$

The error is always negative so the measured density is always less than the true average density within the aperture. For the error to be less than 1%, then

$$a \leq \frac{1}{G}\sqrt{\frac{Do}{19.2}} < \frac{0.23\sqrt{Do}}{G} \qquad \text{II-16}$$

Substituting for a in the definition of the variable U gives

$$U \leq \frac{KG}{2} \cdot \frac{0.23\ Do}{G}$$

$$\leq 0.26\ Do \qquad \text{II-17}$$

Hence, U and V are normally less than 1 for the density range over which the microdensitometer will give less than 1% error.

In order that the error caused by a density gradient across an aperture is minimal, equation II-18 is used to define the aperture size for all the measurements in a scan to be accurate to 1%

$$a = \frac{1}{10}\left(\frac{\sqrt{D}}{G}\right)_m \qquad \text{II-18}$$

where $\left(\frac{\sqrt{D}}{G}\right)_m$ is the maximum value of $\frac{\sqrt{D}}{G}$ in a scan. This value can usually be measured from handscans of an object before a scan is made.

2.2.2. Microdensitometer Noise

The noise introduced by a microdensitometer can be measured by holding neutral density filters in the measuring beam. Figure 2.3 shows the RMS density noise σ_D plotted against Joyce-Loebl density (Ring and Worswick, 1974). At high densities, or with small apertures, the amount of transmitted light is low and the noise due to photon statistics dominates. (NOTE: At an optical density of 5, only one in 10^5 photons is transmitted). The digitising electronic system also introduces noise, but the quantity is small and independent of the density and aperture in a measurement.

The machine should always be operated so that emulsion noise dominates. Since L4 emulsion contains about 15 tracks μm^{-2} per unit density (Coleman, 1974), the signal-to-noise ratio, due to the number distribution of tracks in L4 emulsion, is

$$\left(\frac{S}{N}\right)_{L4} = \sqrt{a^2 15.D} \qquad \text{II-19}$$

where "a" is the aperture size in microns and "D" is the optical density of the emulsion.

Worswick (1975) measured the signal-to-noise ratio of the Joyce-Loebl microdensitometer - L4 combination and found

$$\left(\frac{S}{N}\right)_{m+L4} \doteq \sqrt{a^2 5.OD} \qquad \text{II-20}$$

The detective quantum efficiency of microdensitometry is the ratio of the measured signal to the emulsion signal to noise, viz:

FIGURE 2.3 RELATIONSHIP BETWEEN MEASURED NOISE AND DENSITY USING JOYCE LOEBL MKIII MICRODENSITOMETER

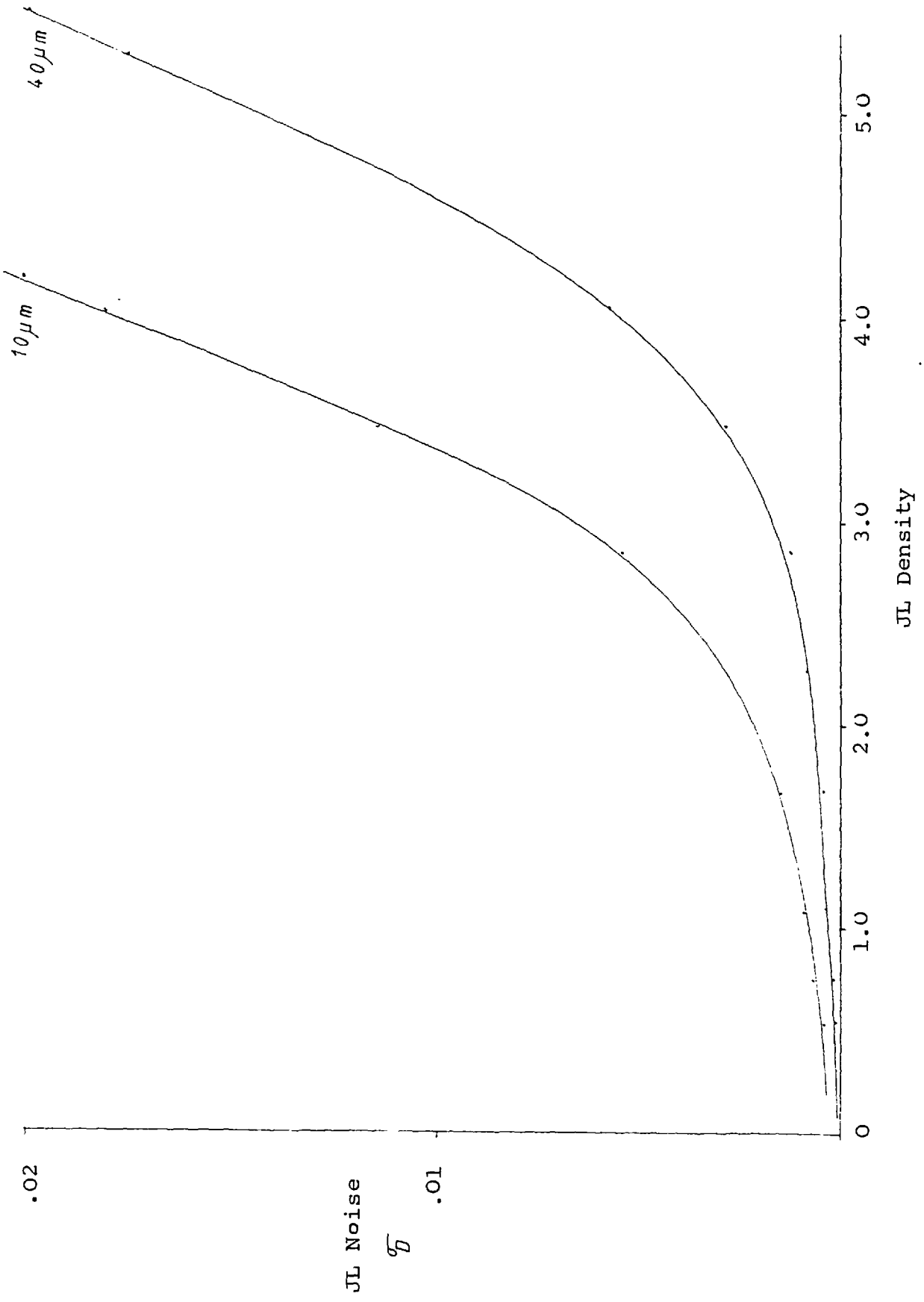

$$\frac{(S/N)_{M+L4}}{(S/N)_{L4}} = \frac{\sqrt{5a^2D}}{\sqrt{15a^2D}} \simeq 0.60 \qquad \text{II-21}$$

Equation II-20 shows that, for the emulsion noise of L4 emulsion to be less than 1% of the signal at any point in a scan, then

$$a_{L4} \geq \frac{100}{\sqrt{5D_L}} \qquad \text{II-22a}$$

where D_L is the lowest density in the scan. Normally, the lowest density in a scan is the density of the sky background. Using data measured by Worswick (1975) a similar calculation for G5 emulsion can be made; giving

$$a_{G5} \geq \frac{100}{\sqrt{D_L}} \qquad \text{II-22b}$$

The aperture must be larger for G5 emulsion because there is a smaller number of tracks per unit density, and hence the emulsion noise is larger.

2.3. The Study of Astronomical Objects with a Microdensitometer

In the previous sections it was shown that a microdensitometer can conveniently access the information stored in an electronograph. Consideration will now be given to the most efficient way in which a microdensitometer can be used to access the data which is necessary for the study of astronomical objects.

Walker (1967) showed that several density readings along a cross-section of a stellar image can be used to calculate an accurate value of the integrated magnitude of a star. However, many objects have an extended luminosity distribution which requires that their surface luminosity be measured at many points to obtain

their integrated magnitude. It was for this reason that the Joyce-Loebl microdensitometer at Imperial College was put under the control of an electronic system which scanned and measured the density of a two-dimensional array of points on an electronograph. When the scan of an extended object is to be made, the following factors must be considered:

(1) the measuring aperture size,

(2) the distance between successive measurements,

(3) the total area to be scanned and the number of measurements in the scan

2.3.1. Aperture Size

The microdensitometer can be used to measure the average density within an area of side 5 μm, or more. The constraints on choosing the optimum size of aperture are:

(1) The aperture must be small enough to give adequate spatial resolution.

(2) The aperture should be as large as possible in order to reduce the emulsion noise. Equation II-22 shows that the highest emulsion noise in a scan is measured at the density of the sky background.

(3) The aperture should be as small as possible in order to reduce the transmission averaging effect. Equation II-18 can be used to calculate the size of aperture which will keep this error below 1% during a scan.

Constraint (1) defines the maximum size of aperture which can be used to study an object. Hence, knowing the accuracy to which the object is to be studied,

the observer must expose his electronographs to a level where the sky background density is greater than that defined by constraint (2). In practice (see chapters 4 and 5), the aperture defined from constraints (1) and (2) is much larger than that needed to minimize the transmission averaging effect. However, scans of the electronographs can be made with a small aperture which reduces the transmission averaging effect, and the results can then be "blocked" to an aperture size defined by constraints (1) and (2).

The process of blocking is shown in figure 2.4. The readings in each square of side a_2 are averaged, giving a result equivalent to that from taking a single reading with aperture a_2, but with a higher accuracy. This is explained in Appendix B.

Thus, studies of an object are made after scanning an electronograph with a small "measuring" aperture and then blocking the results to a larger "analyzing" aperture. The measuring aperture is that aperture which reduces the transmission averaging effect to the required accuracy, and the analyzing aperture is that aperture at which the emulsion noise is reduced to the required accuracy. These apertures are generally calculated by using information from handscans through the centre of an object and applying equations II-18 and II-22.

The analysis in Appendix B assumes that the emulsion noise is randomly distributed. In fact, there are additional effects caused by scratches of lumps of dirt which cause very high, localised errors. These additional sources of noise can be recognised and removed before blocking; this process is described in

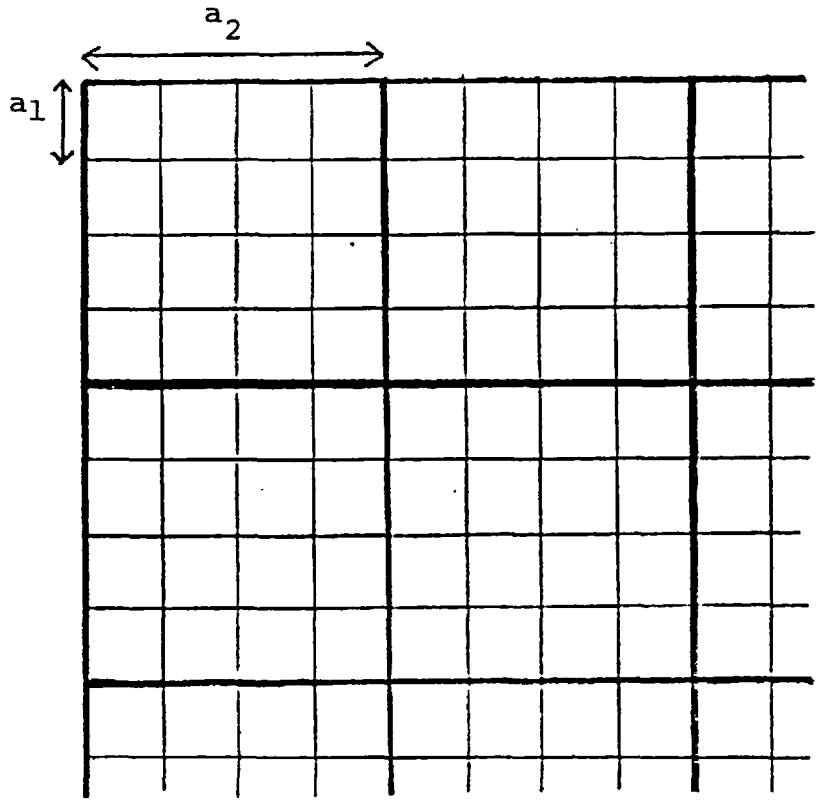

NOTE: The length of a_2 is an integral number times the length of a_1.

FIGURE 2.4 THE PROCESS OF BLOCKING

more detail in section 3.7. Care must be taken that such effects are removed, or marked for future attention, because they are less easily recognised after blocking and may be mistaken to be a real object.

The above analysis defines the measuring and analysing apertures to be used for studies of most electronographs. However, for very accurate studies of, for instance, the luminosity profile of an object, there is another constraint to be considered. The constraint is the following:

"the analysing aperture must be small enough for the average density which is measured to be equal to the central density within the aperture, to the required accuracy".

NOTE: Second-order gradient effects may be negligible within the "measuring" aperture, but within the larger "analysing" aperture this may not be the case.

Inaccurate profiles of an object may be drawn when the average density is not equal to the central density. The error involved can be found by studying the profile of a star, i.e. a point source, because it will have a larger gradient, and rate of change of gradient than that of an extended object of the same density on the same electronograph. The profile of a star can be approximately represented by (see Appendix C),

$$D = Doe^{-kx^2} \qquad \text{II-23}$$

A computer program (APTUR - see Appendix D) was written to simulate the measurement of the average density within analysing apertures of various sizes

centred on a star profile. The density gradient changes rapidly at the centre of a star profile (see Appendix C), so the measured average density through large apertures will be less than the central density within the aperture. The error in the measurement of the central density of a stellar profile was calculated by the computer program and the results are shown in a graph in figure 2.5a. This graph shows that, for the central density to be measured to an accuracy of 1%, the size of the analysing aperture(a) should be less than one-tenth of the full width at half the maximum density of a star profile (S) i.e.

$$a < \frac{S}{10P} \quad \text{mm} \qquad \text{II-24}$$

where P is the plate-scale in arc second per mm on the electronograph. Slightly higher rates of change of gradient are found elsewhere on a star profile (see Appendix C) so, for accurate studies of stellar like objects, the size of the analysing aperture should be less than the value calculated using equation II-24.

This constraint is only important at places where there is a high rate of change of gradient i.e. in stellar like features, and it is only applicable when accurate profiles are needed. For morphological and photometric studies of most objects, any stellar like parts are of little interest because they are unresolved so this constraint is not applied.

2.3.2. Step Length

The "step-length" of a scan is the distance between measurements; it is generally the same length in the x and y directions of a scan. The step length can

(a)

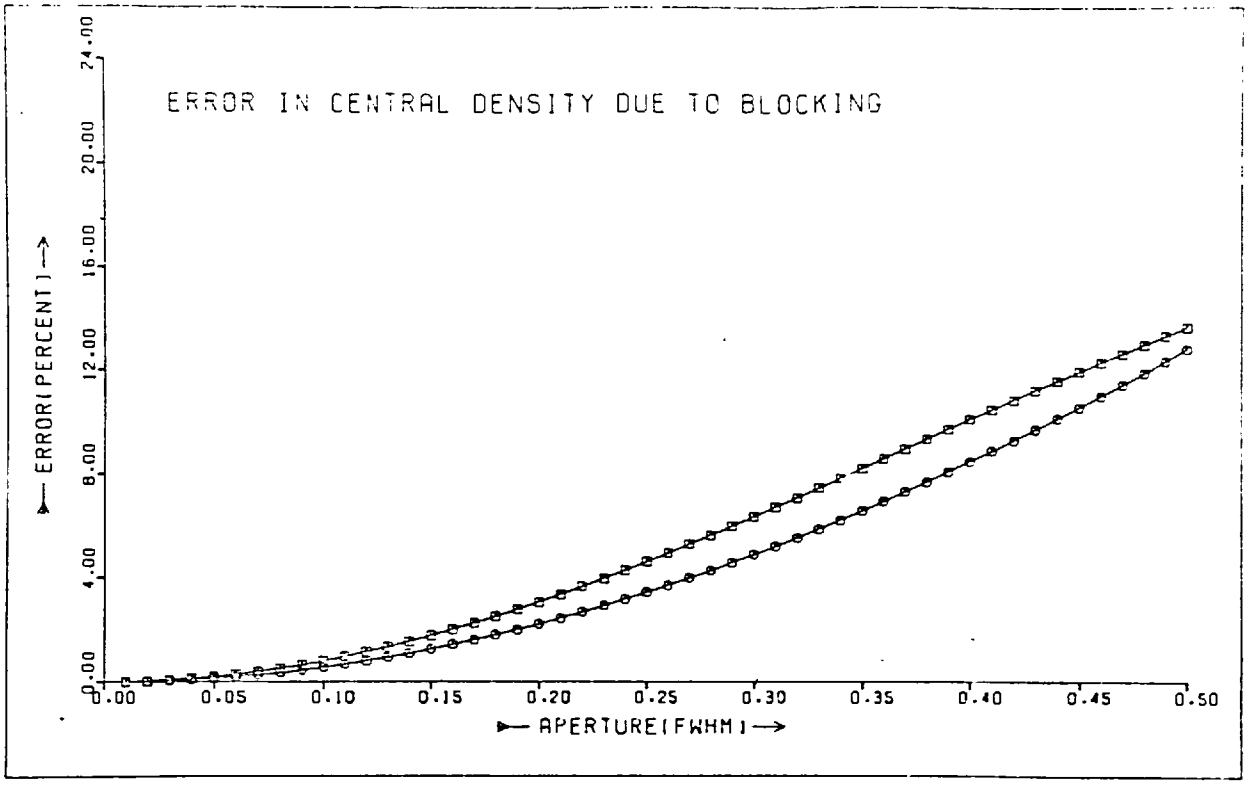

NOTE: THE POINTS MARKED BY SQUARES ARE FOR THE APERTURE CENTRED ON THE CENTRAL DENSITY
THE POINTS MARKED BY CIRCLES ARE FOR AN APERTURE CENTRED HALF AN APERTURE WIDTH FROM THE CENTRAL DENSITY

(b)

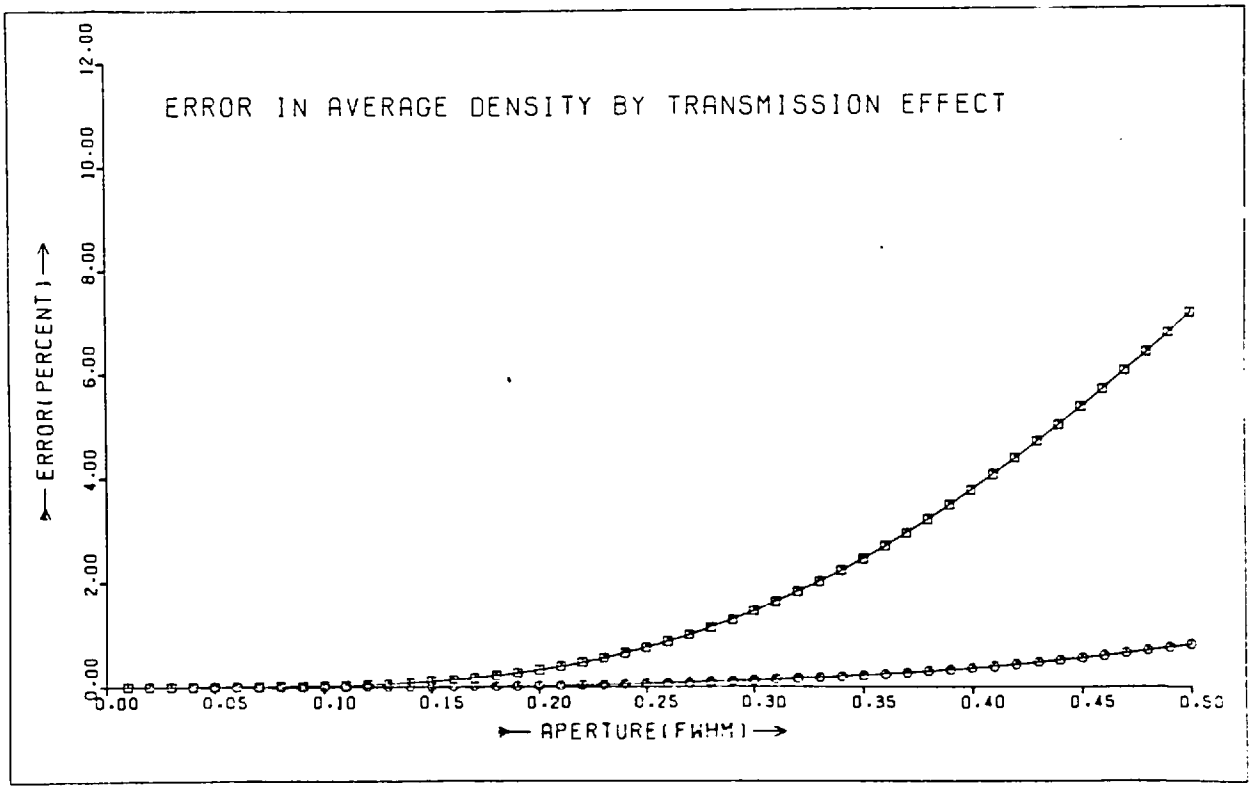

FIGURE 2.5. Computations of the error caused by
(a) the process of blocking, and as a comparison,
(b) the transmission effect

be chosen equal to, larger than, or smaller than the aperture size. If the step length is larger than the aperture size then some of the available information is not sampled. Conversely, if the step length is smaller than the aperture size then the information is oversampled. Oversampling is not itself a problem, but is does mean that more readings have to be taken than are otherwise necessary. Hence, oversampling causes more time to be spent in microdensitometry and in analysing the results. For these reasons the step length is generally chosen to equal the aperture size.

2.3.3. Scans of the Images of Extended Objects

The aperture and step length of a scan have to be chosen so that the measurements are to the required accuracy. The information needed to calculate the aperture and step length can be obtained from a handscan through the nucleus of the image. The parameters to be measured are

Z: The density of the sky background

Dm: The maximum density of the object measured from the sky background density

G: The maximum density gradient of the image

R: The density of the image at which G is measured

These parameters can be used to calculate the measuring aperture (a_T) and step length using equation II-18, for the measurements to be to 1% accuracy; viz

$$a_T < \frac{1}{10}\sqrt{\left(\frac{R}{G}\right)_m} \qquad \text{II-25}$$

The analysing aperture can also be calculated, using equation II-22; e.g. for L4 emulsion and an accuracy of 1%

$$a_E > \frac{100}{\sqrt{5Z}} \qquad \text{II-26}$$

For each of the galaxies studied in Chapters 4 and 5 these parameters are given to indicate why the scanning apertures were chosen.

Scans made of an extended object will usually entail many measurements to be made of the density on an electronograph over a period of several hours. During this time the zero point of the readings may drift by as much as 0.002D per hour (Worswick, 1975) which complicates the data analysis. In addition, the total number of readings becomes very high. However, two or more scans of an electronograph can be made which cover different regions of an object e.g. nucleus, intermediate and outer regions. Each scan need only use the aperture and step length appropriate for the region being scanned. For instance, no large density gradients and only low densities are found in the outer regions of extended objects so a larger step length and aperture can be used than that needed for the scan of the nucleus. Also, small apertures and step lengths are only necessary in the nuclear region of an object where densities and gradients are high, but the nuclear region is usually small compared to the whole object so not many readings are necessary. Hence, a smaller total number of measurements will be made and the scanning and data analysis time can be reduced to less than half an hour per scan.

2.3.4. Scans of a Star Image

The integrated luminosity of a star image is obtained by finding the integrated density, or volume, of the star image. The volume can be found by assuming that the image is circular and taking readings along a central cross-section of the image (Walker, 1967; Hewitt, 1969). However, this method does not use all the available information and will be in error if the star image is non-circular because of the effects of trailing, telescope misalignment or image tube distortions.

Alternatively, the whole star image can be scanned and its volume found either by integrating the readings (Pilkington, 1972; Newell and O'Neill, 1974; Purgathofer, 1974), or by fitting gaussian profiles to the data (Zinn & Newell, 1972). The technique of fitting profiles to the data is generally the most accurate, but involves complicated computational methods and the measurements must be very accurate. The method of Newell & O'Neill (1974), however, involves only simple data processing and needs only a short scan of a star to be made. The measuring aperture is chosen so that the average accuracy of the readings is high, even though particular readings may be very inaccurate. Hence, scans use larger apertures and less time than other methods. The volume of the star image is found using the program VOL (see Appendix D) which sums the readings in a scan, starting from the centre of the image, until the desired accuracy is reached. For example, the integrated magnitude can be calculated to 1% accuracy on a star image which has been appropriately exposed with a plate scale of $25''$ mm^{-1}, in seeing of $4''$. The measurements will be taken from a scan of 35 by 35 steps using an aperture

and step length of 20 μm and 10 μm, respectively.

2.3.5. The Study of Colour

The colour, and other parameters, of an object can be calculated from measurements of the luminosity transmitted through filters with different bandpasses. If L_1 and L_2 are the luminosities of a point P observed through, say, the B and V filters, then the colour (C) at the point P can be calculated using an equation of the form

$$C = -2.5 \log\left(\frac{L1}{L2}\right) \qquad \text{II-27}$$

The exact form of this equation is given in the next chapter.

If scans are made of electronographs exposed through these filters, then the colour at each point on the object can be calculated

$$C_{x_1,y_1} = -2.5 \log\left(\frac{{x_1,y_1}^{L_1}}{{x_2,y_2}^{L_2}}\right) \qquad \text{II-28}$$

where x_1,y_1 are the co-ordinates of P in scan 1, and x_2 and y_2 are the co-ordinates of P in scan 2. The two co-ordinate systems will generally be related by a rotation and translation vector. It will probably also be necessary to interpolate between two measurements in scan 2 in order to find the exact luminosity of P through filter 2. The rotation/translation vector plus interpolation makes the data analysis fairly complicated and time consuming. However, the data analysis can be simplified by ensuring that the scans are made parallel to each other. When this is done the co-ordinate systems of the scans will be related

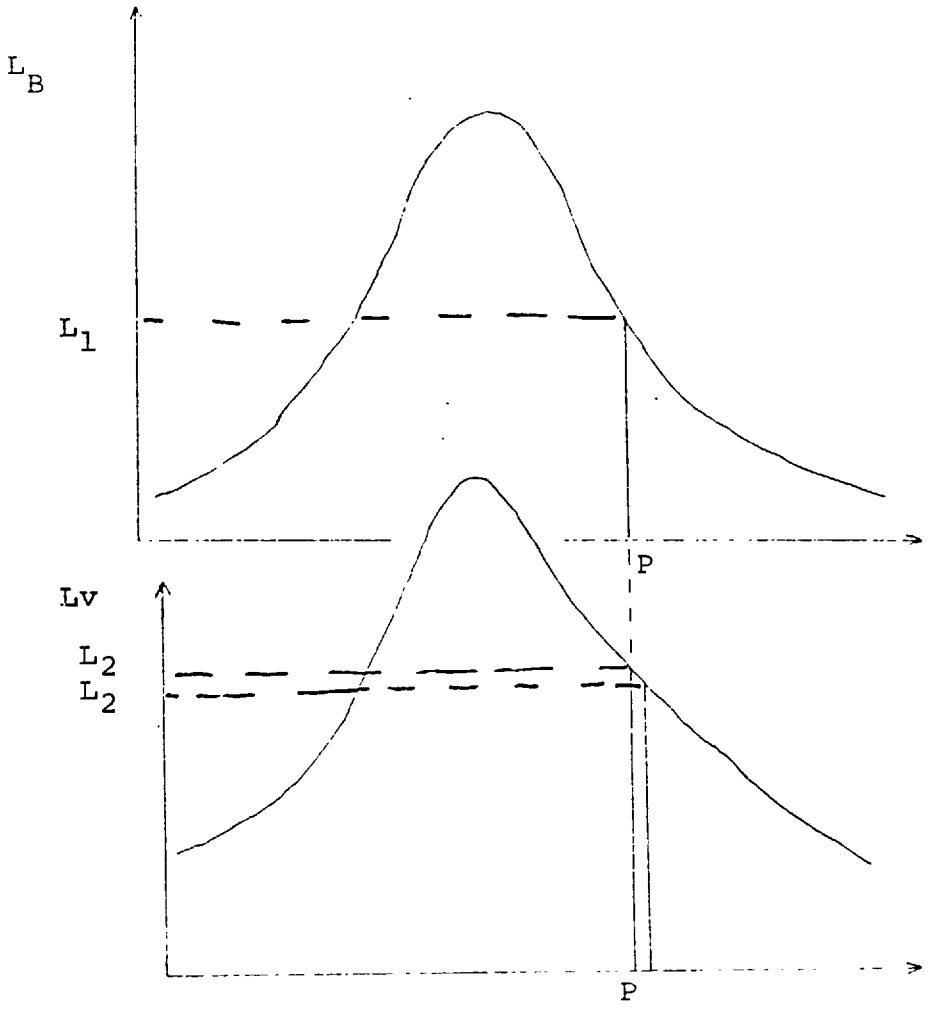

FIGURE 2.6 COMPARISON OF THE LUMINOSITIES THROUGH TWO FILTERS

only by a translation vector.

The scans can be made parallel to each other by making them parallel to a line found on both electronographs. This line can be chosen to be a line connecting two stars, but it is normally taken to be the line defined by the edge of the electronograph. This has the advantage that the edge of the electronograph is normally aligned with the North-South or East-West directions so the orientation of an object can be quickly found.

The data analysis can also be simplified by using a step-length (Δ) in the scans which makes interpolation unnecessary. This occurs when the error caused by misalignment of the scans is less than errors from other causes. The maximum misalignment of two parallel scans is half a step length in the x and y directions. If L'_2 is the luminosity of the nearest point in the second scan to the point P in the first, then

$$L'_2 < L_2 + \frac{G_2 \Delta}{\sqrt{2}} \qquad \text{II-29}$$

where G is the maximum gradient in the second scan and $\Delta/\sqrt{2}$ is the maximum displacement of the two scans (see figure 2.6).

The error in the calculation of the colour at point P will be of order Λ, where

$$\Lambda = C' - C = -2.5 \log \frac{L_1}{L'_2} - (-2.5 \log \frac{L}{L_2} 1)$$

$$= 2.5 \log \left(\frac{L_2}{L'_2} \right) \qquad \text{II-30}$$

In the worst case

$$\Omega_{max} = 2.5 \log\left(\frac{L_2}{L_2 + G_2\Delta/\sqrt{2}}\right) \qquad \text{II-31}$$

Since Δ is small, then $\frac{G_2\Delta}{L_2\sqrt{2}}$ will be small and equation II-31 can be expanded to

$$\Omega_{max} = \frac{2.5}{2.3} \frac{G_2\Delta}{L_2\sqrt{2}} \qquad \text{II-32}$$

Normally, the accuracy(Ω) to which a scan is to be made is known, so the necessary step length (Δ) between measurements can be calculated, viz

$$\Delta = 1.30\Omega_{max}\left(\frac{L}{G}\right)_{min} \qquad \text{II-33}$$

Equation II-33 is used to calculate the step lengths of scans of b and V electronographs. The step length is calculated for the maximum error (Ωmax), rather than the average error, because misalignment of scans causes a systematic error and the calculation of colour must be to the required accuracy, whatever the misalignment.

If the luminosities L_1 and L_2 are measured with an accuracy of 1%, then the colour (c) of an object can be measured to an accuracy of approximately 0.02 magnitudes, assuming the scans are perfectly aligned. Hence, the maximum error in the calculation of the colour caused by misalignment of the scans should also be about 0.02 magnitudes. Substituting this value in equation II-33 gives

$$\Delta = 0.03\left(\frac{L}{G}\right)_{min} \qquad \text{II-34}$$

The value $(L/G)_{min}$ is usually measured close to the point where the gradient (G) is a maximum. Hence, L/G is usually measured at the point of maximum gradient on an object and this value is used to calculate the step length for a scan. When the required step length for a scan is less than a microdensitometer is capable of, interpolation between measurements must be made.

Equation II-34 can also be used to calculate the accuracy to which two scans should be made parallel, i.e. for the scans to be related by a translation vector only. If the scans are aligned so that the centres of the object in the two scans are co-incident, then the end points of the scans must not be greater than $\Delta/2$ distant from each other. Thus the maximum angle of rotation is given by

$$\alpha = \frac{\Delta/2}{L/2} = \frac{\Delta}{L} \quad \text{radians} \qquad \text{II-35}$$

where L is the length of a scan. Typically, α is 0.01 radians (0.6^{o}), but scans can be aligned to about 0.002 radians.

CHAPTER 3

ASTRONOMICAL OBSERVATIONS AND THEIR ANALYSIS

3.1. Observing Procedure

Electronography is an ideal technique for the study of galaxies because its relatively high D.Q.E. permits the detection of faint extensions within a reasonable exposure time, and its linearity facilitates the study of bright nuclei where luminosity gradients are high. Some galaxies have such a high range of luminosities that it is necessary for two exposures, of long and short duration, to be made in order that both bright and faint features are exposed to an optimum level. In section 2.3.3 it was shown that scans should be made of the nucleus, intermediate and outer regions of a galaxy image on an electronograph. These scans can be made on electronographs exposed to the appropriate level and they can easily be compared with each other because electronography is a linear process.

Care must be taken when observations of an object are made to ensure that the constraints defined in section 2.3.1 permit the images to be studied to the required accuracy and detail. Consider, for example, electronographs of a stellar like object which were taken on a telescope with a plate-scale of $25''$ mm^{-1}. If the seeing was $1''$ and the electronograph was exposed to a background density of 1D on L4 emulsion, then the aperture "a" is defined

$$a > \frac{100}{\sqrt{5D_{sky}}} .10^{-3} \text{ mm} > 45\mu\text{m} \qquad \text{III-1}$$

for the emulsion noise to be less than 1%, using equation II-18. The aperture needed for the profile of the object to be measured to a similar accuracy is defined by equation II-25. Therefore,

$$a_{pr} < \frac{S}{10\rho} \quad \text{mm} < \quad 4\,\mu\text{m} \qquad \text{III-2}$$

Thus, this example shows that it is impossible to study the profile of this object to the desired accuracy. This does not stop other studies of the object from being made, but it does show that much thought has to be given to the type of object to be observed, the exposure time and the telescope plate-scale for the observations.

The field size of a spectracon is small (30 mm by 10 mm, which is equivalent to $12.5^{\prime}$ by $4^{\prime}$ with a plate-scale of $25''.\text{mm}^{-1}$, or $3^{\prime}$ by $1^{\prime}$ at $6''.\text{mm}^{-1}$) so the region of a large galaxy to be studied may not lie within the field covered by the spectracon. It is possible, though time-consuming, to take several overlapping exposures of a large object, but these objects are usually observed on telescopes with an appropriate plate-scale. The more distant, or smaller galaxies can normally be exposed on a single electronograph.

Since the spectracon applicator holds a strip of film on which six electronographs can be stored, it is possible to store a long and a short exposure electronograph of a galaxy through two or three filters on one strip of film. If a galaxy is observed through only two filters, for example the B and V filters, then exposures of standard stars through each filter can be stored on the same strip of film. This is very convenient for both storage and data retrieval.

Unexposed emulsions are abrasion sensitive so they have to be handled with extreme care, especially when the applicator is being loaded. Latent image fading can occur if the exposures are left for a long time before being developed (Coleman, 1974), but most electronographs are developed within a few hours of exposure. There are several types of emulsion which have been used with the spectracon, but L4 emulsion is preferred because it has the better characteristics (see Chapter 1). However, observations through narrow band filters, or of faint objects, are made with faster emulsions, even though exposures are limited to a lower density due to the lower dynamic range of these emulsions.

When the electronographs are returned to the laboratory it is convenient to make all the scans of one galaxy consecutively. They can then be transferred to adjacent files on a computer tape which facilitates the data processing. In order to reduce the delays in the data processing procedure, programs were written which allow scans to be displayed on a graphics terminal with a facility for interactive processing of the data by the user.

3.2. Quick-Look Displays of Microdensitometer Scans

As it can take several days between making a scan and seeing the results displayed on paper, the author has developed several programs which can display the results of a scan on a Tektronix graphics terminal. The terminal is directly linked to the college CDC 6400 computer with a fast line facility which permits graphical displays of data stored on computer discs. The programs read the data from disc and create displays

using parameters inserted by the user. Hence, if the parameters are incorrect the user can change them and view the corrected display immediately.

The data is stored on disc using the program TRANS (see Appendix D) which reads the data from an archive tape, blocks it as necessary, and writes it to a disc file together with some information needed for the display programs. Owing to computer constraints in storage space and the time allowed for display, the blocked scan normally consists of less than 10,000 points. There are generally many more points in a full scan so the terminal is mainly used for quick look displays and checks in preparation for more detailed studies of a scan by other programs which are described later. The data is displayed by the programs SLARD, SIMMAP and XSEC (see Appendix D). These programs are invaluable in the processing of data from electronographs, but they have also been used to advantage in the study of stellar models (Reay et al, 1976) and speckle interferometry (Beddoes et al, 1976).

The program SLARD provides a quick, simple display of the readings in a scan, and uses the least computer time. An example display is shown in figure 3.1a. The program is used to find the range of density in a scan and the display is used to detect the effect of any scan errors. For example, when the range of density in a scan is higher than that of the wedge used for scanning, then "topping" occurs. This is easy to detect on a SLARD display.

SIMMAP displays contour maps of an array of readings (see figure 3.1b). The contour heights to

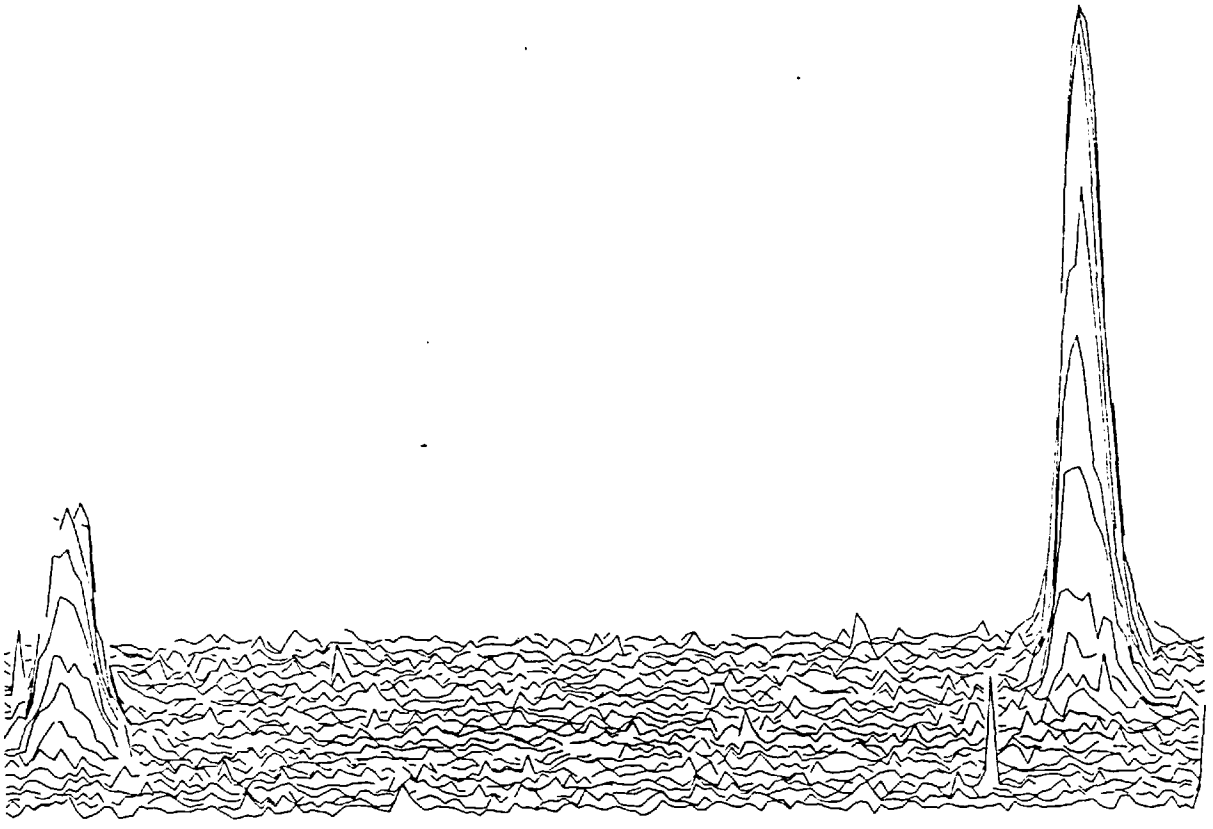

Figure 3.1a LARD display

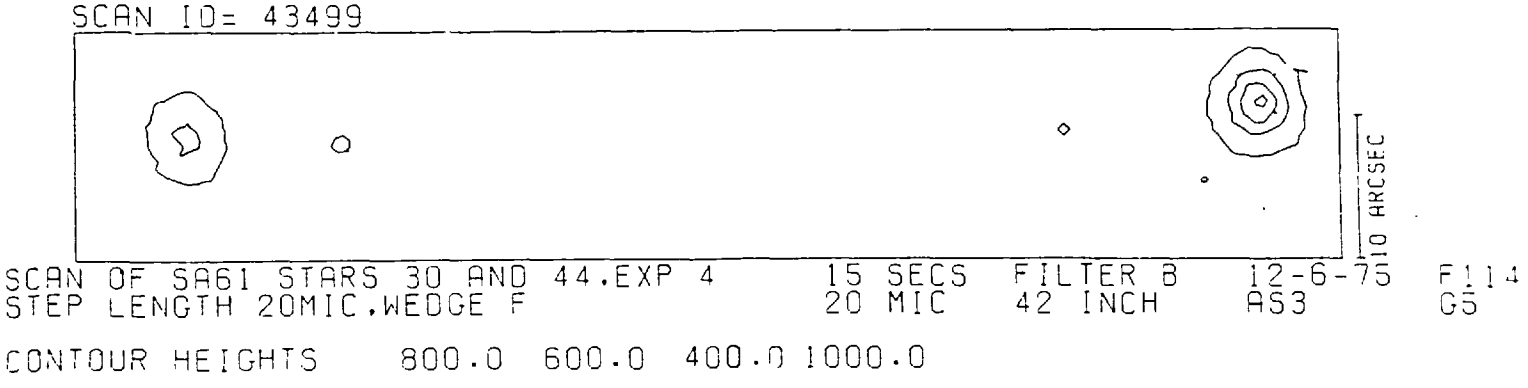

Figure 3.1b SIMMAP Display

FIGURE 3.1 QUICK LOOK DISPLAYS

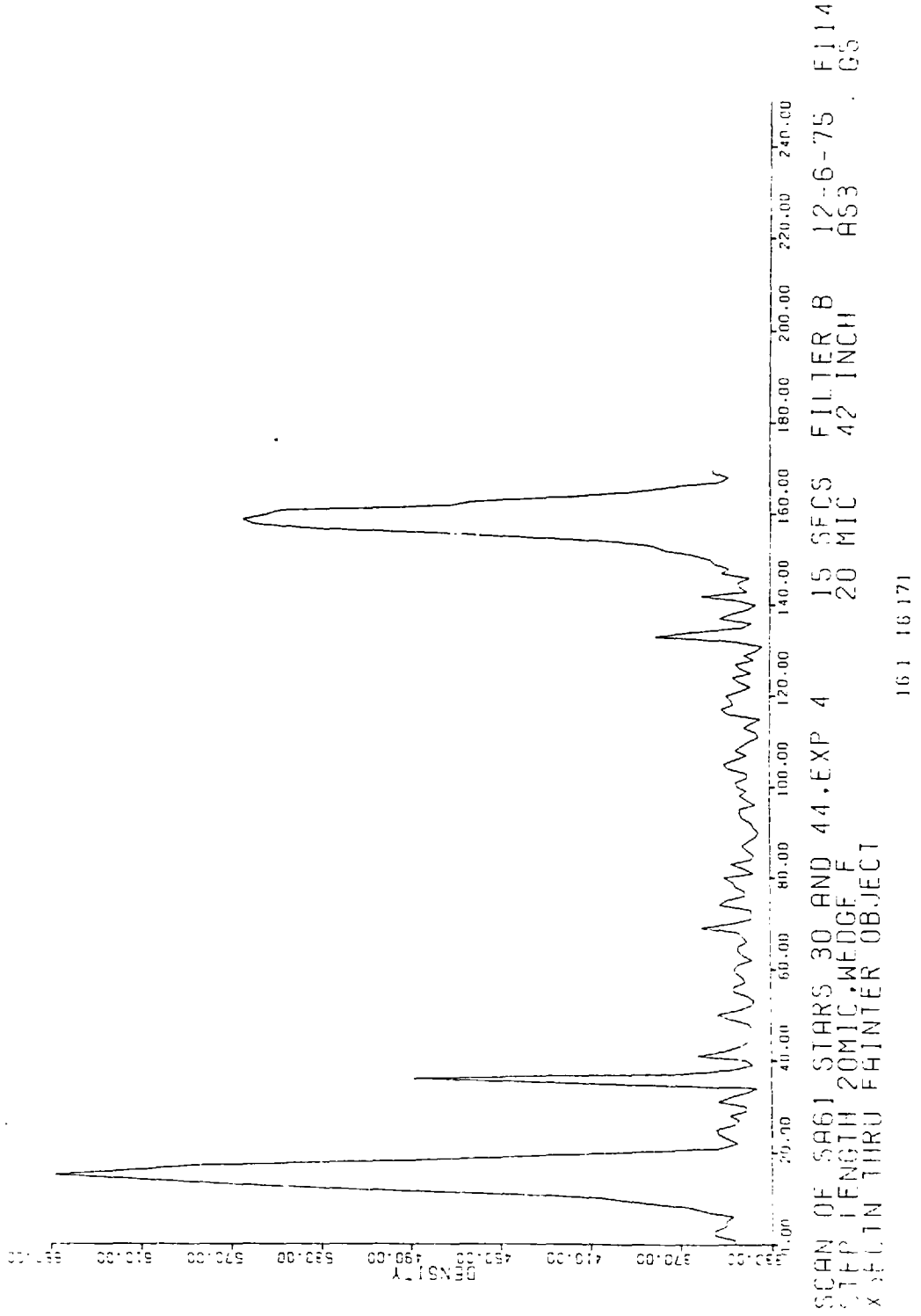

Figure 3.1c XSEC Display

FIGURE 3.1 QUICK LOOK DISPLAYS

be displayed are input to the program by the user, so several contours can be drawn to determine which ones show the most information.

The program XSEC uses the readings in a scan to draw a profile of an object. The user specifies the end points for the profile, so a profile along any direction is possible.

The programs SLARD, SIMMAP and XSEC all permit real-time interaction by the user to change parameters of a display. Hence, they were designed to be very efficient in their use of computer time. Each program allows the display of a portion of the data array and, when necessary, prints the display on microfilm for storage.

For most exact morphological and photometric studies, the programs MAP and CROSS (see Appendix D) are used to produce maps and profiles of the luminosity distribution in a galaxy. These programs can be used to process large arrays of data in order to calculate photometric parameters of a galaxy; they will be described in detail in the following sections.

3.3. Photometric Studies

In section 2.1 it was shown that the optical density (d) at a point on an electronograph is proportional to the total number of photons detected from a point on the galaxy (n_G), plus the number from the sky background, viz

$$D = K_1 (n_S + n_G) \qquad \text{III-3}$$

$$= K_1 n_S + K_1 n_G$$

where K_1 is a constant. Under the conditions defined in the previous chapter, the reading (R) from a microdensitometer is proportional to the density being measured. Thus, the density can be expressed in the form

$$D = C_i\ (R-Ro) \qquad \text{III-4}$$
$$= C_i\ (R-Rs) + C_i\ (Rs-Ro)$$

where C_i is a constant which depends on the wedge that is used for the reading, Ro is the reading at zero density which is constant for a scan (though it will vary from one scan to another as the offset density varies), and R and Rs are the readings of the galaxy plus sky background density and of the sky background density, respectively. Combining equations III-3 and III-4 gives

$$K_1 n_G = C_i\ (R - Rs) \qquad \text{III-5}$$

Equation III-5 relates the reading (R) at a point on an electronograph to the total number of photons received from that point on the galaxy. If the exposure time of the electronograph is 'T' seconds, then

$$n' = \frac{n_G}{T} \qquad \text{III-6}$$

where n' is the photon flux from the point on the galaxy. The photon flux is used to define the surface brightness (m_s) of the galaxy, viz:

$$m_s = K_2 - 2.5 \log_{10} n' \qquad \text{III-7}$$

where K_2 is a constant. Hence, using equations III-5, III-6 and III-7, the surface luminosity of a galaxy can be related to the reading on the electronograph by

$$m_s = K_2 - 2.5 \log_{10}\left(\frac{C_i}{T K_1}\ (R-R_s)\right)$$

$$= K + Ko - 2.5 \log_{10}\left(\frac{R-R_s}{T}\right) \qquad \text{III-8}$$

where Ko is a constant defined by the wedge used for the reading, and K is a constant for a certain telescope/spectracon/filter/emulsion/microdensitometer system. Hence, the absolute surface luminosity of a galaxy can be measured if the constant 'K' is calculated by observing previously calibrated stars under the same conditions as the galaxy (see next section).

The integrated magnitude of a galaxy within a specified area can also be calculated. If 'I' is the number of measurements in a scan within an area 'A', then

$$A = I\ (S.P)^2 \qquad \text{III-9}$$

where 'S' is the step length between measurements in the scan, and 'P' is the plate scale of the electronograph. The integrated magnitude within the area A can be defined

$$m = K+Ko-2.5 \log\left[\frac{1}{T}\sum_I (R-R_S).(S.P)^2\right] \qquad \text{III-10}$$

$$= K+Ko-2.5 \log\left[\frac{S^2P^2}{T}\sum_I (R-R_S)\right]$$

$$= K+Ko+K'-2.5 \log_{10}\left[\frac{1}{T}\sum_I (R-R_S)\right]$$

The term $\sum_I (R-R_S)\ (S.P)^2$ is the volume of density of an image on an electronograph. If this term is measured for a star of known magnitude (m) using the method described in section 2.3.3, then the constant 'K' can be calculated.

Equations III-8 and III-10 can be used to find the surface and integrated luminosities of a galaxy, but for accurate photometry, corrections have to be made which allow for the extinction of the atmosphere and which calibrate the colour sensitivity of the detecting system. When the luminosity of a galaxy is measured through B and V filters, then the instrumental magnitudes can be defined

$$b = -2.5 \log_{10} \frac{R_B - R_{B,S}}{T_B} \qquad \text{III-11}$$

$$v = -2.5 \log_{10} \frac{R_V - R_{V,S}}{T_V}$$

These magnitudes can be corrected for atmospheric extinction using the formulae (Hardie, 1962)

$$v_o = v + K_v \sec z \qquad \text{III-12}$$

$$(b-v)_o = (b-v).J - K_{bv} \sec z$$

where z is the angle from the zenith, and secant z represents the relative air mass through which the observations are made. These formulae transform the observed instrumental magnitudes b,v to the values $(b-v)_o$, v_o which correspond to the luminosities which would be observed outside the earth's atmosphere. J and K_{bv} are usually within 1% of 1 and 0 respectively, whilst K_v may typically be 0.15 magnitude per air mass

on a relatively clear night. Since most observations are made very near the zenith, these corrections are not made except for the most accurate photometry. The constants K_v, J, and K_{bv} may be found by observing calibrated stars at various positions in the sky. As these constants may vary during a night, they should be measured within a short time of the observations of a galaxy and should be nearby in the sky.

Although a particular combination of photocathode and filter may provide a good approximation to the standard defined by Johnson and Morgan (1953), it will in general differ. Therefore, two photometers may measure the same value of colour for one galaxy, but their measurements of the colour for another galaxy will probably differ. The results can be calibrated to a standard by transformation equations which include a colour index term. Specifically, (Hardie, 1962)

$$V = v_o + g\,(B-V) + h \qquad \text{III-13}$$

$$B-V = \mu\,(b-v)_o + \varepsilon$$

where g, h, μ, ε are co-efficients which can be determined empirically by solving the formulae above using stars of known V and B-V. In order to do this, only two stars with known magnitudes V_1, V_2 and colours $(B-V)_1$, $(B-V)_2$ need to be observed.

$$\mu = \frac{(B-V)_1 - (B-V)_2}{(b-v)_1 - (b-v)_2} \qquad \text{III-14}$$

$$\varepsilon = (B-V)_1 - \mu(b-v)_1$$

$$g = \frac{(V_2-V_1) - (v_2-v_1)}{(B-V)_1 - (B-V)_2}$$

$$h = V_2 - v_2 - g(B-V)_2$$

The calibration stars should have very different colours if the constants are to be calculated accurately, but the accuracy can be much improved if the constants are calculated from the observations of many stars. To facilitate this calibration, Priser (1974) has published maps and magnitudes of groups of stars which can be observed with convenient exposure times using image tubes.

When an S11 photocathode is used for the observations the colour corrections are normally less than 2% because this photocathode has a spectral response which is similar to that used to define the standard U,B,V system(Johnson & Morgan, 1953). Therefore, except for the most accurate photometry, equations III-14 above can be replaced by (e.g. Ables 1971; Beaver et al, 1974).

$$V = v + K_v \qquad \text{III-15}$$
$$B-V = b-v + \varepsilon$$
$$\therefore B = b+K_v+\varepsilon = b + K_B$$

The constants in these equations may be found from observations of only one standard star, though much greater accuracy is possible if several stars are observed.

An alternative method of calibrating the measurements of the luminosity of a galaxy is to make use of published photoelectric observations of the same object. Published values can be substituted in equations III-15 to determine the calibration constants.

This method simplifies the calibration, but the results are not as accurate because

(1) only one set of measurements is used so the accuracy is low

(2) no measurement is made of the characteristics of the atmospheric extinction, hence no corrections can be made for it

(3) If the published observations were inaccurate due to unknown errors then these errors will affect the calibration

3.4 Integrated Magnitudes

In electronography, each measurement of luminosity is made within a small, square-shaped aperture. In the previous section it was shown that, when the readings are summed within a large area, the integrated magnitude of a star or galaxy within that area can be calculated. If this large area is rectangular then the summation of readings is simple. However, photo-electric observations of the integrated magnitudes of galaxies are generally measured through circular apertures so, for comparisons, the readings from an electronograph should be summed over the same circular areas. When the distance between readings is small compared to the size of an aperture, then the summation of readings gives an accurate measurement of the integrated luminosity of a galaxy through that aperture. When the size of the aperture is reduced, the measurement of integrated magnitude becomes less accurate. A computer program (DIA - see Appendix D) was written by the author to simulate a measurement of

integrated luminosity within a circular aperture, and to calculate the errors involved. The results of this program are shown in figure 3.2.

An analysis shows that simulated integrated magnitudes within a circular aperture can be calculated to within 1% accuracy for apertures over 5 steps in diameter and centred on an object with a near gaussian luminosity distribution. This corresponds to a diameter of $0.5\hat{''}$ on a typical scan. Due to the effects of atmospheric seeing, the luminosity gradients of any object will be less than, or equal to, that of a stellar object of the same peak luminosity. When the luminosity gradients within the aperture are lower, then the electronograph must be scanned with a smaller step-length. In the limiting case when the luminosity gradient is constant and zero, then the smallest aperture within which the magnitude can be measured to an accuracy of 1%, is 25 steps in diameter (typically $2.5\hat{''}$). As most measures of a galaxy's integrated magnitude are made through apertures which are tens of arcseconds in diameter, this is clearly not a limitation. Therefore, measurements through many large and small sized apertures can be used to determine the luminosity profiles of galaxies with circular symmetry (see Chapter 4). The data in figure 3.2 can be used to define the smallest aperture which can be used for such studies.

A subroutine in the program MAP (see Appendix D) can be used to find the integrated magnitudes of galaxies within specified apertures using the summation method. It can also be used to find the integrated magnitude of a galaxy within a specified surface luminosity level.

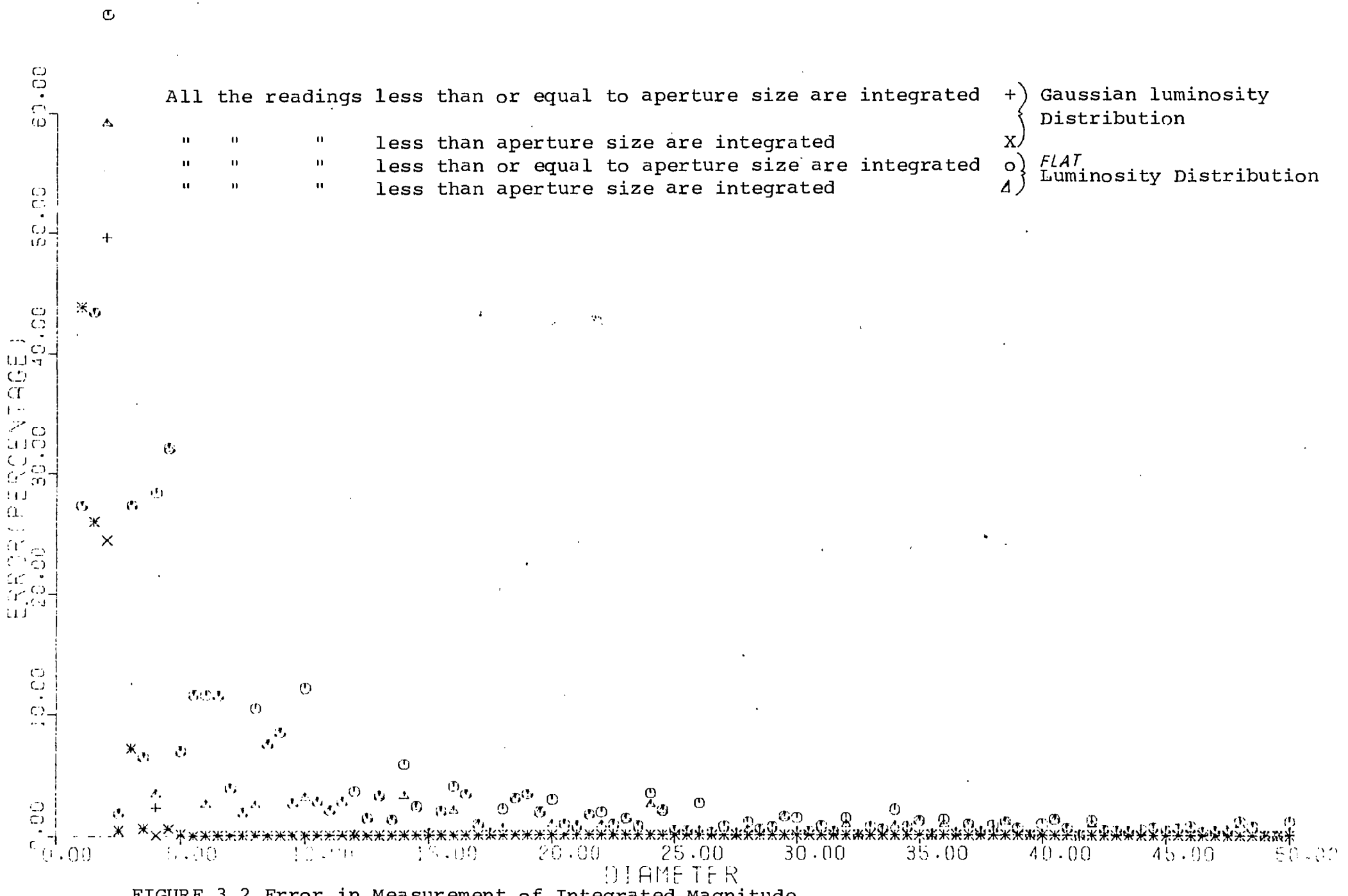

FIGURE 3.2 Error in Measurement of Integrated Magnitude

3.5 Morphological Studies

Equation III-8 showed that a microdensitometer reading of a density on an electronograph can be directly related to the surface luminosity of a galaxy at the point of measurement. As the morphology of a galaxy is studied by comparing the luminosity at various points over its surface, the technique of scanning electronographs provides a direct means for morphological studies. This gives electronography an advantage over photography where the readings have to be corrected for the non-linear exposure-density relationship which reduces the accuracy of the results (see Chapter 1).

By drawing contour levels through an array of readings, a contour map may be drawn from which a morphological study can be made. Contour maps of scans are drawn by the program MAP which blocks the data, as necessary, to reduce noise (see section 2.3.1) and displays the results on paper, microfilm, or on a graphics terminal. This program is run in batch mode because the whole scan, stored on magnetic tape, is used to produce the map. The contour levels which show the most information can be chosen from studies with the program SIMMAP (see section 3.2).

The program can also draw colour (B-V) maps if the scans of the B and V electronographs of a galaxy are made parallel to each other to the required accuracy (see section 2.3.2) and can be aligned. Substituting equations III-11 into III-15 gives

$$B-V = \mathcal{E} + 2.5 \log_{10}\left(\frac{T_B}{T_V}\,\frac{(R_V-R_V,s)}{(R_B-R_B,s)}\right) \qquad \text{III-16}$$

Morphological studies of the variations of the surface colour of a galaxy can be made without determining the constant $\mathcal{E}$. Hence, measurements of the luminosity (R_V and R_B) of a point on the galaxy can be directly related to the colour at that point; the only errors involved are those of the measurement and that due to a misalignment of the scans.

Contour maps are a convenient and simple way of displaying information for general morphological studies. However, contour maps do not display all the information available and detailed studies are difficult to make. Ideally, all the information should be displayed so that the eye can quickly assimilate it. The electronograph itself displays all the information in a reasonable form, but the human eye is not capable of accessing all the information that is available at high and low densities. Hence, a future study, using more sophisticated computing techniques, should attempt to display the information in greater detail than is possible with either contour maps or the grey scale of an electronograph. For example, coloured displays might be employed.

Profiles of a galaxy can be drawn using the program CROSS (see Appendix D) which operates in a similar manner to the program XSEC, but on the data contained in a large scan, stored on magnetic tape. The program can also be used to draw colour profiles, in which case equation III-16 is used to calculate the colour index (B-V) at each point on the profile. If the galaxy has a circularly symmetric luminosity distribution then a more accurate profile can be drawn by averaging the readings of all points at the same

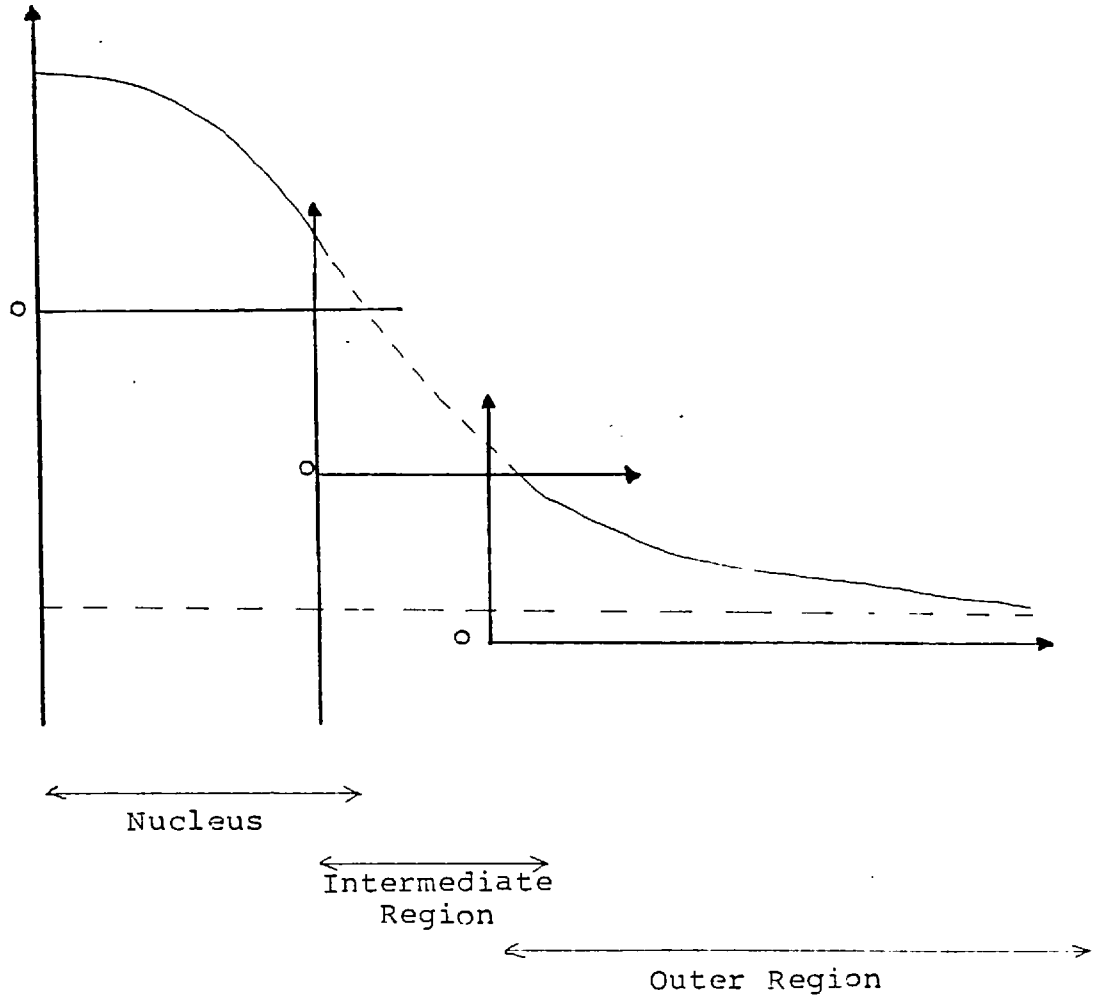

FIGURE 3.3. This figure shows how the profile of a galaxy can be formed using readings obtained from scans of the nucleus, intermediate region and outer region.

distance from the nucleus of the galaxy.

When several scans are made of a galaxy (e.g. one each of the nucleus, intermediate and outer regions), the scans of the central regions will not contain direct measurements of the sky background. In addition, each scan will probably have a different offset density (Ro - see equation III-4) so the calibration of these scans is not straight forward. However, if a luminosity profile is drawn using the readings from each scan, then it should be continuous (see figure 3.3). Hence, the offset density for each scan can be determined and the scans calibrated.

3.6. Photocathode and Mica Non-Uniformities

In the previous sections the analysis of data stored in electronographs was discussed and it was assumed that the R.Q.E. of electronography is uniform across an electronograph. However, variations in the sensitivity of the photocathode and the thickness of the mica window affect the R.Q.E. Hence, corrections must be made in order that the analysis described in the previous sections might be valid.

Variations in the R.Q.E. are caused by the following:

(1) Due to the manufacturing process, the sensitivity of a photocathode can vary slowly across its surface, by up to ±10%.

(2) Dead spots and scratches on the photocathode cause areas of null sensitivity.

(3) The mica window can have strips of its surface removed, which increases the

sensitivity in these areas.

(4) Dirt on the emulsion or mica reduces the sensitivity.

(5) Emulsion defects cause sensitivity variations (see section 1.4)

Most of these effects can be reduced by using only good, clean spectracons and emulsions for observations, but they can never totally be removed. Hence, they must be calibrated out of the results. The sensitivity of the system can be calibrated by taking an electronograph of a uniform light source; the density at each point on the electronograph will be proportional to the sensitivity at that point.

The sensitivity (ρ) at any point P can be given as a percentage of the maximum sensitivity by the equation:

$$\rho_P = \frac{R_p - Ro}{R_{max} - Ro} \times 100\% \qquad \text{III-17}$$

where Ro is the reading of zero (film) density, Rmax is the reading at maximum density on the calibration electronograph, and R_p is the reading at the point P.

If the reading from an electronograph of a galaxy at the point P is ${}_GR_p$ then the corrected reading, i.e. the reading which would have been measured at maximum sensitivity is

$${}_GR'_P = ({}_GR_P - {}_GR_O)\ \frac{100}{\rho_P} + {}_GR_O \qquad \text{III-18}$$

where ${}_GR_O$ is the zero (film) density on the electronograph

of the galaxy.

Walker (1970) showed that the variations in sensitivity can be corrected at all points on an electronograph by measuring the sensitivity at several points on the calibration electronograph and assuming that the sensitivity at other points can be calculated by linear interpolation between the measured points. This method works well when the distance between calibration measurements is small compared to the sensitivity variations. The accuracy can be improved by fitting a two-dimensional polynomial to the measured points (Chincarini et al, 1974). However, both of these methods give poor corrections when the sensitivity varies rapidly; for example, a step in sensitivity can occur where there is a change in thickness of the mica window.

A more general method is to scan the calibration electronograph and match each point on this scan to the corresponding point on the scan of an electronograph to be studied. The scans have to be matched in the same manner, and to the same accuracy, as that described in section 2.3.3. If the sensitivity varies slowly, the scan of the calibration electronograph can be made with a large aperture which will reduce emulsion noise. The programs MAP and CROSS (see Appendix D) correct the readings in a scan for sensitivity variations by using this method. The programs use equation III-18 to calculate the corrected reading. Worswick (1975) showed that, even when corrections for photocathode variations are made, the accuracy of the measurements will normally be worse than 2%.

Three spectracons (B275, AS3 and AS7, were

used to obtain the electronographs studied in this thesis. The variations in sensitivity due to these spectracons were derived from electronographs of a uniform light source and are discussed below.

3.6.1. Spectracon B275

This spectracon, which has an S11 type photocathode, was used at the Boyden Observatory on a 1.5 m. telescope which has a plate-scale of $8.80'' . mm^{-1}$. The effective field size was about 3.7° by 1.3°.

Maps and cross-sections of B275 are shown in figure 3.4. They show that there is a sensitivity variation of about $\pm$ 10% along the length of the photocathode. Calibration electronographs through different filters were not taken with this spectracon before it suffered an accident. Hence, any variations in the sensitivity of this spectracon with colour are not known, but may be assumed to be negligible. Experience with other spectracons (see below) shows that the differences in colour sensitivity are normally less than $\pm$ 2%.

The galaxy NGC 3521 (PKS 1103 + 02) was observed with this spectracon (see chapter 4). The area of the galaxy's image is larger than the field covered by the spectracon, so the studies of this galaxy are corrected for the sensitivity variations.

3.6.2. Spectracon AS3

This spectracon was used at the prime focus of the 2.5 m. Isaac Newton Telescope at Herstmonceux, and on the 1.1 m. telescope at Flagstaff,

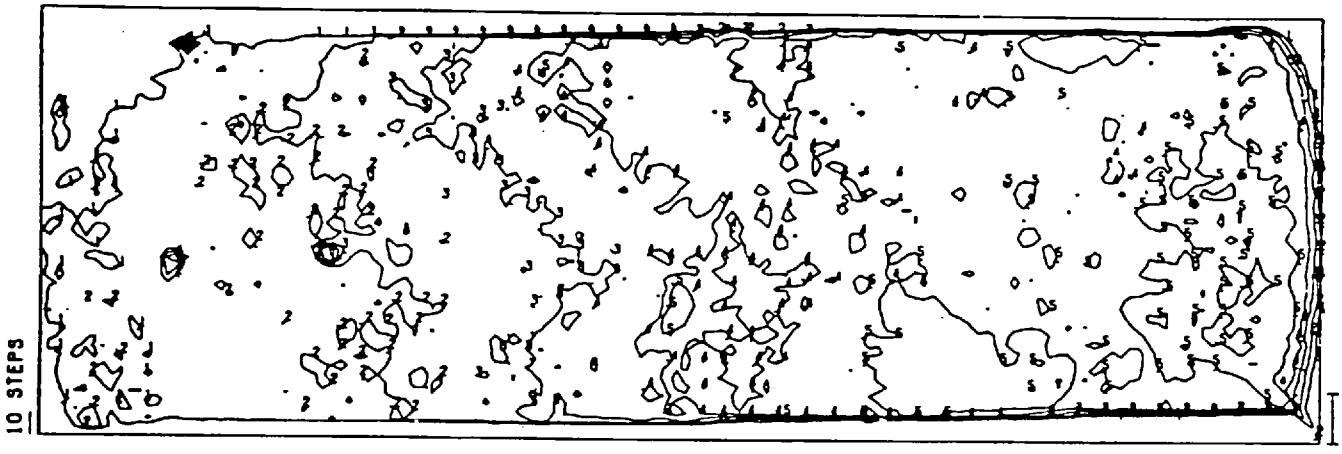

Interval between contour levels is 8% of sensitivity

FIGURE 3.4 SENSITIVITY VARIATIONS ON SPECTRACON B275

Arizona. It has a bi-alkali photocathode which has a response which is similar to that of an S11 photocathode. The plate-scales of the observations were $25.65\hat{''}.mm^{-1}$ and $24.1\hat{''}.mm^{-1}$ respectively, so the field size covered by the electronographs taken on these telescopes was about $4\hat{'}$ by $12\hat{'}$.

Maps and cross-sections of the sensitivity of this spectracon are shown in figure 3.5. The variations in sensitivity are much less than those of B275 and are less than $\pm 2\%$ in the central regions of the photocathode. Therefore, when an image of a galaxy appears wholly on this region, corrections for the variations in sensitivity will be small. The maps show that, outside the central region, the variations in sensitivity are larger. In particular, at the edge of the photocathode there is a difference in sensitivity with colour of about $\pm$ 10%. The approximate positions and sizes on the photocathode of the galaxies which are studied in this thesis are shown figure 3.6.

Electronographs of galaxies and some calibration tests which were taken with this spectracon show that some dust had accumulated on the spectracon windows during the observations at Flagstaff. Fortunately, the studies of galaxies in this thesis were not affected by this problem. This suggests that calibration tests of a spectracon should not only be taken of a uniform light source in the laboratory, but also in the operating position on the telescope.

3.6.3. Spectracon AS7

Only the galaxy 1ZW208 is studied in this

FIGURE 3.5 Maps of the Variations in Sensitivity due to Spectracon AS3

The interval between contour levels is approximately 9% of the total sensitivity.

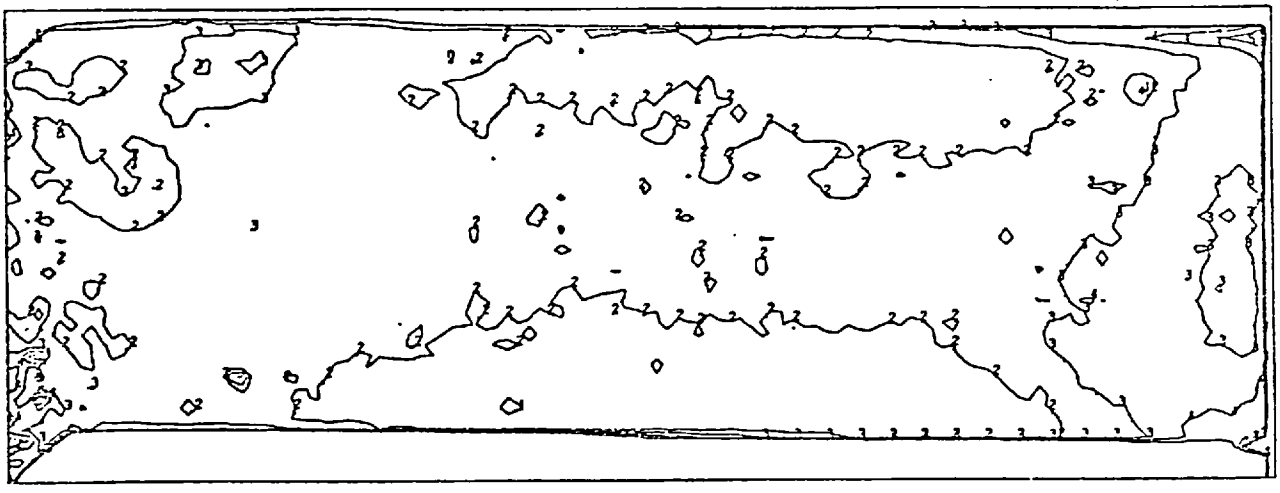

B Filter

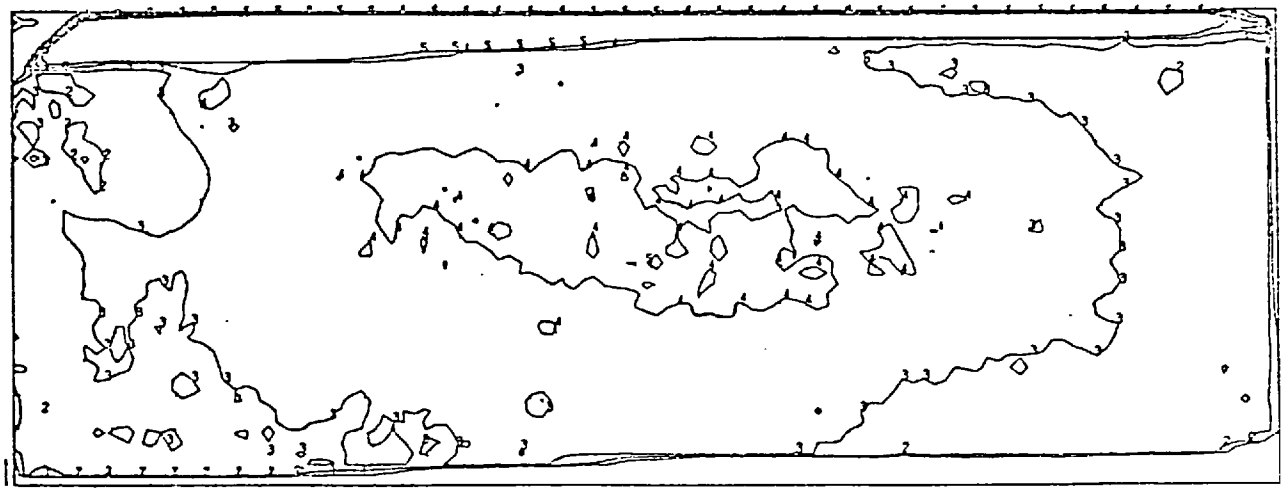

V Filter

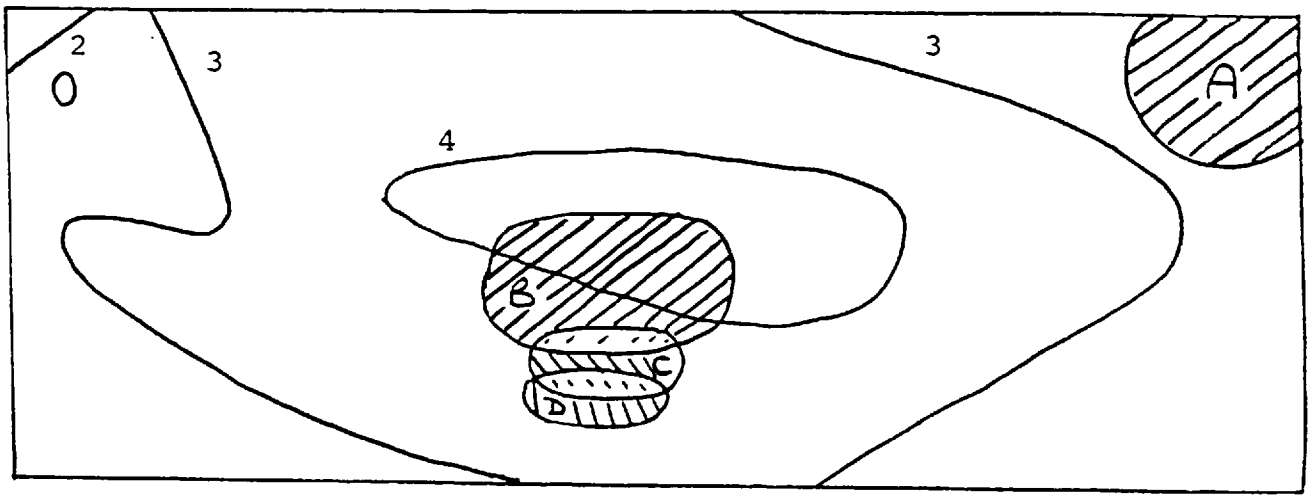

Region A - NGC 4881

Region B - 1ZW129, 1ZW165, 1ZW206, 1ZW86

Region C - 1ZW92

Region D - 1ZW41

Note: The contours are approximately those from figure 3.5, V filter.

FIGURE 3.6 POSITIONS OF GALAXIES ON THE FIELD COVERED BY AS3

thesis from observations made with this spectracon. The observations were made on the 1.8 m. telescope at Flagstaff, Arizona. Measurements of the stars in M15 show that this telescope has a plate-scale of $6.64''.mm^{-1}$. 1ZW208 covers an area of about 4 mm by 4 mm ($25''$ by $25''$) on the electronographs. The spectracon has an S-20 photocathode. Tests show that the variations in sensitivity due to this spectracon are less than $\pm$ 5% over the whole field. There are, however, two scratches on the photocathode. These appear on all electronographs and their effect on the study of 1ZW208 is discussed later (see section 5.2).

3.7. Noise Spikes and their Removal

Often there are measurements in a scan which give much higher readings than their neighbours which are normally caused by a speck of dirt on the emulsion. These erroneous measurements, or noise spikes, are easily distinguishable from stars by their size (they are much smaller than stars), large gradients and their rapid changes in gradient. Similar problems are caused by dead spots (areas of zero sensitivity) on the photocathode which cause large dips in the values of the readings in a scan. These erroneous readings can contribute to the errors in a measurement of a galaxy's luminosity so it is occasionally necessary to remove them.

The main characteristics of these noise spikes are their large gradients and rapid gradient changes. The maximum gradient and gradient change in a scan are normally found on the brightest star or in the nucleus of a galaxy (see Appendix C). Hence, noise spikes are found by measuring the gradient and change of

gradient at every point in a scan and comparing them with the maximum possible for that scan. If the measured gradient or gradient change is larger than the maximum possible then the point of measurement must be artificially affected by a noise spike and can be corrected by reducing it to a level consistent with its neighbours (see figure 3.7).

A computer program was written and developed by the author to search for, and remove, noise spikes by this technique. The program is not intended to reduce or affect normal emulsion noise which might introduce large gradients or rapid changes in gradient. Hence, the program only finds those noise spikes which are more than three standard deviations above the noise level. The program can run automatically and remove all noise spikes in a scan, but it can also be used interactively. In interactive mode the program displays on a graphics terminal each noise spike and the proposed correction. The operator can permit or disallow the correction to be made. At present, the program only looks for spikes which are smaller than the seeing diameter, but more sophisticated programs are being considered.

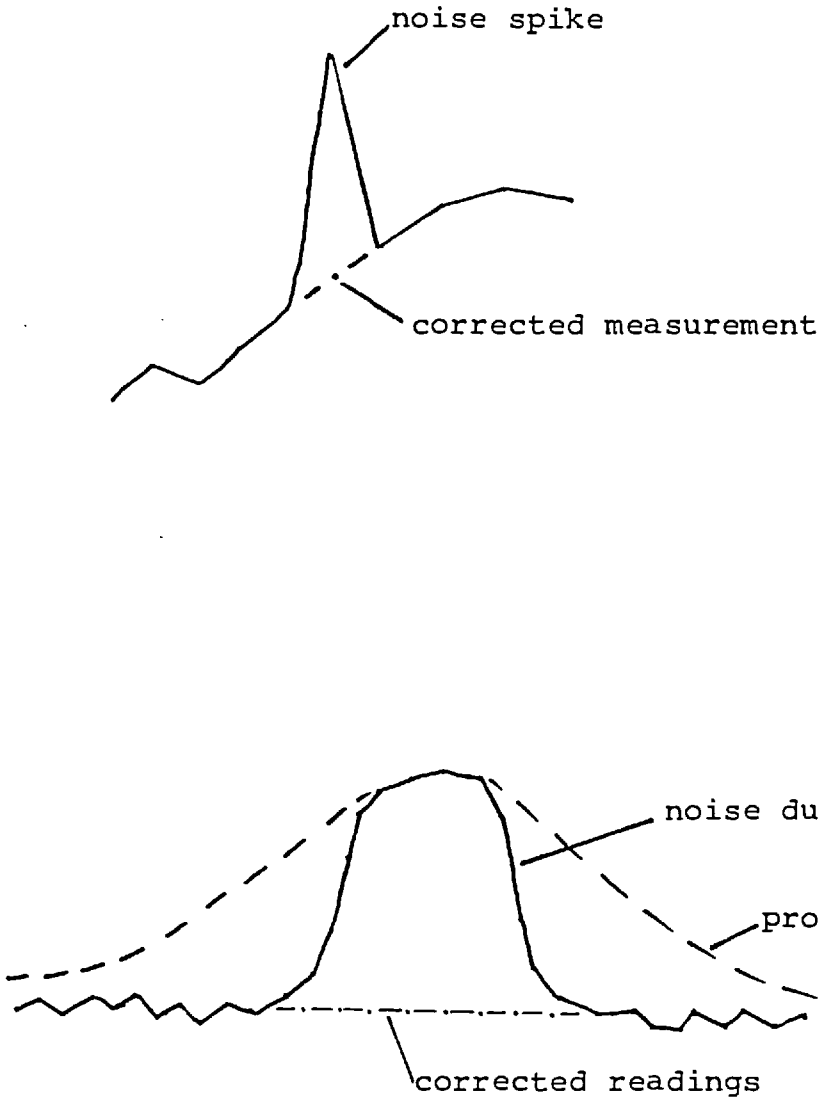

FIGURE 3.7 THE CORRECTION OF NOISE SPIKES

CHAPTER 4

A STUDY OF GALAXIES WITH COMPACT NUCLEI

Zwicky (1971) has measured some photometric parameters of many compact galaxies. However, due to their wide range of surface luminosities and luminosity gradients (see section 1.1), it is difficult to study the morphology of these galaxies with techniques other than electronography. Sargent (1970), Kormendy (1977) and Fairall (1978) showed that some galaxies which are called "compact" are ellipticals, and some are SO galaxies. Sargent (1970) also showed that compact galaxies have a variety of spectral types which indicates that they are not all in the same evolutionary phase. A study of the morphology of galaxies which have been termed "compact" may help to determine their properties and might indicate their relationship with other galaxies. This chapter, and the next, present a study of galaxies with compact nuclei or compact parts. The galaxy NGC4881 is also studied because it has not been termed compact and it has previously been observed in detail, allowing a comparison to be made between this study and previous work.

The compact galaxies observed were chosen for their apparent brightness (generally m_p is greater than 15), convenient observing position in the sky, for being easy to find, and for their compactness. The sample is not large, or statistically representative, but there should be enough information to indicate some parameters of compact galaxies. The telescopes used

for the observations are listed in table 4.1. In sections 3.7 and 4.2 a summary of the photocathode sensitivities and the calibration procedure for these studies are given, respectively.

Where possible, luminosity profiles and some photometric parameters are measured for each galaxy. Apparent recession velocities are given for each galaxy, corrected to the centre of our galaxy. Absolute magnitudes and distances are calculated, assuming the Hubble constant is 50 $km.sec^{-1}. Mpc^{-1}$. In order to compare compact galaxies with other galaxies, and to determine whether they actually are compact, a definition of compactness must first be made.

4.1. Compactness of a Galaxy

Logically, a galaxy which is termed "compact" should have a higher surface luminosity over the compact area than other galaxies at the same distance. Zwicky (1966) searched for compact galaxies by studying galaxies which are at a distance where their nuclei are near stellar in size. Those galaxies which he found to have an average surface brightness greater than 20 $mag.arcsec^{-2}$ were termed compact. By varying the constraints slightly, a study can determine whether a galaxy is compact, very compact or extremely compact. Zwicky's measurements were mostly qualitative so, whilst the technique is fairly successful in finding compact galaxies, quantitative comparisons between galaxies can not be made. The compact galaxies described in this thesis were all defined as such by Zwicky (1971).

TABLE 4.1 TELESCOPES USED FOR OBSERVATIONS

Telescope	Aperture	Focus	F number	Plate Scale
Isaac Newton Herstmonceux G.B.	2.5 m	Prime	f/3.3	$25.65''.mm^{-1}$
Rockefeller Reflector Boyden Observatory S.A.	1.5 m	Cassegrain	f/16	$8.80''.mm^{-1}$
Flagstaff U.S.A.	1.1 m	Cassegrain	f/8	$24.1''.mm^{-1}$
Perkins Telescope Flagstaff U.S.A.	1.8 m	Cassegrain	f/18	$6.64''.mm^{-1}$

Weedman (1976) accurately compared the luminosity of the nuclei (the compact part) of galaxies by measuring the integrated luminosity from the central 4.2 kpc (diameter) of each galaxy. This technique was sufficiently accurate for Weedman to show that there is a correlation between nuclear magnitudes and redshifts of galaxies. However, it gives little information about the compactness of the nucleus because the size of the area over which the galaxy has a high luminosity is not measured, i.e. a compact galaxy which has a high surface brightness over a region 1 kpc in diameter could appear, when measured by Weedman's technique, to have a nuclear luminosity which is the same as that of a less compact galaxy with a lower surface luminosity spread over 4.2 kpc.

Neither Zwicky's (1971) nor Weedman's (1976) techniques can be used to accurately compare galaxies that have been termed compact under the definition at the beginning of this section. Kormendy (1977) tried to compare compact galaxies with other galaxies by comparing maximum luminosity and average luminosity over the whole of each galaxy, but neither of these quantities takes into account the size of the area over which a galaxy has a high luminosity. Thus, in order to make possible quantitative comparisons between galaxies, the author has made the following definitions:

(1) The radius of compactness (r_c) is the distance in parsecs from maximum luminosity at which the gradient of the integrated luminosity - radius curve is equal to 1 magnitude per kiloparsec. This gradient was found to be an optimum after studying

many integrated madnitude - radius (see sections later in this chapter) curves because it is generally at a radius which is

(a) beyond the high luminosity gradients of the nucleus where a small change in position causes a large change in the measured surface luminosity,
and

(b) within the outer regions of a galaxy where the luminosity is low and difficult to measure except with long, time-consuming exposures.

(2) The compactness of a galaxy is indicated by the average surface luminosity within the radius of compactness of the galaxy.

(3) The average surface luminosity within the radius of compactness is given by:

$$\overline{m_c} = M_c + 2.5 \log (\pi r_c^2) \qquad \text{IV-1}$$

where M_c is the integrated magnitude within the radius of compactness, as measured through a V filter. This filter was chosen to define a wavelength range for measurements of compactness because galaxies normally appear most luminous in this wavelength range.

(4) In order to compare the compactness of galaxies at different distances, the compactness of a galaxy must be defined at a standard distance. This distance is usually taken as 10 pc. The difference in magnitude between a galaxy at distance R and another at 10 pc is defined as the distance modulus K, where:

$$K = -5 \log \frac{R}{10}$$

$$K = -25 - 5 \log \frac{V}{H} \qquad \text{IV-2}$$

where R is the distance of the galaxy in parsecs, V is its recession velocity and H is Hubble's constant.

(5) The compactness (C) of a galaxy can now be defined as the average surface luminosity within the radius of compactness at a distance of 10 pc. Thus

$$C = K + \overline{m}_c$$

$$= K + 2.5 \log (\pi r_c^2) + M_c \qquad \text{IV-3}$$

When galaxies are at a distance where the angular diameter of the galaxy is comparable to the "seeing" in an observation, the galaxy will appear less compact. In sections 4.4 to 4.7 the observations of some compact galaxies are discussed and the results are summarised in section 4.9.

4.2. Calibration of Electronographs

The observations of galaxies at Flagstaff, Arizona, were calibrated by taking observations of stars with photoelectrically measured luminosities. For each set of observations of a galaxy, exposures were made through B and V filters of the stars numbered 30 and 44 in the field SA61 (Baum,1976, see fig. 4.1). These stars were chosen because they both lie conveniently within the field of the spectracon and they have different colour indices which facilitates

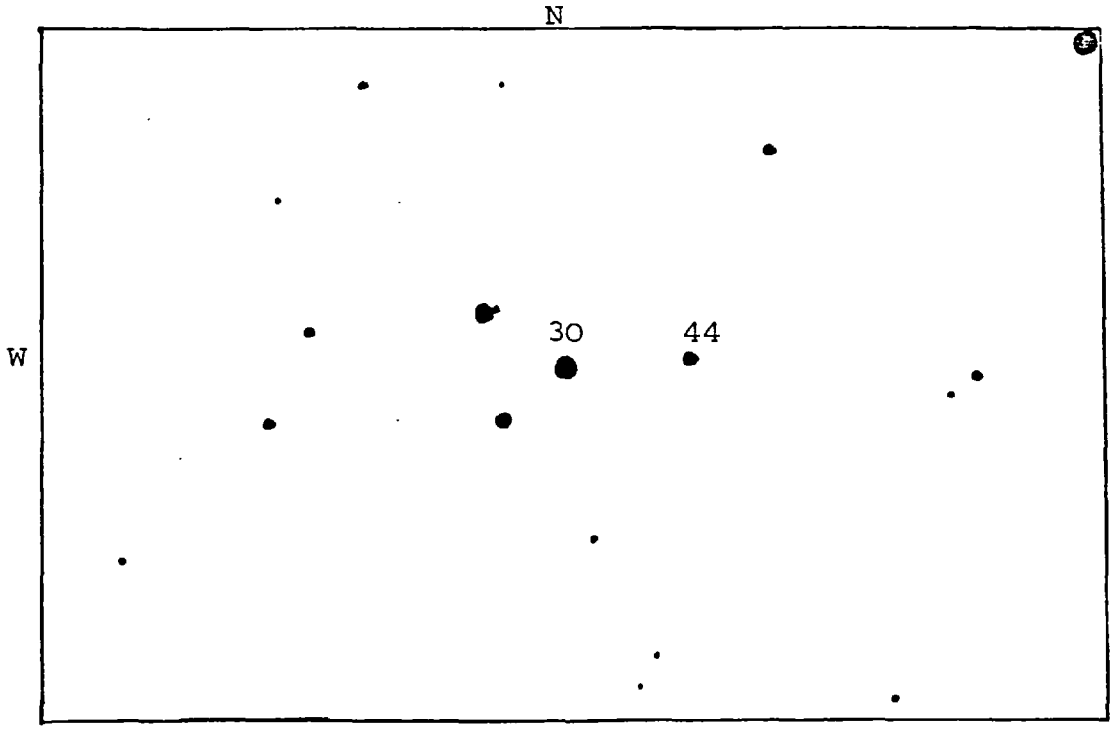

R.A. (1950) 17-00-46

Dec. (1950) +29-53.3

FIGURE 4.1 THE FIELD CONTAINING STARS 30 AND 44 OF SA61

	V	B-V
Star 30	11.39	1.13
Star 44	12.58	0.69

the calibration. The accuracy of the calibration would have been greater if more stars had been observed but this was not necessary because other problems (described below) reduced the accuracy to a greater extent. The technique described in section 3.3 was used to make the observations and the calibration.

The stars required exposures of only 10 seconds. This led to large errors (about $\pm$ 5%, see below) in the timing of exposures because the camera shutter was operated manually. Also, the exposures were too short for the sky background to show on the electronograph so the positions of the star images on the photocathode are not known. Hence, the sensitivity of the photocathode at the position of the star image can not be found and corrections for sensitivity variations can not be made. Measurements of absolute luminosities are therefore not as accurate as they might have been, but studies of the morphology or variations in colour of an object are not affected.

The lesson learnt from this is that, for greater accuracy, calibration exposures on this size of telescope should be made with either:

(1) fainter (about 15 mag.) stars, or
(2) stars of the same brightness, but the exposures should be trailed, as described in section 2.3.

Either of these methods will allow longer, more accurately timed, exposures which will show the sky background and therefore the position of the stars on the photocathode.

The instrumental magnitudes of the stars were found using the technique of Newell and O'Neill (1974) which was described in section 2.3.3. Table 4.2 lists the results obtained from each electronograph in the calibration. A description of the exposure and of the scan of the stars is given in column 1. The instrumental magnitudes of the stars were measured from each exposure and the results listed in columns 2 to 5. The analysis in section 3.3 showed that these instrumental magnitudes depend on the parameters of the scan and the exposure of the electronograph. Therefore, each magnitude in columns 2 to 5 has been corrected to appear as that from a scan with wedge F and a 20 μm step-length on a 1 second exposure. The parameters change for each set of scans according to the state of the microdensitometer. For instance, if the previous scan was of a galaxy using the D wedge and 20 μm step-length, then the stars were also scanned with these parameters. This reduced the setting-up time before the scan of the stars, but did not reduce the accuracy of the results because checks were made that the parameters gave the required accuracy. The results in rows 6 and 7 are repeat measurements of the results in rows 1 and 4, respectively. However, a new potentionmeter in the microdensitometer introduced an extra factor into these results (see notes in table 4.2).

The results in columns 2 to 5 are each affected by:

(1) an error in the measurement of the exposure time

	DESCRIPTION	v_{30}	v_{44}	b_{30}	b_{44}	$v_{44}-v_{30}$	$b_{44}-b_{30}$	$(b-v)_{30}$	$(b-v)_{44}$	$(b-v)_{30}-(b-v)_{44}$	NOTES
	SA61	11.39	12.58	12.52	13.27	1.19	0.75	1.13	0.69	0.44	
1	F14, B=15, V=8 Wedge F, 20 um	-9.75	-8.57	-8.63	-7.87	1.18	0.76	1.13	0.70	0.43	
2	F130, B=15, V=8 Wedge F, 10 um	-9.91	-8.71	-8.66	-7.88	1.20	0.78	1.25	0.83	0.42	
3	F115, B=20, V=8 Wedge D, 20 um	-9.71	*	-8.60	-7.78	*	0.87	1.11	*	*	v_{44} spoiled by emulsion defect
4	F111, B=16, V=8 Wedge J, 10 um	-9.87	-8.66	-8.84	-8.02	1.20	0.81	1.01	0.63	0.39	
5	F128 B=60, V=30 Wedge D, 10 um	-7.72	-6.63	-6.63	-5.95	1.09	0.68	1.09	0.68	0.41	L4 emulsion. These results indicate that G5 blackens 6.8 times faster than L4 emulsion.
6	F114, B=15, V=8 Wedge F, 10 um	-9.78	-8.59	-8.74	-7.95	1.19	0.79	1.03	0.63	0.40	Ratio of row 6 to row 1=1.05 $\pm$ 0.02
7	F111, B=16, V=8 Wedge F, 10 um	-10.05	-8.85	-8.97	-8.17	1.20	0.81	1.08	0.69	0.39	Ratio of row 7:row 4=1.17$\pm$0.02
	Average of rows 1 to 4	-9.83	-8.66	-8.73	-7.93	1.17	0.80	1.10	0.73	0.37	

TABLE 4.2 THE CALIBRATION MEASUREMENTS

(2) an error in the integration of the density volume of the star

(3) the system efficiency over the area covered by the star image, which is not known

A comparison of the results in rows 6, and also rows 4 and 7, shows that (2) is between $\pm$ 1% and $\pm$ 2%, as expected. The system efficiency at the position of star "30", through a V filter, is termed $\beta_{30,V}$. The efficiencies $\beta_{30,B}$; $\beta_{44,V}$; $\beta_{44,B}$ are similarly defined. These values will be different for each set of exposures.

Column 6 records the difference in V luminosities of the two stars, as measured from each V electronograph. The difference in B luminosities is recorded in column 7. These results are not affected by an error in the exposure time because the measurements of each star are from the same exposure. However, the position of an image on the photocathode changes from one pair of electronographs to another. Hence, the sensitivity at a star image, and the ratio of the sensitivities at the two star images ($\beta_{30,V}/\beta_{44,V}$ and $\beta_{30,B}/\beta_{44,B}$) will change. The variation in the results, due to this change, can be predicted from the studies of spectracon AS3 in section 3.6.2 as about $\pm$ 3% and $\pm$ 4% for the V and B electronographs, respectively. The results in table 4.2 indicate that the variations are $\pm$ 4% and $\pm$ 7%, respectively. However, the results from L4 emulsion appear especially low, probably due to an emulsion defect (see section 1.4). When the L4 results are

ignored, the variations are $\pm$ 1% and $\pm$ 4%, respectively, which are comparable to those predicted. The variation in the difference of V luminosities seems especially low when it is considered that the measurements are only accurate to $\pm$ 2%. This is probably due to the small number of measurements involved.

Since the B and V exposures were taken consecutively, the star images appear on the same point of the photocathode for each pair of exposures. Hence, the colours (b-v) given in columns 8 and 9 are affected by an error in the exposure time, and the ratio of the sensitivities for the B and V exposures at each star image ($\beta_{30,B}/\beta_{30,V}$ and $\beta_{44,B}/\beta_{44,V}$) will change from one set of exposures to another. The studies of this spectracon in section 3.6.2 showed that the variation in the difference of sensitivities would be less than $\pm$ 2% for each star. The standard deviation of the results in columns 8 and 9 is about $\pm$ 7%. Thus the exposure time must have been accurate to about $\pm$ 5%.

For each pair of electronographs, the results in columns 8 and 9 are affected by the same timing error. The ratios of columns 8 and 9, listed in column 10, are therefore independent of exposure time. The variation in the results in column 10 is due to

(1) the error in the integration of the density volume of each star image (see above), and

(2) a change in the ratio of the B and V sensitivities ($\beta_{30,B}\,\beta_{44,V}/\beta_{30,V}\,\beta_{44,B}$) from one point to another.

The measured variation is $\pm$ 2%, which is comparable to

the error introduced by the volume integration alone. Therefore, the change in the ratio of B and V sensitivities, over the region covered by the stars, must be less than $\pm$ 1%. The discrepancy between the average colour difference of column 10 and the true colour difference of the stars is probably caused by this spectracon having a slightly different photometric response from the system used to define the U, B and V standards (Johnson and Morgan, 1953). A comparison of the response of this spectracon with the response of the system used by Johnson and Morgan showed that the discrepancy is largely due to this factor.

The total error in a reading is about $\pm$ 8% (by propogation of the errors given above), so it is not possible to study the effects of any changes in emulsion sensitivity, or in the extinction of the sky, because these would have a much smaller effect.

By averaging the instrumental magnitudes of each star and applying equations III-19 and III-21, the calibration constants can be calculated, viz.

$$k'_V = V-v = 21.1 \pm 0.1 \text{ magnitudes} \qquad \text{IV-4}$$

$$k'_B = B-b = 21.1 \pm 0.1 \text{ magnitudes}$$

Hence, the colour index of an object can be calculated:

$$B-V = (b-v) + k'_B - k'_V \qquad \text{IV-5}$$

$$= (b-v) \pm 0.13 \text{ magnitudes}$$

The constants k'_V and k'_B will be used to find absolute integrated magnitudes of the studies in chapters 4 and 5 using equation III-8. However, several scans of one object may be made with different

step-lengths. From equation III-8, it can be shown that each scan would need a different calibration constant. Therefore, it is preferred to transform the constants k'_V and k'_B to the constants k_V and k_B and to use these with equation III-6. This permits the surface luminosity of an object to be compared from scan to scan without changing constants. When integrated magnitudes are calculated a correction for step-length plate-scale can then be made.

Comparing equations III-6 and III-8 shows that

$$k_V = k'_V + 2.5 \log_{10} (\text{STEP} \times \text{PLATE-SCALE})^2$$
$$= 21.1 \pm 0.1 - 1.62 \pm 0.01 \qquad \text{IV-7}$$
$$= 19.5 \pm 0.1$$

Similarly $k_B = 19.5 \pm 0.1$

The errors in k_V and k_B are directly related to the errors in the measurements of k'_V and k'_B because the errors in the STEP and PLATE-SCALE are only about 1% i.e. much smaller.

4.3 NGC 4881

NGC 4881 is a galaxy in the Coma cluster which Rood and Baum (1967) classified as E0 while de Vaucouleurs (1971), from inspection of a well exposed 200 inch telescope plate, classified it as an S0. Ables and Ables (1972a), from studies of the profile of the galaxy, suggest that this galaxy is most likely to be a lenticular S0. The classification of the galaxy is difficult as it is of small apparent diameter, about one minute of arc at 25 magnitude per arcsec^2. A summary of its elements is given in table

4.3 (Source: de Vaucouleurs and de Vaucouleurs, (1964). A finding chart has been published by Rood and Baum (1967).

Table 4.3 Elements of NGC 4881	
R.A (1950)	12h. 57.5 m
Dec. (1950)	+ 28° 31'
Magnitude (m_{pg})	14.5
Type	EO/SO ?
Dimensions	$60^{\hat{n}}$ x $60^{\hat{n}}$
Corrected Apparent Radial Velocity	6705 km.sec^{-1}

This galaxy has been studied by several authors using various techniques. Ables et al (1972a) have compared these results and shown that the photographic photometry of Rood and Baum (1967) is in error. A comparison will be made of the profiles of NGC 4881 as found by Ables et al (1972a) and the present study.

4.3.1 Observations

The electronographs used for this study are listed in table 4.4. The observations were especially affected by atmospheric extinction because the galaxy was three hours from the zenith when it was observed. The amount of extinction could not be reliably measured at this position. The accuracy of the absolute photometry is therefore reduced, but a comparison of this study with previous studies is still possible and of interest.

FIGURE 4.2 ELECTRONOGRAPH OF NGC 4881 MAGNIFIED APPROXIMATELY 6.3x

Table 4.4 Electronographs of NGC 4881

Date	Telescope	Plate-Scale	Emulsion
12 June 1975	1.1 metre Flagstaff	$24.1\text{Å}.\text{mm}^{-1}$	G5

Spectracon

AS3

Electronograph	Exposure	Filter
F111a	45 min.	B
F111b	34 min.57s	V

The image of NGC4881 fell on a corner of the photocathode so parts of the galaxy do not appear on the electronograph (see figure 4.2). However, there is enough information for a partial study to be made. An optical density of 3 was reached on the electronograph F111b at the nucleus. This density is on the non-linear part of the density-exposure curve of the emulsion used for the exposure (G5 emulsion, see section 1.4). Therefore, small corrections had to be made in the data analysis to correct for this.

4.3.2 Morphological Studies

The main results which were obtained from handscans of the electronographs using the micro-densitometer are listed in table 4.5. With this information, it was decided that a scan of the galaxy on each electronograph should be made with a step length and aperture size of 10 μm. Contour maps of these scans are shown in figure 4.3, the scans are

Table 4.5 Principal Elements of Handscans of NGC4881

seeing (S) = 4.5″ = 180 μm

Electronograph	F111a	F111b
Z	0.3	0.3
Dm	2.0	2.7
G	0.013	0.013
R	1.5	2.0
Gs	0.016	0.016
a_T	20	10
a_e	80	80
Δ	3	4

FIGURE 4.3 ISOPHOTE MAPS OF NGC 4881

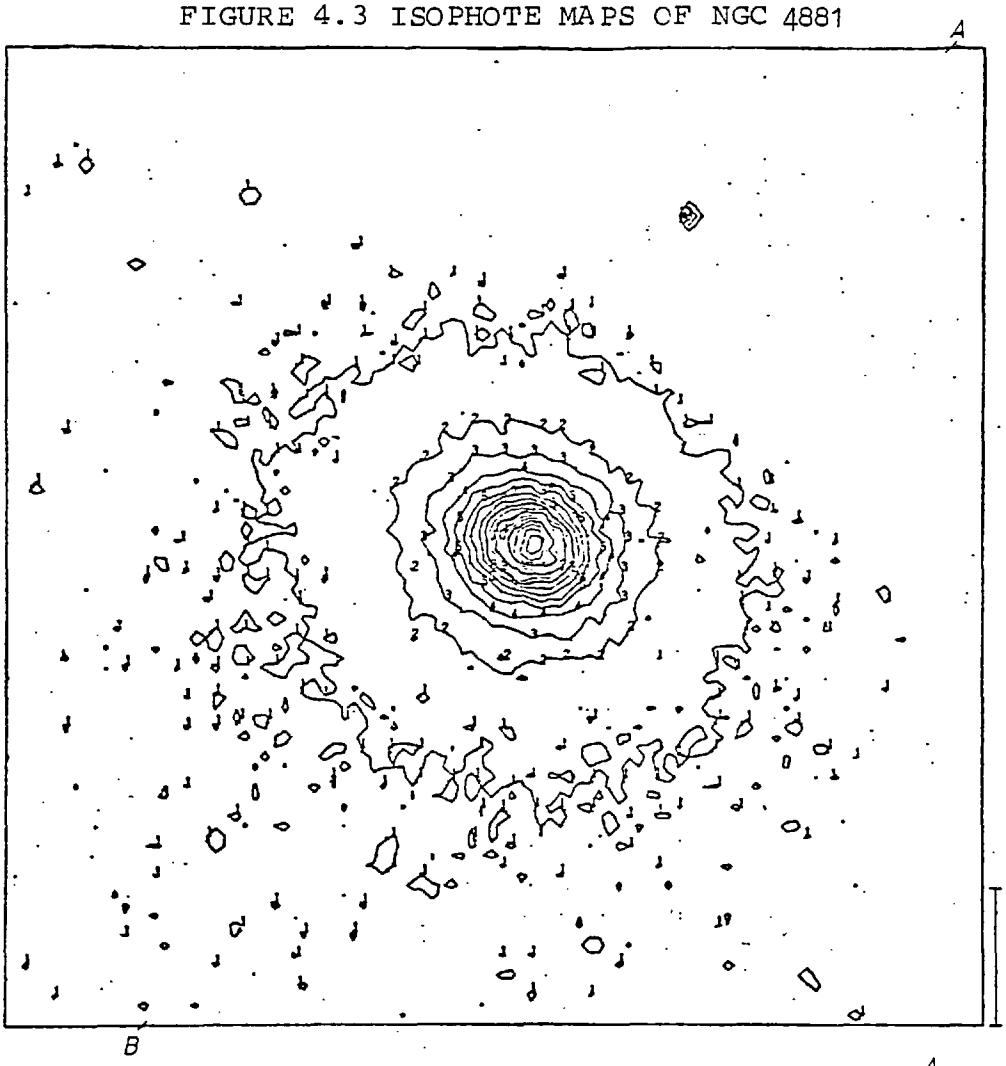

Electrono-
graph F111b
Filter V

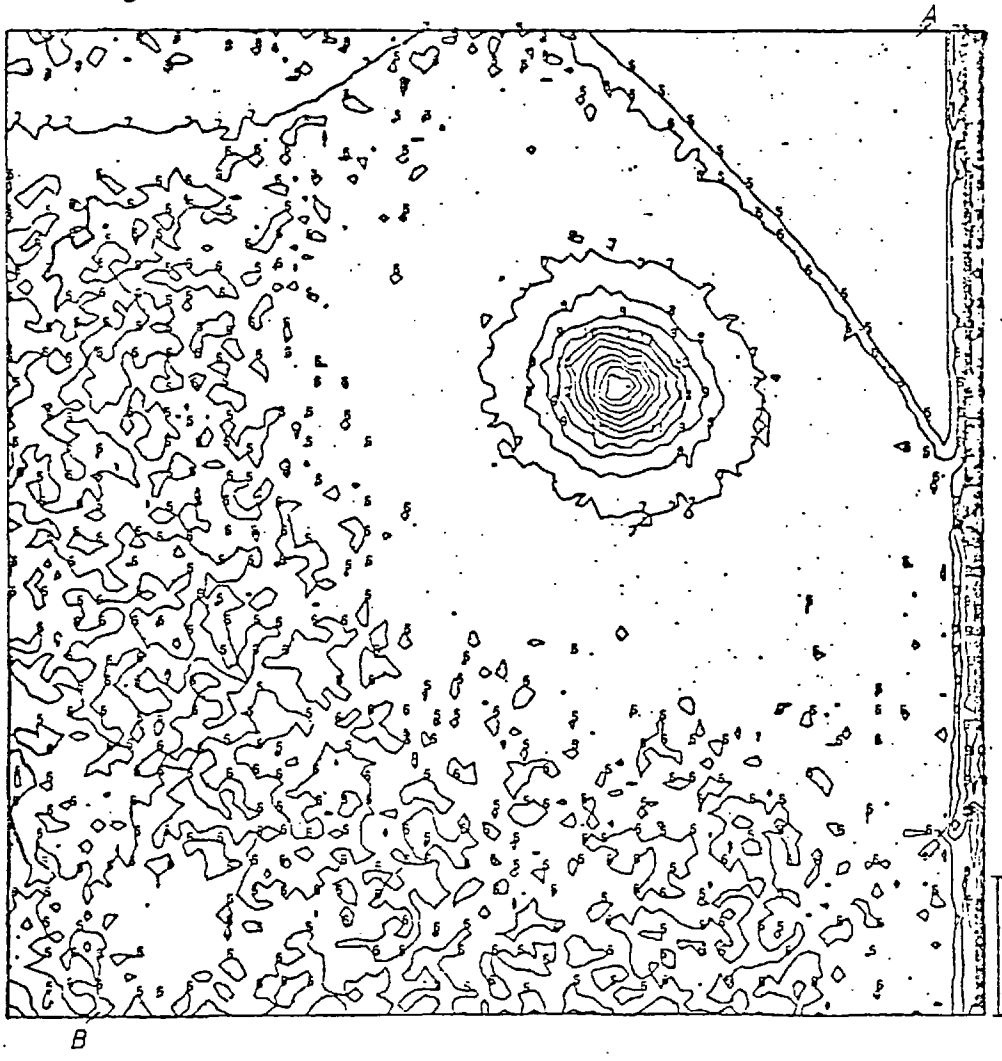

Electrono-
graph F111a
Filter B

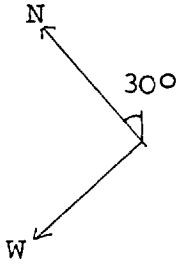

blocked to an analysing aperture size of 30 μm to reduce the effects of emulsion noise. (The contour levels are set at equal intervals). The edges of the photocathode are clearly shown in the scan of the B exposure, but they are not seen in the scan of the V exposure because of the choice of contour heights. The centre of the galaxy comes within 15$\hat{''}$ (0.6 mm) of the edge and only the bottom left hand quadrant of the galaxy is not near, and therefore unaffected by the photocathode edge.

Cross-sections along the lines A-B for each colour have been drawn for the galaxy (see figure 4.4). These confirm that there is less than $\pm$ 2% photocathode sensitivity variation in the bottom left hand quadrant of the scan (see section 3.7). The galaxy can be detected to a radius of 25$\hat{''}$ from these scans at 24 magnitude arcsec^{-2}.

4.3.3 Photometric Studies

As this galaxy has circular symmetry, Ables and Ables (1972a) averaged all their measurements of the luminosity at each radius to produce an accurate luminosity profile. This method gives a much more accurate profile of the galaxy than that found from a simple cross-section.

This method can not be used to its full advantage in this study as three quadrants of the galaxy are affected by the edge of the photocathode. However, the lower left hand quadrant of the galaxy appears on a region of uniform, to within $\pm$ 2%, photocathode sensitivity (see section 3.7). Therefore,

FIGURE 4.4 CROSS-SECTIONS THROUGH NGC4881
AT POSITION ANGLE 75° (NE TO SW)

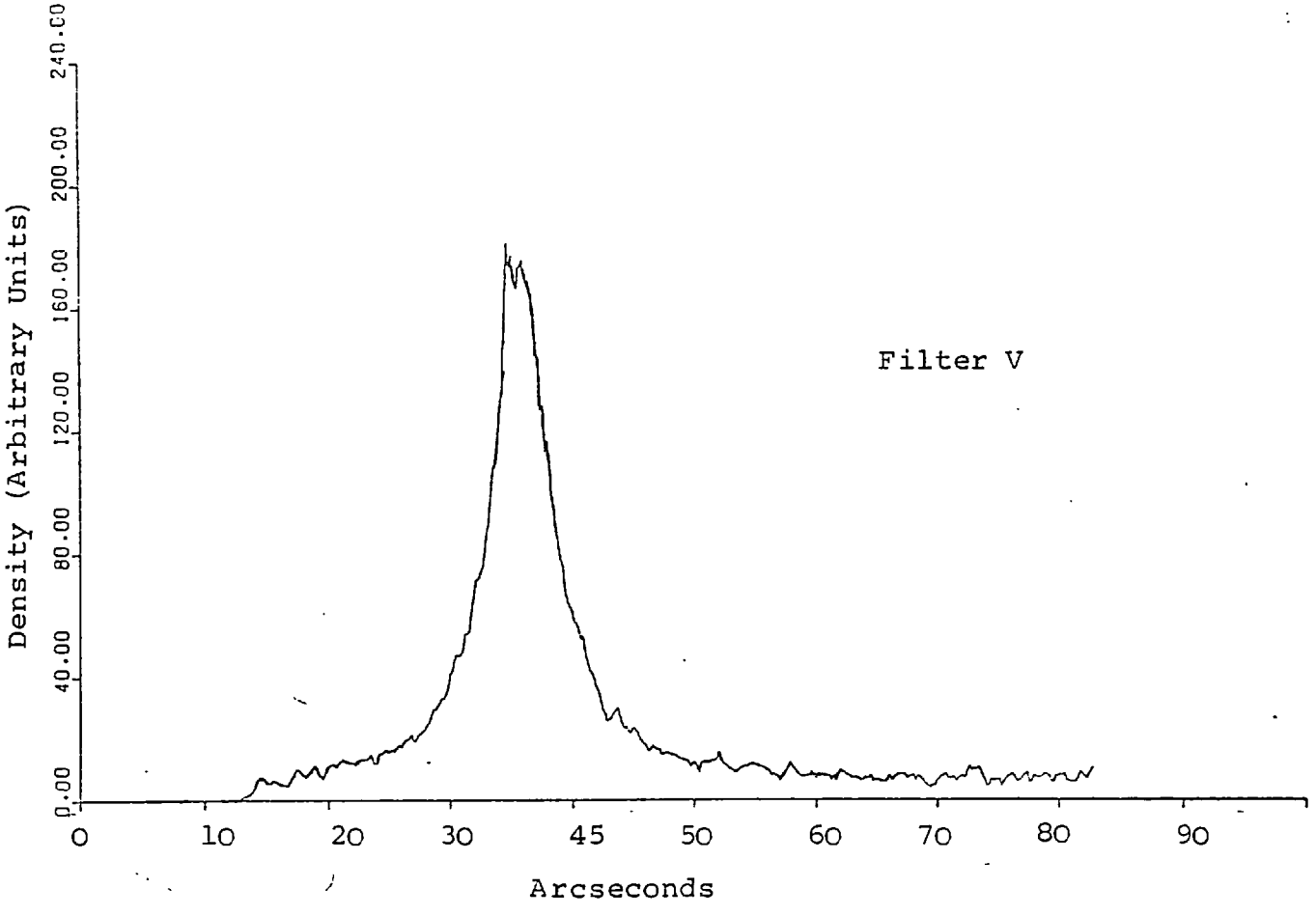

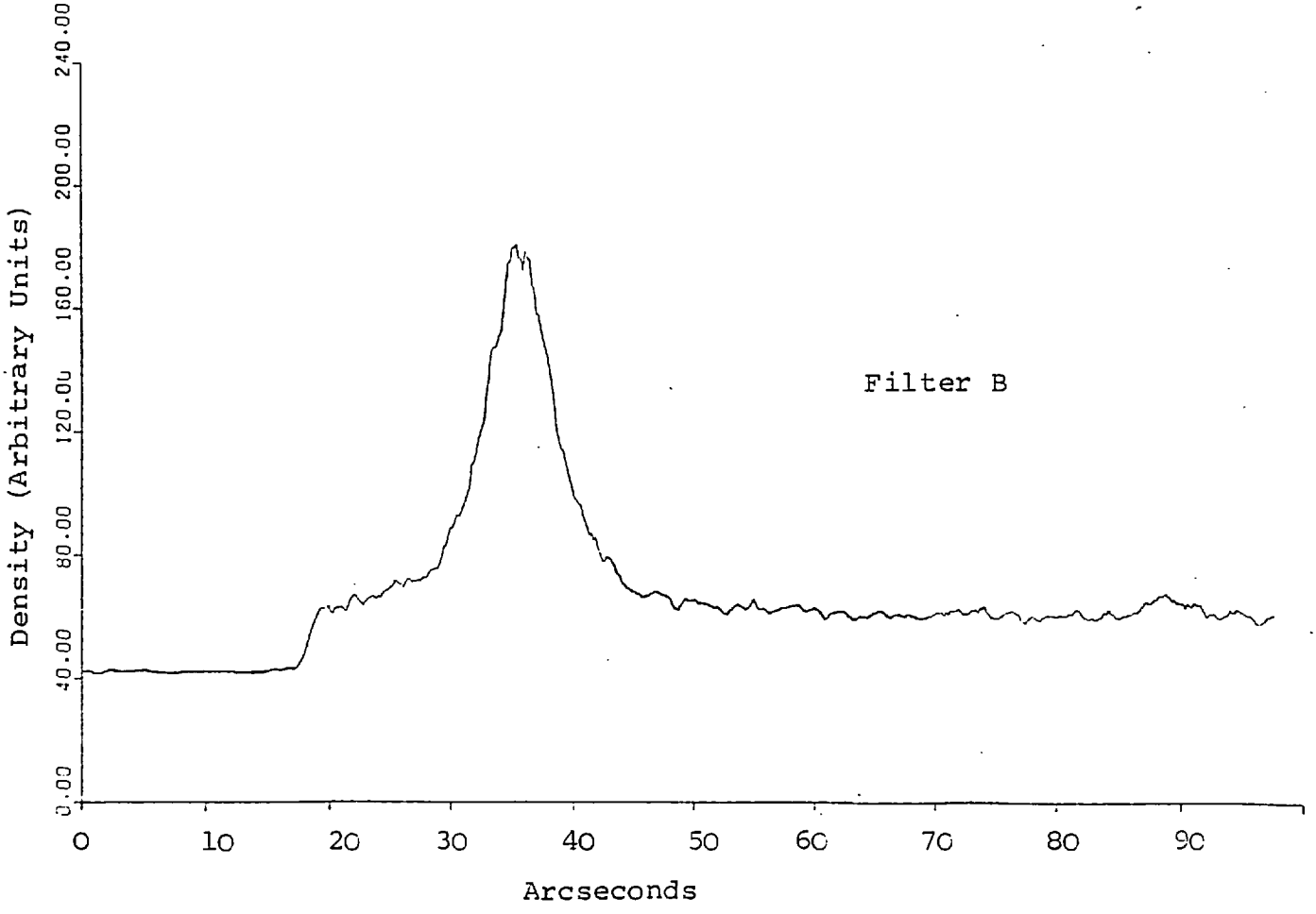

the above method can be applied in part to the measures of luminosity in this region in order to find the luminosity profile of the galaxy. As only one quarter of the galaxy image is used, the noise in the data is increased to a level that would have been obtained from data on a whole image which had been exposed for a half of the time, i.e. about 18 mins. for the V filter and 22.4 minutes for the B filter. The profiles found with this procedure are shown in figure 4.5 and were calibrated using the results in section 4.2. The constants used for the calibration were corrected in order to allow for the wedge which was used for scanning the electronographs and for the different photocathode sensitivity at the position of the galaxy. In the region of the galaxy the photocathode sensitivity is 10 $\pm$ 2% greater for the B electronograph and 10 $\pm$ 2% lower for the V electronograph than in the region where the stars were measured (see section 3.7).

The profiles NGC4881 which were measured by Ables and Ables (1972a) are shown in figure 4.6. These profiles were measured from electronographs exposed for 60 minutes on a 1.5 metre telescope and are therefore much more accurate at large distances from the nucleus than the profiles measured for the present study. The electronographs used by Ables and Ables were also taken in good "seeing" conditions which permitted more accurate studies of the nucleus.

A comparison of the profiles of NGC4881 which were measured by Ables and Ables (1972a) and by the author yields the following points:

FIGURE 4.5 LUMINOSITY PROFILES OF NGC 4881

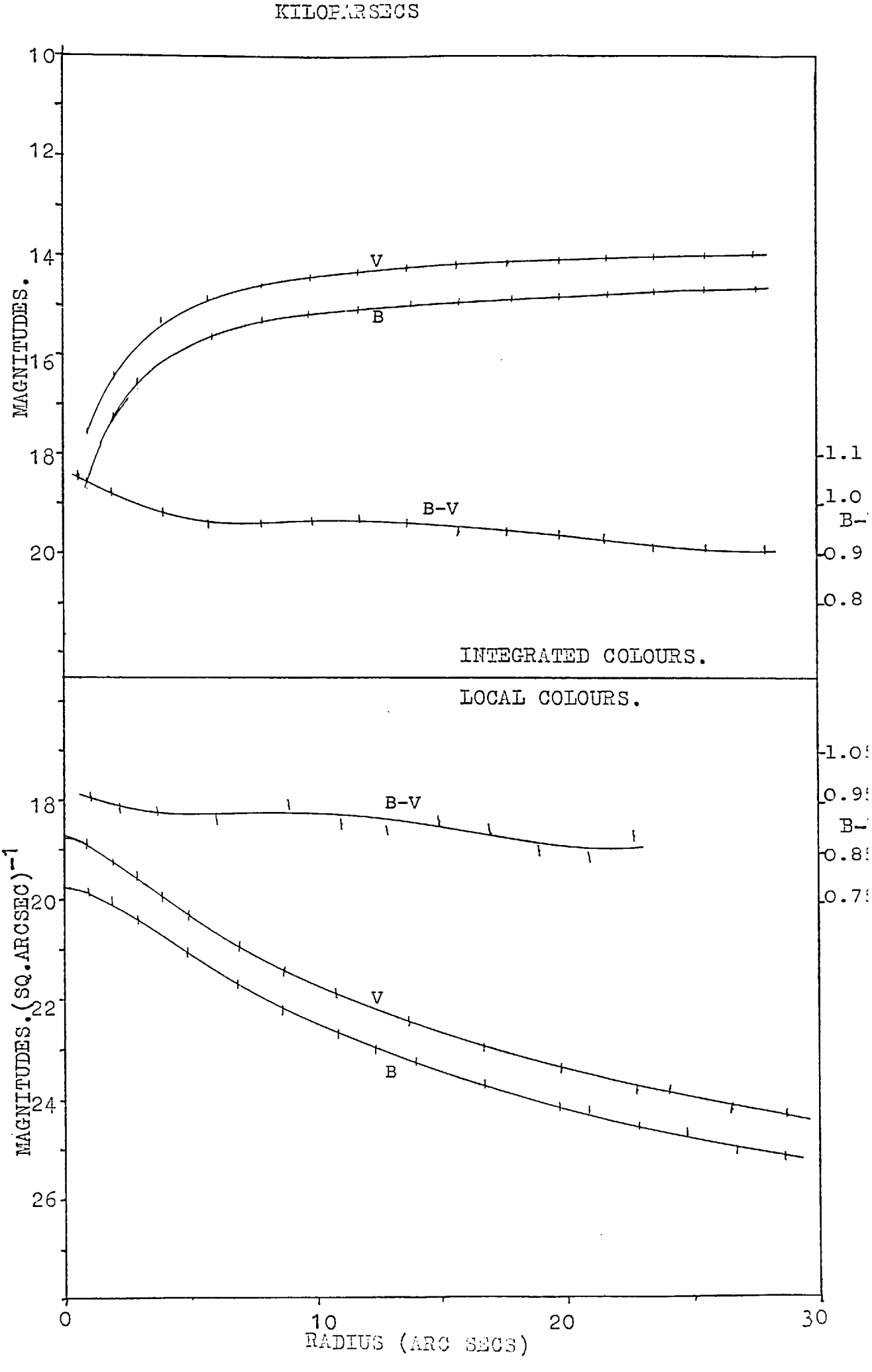

FIGURE 4.6 LUMINOSITY PROFILES OF NGC 4881 (ABLES AND ABLES, 1972)

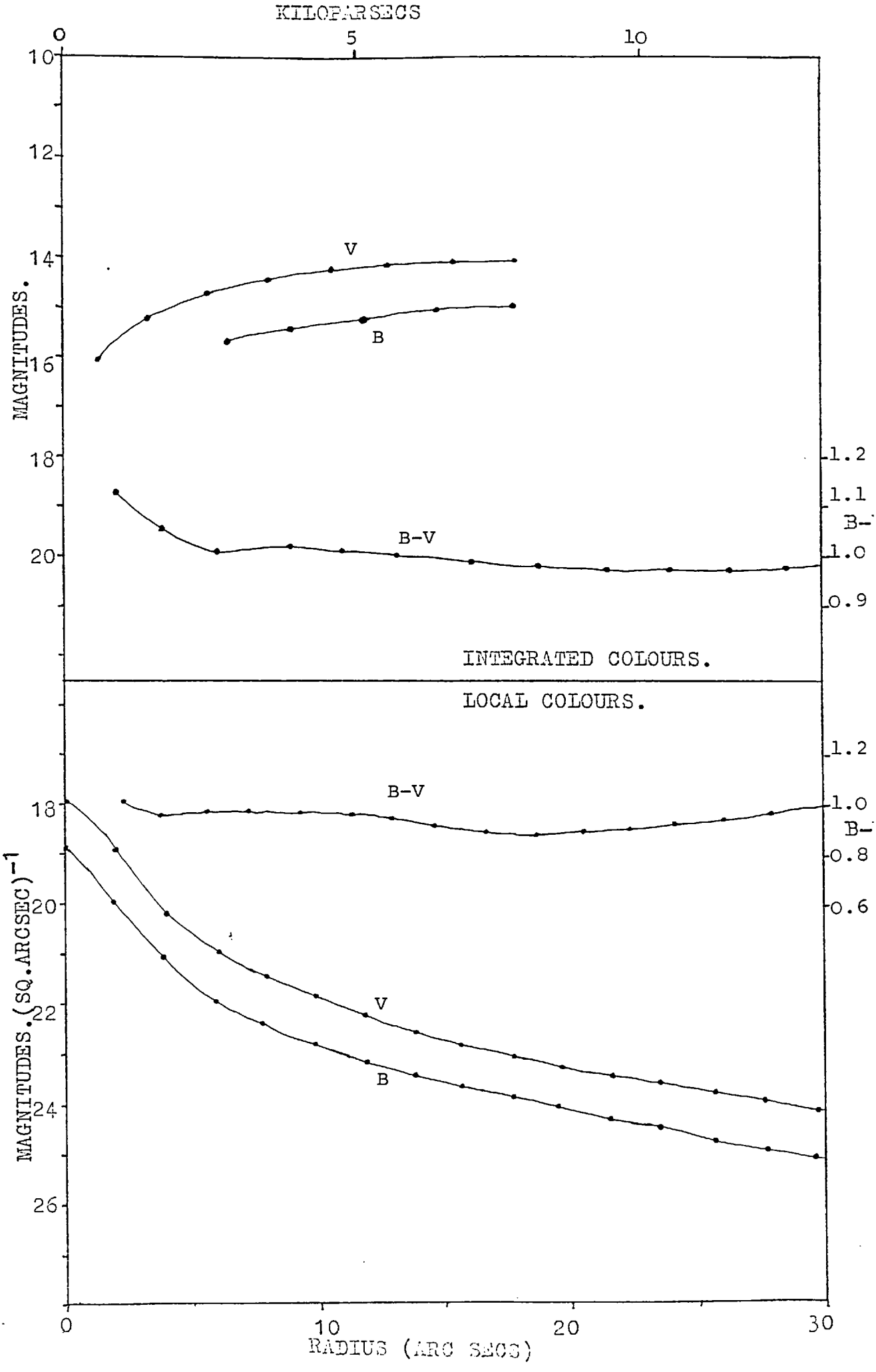

1. The nuclear luminosity profiles in the present study are affected by poor seeing to a radius of about 7".

2. Within experimental error, the profiles of the intermediate regions of the galaxy which were measured in the two studies are the same, but the profiles in the present study are noisier because the electronographs were of a shorter exposure time on a smaller telescope than used by Ables and Ables.

3. The colour profiles are also the same, within experimental error, but again the present study gives noisier results owing to the telescope and exposure times involved. Ables and Ables measured a higher colour index in the nuclear region than that found in the present study, this is probably caused by a combination of poor seeing and a slight over-exposure of the V electronograph in the present study.

4. The calibration of the electronographs in the present study appears in error when the results are compared with Ables and Ables. Measurements from the V electronograph appear to be 0.05 magnitudes too faint and the B electronograph appears to be measured 0.05 magnitudes too bright. These differences cause a discrepancy of 0.1 magnitudes in the B-V measurements. The discrepancy is within the error of the calculation of the calibration constants. One might think that the calibration constants should be defined using the results in this section, rather than using the measurements of standard stars. However, the accuracy of the measurements of NGC4881 is much lower

than the measurements of standard stars due to the atmospheric extinction and the position of the image on the electronographs. Hence, the calibration constants calculated from the measurements of standard stars in section 4.2 will be used to calibrate all other measurements of the luminosity of galaxies in this thesis.

Table 4.6 Photometric Parameters of NGC4881

Integrated magnitude (through a 36″ diaphragm)	B	15.0
	V	14.0
	B-V	0.9
Peak observed surface brightness (magnitude arcsec^{-2})	B	19.8
	V	18.8
	B-V	1.0
Maximum detected radius		30″
V magnitude within 4.2 kpc diameter		15.3
K		-35.65
Core radius		1.6 kpc (2.6″)
Core magnitude		16.0
Compactness		-2.4 ± 0.4

Calibration constants $K_B = 19.6 \pm 0.1$

$K_V = 19.4 \pm 0.1$

4.4. 1ZW166

This galaxy has been studied by Zwicky (1971) and Sargent (1970). (In Sargent's paper it is erroneously named 1ZW165). The results from a three colour (U,B,V) study of 1ZW166 are presented in this section. The principal elements of 1ZW166 are given in table 4.7. (Source:- Zwicky, 1971)

Table 4.7 Principal Elements of 1ZW166

R.A. (1950)	16^h 47.0m
Dec. (1950)	+ 48° 47'
Magnitude (m_p)	14.6
Dimension	$10''$
Corrected apparent recession velocity	7819 km.sec^{-1}

4.4.1 Description

1ZW166 has been described by Zwicky (1971) as a "post-eruptive, very blue, patchy and very compact" galaxy with curved jets from the East to North and West. Sargent (1970) describes it as a slightly elliptical galaxy which is about $10''$ (7.5 kpc) in diameter, positioned $1.5'$ south of MCG 8-31-1 (see figure 4.7).

Sargent has studied the spectrum and found sharp emission of the Balmer and forbidden OII lines. As the lines are not spectrally resolved, the emitting gas must have a velocity dispersion of less

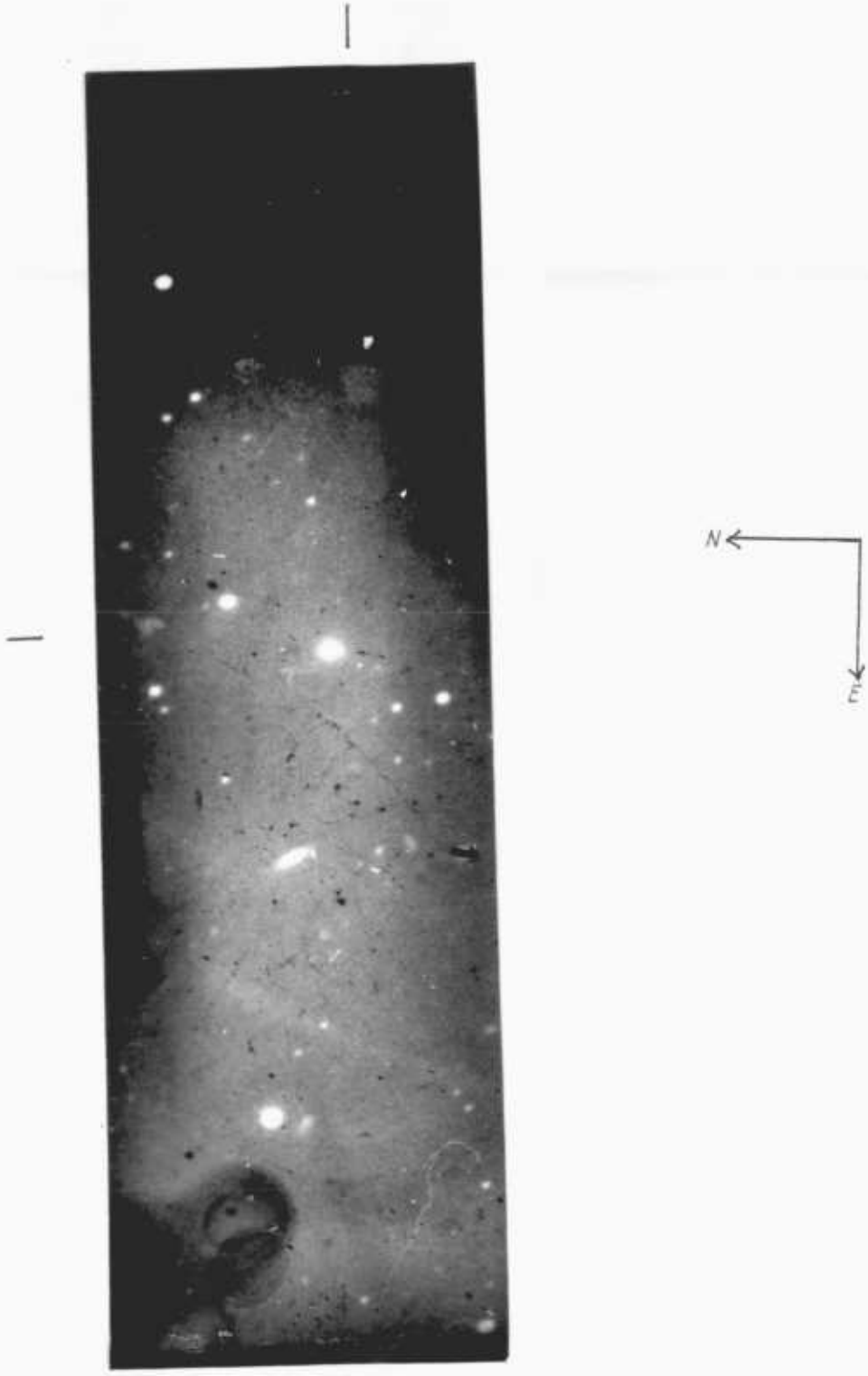

FIGURE 4.7 ELECTRONOGRAPH OF 1ZW166 MAGNIFIED APPROXIMATELY 6.3x

than 450 km.sec^{-1} (Sargent, 1970). Sargent attributed the emission lines to excitation by hot stars.

4.4.2 Observations

The electronographs used for this study are listed in table 4.8. The seeing diameter during the observations was 3$^{\prime\prime}$ at F.W.H.M, measured from a star profile. The prime focus of the telescope was used.

Table 4.8 Electronographs of 1ZW166

Date	Telescope	Plate-Scale	Emulsion
19 June 1975	I.N.T. 2.5 metre	25.65".mm^{-1}	L4

Spectracon

AS3

Electronograph	Exposure	Filter
I171a	12m	B
I172b	20m	U
I172b	20m	V

Plate I171a was interrupted by cloud but continued afterwards. All of these electronographs show the effects of variations in the sensitivity of the photocathode and emulsion defects. The maps of the photocathode sensitivity (see section 3.7) do not show any variations as large as those that appear on

Table 4.9 Principal Elements of Handscans of 1ZW166

Electronograph	I171a	I172a	I726
Z	0.3	0.2	0.8
D_m	1.8	1.5	3.5
G	0.01	0.01	0.02
R	1.5	1.2	2.5
G_s	0.02	0.02	0.05
a_T	10	10	5
a_e	70	70	50
Δ	3	3	3

these electronographs. This implies that there were defects in the sensitivity of the emulsion - these are impossible to correct. This means that the information found in this study will be of poor quality.

The Joyce-Loebl microdensitometer was used in the hand-scanning mode in order to find the principal parameters of the image of 1ZW166 on the above electronograph. These parameters are given in table 4.9. With these results, it was decided to scan the nucleus of the galaxy in each electronograph using a step-length and aperture size of 10 μm. A scan of the nucleus on electronograph I172b was not made because the image was too dense in this region for the microdensitometer to measure. The outer regions of the galaxy were scanned with a step-length and aperture size of 20 μm.

4.4.3 Morphology

Maps of the scans of the nucleus from the B and V electronographs are shown in figure 4.8. On the map of electronograph I171a, there is a dense point (marked A) near the galaxy which was caused by a spot of dirt on the electronograph. Maps of the scans of the outer regions of this galaxy are shown in figure 4.9; only the lower contour levels are drawn in order to show the distribution of luminosity in the outer regions of this galaxy.

Map of electronograph I172b (V filter): This electronograph was unfortunately over exposed so studies of the nucleus are impossible. This map shows

FIGURE 4.8 MAPS OF THE NUCLEUS OF 1ZW166

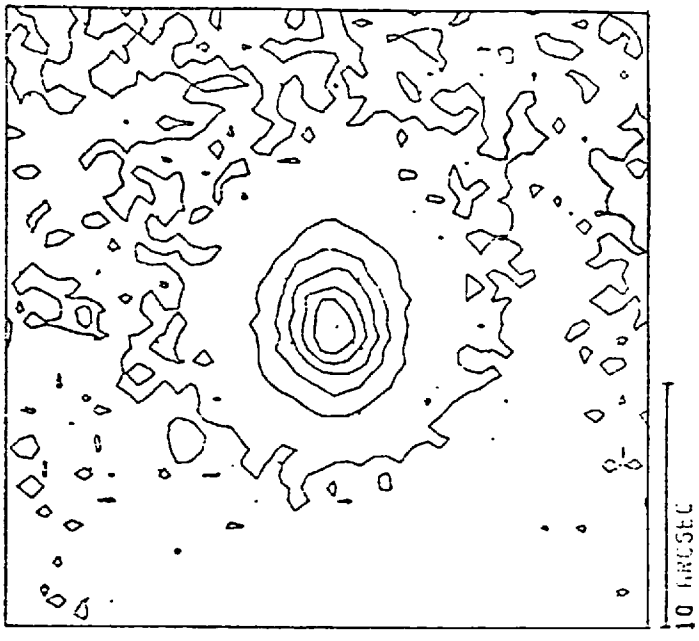

(i)

Electronograph I172a
Filter V

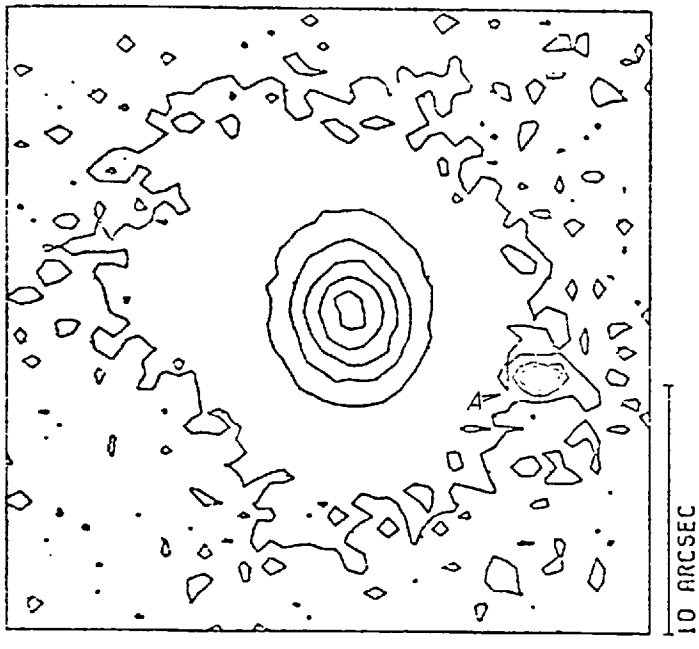

(ii)

Electronograph I171a
Filter B

FIGURE 4.9 MAPS OF THE OUTER REGIONS OF 1ZW166

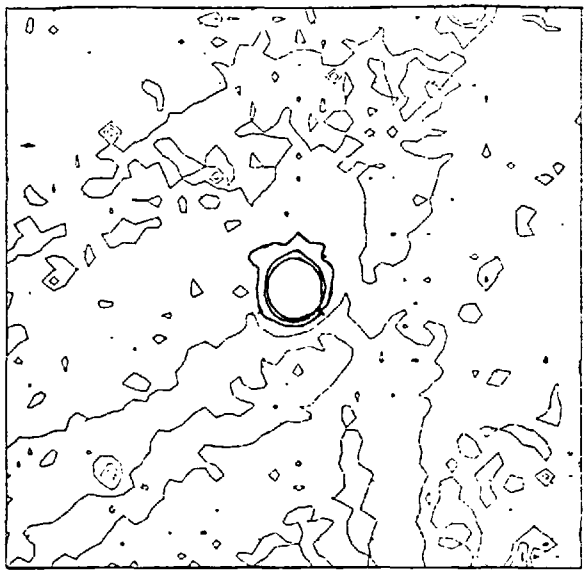

(i)

Electronograph I172a
Filter U

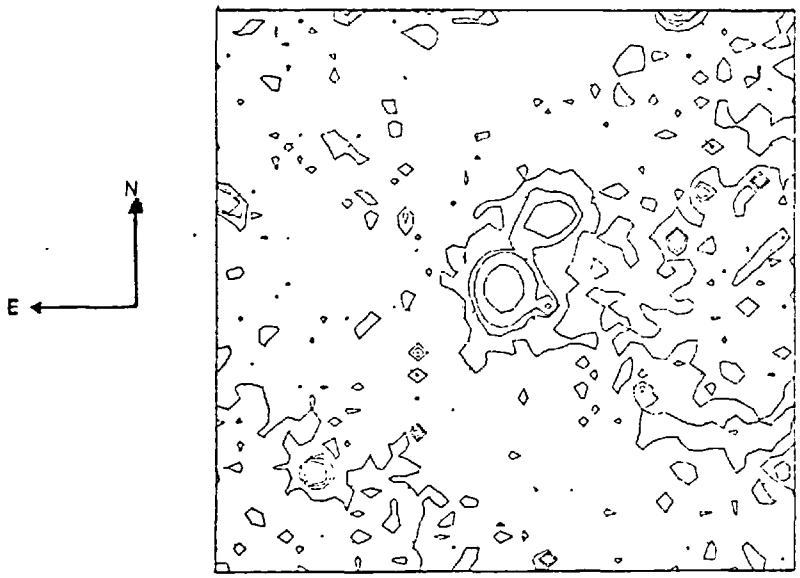

(ii)

Electronograph I171a
Filter B

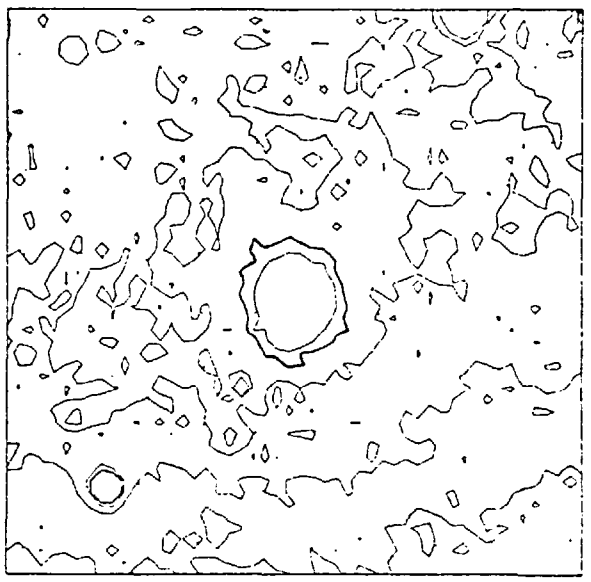

(iii)

Electronograph I172b
Filter V

that there is a fall in the background density from the central region of the galaxy to the bottom of the scan. This fall in density is about 10% which is much higher than that produced by the variation in sensitivity of the spectracon (see section 3.7). The variation over this region on this electronograph must therefore have been caused by an emulsion defect (see section 1.4). To the North of the galaxy the sensitivity of the spectracon varies by about $\pm$ 2% (section 3.7). In this region 1ZW166 can be detected to a radius of 20$\hat{''}$ at about 24 mag.arcsec^{-2}, which is larger than measured by Sargent (1970). The contours show that it has an axis ratio of 0.86 $\pm$ 0.03 at 4$\hat{''}$ radius.

Maps of electronograph I171a (B filter): The map of the region around the galaxy shows that the background density is low in the region to the south-east of the galaxy and high to the west. This variation is about $\pm$ 10% across the scan and $\pm$ 5% within 10$\hat{''}$ of the centre of the galaxy. It is much greater than the variation in the sensitivity of the spectracon in this region (see section 3.7) so it must be due to defects in the emulsion.

This map also shows what appears to be a faint companion of 1ZW166 to the north-west. No evidence for this companion appears on the "V" electronograph even though the exposure time was greater. Hence, this faint, extremely blue region is probably caused by an emulsion defect. A study of the galaxy shows that it is oval, with an axis ratio of 0.81 $\pm$ 0.03 at 4$\hat{''}$ radius.

Maps of electronograph I172a (U filter): The map of the outer regions of 1ZW166 shows that there is a dip in the background density to the south and east of the galaxy. This must also be caused by an emulsion defect. The variation in sensitivity can not be corrected so it is impossible to perform accurate photometry of the outer regions of the galaxy on this electronograph. The map of the nucleus of 1ZW166 also shows the effects of the dip in sensitivity to the south of the galaxy. This map shows that the axis ratio of 1ZW166 is 0.78 $\pm$ 0.06 at $4^{\prime\prime}$ from the centre. The large error is due to the effects of the variations in sensitivity.

All the electronographs are badly affected by variations in the sensitivity of the emulsion, thus removing the possibility of studying the extensions of 1ZW166 which were observed by Zwicky (1971). However, the nucleus has been found to be small ($4^{\prime\prime}$) and oval, in agreement with Zwicky (1971). The axis ratio is measured as 0.83 $\pm$ 0.03. Exposures which are taken under better "seeing" conditions will be necessary in order to observe features in the nucleus.

4.4.4 Photometry

As the electronographs which were taken through the U and V filters are adversely affected by emulsion sensitivity variations, only the electronograph taken through the B filter is used for photometric studies. However, this to is affected by sensitivity variations which restrict photometric studies to the region around the nucleus of the galaxy where the variations are small.

The observations can not be calibrated directly because standard stars were not observed at the same time as this galaxy and no photometric measurements of it are available. However, an estimate of the luminosity is required and an approximate calibration can be made by using the constants which were measured at the Flagstaff observatory (see section 4.3) and making allowances for the diameter of the telescope, the plate-scale on the electronograph and the emulsion used (see the note below). The calibration constant which was calculated from these considerations is given in table 4.10, it also includes a correction for the wedge used to scan the electronographs. The extinction by the atmosphere (the I.N.T. is about 1000m. lower than the Flagstaff observatory) was not measured and is therefore not included in the calibration. Since this is a poor method of calibration, a large error is put on the value of the calibration constant.

Table 4.10 lists some of the principal photometric parameters of 1ZW166 which were found from measurements of the B electronograph. The parameters referring to a V magnitude are found from the B measurement by assuming that 1ZW166 has a colour of $B-V = 0.5 \pm 0.1$. This figure was deduced by studying the luminosity on the B and V electronographs at several points around the nucleus of the galaxy.

NOTE: The calibration constants were calculated using the results from section 4.2 and making corrections for the emulsion, telescope diameter, plate-scale and wedge used for scanning. Therefore, for the study of this object (using equation IV-7):

Table 4.10 Photometric Parameters of 1ZW166

Integrated luminosity within a radius of 10″	B	15.5
Observed peak surface luminosity	B	19.5
Maximum detected radius	B	15″ 11.3 kpc
V magnitude within 4.2 kpc diam.		15.8
K		-35.9
Core radius		$1.5.10^3$ pc
Core V magnitude (assuming B-V 0.5).		15.1
Compactness (no correction for seeing effects)		-2.7 ± 0.6

$k_B = 19 \pm 0.5$

$k_V = 19 \pm 0.5$

$$k_B = 19.5-2.0+2.5 \log_{10} \frac{2.5}{1.1}^2 +2.5 \log \frac{25.65}{24.1}^2 - 0.44$$

$$= 19.0 \pm 0.5$$

Similarly $k_V = 19.0 \pm 0.5$ IV-8

These results have large errors because the correction for emulsion sensitivity is very approximate and there is no correction for the extinction of the atmosphere.

4.5 1ZW86 (NGC 5603)

NGC 5603 was considered to be a compact galaxy by Zwicky (1971) and numbered 1ZW86 in his catalogue. Holmberg (1931) included NGC 5603 in his list of double galaxies, the associated galaxy being 2.5' to the north-west with a photographic magnitude of 15.0. 1ZW86 has a photographic magnitude of 14.0 and a recession velocity of 5779 $km.sec^{-1}$ (Kormandy, 1977 - see table 4.11). Holmberg (1931) suggested that these galaxies are a double system because they have a small apparent separation and they have similar dimensions and luminosities. Palomar sky survey photographs of the field show no evidence of a bridge or tidal effects. No reference to a measurement of the recession velocity of the second galaxy, or any other reference to the possibility that they may be a double system, can be found by the author.

A study of 1ZW86 in the B and V colours is presented in this section. The elements of 1ZW86 are given in table 4.11.

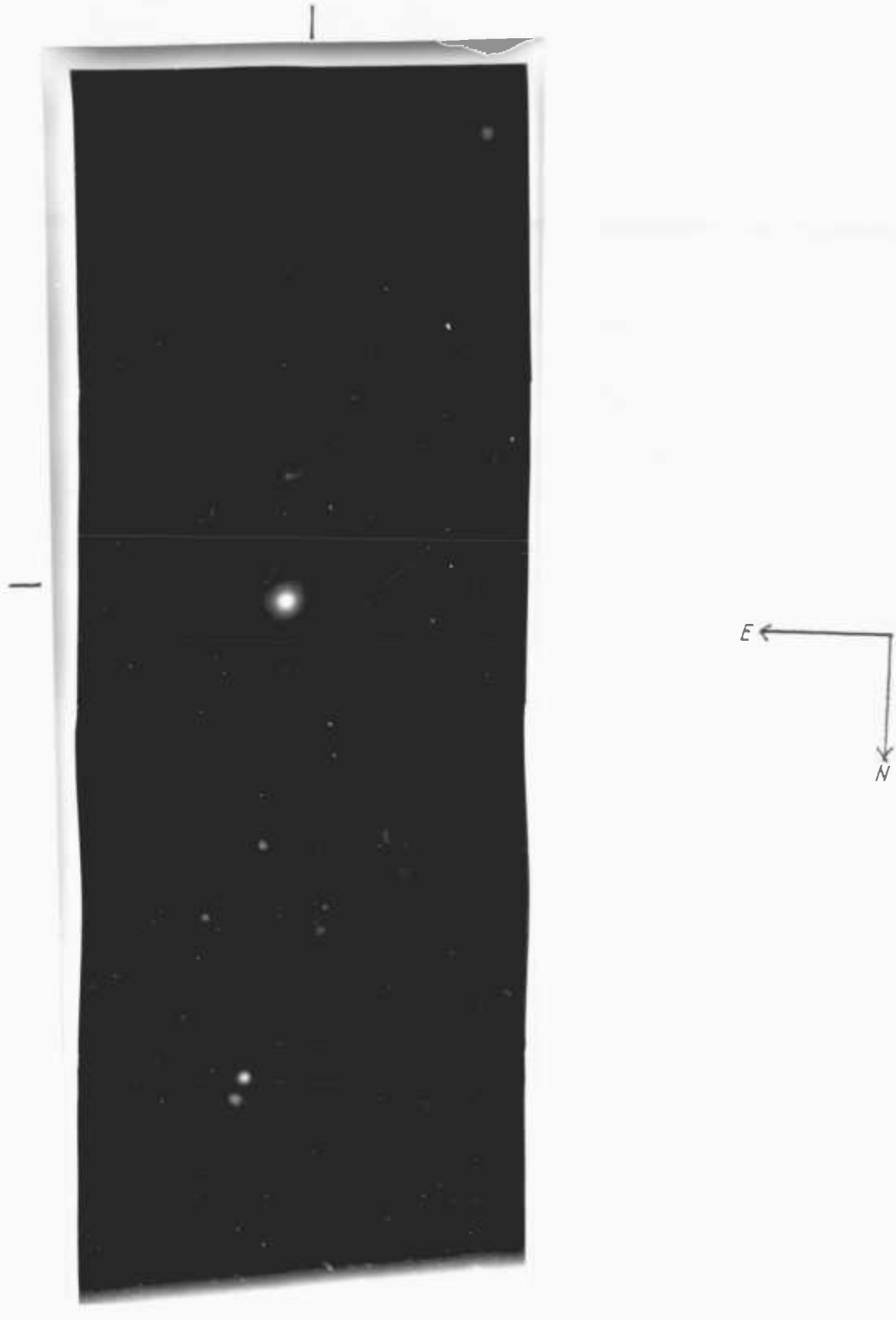

FIGURE 4.10 ELECTRONOGRAPH OF 1ZW86 MAGNIFIED APPROXIMATELY 6.3x

Table 4.11 Elements of 1ZW86 (NGC 5603)

R.A. (1950)	14h.22.1m
Declination (1950)	+40°36'
Magnitude: m_{pg}	14.0
V within 29″ aperture	13.58
B-V "	0.99
Type	E0
Dimensions	50″ by 50″
Corrected Apparent Recession Velocity	5779 km.sec^{-1}

4.5.1 Description

In the R.N.G.C. (Sulentic and Tifft, 1973), NGC 5603 is described as "a round galaxy with a high surface brightness, possessing the normal elliptical characteristics". Zwicky (1971) described the galaxy as "a large, spherical disc compact with an extended halo".

4.5.2 Observations

The electronographs used for this study are listed in table 4.12

Table 4.12 Electronographs of 1ZW 86

Date	Telescope	Plate Scale	Emulsion	Spectracon
15 June 1975	1.1 metre Flagstaff	24.1″.mm^{-1}	L4	AS3

Electronograph	Exposure	Filter
F128e	25 min	V
F128f	40 min	B

Table 4.13 Principal Elements of Handscans of 1ZW86

Electronograph	F128e	F128f
Z	0.16	0.16
D_m	0.96	0.56
G	0.005	0.002
R	0.8	0.45
G_s	0.009	0.005
a_T	20	50
a_E	100	100
Δ	5	5

The full width at half the maximum density of a star profile during the observations was measured to be 160 μm, approximately 4". The principal measurements from handscans of these electronographs are listed in table 4.13.

4.5.3 Morphology

With the results in table 4.13, it was decided that three scans of each electronograph of 1ZW86 would be necessary for morphological studies. These scans had a step length of 5, 20 and 40 μm with an aperture of 10, 20 and 40 μm respectively. They are used for studies of the nucleus, the area at intermediate radius, and the regions distant from the centre of the galaxy. Maps of these scans are shown in figures 4.11 and 4.12.

The scans of the outer regions of the galaxy show apparent variations in the sky background density. These are due to variations in the sensitivity of the photocathode (see section 3.7) and are only about $\pm$ 2%. The variations are within the accuracy which is necessary for the study of this object so no attempt is made to calibrate them out.

On both maps the galaxy can be detected to a radius of 50", in good agreement with the results of Holmberg (1931). These maps, and those of the nucleus and intermediate regions (fig. 4.12) do not show any evidence of tidal effects which might have been seen if this galaxy is a member of a double system. There is certainly no evidence of a luminous bridge extending from 1ZW86, down to a level of 26 mag.arcsec^{-2}.

FIGURE 4.11 ISOPHOTE MAPS OF 1ZW86 V FILTER

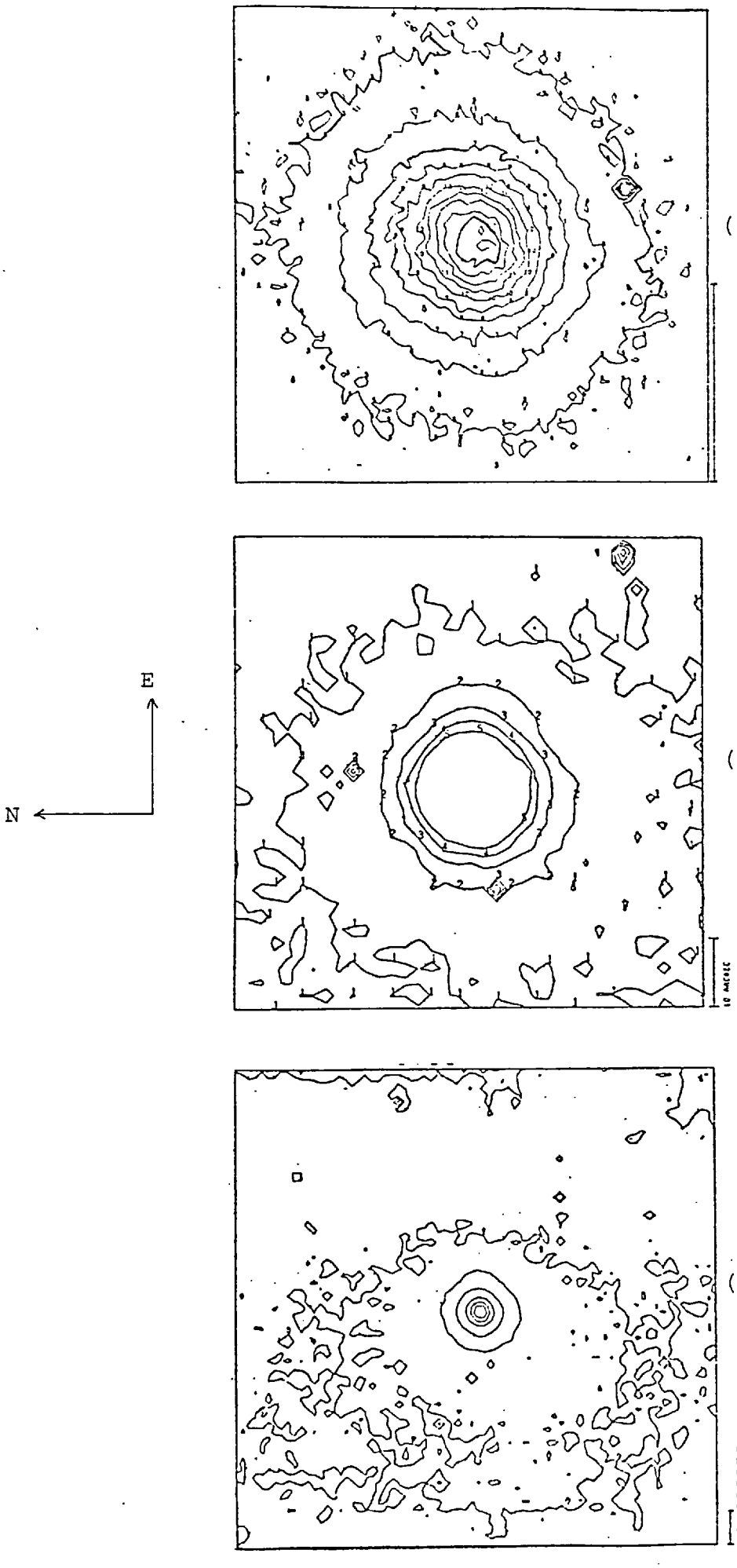

FIGURE 4.12 ISOPHOTE MAPS OF 1ZW86 - B FILTER

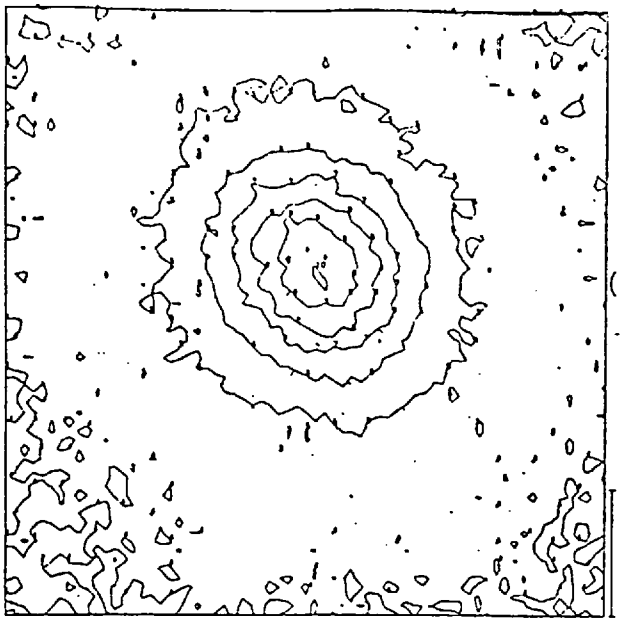

(i) Nucleus

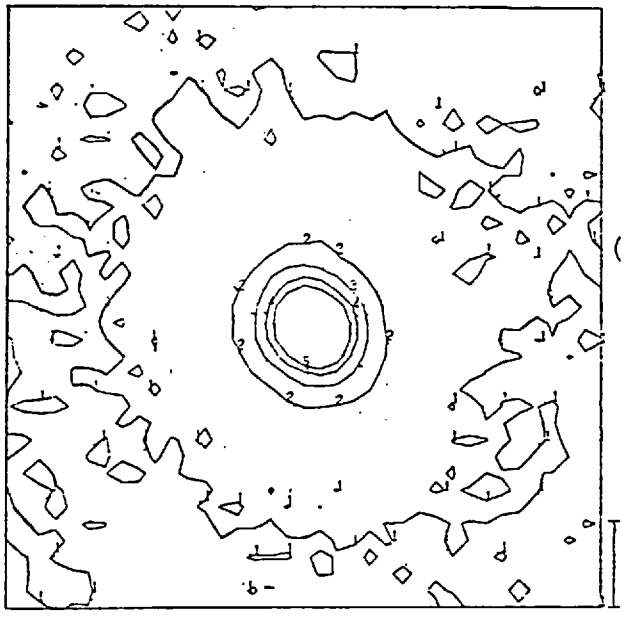

(ii) Intermediate Region

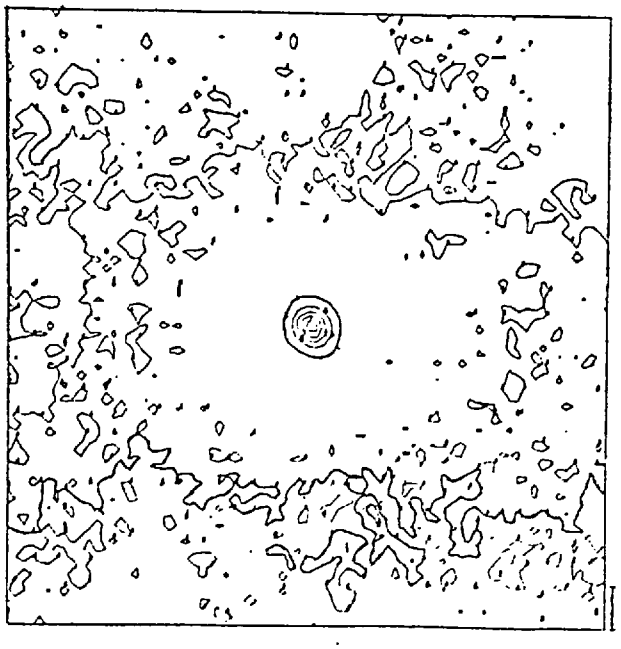

(iii) Outer Regions

Cross-sections of 1ZW86 from scans of electronograph F128e are shown in figure 4.13: they are in the north-south and east-west directions. The profiles show that 1ZW86 has a very bright nucleus and an extended faint halo, as suggested by Zwicky (1971) and Kormendy (1977).

During the observing session, it was found that the images on some of the electronographs were slightly elongated. The cause of this drift was not conclusively proven but it was thought that it was most probably caused by a drift in the focus of the telescope. Unfortunately, this affected the electronographs which are studied in this section and no other electronographs of 1ZW86 are available. The exact effect of the drift is not known and could only be corrected by deconvolution if its characteristics were well known. However, no bright stars appear on the plates which would have enabled these characteristics to be measured with sufficient accuracy.

NOTE: The effect on a star is to give it an axis ratio of about 0.95 at a radius of five arcseconds, but at a radius of 10 arcseconds the axis ratio is 0.995.

Measurements of electronographs F128e and F128f give the axis ratio of 1ZW86 at a radius of 5" as 0.95 ± 0.02 and 0.85 ± 0.02, respectively. This shows that electronograph F128f was more affected by focus drift. Measurements of faint star images in each electronograph indicate that the axis ratios which were measured were both caused by the focus drift and that the axis ratio is probably 1.0 ± 0.04 (Zwicky, 1971 described the galaxy as spherical).

FIGURE 4.13 CROSS-SECTIONS THROUGH THE CENTRE OF 1ZW86, V FILTER

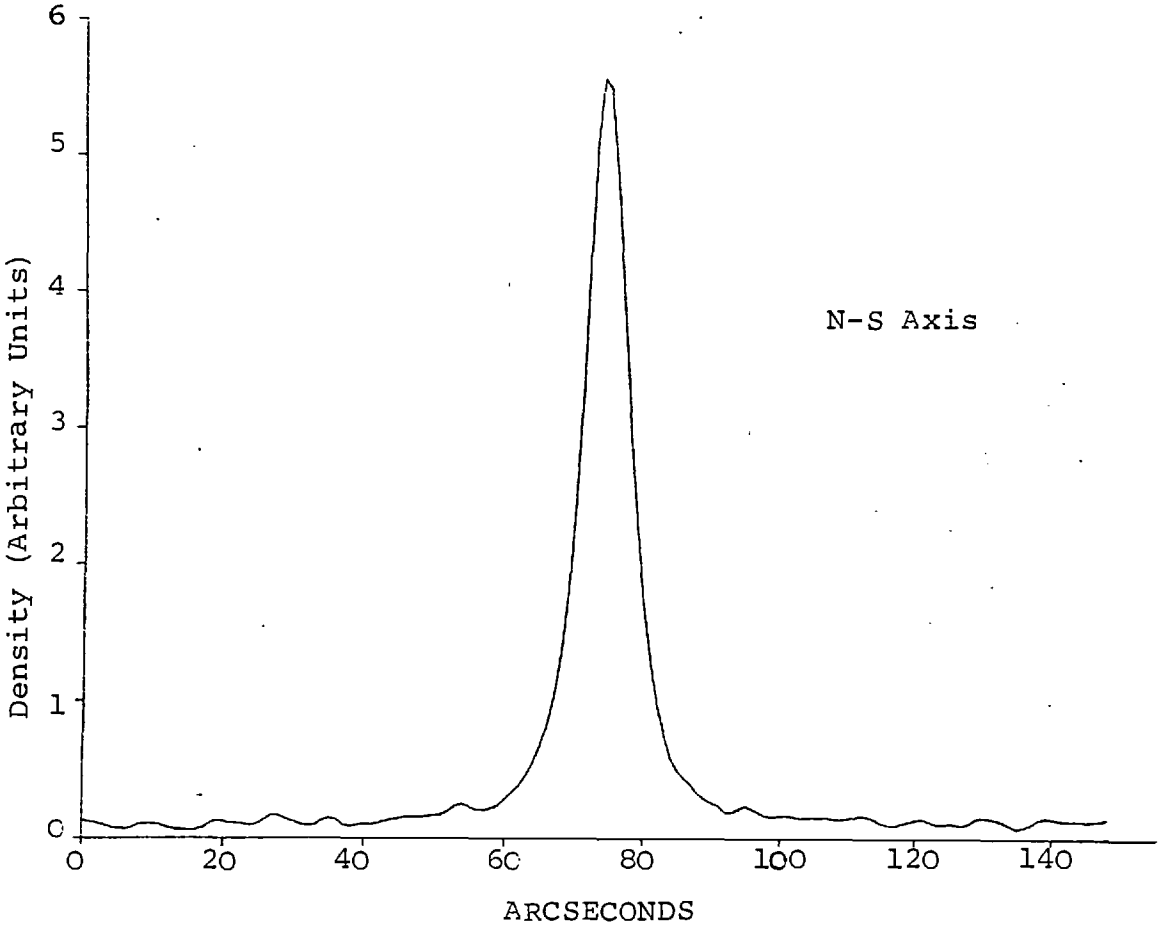

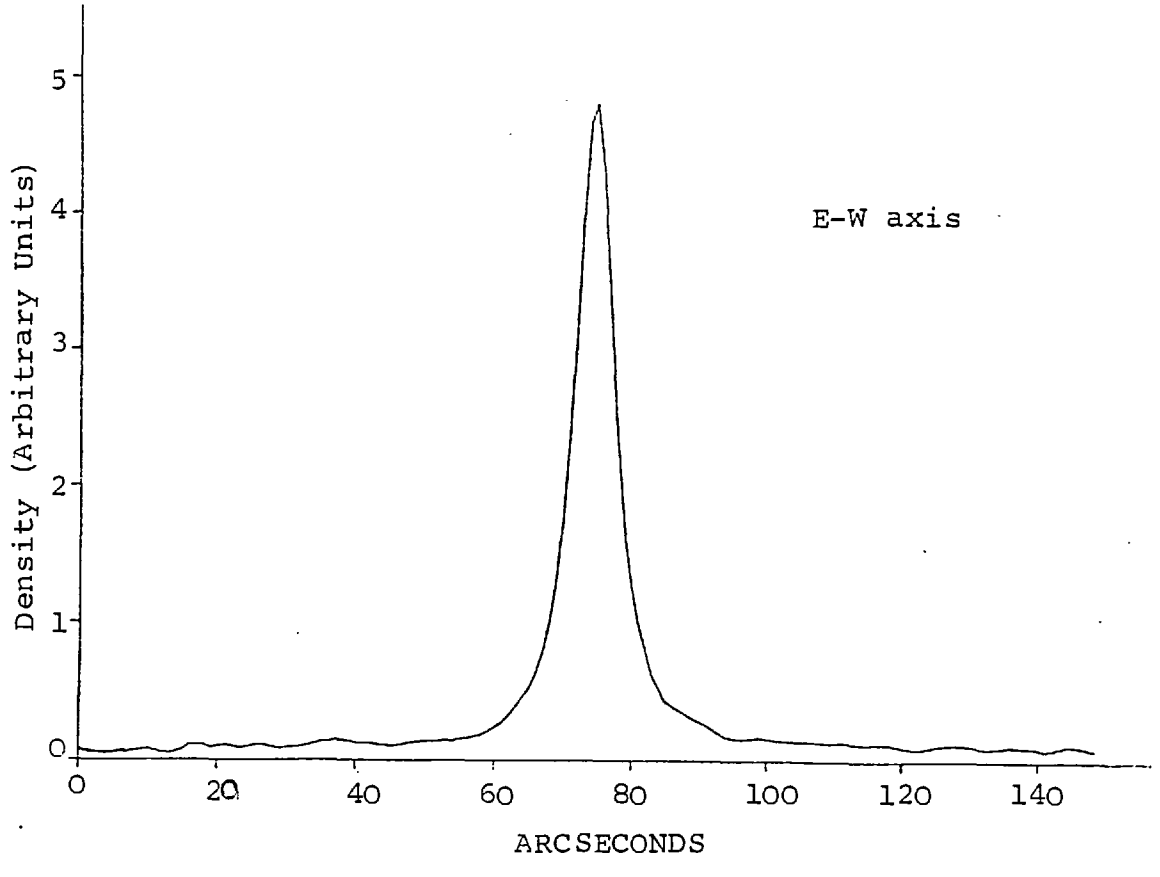

4.5.4 Photometry

As electronograph F128f was not affected by focus drift (see above), it is not possible to draw accurate profiles of the B luminosity or B-V colour. The V luminosity profiles are shown in figure 4.14. The effect of focus drift is small (see above) and the profiles are accurate enough for some information to be measured. The profiles were drawn by integrating all the luminosity within a specified contour level and equating this to an integrated luminosity within a radius r , where

$$r = A/\sqrt{\pi}$$

and A is the area enclosed by the contour. This method allows all the measurements of the luminosity of the galaxy to be used to draw a luminosity profile, even though the luminosity distribution is not circularly symmetric.

Table 4.14 shows the photometric parameters of 1ZW86 which were measured in this study. The integrated magnitudes are in good agreement with the photo-electric measurements of Kormendy (1977), within experimental errors. The colour and luminosity profiles of 1ZW86 are very similar to those which were found for NGC 4881, but 1ZW86 is 0.35 magnitudes brighter when their absolute magnitudes are compared.

4.6 1ZW129

The results from a two colour, B and V, photometric study of the compact galaxy 1ZW129 are presented in this section. Sargent (1970) studied

FIGURE 4.14 LUMINOSITY PROFILES OF 1ZW86

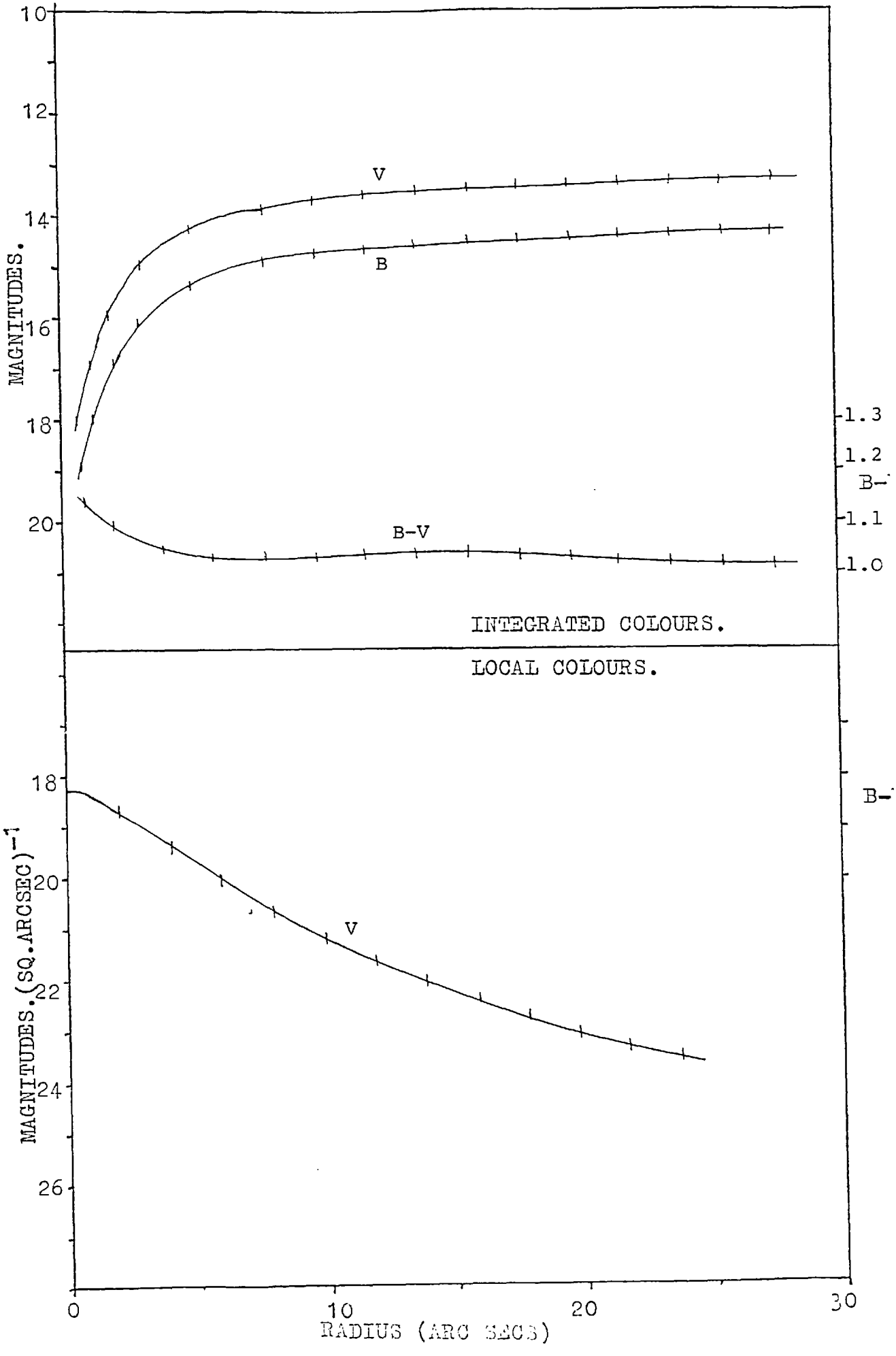

Table 4.14 Photometric Parameters of 1ZW86 (NGC 5603)

Integrated magnitude within a 50″ diaphragm	B	14.3
	V	13.3
	B-V	1.0
Maximum surface brightness	V	18.2
Maximum detected radius	V	50″
	B	50″
V magnitude within 4.2 kpc diameter		13.9
K		-35.3
Core radius		1.5 kpc (2.7″)
Core magnitude		15.2
Compactness		-3.0 ± 0.5
Calibration Constants (Corrected for emulsion and scanning wedge)	k_B	$= 17.9 \pm 0.2$
	k_V	$= 17.9 \pm 0.2$

the spectrum and found Balmer lines in absorption and the forbidden OII (372.7 nm) line in emission. Sargent erroneously named this galaxy 1ZW128 (Zwicky, 1971). Some elements of 1ZW129 are given in table 4.15 (Sargent, 1970).

Table 4.15 Elements of 1ZW129

R.A. (1950)	15h.54m.9s
Declination (1950)	+42° 01'
Magnitude (m_{pg})	14.3
Corrected Apparent Recession Velocity	10482 km.sec^{-1}

4.6.1. Description

Zwicky (1971) described this galaxy as "red, elliptical and disk-like with a faint halo". Sargent (1970) described the image as "structureless and 10″ (10 kpc) in diameter".

A Palomar Sky Survey photograph of the field (fig. 4.15) shows two galaxies within 80″ of 1ZW129. The brighter is MCG 7-33-16, a 14-magnitude galaxy about 80″ NW of 1ZW129, which corresponds to 80 kpc if they are at the same distance. The fainter galaxy, 60″ to the east of 1ZW129 appears to be more distant and unlikely to be connected. These galaxies are not studied in this section, but the possibility that there might be a connection between either of these galaxies and 1ZW129 is examined.

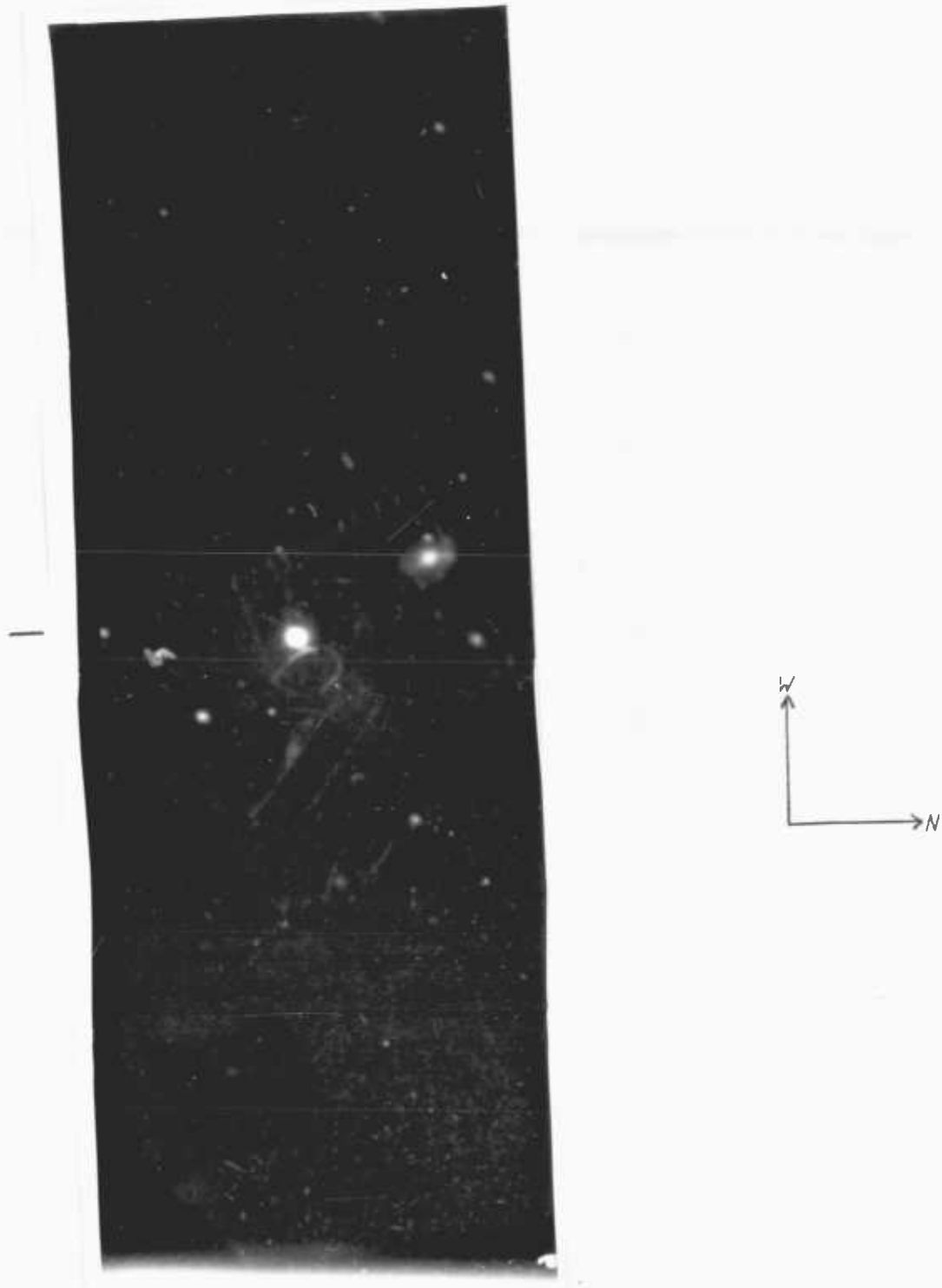

FIGURE 4.15 ELECTRONOGRAPH OF 1ZW129 MAGNIFIED APPROXIMATELY 6.3x

4.6.2 Observations

The electronographs used for this study are listed in table 4.16.

Table 4.16 Electronographs of 1ZW129

Date	Telescope	Plate-Scale	Emulsion	Spectracon
15 June 1976	1.1 metre Flagstaff	$24.1^{\text{n}}.\text{mm}^{-1}$	G5	AS3

Electronograph	Exposure	Filter
F129b	15 min.	B
F129c	5 min.	V
F129d	15 min.	V

The nucleus of 1ZW129 was overexposed on electronograph F129d (see section 1.4). Hence, for observations with the V filter, electronograph F129c is used for studies of the nuclear region and the longer exposure on electronograph F129d is used for studies of the fainter parts of the galaxy. On electronograph F129d scratches appear within 20^{n} of the nucleus (see figure 4.17), but this is outside the area of study. On the night of observation the seeing, as determined from the profile of a standard star, was about 3.5^{n} (FWHM).

All of these electronographs show a slight elongation of the stellar images which is probably caused by improper telescope focussing, this effect is discussed more fully in section 4.6.4. The images were too faint to accurately determine the parameters of the effect or even its amplitude so

Table 4.17 Principal Parameters from Handscans of 1ZW129

seeing (s) = 3.5″ = 150 μm

Electronograph	F129b	F129c	F129d
Z	0.19	0.06	0.17
D_m	1.47	0.90	3.5
G	0.0016	0.005	
R	1.0	0.7	
G_s	0.014	0.010	
a_T	20	20	
a_e	200	200	
Δ	4	4	

corrections could not be made. The implications of this are discussed below.

4.6.3 Morphology

Handscans of the galaxy, using the Joyce-Loebl microdensitometer, were used to produce the parameters of the image of 1ZW129 which are listed in table 4.17. These results indicated that, for studies of the nucleus, electronographs F129b and F129c should be scanned with a step-length and aperture of 10 μm. Similarly, the outer regions of the galaxy and its surrounding area should be studied by scanning electronographs F129b and F129d with a step-length and aperture of 20 μm.

Figures 4.16 and 4.17 show maps of the scans of the area around 1ZW129. In figure 4.16 the maps have been blocked to 200 μm aperture in order to reduce the signal-to-noise ratio to 1% which should permit faint extensions of the galaxy to be seen. N.B. The contour levels in these maps do not have equal density intervals between them and they should not be used to infer luminosity gradients. These contours were chosen to show the extensions of the galaxy and the effects of spectracon sensitivity variations. It was shown in section 3.7 that the sensitivity of the photocathode is uniform, to within 1%, within 20" of the centre of 1ZW129. Also, on electronograph F129b (B filter), there is a 5% increase in sensitivity to the left hand side of the scan, but this is not corrected because it does not affect the present study. 1ZW129 appears on the central region of the photocathode; the edge of the photocathode

FIGURE 4.16 MAPS OF 1ZW129 AND SURROUNDING AREA
(BLOCKED TO 200 μm)

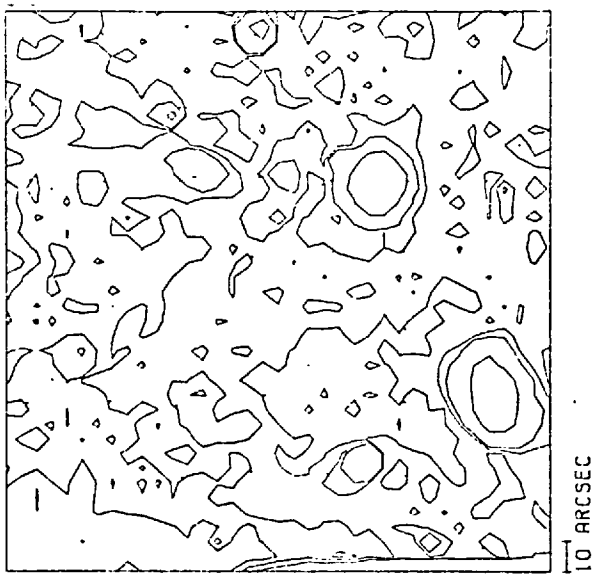

Plate F129b
B Filter

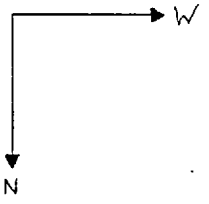

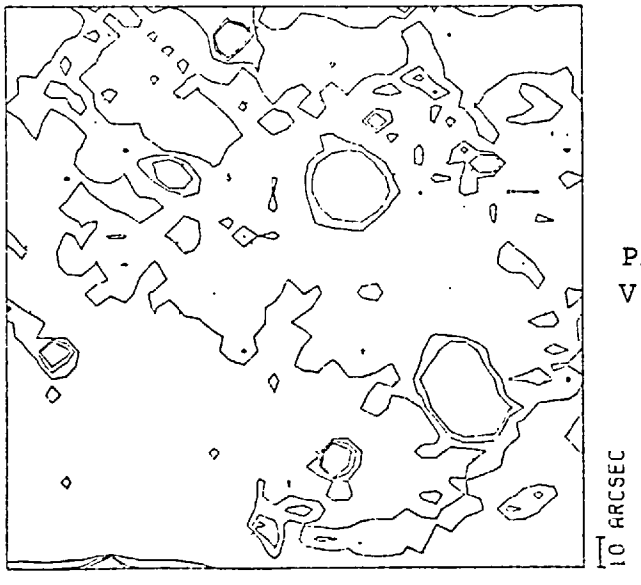

Plate F129d
V Filter

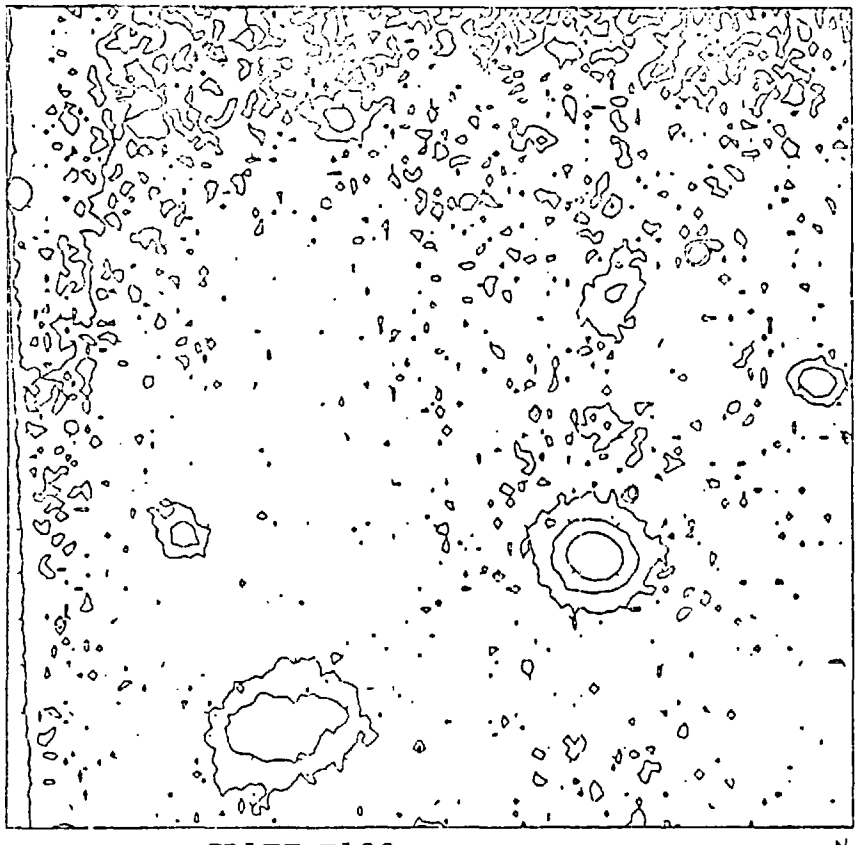

PLATE F129B - B FILTER

10 ARCSEC

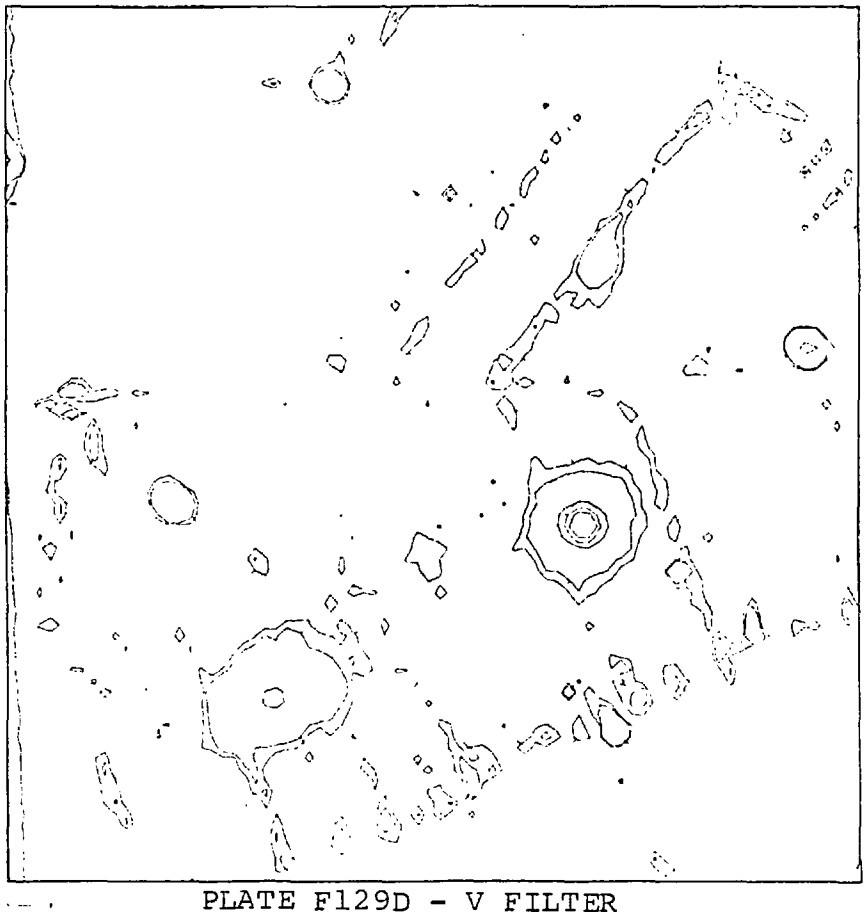

PLATE F129D - V FILTER

10 ARCSEC

FIGURE 4.17 MAPS OF 1ZW129 AND SURROUNDING AREA

(BLOCKED TO 20 μm)

coincides with the bottom edge of these scans.

In figure 4.17 the contour level at 5% above the sky background (brightness 22 mag per square arcsecond) shows no connections between the galaxies. The maps indicate that the halo of 1ZW129 is uniform (i.e. no major disruptions are visible), but longer exposures are necessary in order to study this in more detail.

Figure 4.18 shows maps of the scans of the nucleus which are unblocked to show details. Maps of the whole galaxy blocked to 60 μm to reduce noise are shown in figure 4.19. In each map the spacing of the contours is about 0.2D. A comparison of these maps shows that 1ZW129, when observed through the B filter, appears to be more elliptical than when observed through the V filter. At a radius of 5″ the axis ratio is 0.80 $\pm$ 0.02 for electronograph F129b, but it is 0.87 $\pm$ 0.02 for electronograph F129c. This difference must have been caused by a focus drift during the exposures. It would have been desirable to use the stars in the scans to study the effects of the focus drift and possibly correct the galaxy image but they are too faint for accurate measurements to be made.

Zwicky (1971) described 1ZW129 as being oval. The present results also indicate that it is elliptical but the focus drift makes any quantative measurements impossible. The luminosity of 1ZW129 is detected to a radius of 18″ (18 kpc), over three times the radius measured by Sargent (1970).

FIGURE 4.18 MAPS OF NUCLEUS OF 1ZW129

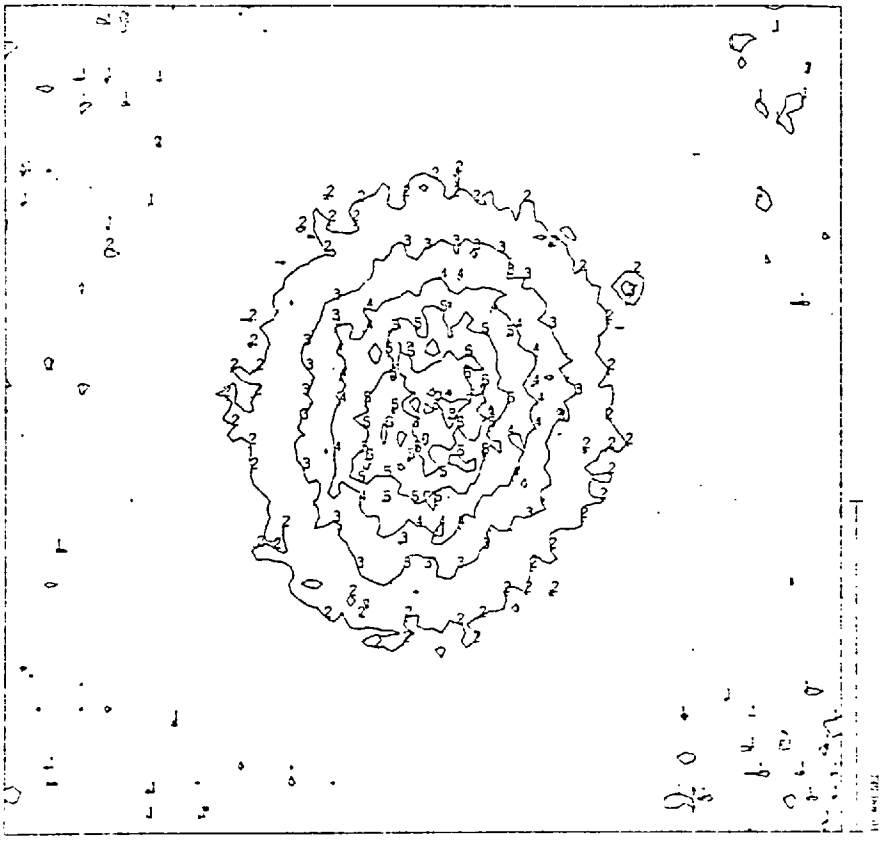

Electronograph F129B
B Filter

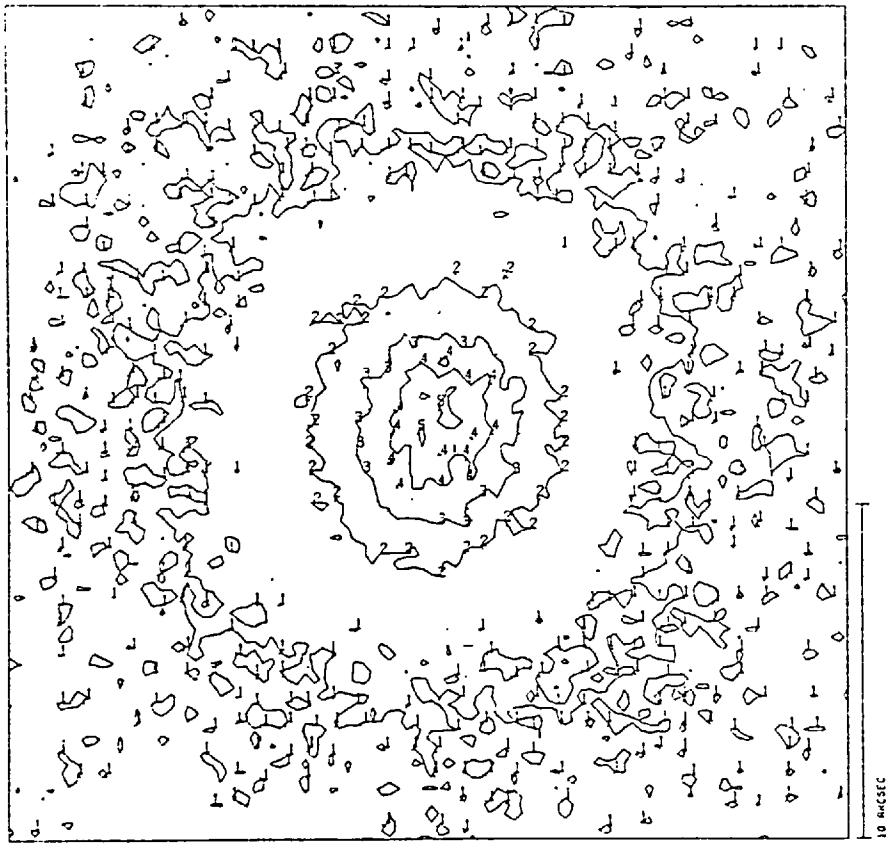

Electronograph F129D
V Filter

FIGURE 4.19 MAPS OF INTERMEDIATE REGIONS OF 1ZW129

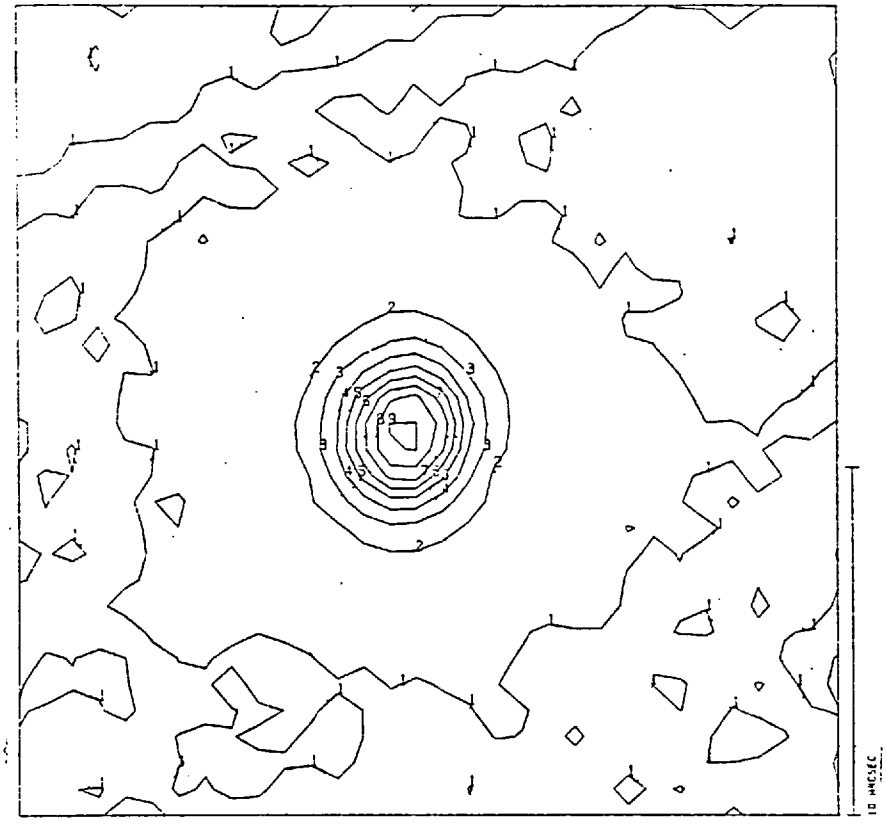

Electronograph F129D
V Filter

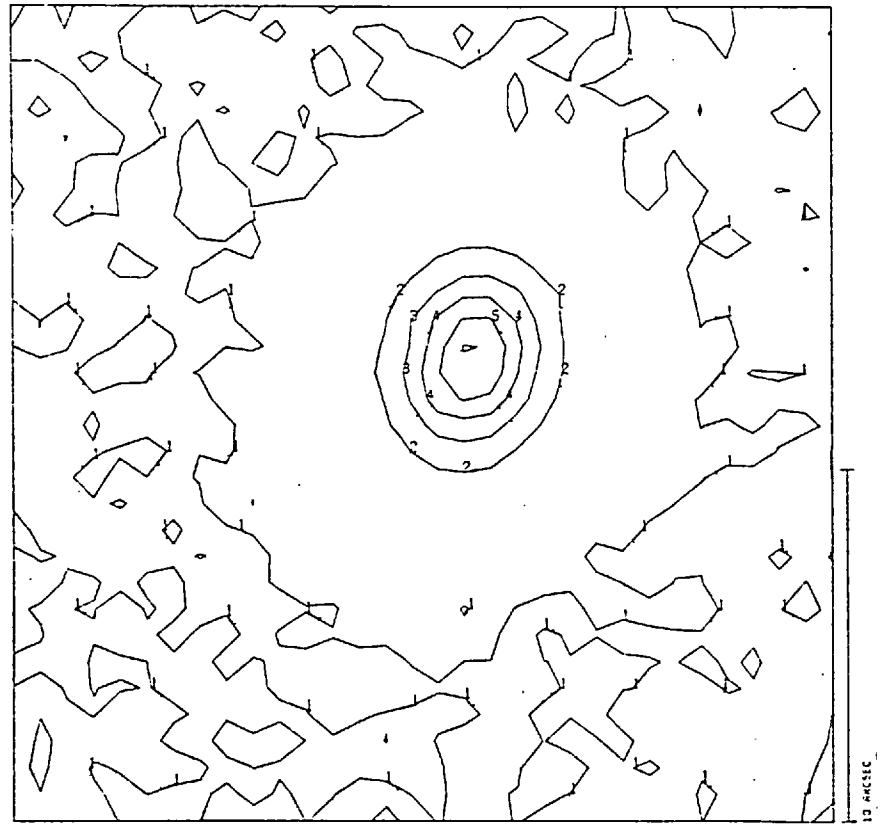

Electronograph F129B
B Filter

4.6.4 Photometry

The integrated magnitudes and maximum surface brightness of 1ZW129 were found using the subroutines in the program MAP (Appendix D), the results are shown in table 4.18. The integrated magnitudes are not affected by focus drift because these involve a computation of the luminosity "volume". The observed peak surface brightness is less than the true value because of the spreading of the light by the effects of seeing and focus drift. However, the object still falls within Zwicky's classification of compact galaxies (see section 4.1).

The measurement of nuclear magnitudes, i.e. integrated V luminosity within 4.2 kpc, shows that, after corrections for distance, 1ZW129 is as bright as the brightest galaxy in the Coma cluster (Weedman, 1977) and about 50% brighter than that of NGC 4881.

Further observations of 1ZW129 are necessary in order to study the local luminosity and colour variations because the focus drift adversely affected the present study. However, it has been shown that 1ZW129 has a very high luminosity within a small central region and that there is no evidence for eruptions within the galaxy or extensions from it to a luminosity level of 26 mag. per square arcsecond.

4.7 NGC 3521 (PKS 1103 + 02)

NGC 3521 is a bright, type Sc galaxy which has been the subject of several studies (Stebbins and Whitford, 1937; Bigay, 1951; Pettit, 1954; Holmberg, 1959; de Vaucouleurs, 1961; Sandage, 1961). In 1970

Table 4.18 Photometric Parameters of 1ZW129

Integrated magnitude within 20″ radius	B	14.8
	V	14.2
	B-V	0.6
Observed peak surface brightness (magnitude arcsec^{-2})	B	19.3
	V	18.3
Maximum detected radius		15″ (15 kpc).
V magnitude within 4.2 kpc diameter		15.9
K		-36.6
Core radius		3 kpc
Core magnitude		15.1
Compactness		-2.6
Calibration constants	$k_B = 19.5 \pm 0.1$	
	$k_V = 19.5 \pm 0.1$	

it was identified with the radio source PKS 1103 + 02 (Merkelijn and Wall, 1970). The principal elements of NGC 3521 are given in table 4.19 (de Vaucouleurs and de Vaucouleurs, 1964). A photograph of the galaxy is shown in figure 4.20 (Sandage, 1961).

Table 4.19 Principal Elements of NGC 3521

R.A. (1950)	11*h* 03.2m
Declination (1950)	+ 00°.02'
Magnitude (V filter, 4' diaphragm)	9.8
Type	Sc
Dimensions	4.2' by 1.4'
Corrected apparent radial velocity	604 km.sec^{-1}

4.7.1 Description

In the Revised New General Catalogue of Galaxies (Sulentic & Tifft, 1973) NGC 3521 is described as a spiral galaxy with diffuse, knotty arms which are tightly bound with many dark lanes. Individual arms are impossible to trace because only discontinuous segments are observed. The nucleus lies in a complex hexagonal lens structure of dimensions 4.2' by 1.4'. The arms can be traced to within 6" of the nucleus which is very small and very bright (Sandage, 1961).

Humason (1936) showed that NGC 3521 has an early type spectrum in common with other Sc type galaxies.

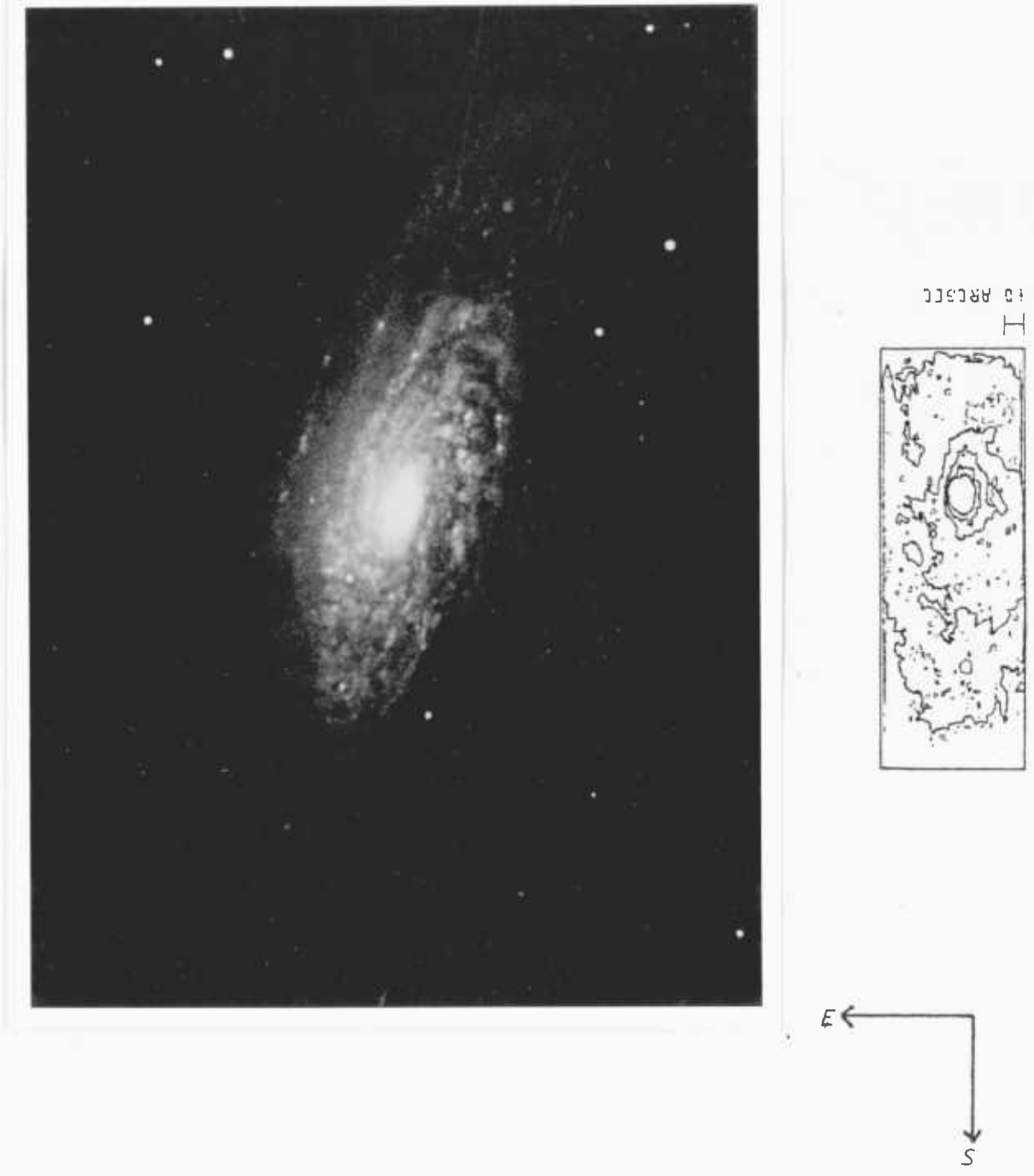

FIGURE 4.20 PHOTOGRAPH OF NGC3521 (SANDAGE, 1961) WITH AN ISOPHOTAL MAP OF THE AREA COVERED BY AN ELECTRONOGRAPH

4.7.2 Observations

The electronographs used for this study were taken on the 1.5m. telescope at the Boyden Observatory in South Africa; they are listed in table 4.20. No standard stars were observed with this telescope so photometric measurements of NGC 3521 by other observers are used to calibrate the present study. During the observations, the seeing was good (estimated as $2^{\hat{n}}$ to $3^{\hat{n}}$ seeing disc) and the extinction low on a clear night. The galaxy extends over a large area and in each case the image covers the whole electronograph.

Table 4.20 Electronographs of NGC 3521

Date	Telescope	Plate-scale	Emulsion	Spectracon
9 April 1973	1.5 metre Boyden	$8.80^{\hat{n}}.mm^{-1}$	L4	B275

Electronograph	Exposure	Filter
B13	20 min	V
B14	20 min	B
B15	20 min	U

The images of the central regions of the galaxy on each electronograph were studied with a microdensitometer in handscanning mode. The principal results of these studies are given in table 4.21 and are used to determine the step lengths and aperture sizes for the two-dimensional scans of the galaxy.

Table 4.21 Parameters of Electronographs of NGC 3521

seeing (s) = 2.5″ = 280 μm.

Electronograph	B13	B14	B15
Z	0.2	0.2	0.1
D_m	2.0	2.0	0.5
G	0.01	0.01	0.003
R	1.5	1.5	0.4
G_s	0.01	0.01	0.003
a_T	15	15	20
a_e	100	100	140
Δ	3	3	3

4.7.3 Morphology

In order to facilitate studies of this galaxy, each electronograph was scanned three times with a different step length and aperture for the measurements. The central $9^{\prime}$ by $9^{\prime}$ of the galaxy, where the luminosity gradients are highest, was scanned with a step length and aperture of 10 μm. These scans give the detailed U, B and V maps of the nucleus shown in figures 4.22, 23, 24. The region of intermediate luminosity (the central $35^{\prime}$ by $44^{\prime}$) was scanned with a step-length and aperture size of 20 μm. and the whole electronograph was scanned with a step length and aperture size of 50 μm. The U electronograph was not scanned in total because its exposure was too short for accurate studies of the extensions of the galaxy to be made. Maps of the scans of the intermediate regions are shown in figures 4.22 to 4.24 and the outer regions are shown in figure 4.21. The 20 μm and 50 μm scans are blocked to analysing apertures of 40 μm and 200 μm respectively in order to reduce the noise from the emulsion.

The maps of the nucleus and intermediate region show "holes" in the luminosity distribution of the galaxy which are caused by point defects on the photocathode of the spectracon. The largest "hole" is about $5^{\prime}$ to the south of the nucleus and is about $1^{\prime}$ in diameter (see section 4.2.1). The photocathode sensitivity variations over the area covered by these maps is small ($\pm$ 2%) so corrections have not been made for them.

Over the area covered by the 50 μm scan the photocathode sensitivity has a large variation ($\pm$ 10%, see section 4.2.1) so these scans were corrected. The corrected maps are shown in figure 4.21. Figure 4.20 shows a 60 minute photograph of NGC 3521 by Sandage

FIGURE 4.21 MAPS OF NGC 3521 (BLOCKED TO 200 μm)

ELECTRONOGRAPH B13 FILTER V

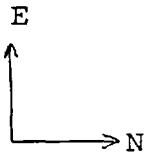

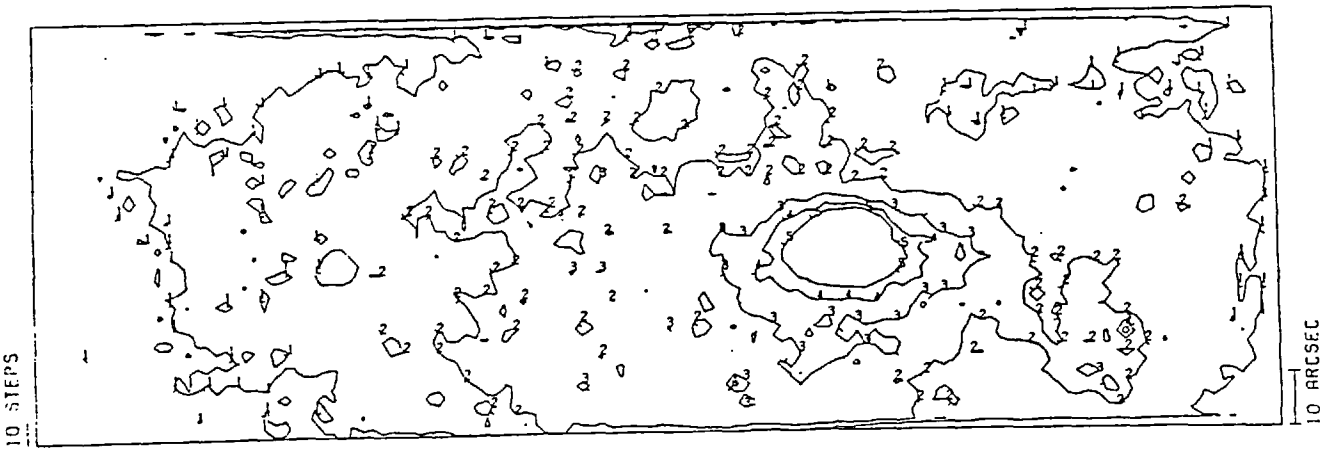

ELECTRONOGRAPH B14 FILTER B

FIGURE 4.22 NUCLEUS AND INTERMEDIATE REGIONS OF NGC 3521 FILTER B

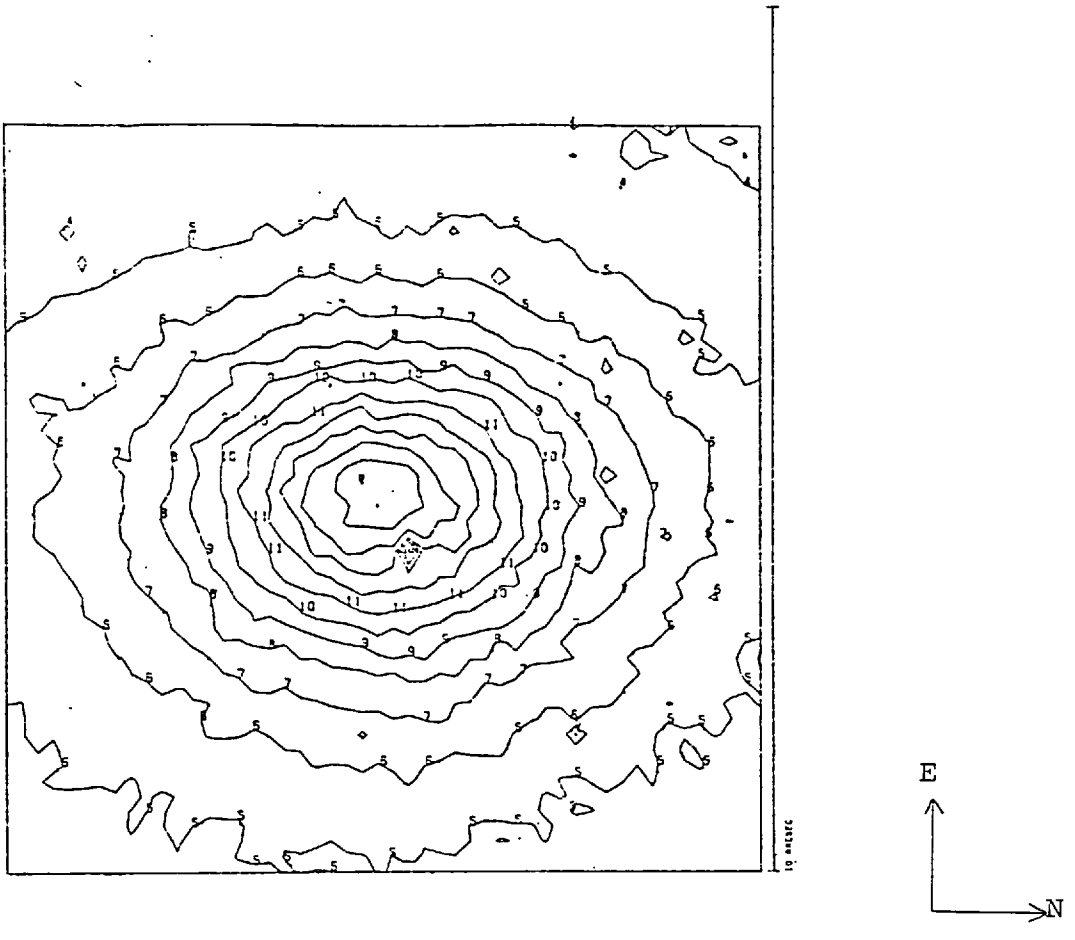

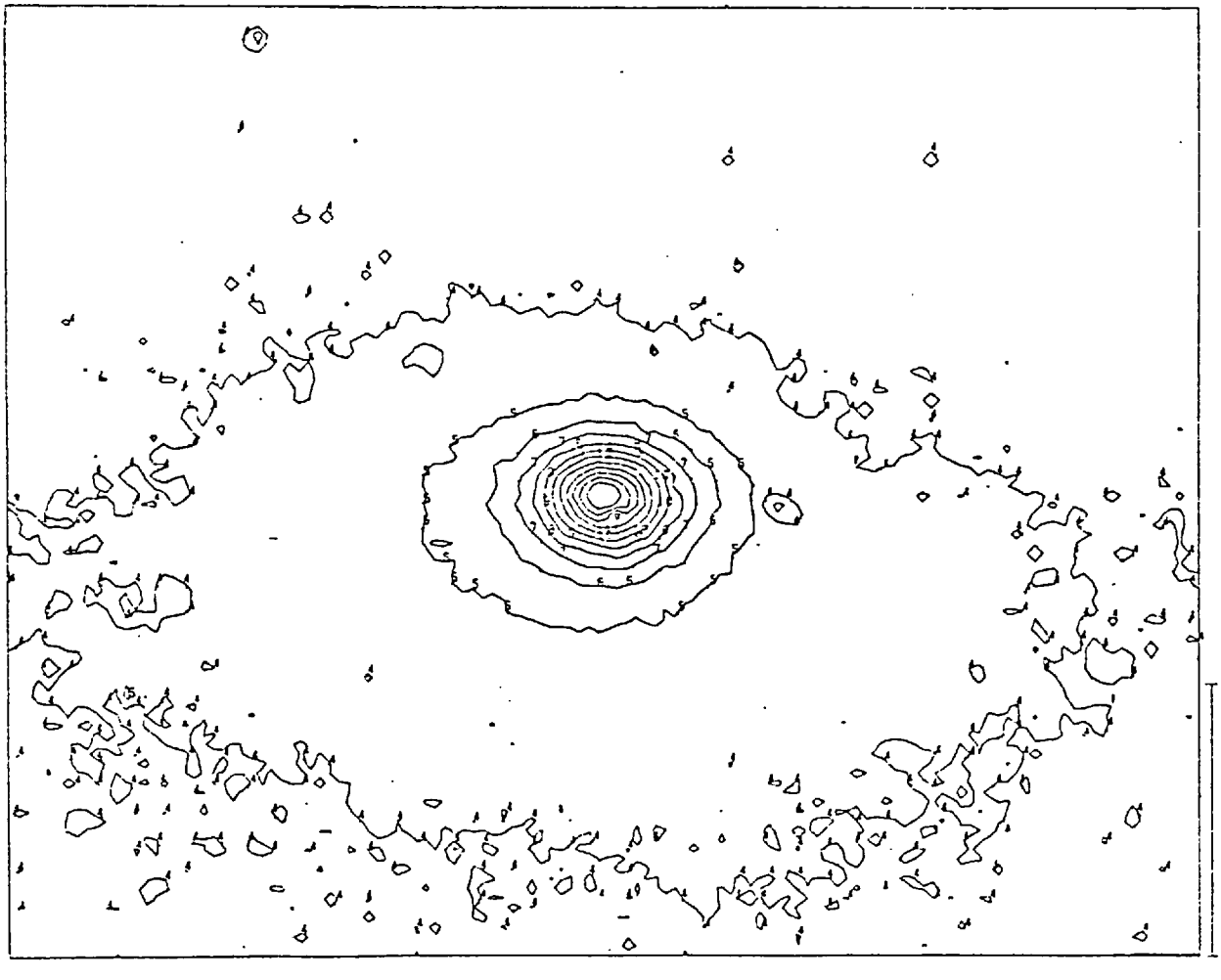

FIGURE 4.23 NUCLEUS AND INTERMEDIATE REGIONS OF NGC 3521 FILTER V

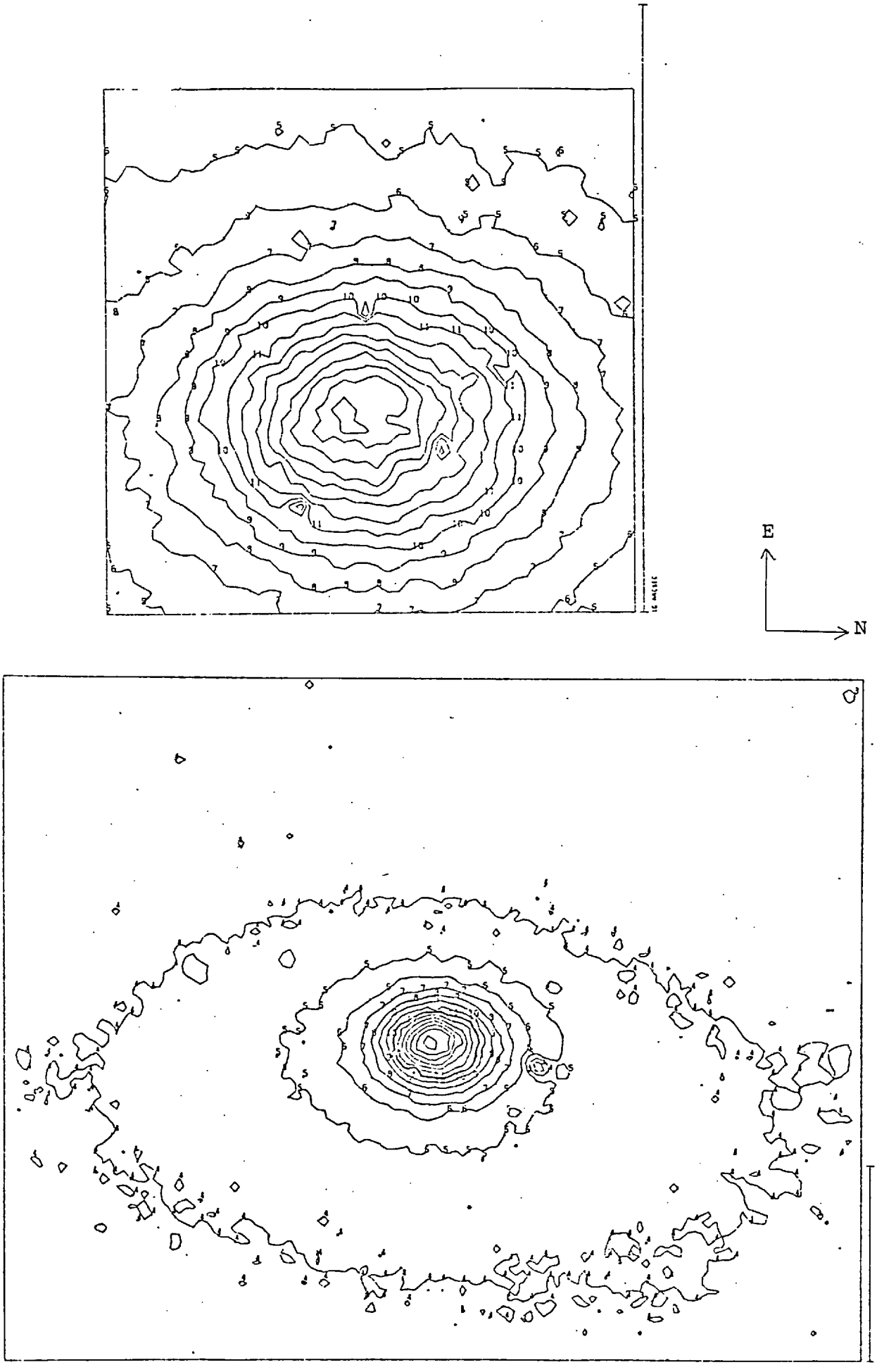

FIGURE 4.24 NUCLEUS AND INTERMEDIATE REGIONS OF NGC 3521 FILTER U

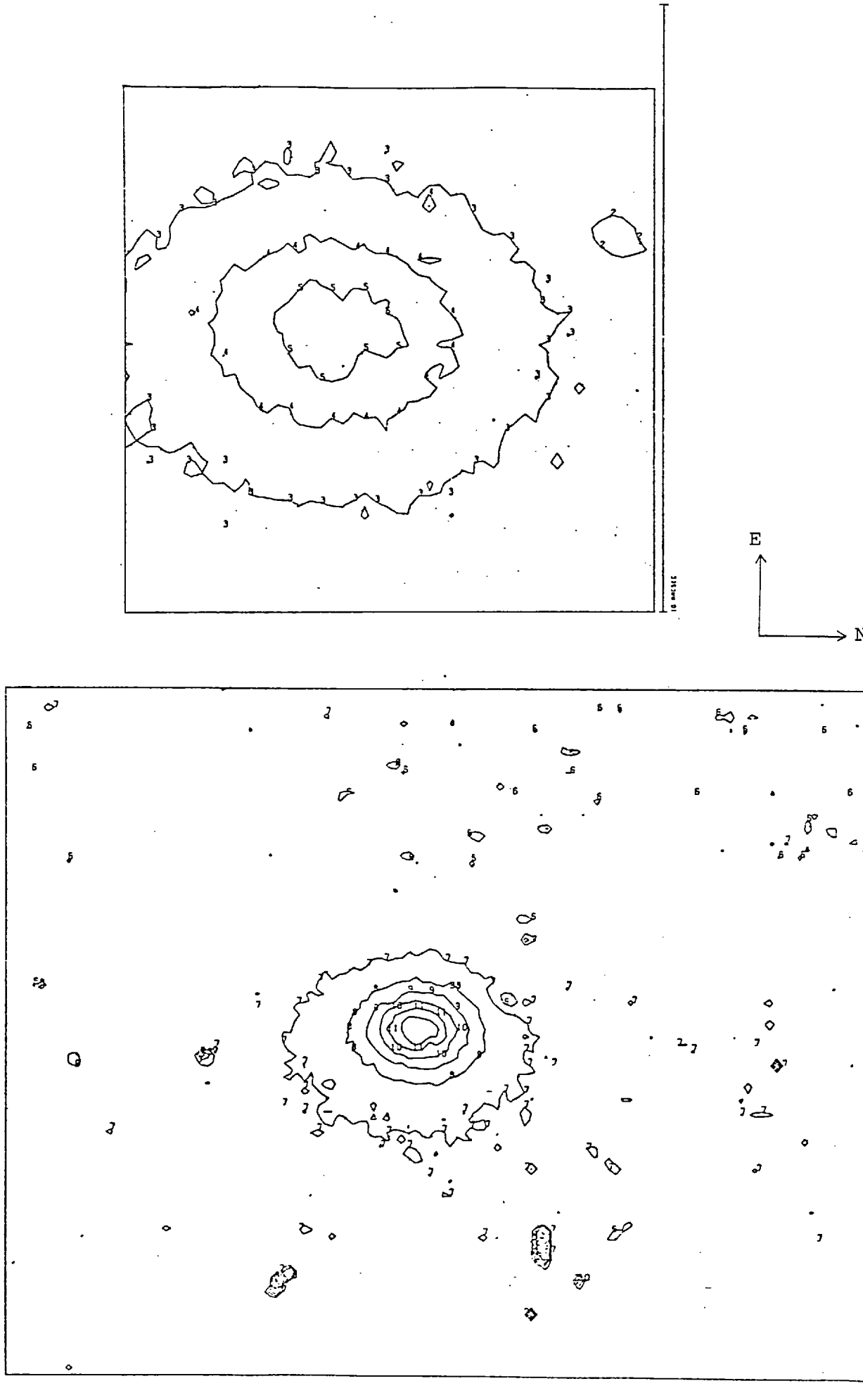

(1961) alongside a map of the corrected 50 μm scan of electronograph B13 drawn to the scale. A photograph of the electronograph is also given. A comparison of these shows that only a small area of the galaxy appears on the electronograph and that more information appears to be present on the photograph, i.e. spiral arms are more visible on the photograph. The photograph was taken on a larger telescope with a longer exposure time, but the efficiency of the technique of electronography should permit the electronographs in the present study to have a similar information content. The apparent lack of information on the electronograph is not real, but is caused by the linearity of the electronographic technique and the inability of the human eye to discern features where the luminosity gradients are low. The contour maps are a poor way of displaying information when the features which are being studied have low luminosity gradients or are in faint regions which are affected by poor signal-to-noise (see section 3.5). A careful study of the contour maps is necessary in order to "see" the stars and bright arms of the galaxy which are visible on the photograph.

The maps of the region of intermediate luminosity of the galaxy show an asymmetry in the luminosity which is caused by the galaxy being at an angle to the line of sight. These maps indicate that the west edge is closer to us than the east edge. Cross-sections through the major and minor axes of the galaxy on electronograph B13 are shown in figure 4.25. The axis ratio of the outer contour on the maps is 0.55 ± 0.02.

FIGURE 4.25 CROSS-SECTION THROUGH CENTRE OF NGC 3521 FILTER V

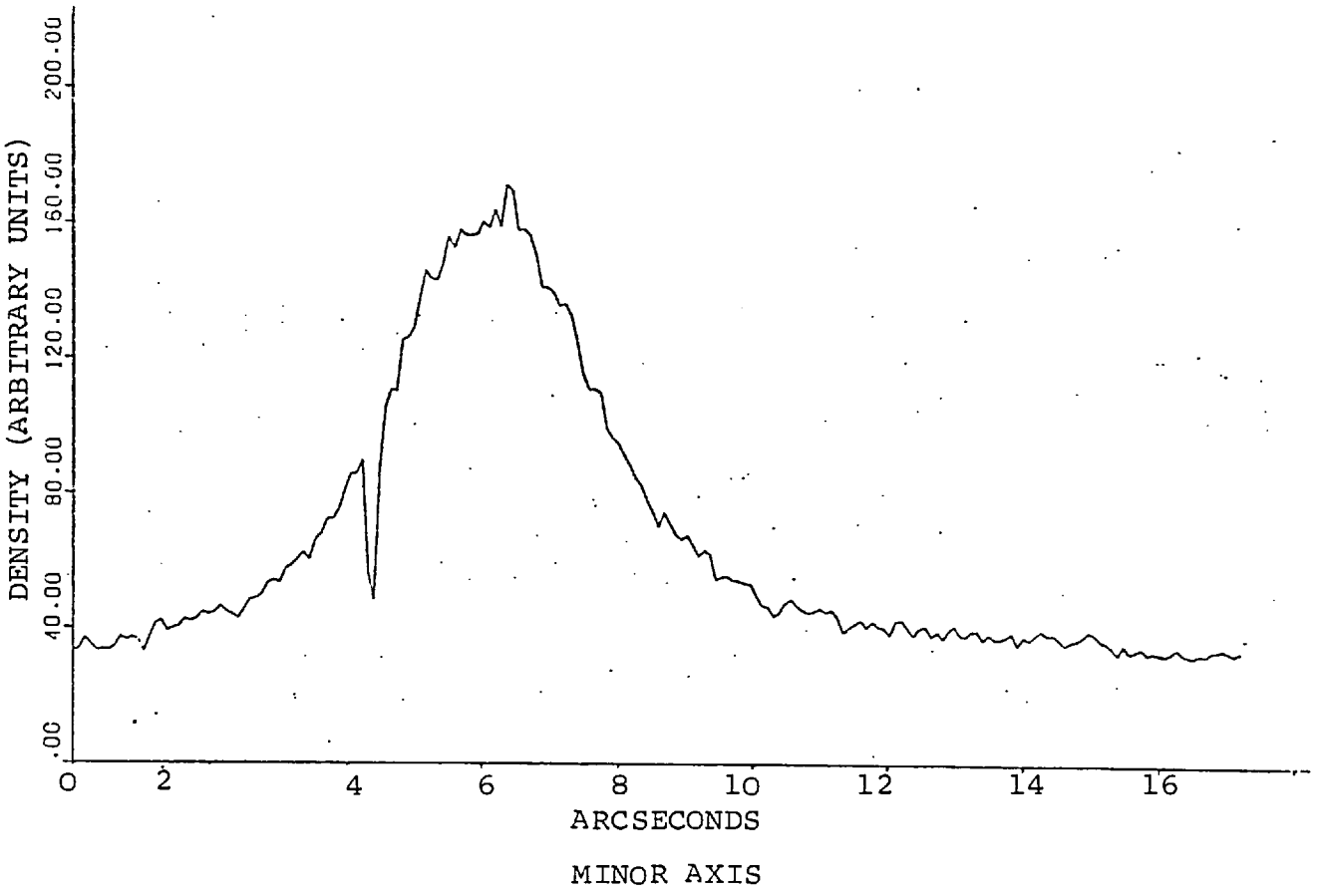

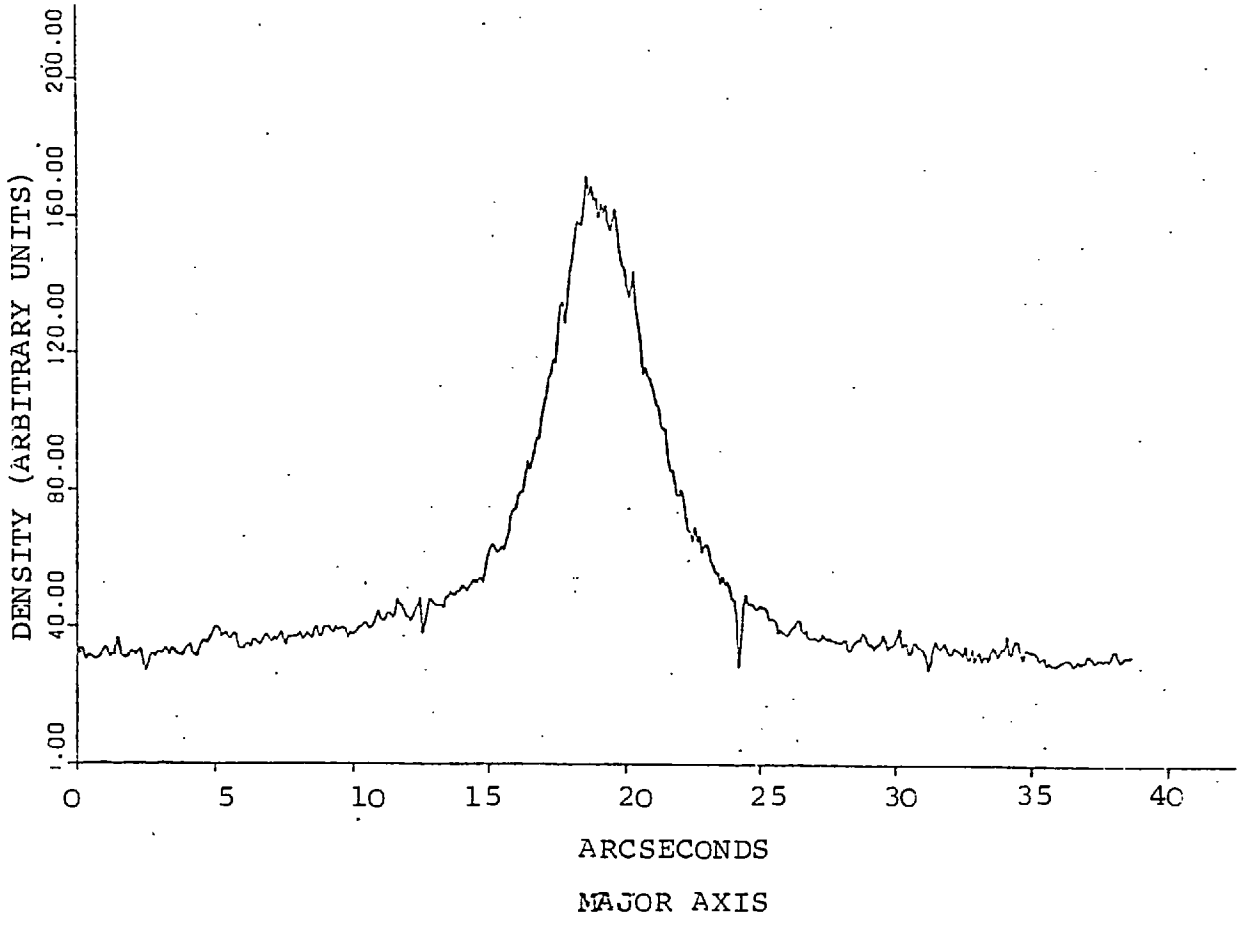

B-V maps of the nucleus were drawn (see figure 4.26) to study the local colour within the galaxy. These maps show that, approaching the centre of the galaxy, its colour becomes redder (i.e. B-V increases). However, within the central 3$^{\prime\prime}$ (200 pc radius) this trend reverses and the centre is slightly bluer than the area around. The centre has a colour index which is 0.2 below the maximum index. Similar zones of opposite colour from the central core have been observed in a variety of galaxies (Tifft, 1969). It has been suggested that the effect may have been caused by a change of about 25% in the seeing diameter during the observations. Although this would have created a low colour index in the centre of the nucleus, it would have caused a high colour index in the outer regions, but this was not observed.

NOTE: The large rise and fall in the colour index at about 5$^{\prime\prime}$ to the south of the centre of the galaxy is caused by the "dead spot" in the photocathode sensitivity (see section 3.7). This "high-low" effect was caused by the image of the galaxy being on slightly different parts of the photocathode on each exposure. The colour index over this map is not affected by this shift in position because the photocathode sensitivity is relatively constant over this region (see above).

4.7.4 Photometry

The integrated luminosity of NGC 3521 has been studied before (see above) so the present study can be calibrated by comparison with the results of other observers. Most of the measurements were made through diaphragms which are larger than the electronograph so the calibration is based on the measurements by Pettit (1954) of the

FIGURE 4.26 B-V MAPS OF NGC 3521

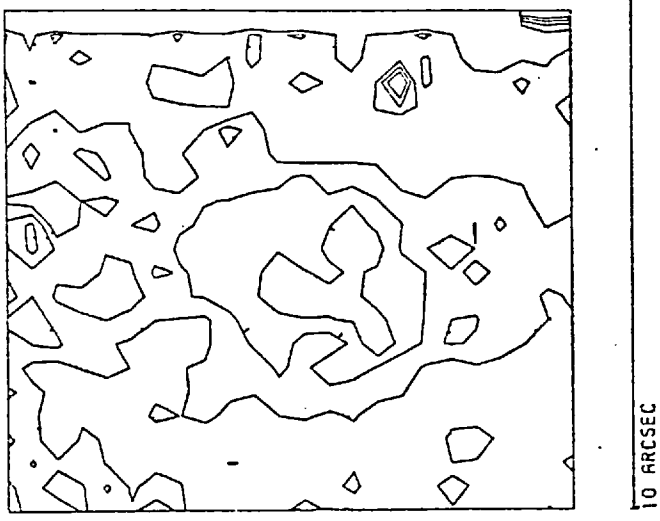

Nucleus

E

N

Nucleus and Intermediate Region

integrated luminosities through a 19^{n} diaphragm (see table 4.22). These measurements are corrected to the U, B, V system by the formula given by de Vaucouleurs (1964). The author has not found any reports of a measurement of the U luminosity through a small diaphragm so the U electronograph is not calibrated.

Table 4.22 Integrated Luminosity of NGC 3521

V	B-V	Diaphragm
11.51	0.93	19^{n}

The B and V electronographs of NGC 3521 were calibrated using the measurements in table 4.22 and some of the principal photometric parameters of NGC 3521 were measured. These parameters are listed in table 4.23.

The luminosity of the nucleus of NGC 3521 is about 1.5 mag. fainter than that of NGC 4881, when measured using Weedman's (1976) technique and allowing for distance. Therefore, Weedman would consider NGC 3521 as having a faint nucleus. However, studies of the compactness show that the nucleus of NGC 3521 is in fact more compact than that of NGC 4881 (see table 4.23). This discrepancy is due to the fact that Weedman's technique does not take into account the area over which the galaxy has a high luminosity.

Table 4.23 Photometric Parameters of NGC 3521

Integrated luminosity within 17.5$\hat{n}$ radius of peak luminosity	B	12.1	
	V	11.2	
	B-V	0.9	
Observed peak surface luminosity	B	16.0	mag.arcsec^{-1}
	V	15.2	"
	B-V	0.8	"
V magnitude within 4.2 kpc (72$\hat{n}$) diameter	V	10.9	
K		-30.4	
Core radius		0.54	kpc (9$\hat{n}$)
Compactness		-4.0 $\pm$ 0.4	

Calibration constants $k_B = 14.5 \pm 0.1$

$k_V = 13.9 \pm 0.1$

(Boyden 1.5 telescope, B275 spectracon, F Wedge, L4 emulsion, 20 μm step).

4.8 Summary

Table 4.24 lists a summary of the results which were given in this chapter. The compactness given in column 5 was calculated using the method given in section 4.1; each measurement of compactness is accurate to $\pm$ 0.4 magnitudes per square parsec. A correction for the effect of atmospheric seeing on these results was not made, although this effect makes the more distant galaxies appear less compact. The effects of "seeing" could have been removed if the seeing profile had been deconvolved from the galaxy profile, but the techniques to do this were not available.

Table 4.24 Compactness of Galaxies

Galaxy	Apparent Recession Velocity (km. sec^{-1})	Core Radius (parsecs.)	Core Magnitude	Compactness
NGC 3521	604	540	11.5	-4.2
1ZW86	5779	1500	15.2	-3.0
NGC 4881	6700	1600	16.0	-2.4
1ZW166	7819	1500	16.1	-2.7
1ZW129	10500	3500	15.1	-2.6

The table shows that NGC 3521 has the most compact nucleus. As it is a fairly close galaxy, it is apparently bright and therefore easy to study in more detail in the future. It is possible that 1ZW166 and 1ZW 129 may have a compactness as high as that of NGC 3521, but the effect of seeing has made them appear less compact.

NGC 4881 appears the least compact, even though some galaxies are more distant and affected by atmospheric "seeing".

These studies indicate that the compact part of a compact galaxy has a diameter of less than 3 kpc, but this figure would probably be nearer 2 kpc if the effects of "seeing" are removed. It would also have a compactness (as defined in section 4.1) of less than -2.5, and possibly even less than -4.0 after removal of the effects of seeing.

CHAPTER 5

A STUDY OF INTERCONNECTED AND COMPACT GALAXIES

Four galaxy systems were chosen from Zwicky's "Catalogue of Eruptive and Post-Eruptive Galaxies" (1971). The systems are not representative, having been chosen mainly for their brightness ($m_{pg} > 16$), convenient observing position in the sky and for being in unmistakeable fields. They were also chosen for their size because the image of the whole system had to lie within the field covered by the spectracon.

5.1. 1ZW41

Zwicky has described 1ZW41 as "interconnected, blue post-eruptive pair of galaxies with compact cores and extended plumes" (Zwicky, 1971). In the morphological Catalogue of Galaxies (Varontsov - Velyaminov, 1962), 1ZW41 is noted as showing an "interaction with tails". The northern component is designated MCG 9-20-33 (N;C) and the southern component 9-20-34 (N). Chincarini and Rood (1974) gave the photographic magnitudes as 14.5 and 15.3 for the galaxies which have a separation of 35" (17.5 kpc). The northern component has an elliptical main body of 7" by 12" with a wide plume to the North which is 15" long. The southern component is 12" by 25" and has a wide plume extending 15" to the West (Sargent, 1970). (see figure 5.1)

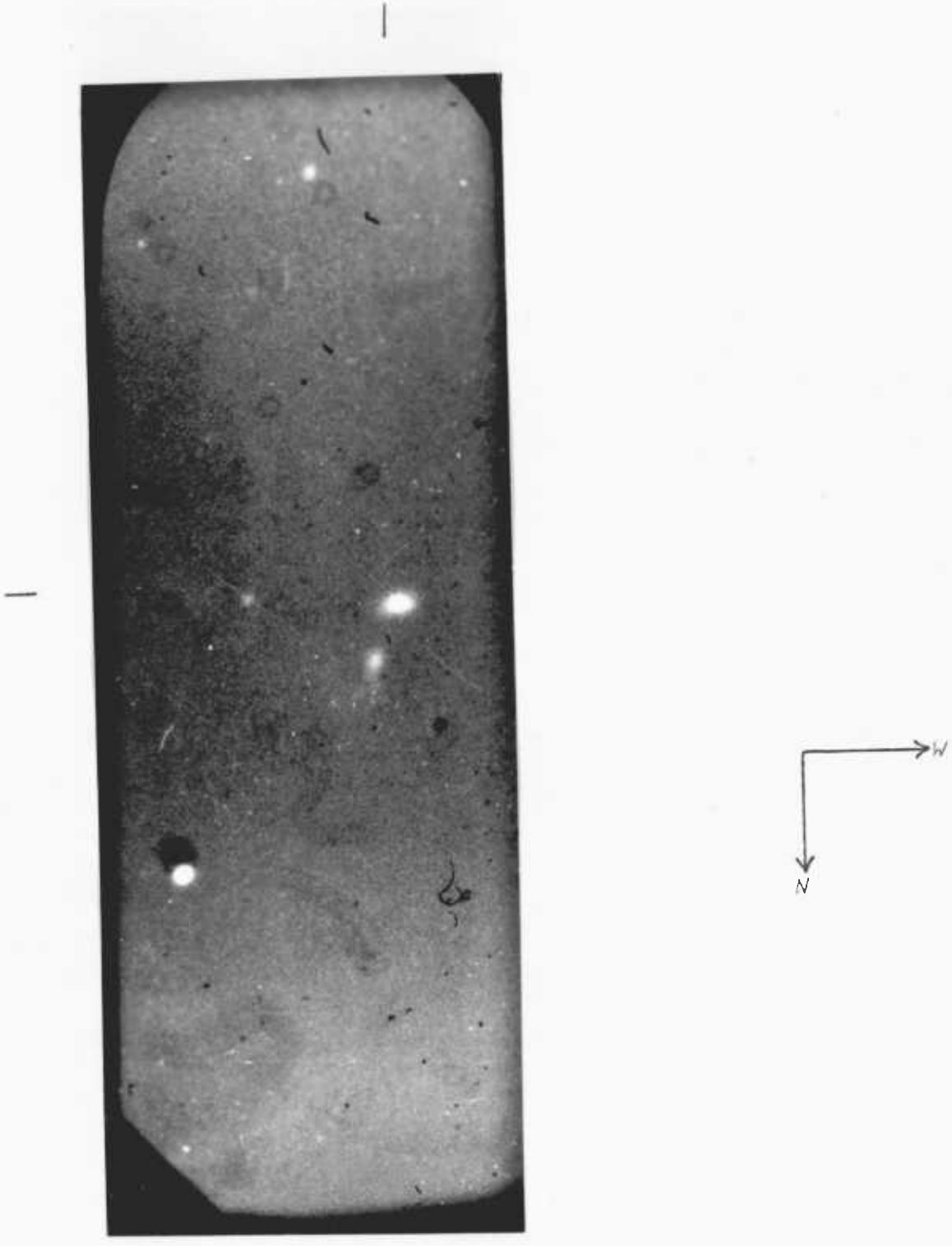

FIGURE 5.1 ELECTRONOGRAPH OF 1ZW41 MAGNIFIED APPROXIMATELY 6.3x

Table 5.1	Elements of 1ZW41
R.A. (1950)	12^h 41.5m
Declination (1950)	+55°10'
Photographic magnitudes	14.5 and 15.3
Dimensions	12″ by 25″ and 7″ by 12″
Separation of Galaxies	35″
Apparent Corrected Radial Velocity	4998 km.sec^{-1}

Zwicky (1971) studied the spectra of the components and both show the Balmer lines in absorption. They also show emission from the forbidden (OII) and (OIII) lines. Sargent (1970) described the spectra as containing sharp emission lines with the southern component having early type absorption lines. He found the northern component was more compact with the emission lines coming from a region less than 5″ in diameter. The southern component has emission from a more extended region which is 12″ in diameter. Zwicky (1971) and Sargent (1970) found that the galaxies have the same redshift.

5.1.1. Observations

The electronographs which are studied in this section are listed in table 5.2.

Table 5.2 Electronographs of 1ZW41

Date	Telescope	Plate-Scale	Emulsion	Spectracon
16 June 1976	1.1m. Flagstaff	$24.1''.mm^{-1}$	G5	AS3

Electronogragraph	Exposure	Filter
F134d	19m 40s	B
F134e	15m	V

The atmospheric seeing during the observations was poor, the full width at half the maximum luminosity of a star was about 5'' (200 μm). The images of 1ZW41 lie just off the central region of the photocathode of the spectracon where there is a large (± 5%) sensitivity variation within the area covered by the object (see section 3.7). This will be discussed later.

The bright component of 1ZW41 was initially studied using handscans from the microdensitometer. The principal results are given in table 5.3. These results give enough information to determine the parameters for scans of 1ZW41 so that handscans of the faint component were not necessary.

5.1.2. Morphology

Studies of the variation in sensitivity of the photocathode in section 3.7 indicated that the variation across the region covered by 1ZW41 is about 5%. However, the density measured on this electronograph is about 10% lower at the bottom edge of this region than

Table 5.3 Principal Elements of Handscans of 1ZW41

Electronograph	F134c	F134d
Z	0.8	0.75
Dm	1.3	1.4
G	0.007	0.007
R	1.0	1.0
Gs	0.01	0.01
a_T	15	15
a_e	110	110
Δ	5	5

at the top. These areas of the electronograph were exposed to sky background luminosity which would have been uniform. Hence, the variation across the image is larger than expected and is probably caused by an additional variation in the sensitivity of the emulsion which cannot be corrected.

Scans of 1ZW41 on each electronograph were made with a step length and aperture size of 20 μm. Normally, a more accurate study would have been made with a smaller step length and aperture, but it is not necessary in this case because the accuracy of the results will be poor due to the variation in emulsion sensitivity. Maps of the scans are shown in figure 5.2, they are blocked to 60 μm in order to reduce the emulsion noise. N.B. The small apparent dip in luminosity which appears between the galaxies is caused by a photocathode defect.

The effects of the sensitivity variation are visible on these maps, especially on the lower part of the scan of electronograph F134e. This makes it impossible to detect any extensions with a luminosity less than 23 mag.arcsec^{-2}, such as the faint plume which was observed by Sargent (1970) to the west of 1ZW41. However, the maps do show that the east edge of the southern component is extended and curved towards the faint component. This effect is very marked and can not be caused by the light from the fainter component causing an "apparent" connection of the type discussed by Hardwick and Morgan (1976) because the luminosity of the faint galaxy is negligible at this distance from its nucleus.

FIGURE 5.2 ISOPHOTE MAPS OF 1ZW41

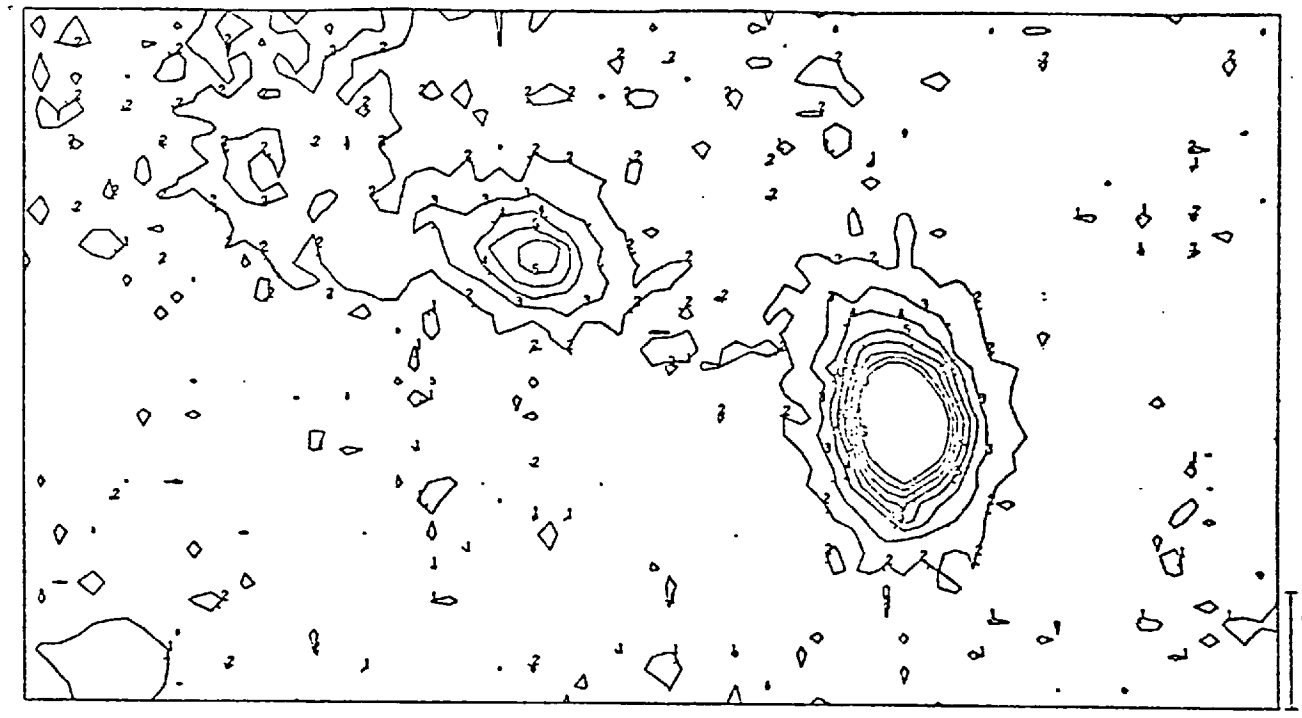

Filter B

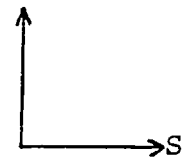

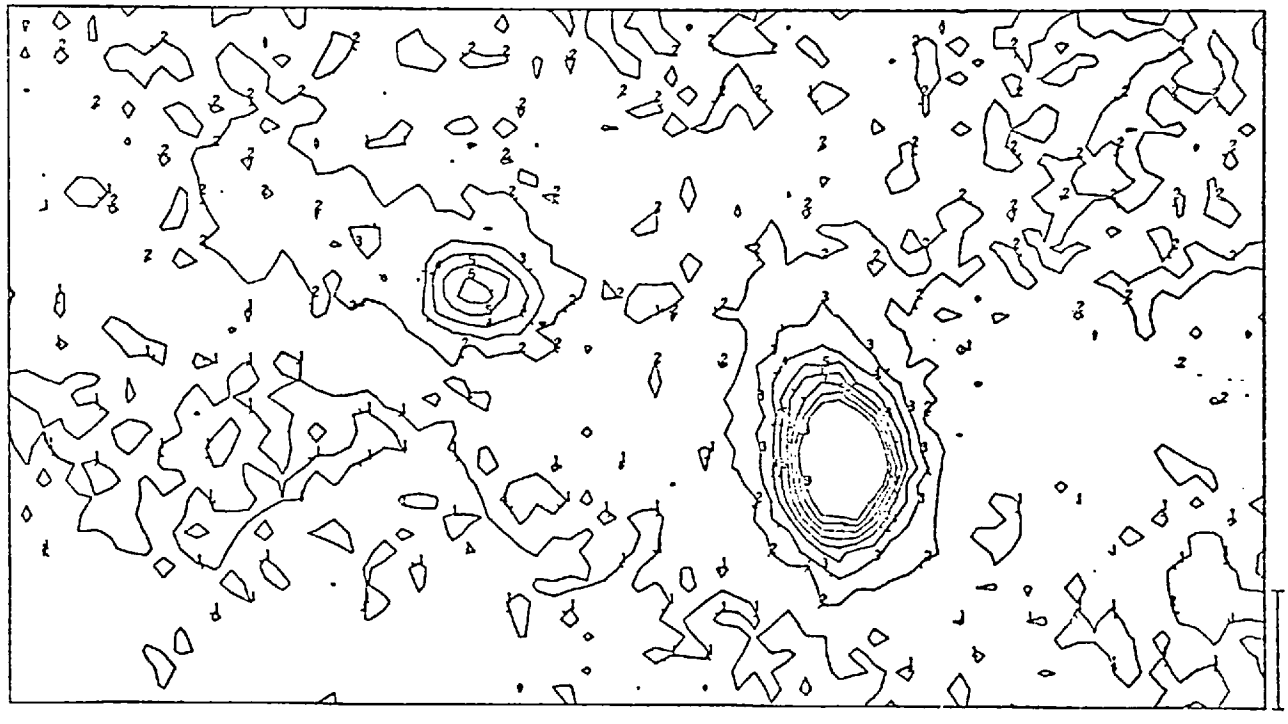

Filter V

The dimensions of the southern component, measured from the electronographs, are 35$^{\prime\prime}$ by 20$^{\prime\prime}$ (17.5 kpc by 10 kpc). However, the sensitivity variation described above will have affected the measurement so the true length of this component must be greater than 35$^{\prime\prime}$. A plume of luminosity which extends from the faint component is visible on both electronographs. It stretches to the North and then curves east. The length of plume is about 20$^{\prime\prime}$ (10 kpc). This component has dimensions of 20$^{\prime\prime}$ by 15$^{\prime\prime}$ (10 kpc by 7.5 kpc). The separation of the galaxies is 35.0$^{\prime\prime}$ (16.8 kpc), a measurement which is in good agreement with the results of Sargent (1970).

No luminosity can be detected between the galaxies at a level which is only 1% above the sky background i.e. a "bridge" can not be detected between the galaxies at a luminosity of 25 mag. arcsec^{-2}. Hence, although the galaxies have a similar colour, 1ZW41 is unlikely to be the result of one galaxy breaking up. However, it is unlikely that the galaxies are a line-of-sight double because the plumes and the luminosity distribution suggest that there is a gravitational interaction between them. They also have identical redshifts (Sargent, 1970). 1ZW41 therefore appears to be caused by an encounter between two distant galaxies. As the velocities of the galaxies relative to each other are not known, one cannot determine if the system is bound.

5.1.3 Photometry

Table 5.4 lists some of the photometric parameters of the components of 1ZW41. The integrated

Table 5.4 Photometric Parameters of 1ZW41

		Bright Component	Faint Component
Integrated magnitude within 22 mag.arcsec^{-2}	B	14.7	15.7
	V	14.4	15.5
	B-V	0.3	0.2
Peak surface brightness observed	B	19.5	20.7
	V	19.2	20.3
	B-V	0.3	0.4
Maximum detected radius	arcseconds	20	13
	parsecs	10	6.5
Axis Ratio		0.67 $\pm$ 0.02	0.70 $\pm$ 0.02
Separation		35.0" = 16.8 kpc	
Calibration constants	k_B	= 19.5 $\pm$ 0.1	
	k_V	= 19.5 $\pm$ 0.1	
Core magnitude		15.2	16.6
Compactness		-1.8	-0.4

magnitudes of the galaxies were found by integrating the luminosity within luminosity levels centred on each galaxy. Since the western edge of the image of the bright component on electronograph F134e lies on a region of low sensitivity which cannot be corrected (see previous section), the measurement of its integrated magnitude is probably low, by up to 1% (0.1 mag.). This makes the galaxy appear slightly bluer. The effect on the fainter galaxy is smaller. Allowing for the errors involved, the components of 1ZW41 appear to have a similar colour (B-V = 0.3) and the brighter component is 1.1 magnitudes brighter than the faint component.

As the sensitivity variations are so large (see previous section), it is not possible to study the local colours of 1ZW41. However, a comparison of the maps shows that the plume from the faint component has a similar morphology and luminosity in each colour. This study found that the plume is fairly blue and has a colour index of 0.1 ± 0.2 which is lower than that of the galaxies.

A measure of the compactness (see section 4.1) of each component (see table 5.4) shows that the compactness of the brighter component is only slightly less than that of the galaxies which were studied in the previous chapter.

5.2. 1ZW208

1ZW208 is a pair of blue, coalesced, spherical compacts (Zwicky, 1971). Sargent (1970, misnamed 1ZW207) describes it as a hard elliptical image,

16″ by 10″ (15.1 by 8.4 kpc). The spectrum has been studied by Sargent and Zwicky who found recession velocities of 8936 km.sec^{-1} (corrected) and 8740 km. sec^{-1}, respectively. Sargent found sharp emission lines in the spectrum and Zwicky reports the forbidden OII line in emission with H_δ, H_ϵ, H_ζ, H_η in absorption.

Table 5.5 Elements of 1ZW208

R.A. (1950)	18h 31.6 m
Declination (1950)	+54° 29'
Photographic magnitude	14.8
Dimensions	10″ by 10″
Apparent Recession velocity	8740 km.sec^{-1}

Table 5.5 lists the elements of 1ZW208 which were given by Zwicky (1971), but Sargent (1970) gave the photographic magnitude as 16.

In the introduction to the "Catalogue of Eruptive and Post-Eruptive Galaxies", Zwicky (1971) suggests that 1ZW208 may be in a class of galaxies which exhibit the phenomenon of having a difference in redshift between the core and the outskirts of the galaxy. In this case, he suggests that this is caused by a gravitational redshift of value 1000 to 2000 km.sec^{-1}.

5.2.1 Observations

The electronographs used for this study are listed in table 5.6.

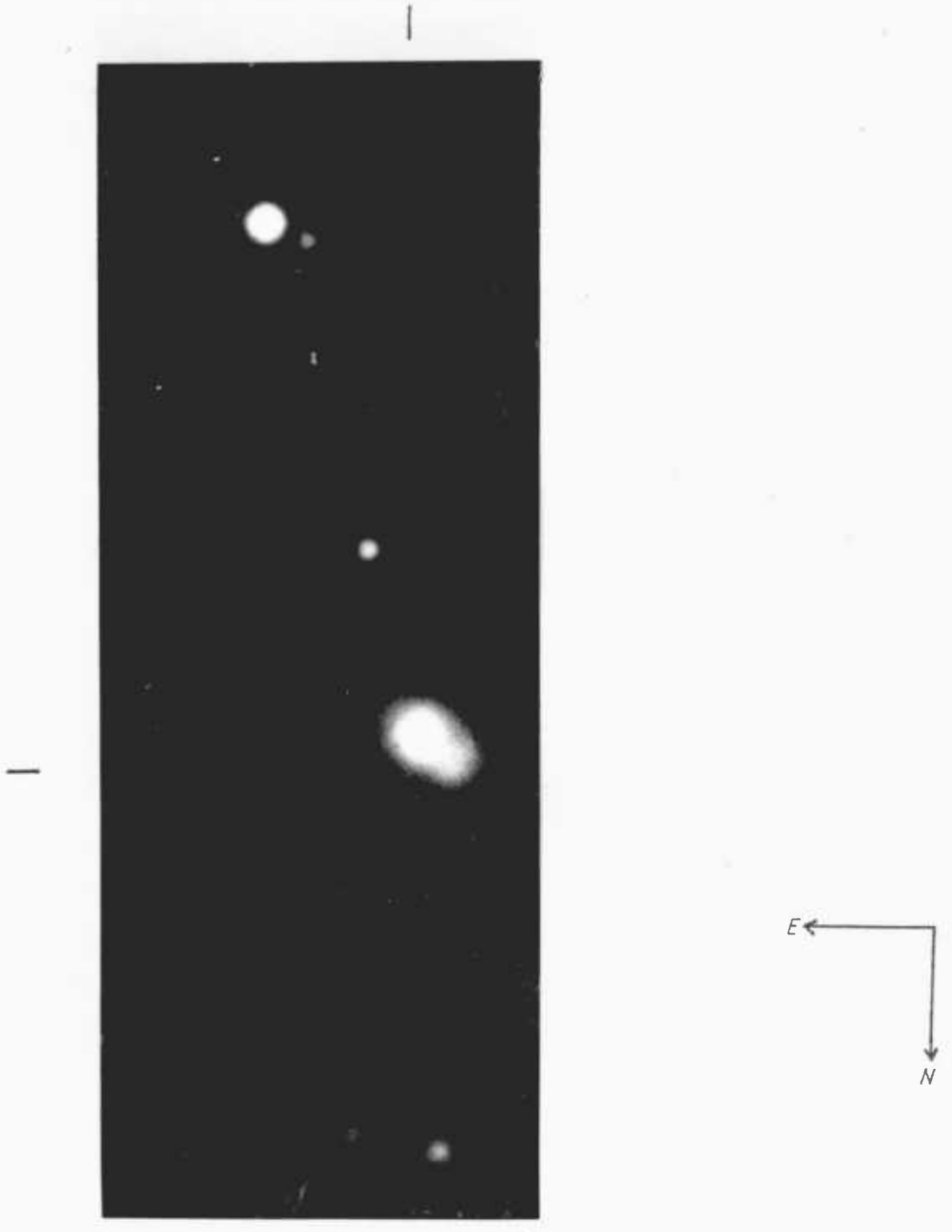

FIGURE 5.3 ELECTRONOGRAPH OF 1ZW208 MAGNIFIED APPROXIMATELY 6.3x

Table 5.6 Electronographs of 1ZW208

Telescope	Plate Scale	Emulsion	Spectracon
1.8m Flagstaff	$6.64\hat{''}.mm^{-1}$	G5	AS7

Date	Electronograph	Exposure	Filter
8 June 1976	F99c	80m105	V
9 June 1976	F101c	100m	B
	F101d	30m	V

The longer exposures were interupted while the focus was checked. The seeing during the observations, derived from measures of stars on the electronograph, was about $3.5\hat{''}$. Handscans of these electronographs using the microdensitometer were used to produce the results which are listed in table 5.7. All the images are slightly affected by scratches on the photocathode, this will be shown later.

The image of 1ZW208 falls on the edge of the curved mica window where the curvature of the window would distort the images (see section 1.3). The image is not corrected for the distortion because the distortion would have only a small effect (less than 5%) on morphological studies, and accurate photometry of this object was not attempted.

5.2.2 Morphology

Each exposure was scanned with a step length and aperture size of 20 μm. Maps of these scans, blocked to an analysing aperture of 100 μm to reduce emulsion noise, are shown in figure 5.4. The

Table 5.7 Principal Elements of Handscans of 1ZW208

seeing (S) = $3.5''$ = 500 μm

Electronograph	F101c	F101d	F99c
Z	0.2	0.2	0.45
Dm	1.4	1.0	2.0
G	0.0014	0.001	0.004
R	1.2	0.8	1.5
Gs	0.004	0.003	0.007
a_T	100	100	30
a_e	200	200	140
Δ	20	20	10

FIGURE 5.4 MAPS OF 1ZW208

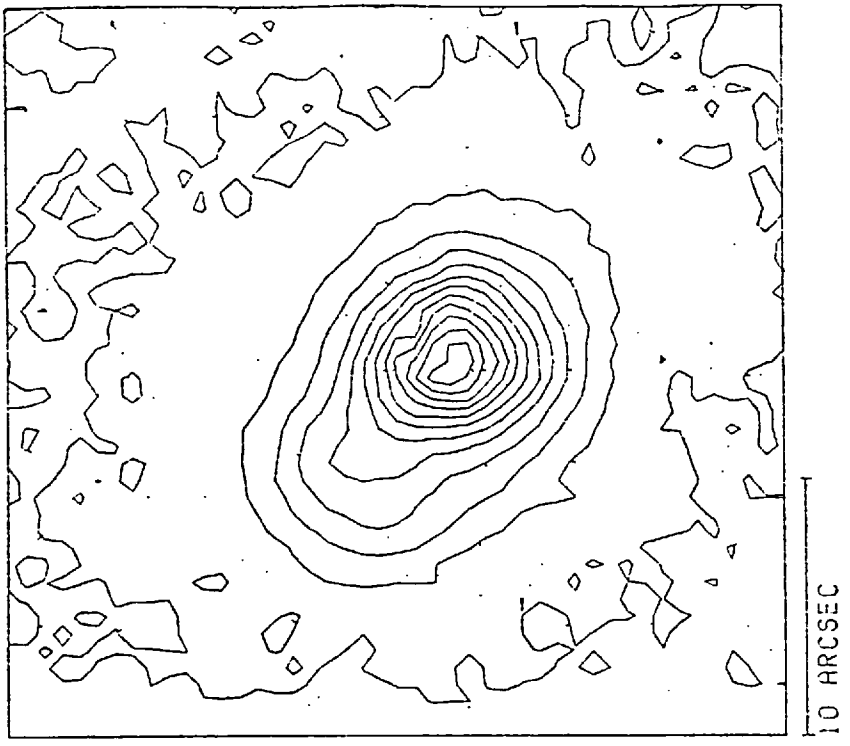

Electronograph F101d
Filter V

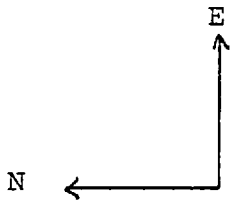

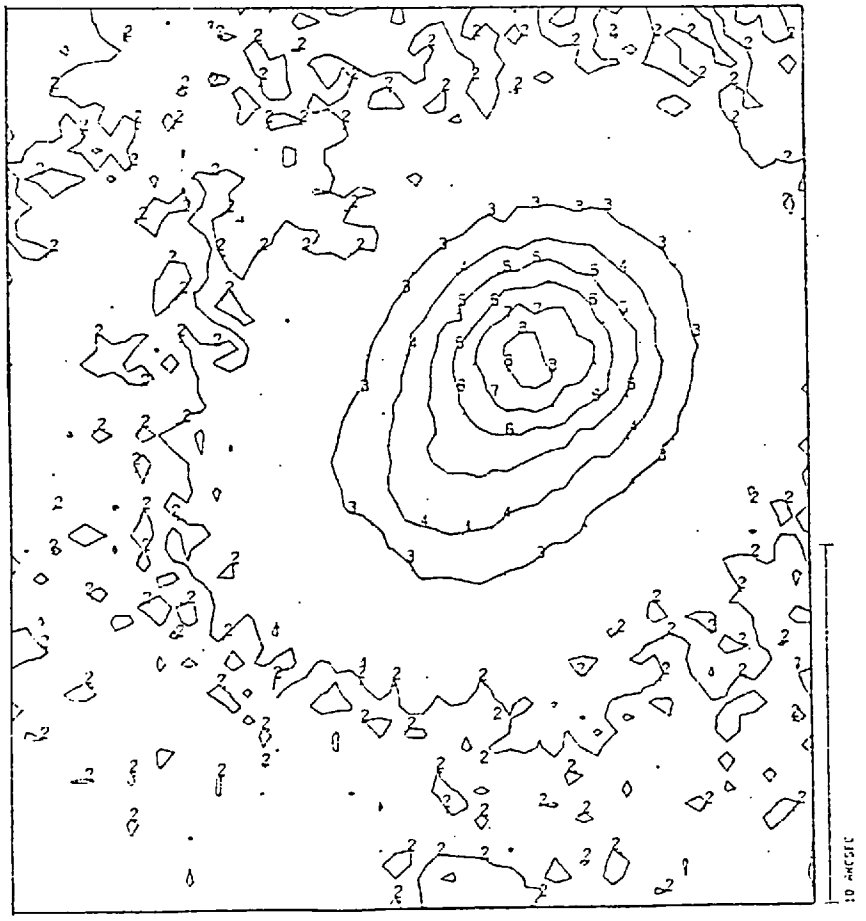

Electronograph F101c
Filter B

scratches on the photocathode appear on these maps as curved lines where the density is low. These maps show that 1ZW208 has axial symmetry and the smoothness of the contours implies that there are no eruptive processes occuring in it. However, cross-sections along the axis of symmetry (shown in figure 5.5) show a second peak in the luminosity which is 5.3" (4.6 kpc) from the main peak. 1ZW208 can be detected to 30" by 20" (26 x 17 kpc) but the main luminosity comes from the central 5". This central core is not much larger than the "seeing".

The electronograph (see figure 5.3) and detailed maps (see figure 5.6) indicate the existence of a faint, elliptical, nebuleus object alongside the bright core of 1ZW208. It is this object which causes the secondary peak in luminosity which is shown on the cross-section (figure 5.5).

NOTE: A small hair on electronograph F99C caused the small dip in density which is shown on the contour map.

The core of 1ZW208 appears to be a bright, circularly symmetric galaxy. The faint object alongside this core may be either:

(1) a galaxy seen in projection

or (2) a galaxy in close proximity to, and interacting with, the bright galaxy,

or (3) matter associated with, or even ejected from, the bright galaxy.

The uniformity of the bright galaxy and the fact that Zwicky (1971) measured a difference in

FIGURE 5.5 CROSS-SECTION THROUGH 1ZW208

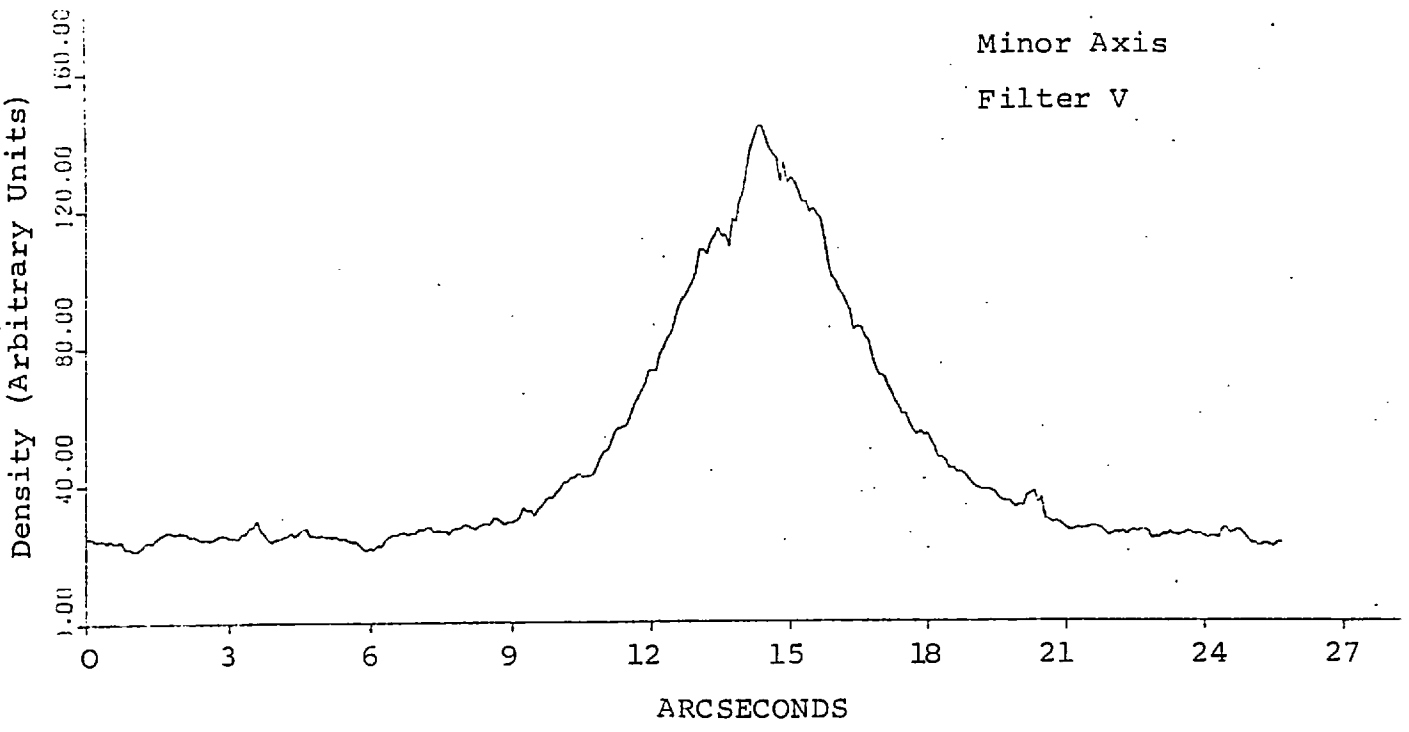

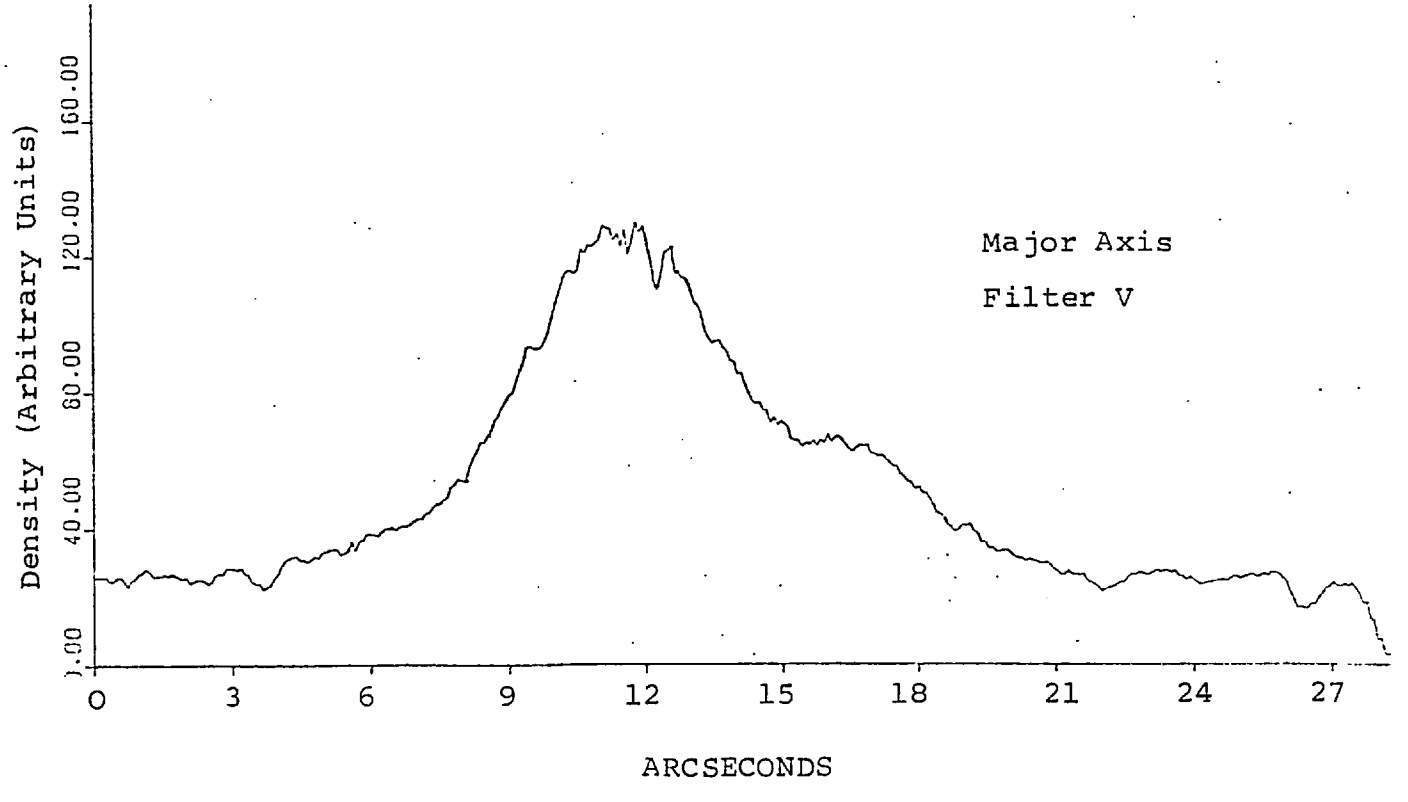

FIGURE 5.6 MAPS OF INTERMEDIATE REGIONS OF 1ZW208

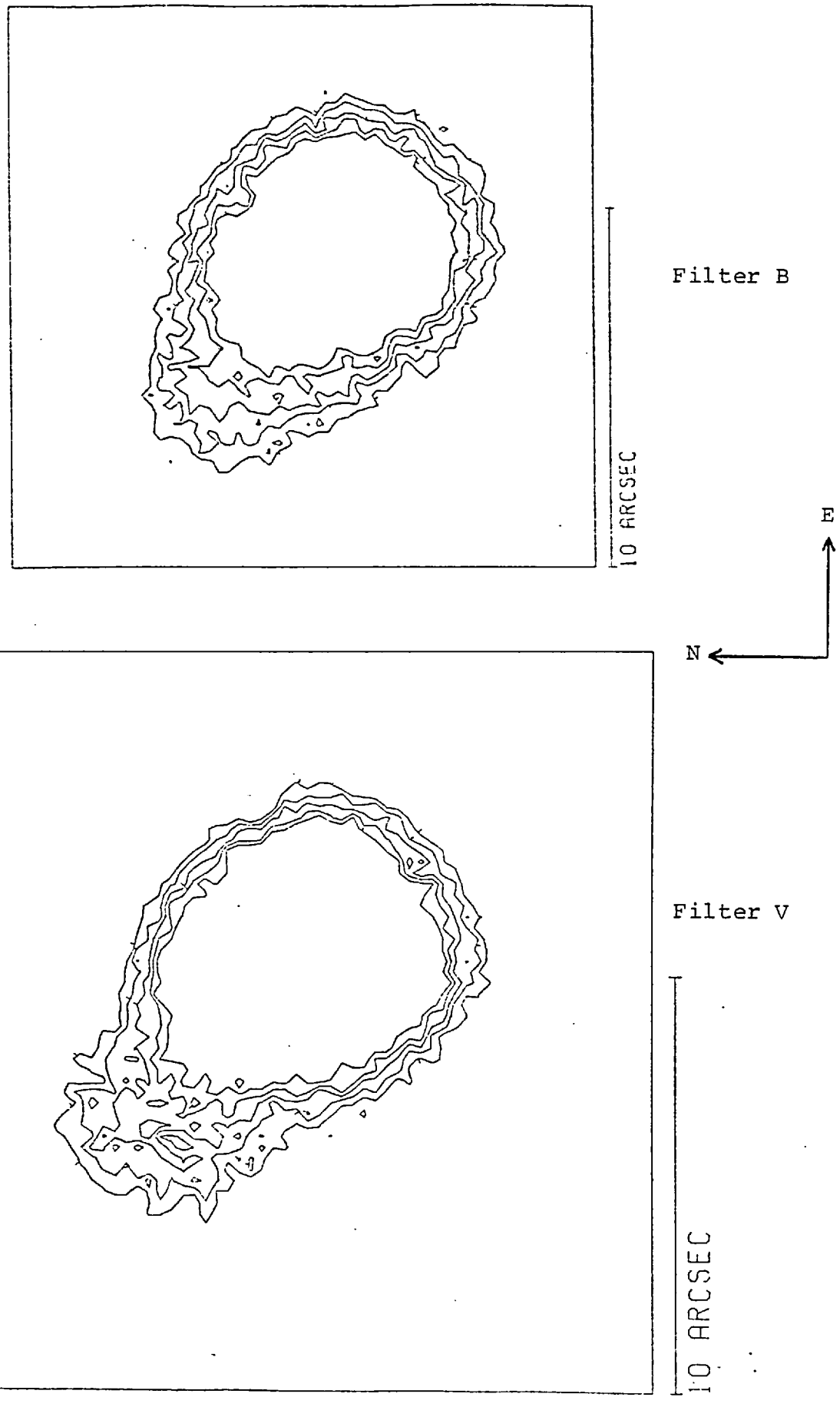

redshift of 1000 to 2000 km.sec^{-1} for 1ZW208 suggests that 1ZW208 is composed of two galaxies seen in projection. Zwicky (1971) suggested that 1ZW208 is composed of two blue spherical compacts, but the contour maps indicate that the fainter galaxy is elliptical, with an axis ratio of 0.6 $\pm$ 0.2.

5.2.3 Photometry

The calibration stars for this telescope were unfortunately over-exposed. In addition, this spectracon has an S-20 response, so a comparison of the B and V results is not possible and no photometric parameters could be measured for 1ZW208.

The difference in luminosity between the two components of 1ZW208 can be estimated by assuming that the luminosity of the faint component is negligible on the far, south-east side of the bright component. The total luminosity of the bright component can then be calculated by integrating only the luminosity on the south-east side, and doubling this value. The luminosity of the faint component and the luminosity difference can then be calculated by subtracting this value from the total luminosity of 1ZW208. The difference in luminosity of the components was calculated as 1.7 $\pm$ 0.5 mags. by this method.

5.3. 1ZW207

This object was described by Zwicky (1971) as a very blue boomerang-shaped, post eruptive galaxy. It has a width of 45$''$ and a photographic magnitude of 15.5. Zwicky (1971) found emission in the Balmer

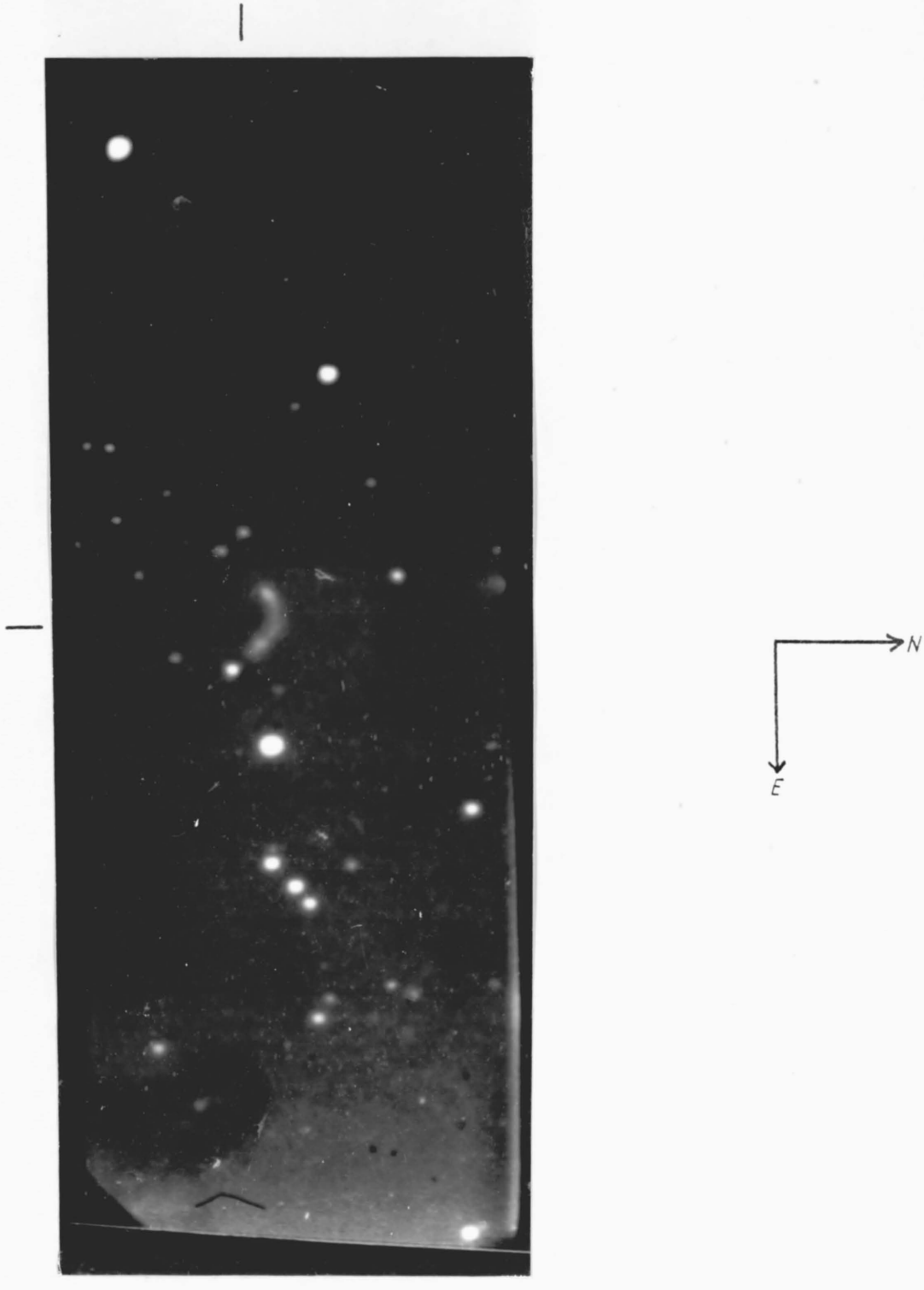

FIGURE 5.7 ELECTRONOGRAPH OF 1ZW207 MAGNIFIED APPROXIMATELY 6.3x

lines and the forbidden OII line and measured a recession velocity of 5535 km.sec^{-1}. Sargent (1970) also described it as a very blue boomerang-shaped object which is composed of bright knots. He found sharp emission lines in the spectrum and measured a recession velocity of 5762 km.sec^{-1} (corrected to the centre of the galaxy). It is suggested by Sargent (1970) that 1ZW207 could be two interacting galaxies of width (end-to-end) 30″ (17 kpc).

Table 5.8 Elements of 1ZW207

R.A. (1950)	18h.30.2m
Declination (1950)	+ 55°14′
Photographic magnitude	15.5
Width	45″
Corrected Apparent Recession Velocity	5535 km.sec^{-1}

5.3.1 Observations

The electronographs listed in table 5.9 are studied in this section. The seeing diameter, measured from a star profile, was about 4″ on this clear night. Measurements of these electronographs by handscanning on a microdensitometer produced the results which are listed in table 5.10.

Table 5.9 Electronographs of 1ZW207

Date	Telescope	Plate-Scale	Emulsion	Spectracon
12 June 1975	1.1m Flagstaff	24.1″.mm^{-1}	G5	AS3

Electronograph	Exposure	Filter
F114a	30m30s	B
F114b	30m10s	V

5.3.2 Morphology

Both electronographs were scanned with a step-length and aperture of 40 μm over a large area containing 1ZW207. No extensions from the object were found to a level of 26 mag.arcsec^{-2}, so maps are shown only of the object and its immediate area (see fig. 5.8). On electronograph F114b the effect can be seen of a gentle rise in the photocathode sensitivity from the top to the bottom of the scan. This sensitivity variation is only about ± 2% across the object.

These maps show that 1ZW207 does contain knots of luminosity which were suggested by Sargent (1970). There are two bright areas of luminosity at each end of 1ZW207, the one to the west being slightly brighter (see next section on photometry). The separation of these two cores is 27″ (15 kpc) and the whole object is contained within an area of 56″ by 35″ (32 x 20 kpc).

A B-V map of 1ZW207 (see figure 5.9) shows that the object is very blue (B-V = -0.5) midway between

Table 5.10 Principal Elements of Handscans of 1ZW207

Electronograph	F114a	F114b
Z	0.25	0.25
Dm	0.35	0.35
G	0.002	0.002
R	0.3	0.3
Gs	0.003	0.003
a_T	40	40
a_e	200	200
	5	5

seeing (s) = $4''$ = 170 μm

FIGURE 5.8 ISOPHOTE MAPS OF 1ZW207

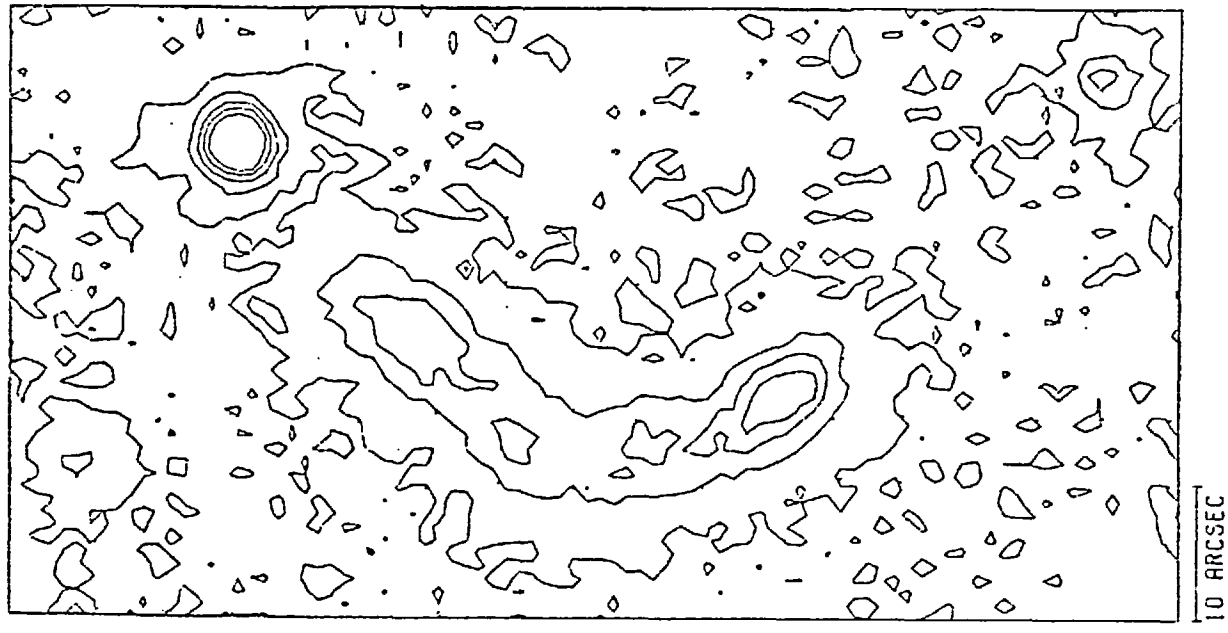

FILTER B

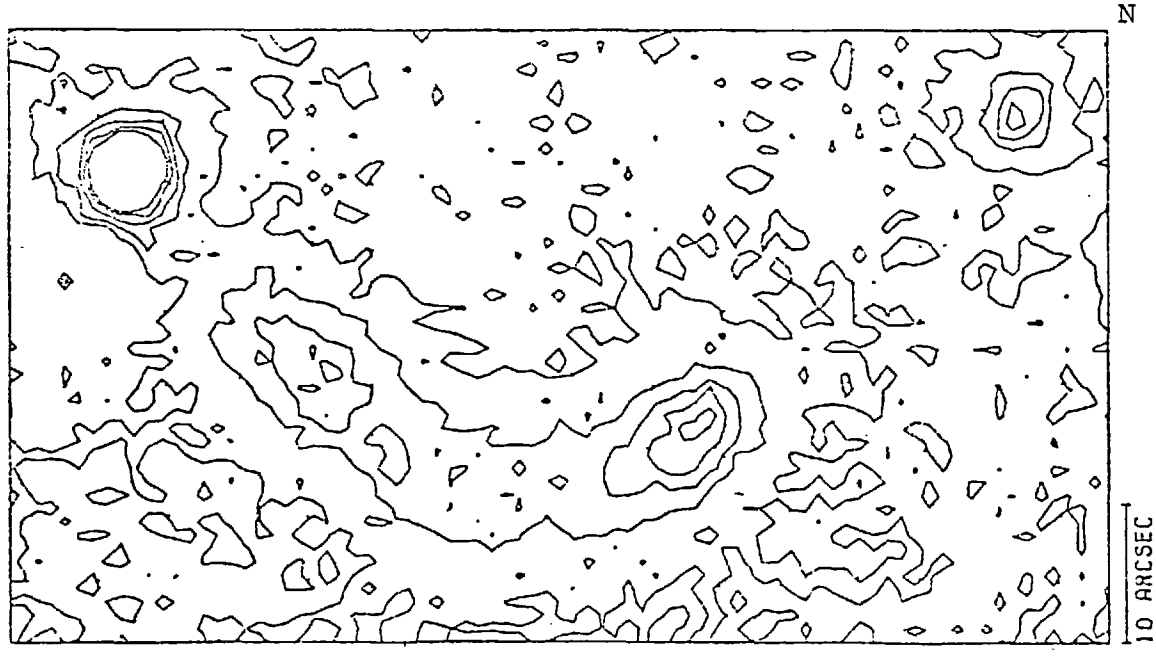

FILTER V

the luminous cores, and in the bright cores are fairly blue (B-V = 0). This shows that 1ZW207 is very blue, as suggested by Sargent (1970), and extremely blue in the centre. It also appears that the knots of luminosity have a similar colour to the rest of the object.

The morphology of 1ZW207 suggests that it is a pair of interacting galaxies which are connected by a bridge of luminous material, containing "knots" of luminosity caused by the interaction of the galaxies. The spectra, colour and small size of the components suggest that they are of similar age, composed of gas and young hot stars, and they may still be evolving.

5.3.3. Photometry

The integrated luminosity of 1ZW207 was found by integrating the luminosity greater than 26 mag. arcsec^{-2} above the sky background. The results agree well with the values given by Sargent (1970) and Zwicky (1971). The luminosity of each component was found by integrating separately the luminosity on each side of a line running midway between the two bright cores. The luminosity in this region is low so any small misalignment of this line has little effect on the calculated luminosities.

This study shows that the components of 1ZW207 are very similar and their luminosity and colour are almost identical. The knots of luminosity are fairly blue (B-V = 0) and the peak surface luminosity of the brightest knot is 23 mag.arcsec^{-2}. The brightest knots have a surface luminosity which is 24 mag.arcsec^{-2} above the surrounding material.

FIGURE 5.9 B-V MAPS OF 1ZW207

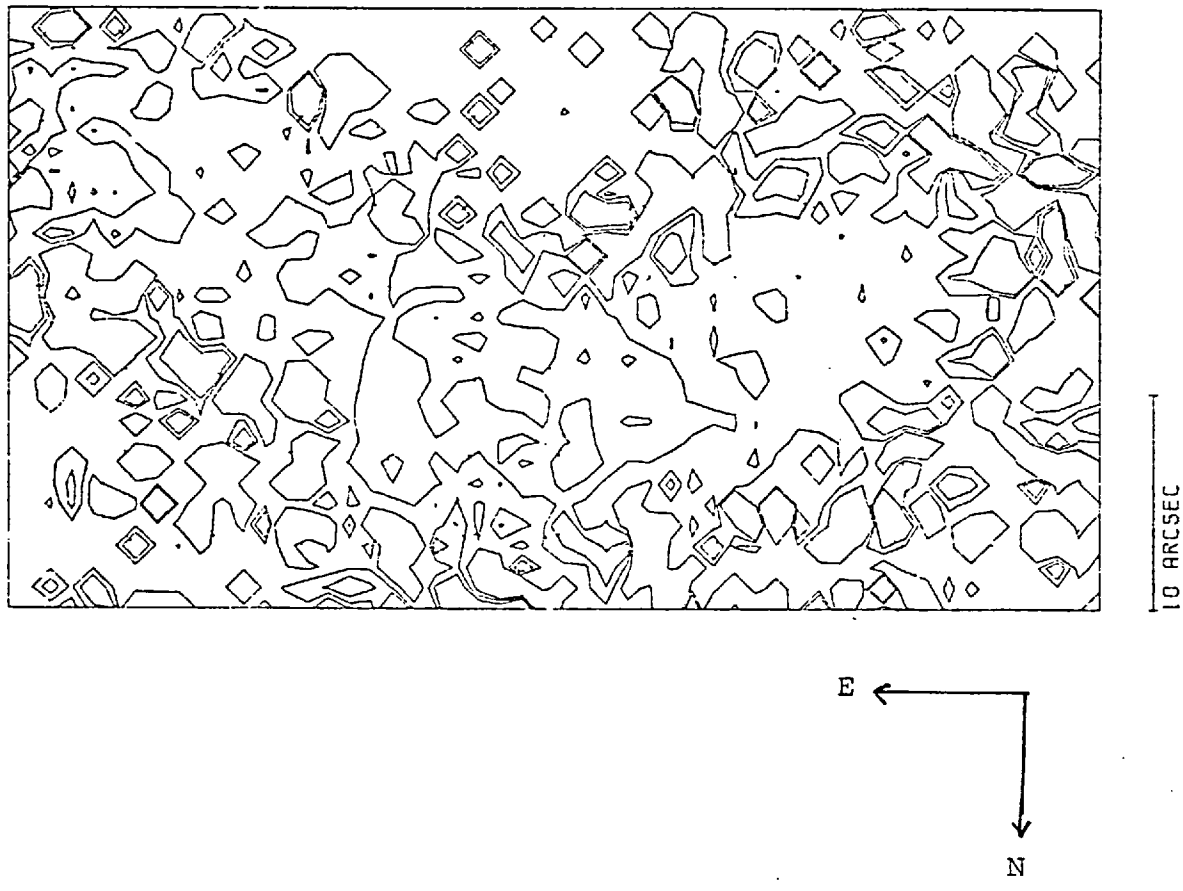

TABLE 5.11 PHOTOMETRIC PARAMETERS OF 1ZW207

Integrated magnitude within 26 mag.arcsec^{-2}	B	15.5
	V	15.6
	B-V	-0.1
Integrated magnitude of West component	B	16.4
	V	16.5
	B-V	-0.1
Integrated magnitude of East component	B	16.5
	V	16.6
	B-V	-0.1
Peak surface brightness observed (magnitude arcsec^{-2})	B	21.9
	V	21.9
	B-V	0
Calibration constants	k_B = 19.5 $\pm$ 0.1	
	k_V = 19.5 $\pm$ 0.1	

5.4. 1ZW92

1ZW92 is a pair of interconnected galaxies, the brighter of which is a compact (Zwicky, 1966). Zwicky studied 1ZW92 on photographs from the Mount Palomar 200 inch telescope and also studied the spectrum of the brighter component. Takada and Kodaira (1972) studied the spectrum of the bright component too and found that, in agreement with Zwicky, it has a recession velocity of 11460 km.sec^{-1}. The recession velocity of the faint component has not been measured. Sandage (1967) made photoelectric measurements of the bright component and these, together with the main elements of 1ZW92 given by Zwicky (1971), are listed in table 5.12. This section presents results from a study of 1ZW92 from observations made through U, B and V filters.

Table 5.12 Principal Elements of 1ZW92

R.A. (1950)		14h39.1m
Declination (1950)		+53°44′
Separation of Galaxies		50″
Bright Component		
Magnitude through 12.2" diaphragm	V	14.84
	B-V	1.01
	U-B	-0.22
Dimensions		7.5″
Recession Velocity		11460 km.sec^{-1}
Faint Component		
Magnitude (m_{pg})		16.3
Dimensions		7″

5.4.1 Description

Figure 5.10 shows a sketch of the field drawn by Zwicky (1966) alongside a print of an electronograph of the field. Zwicky's sketch shows a connecting bridge between the two galaxies and a faint spiral arm emanating from the eastern component to the North. This arm is also visible on the Palamar sky survey charts. The results of the morphological studies of 1ZW92 by electronography are given in section 5.4.2.

The brighter galaxy is described as oval and compact with a hard luminous core less than 2″ (2.2 kpc) in diameter and a faint halo about 7.5″ (8.3 kpc) in diameter. The apparent photographic magnitude of this galaxy was given as 14.4 (Zwicky, 1966) and 15.2 (Zwicky, 1971), but no reason is known for this difference. The former value is more consistent with the measurements of Sandage (1967) (see table 5.12). The results of the photometric studies of 1ZW92 by electronography are given in section 5.4.3.

The spectrum of the brighter component shows the lines H, He II, (OII), (OIII), (Ne III), (Ne V), C III, C IV, (OI) and others in emission (Zwicky, 1966; Takada and Kodaira, 1972). Takada and Kodaira found the electron temperature $T_e = (1.4 \pm 0.4)\ 10^4 K$ from the intensity ratio of the OIII lines. They also estimated the electron number density $N_e = (10^0 - 10^1) \times \varepsilon^{-\frac{1}{2}}\ cm^{-3}$ from the absolute flux of H_β (where ε denotes the filling factor). The mass of gas in the H_β emitting region was found to be $(10^8 - 10^9) \times \varepsilon^{\frac{1}{2}}\ M_\odot$. From the spectroscopic characteristics of the galaxy, Takada and Kodaira interpreted it as being a dense aggregate of gas and normal stars.

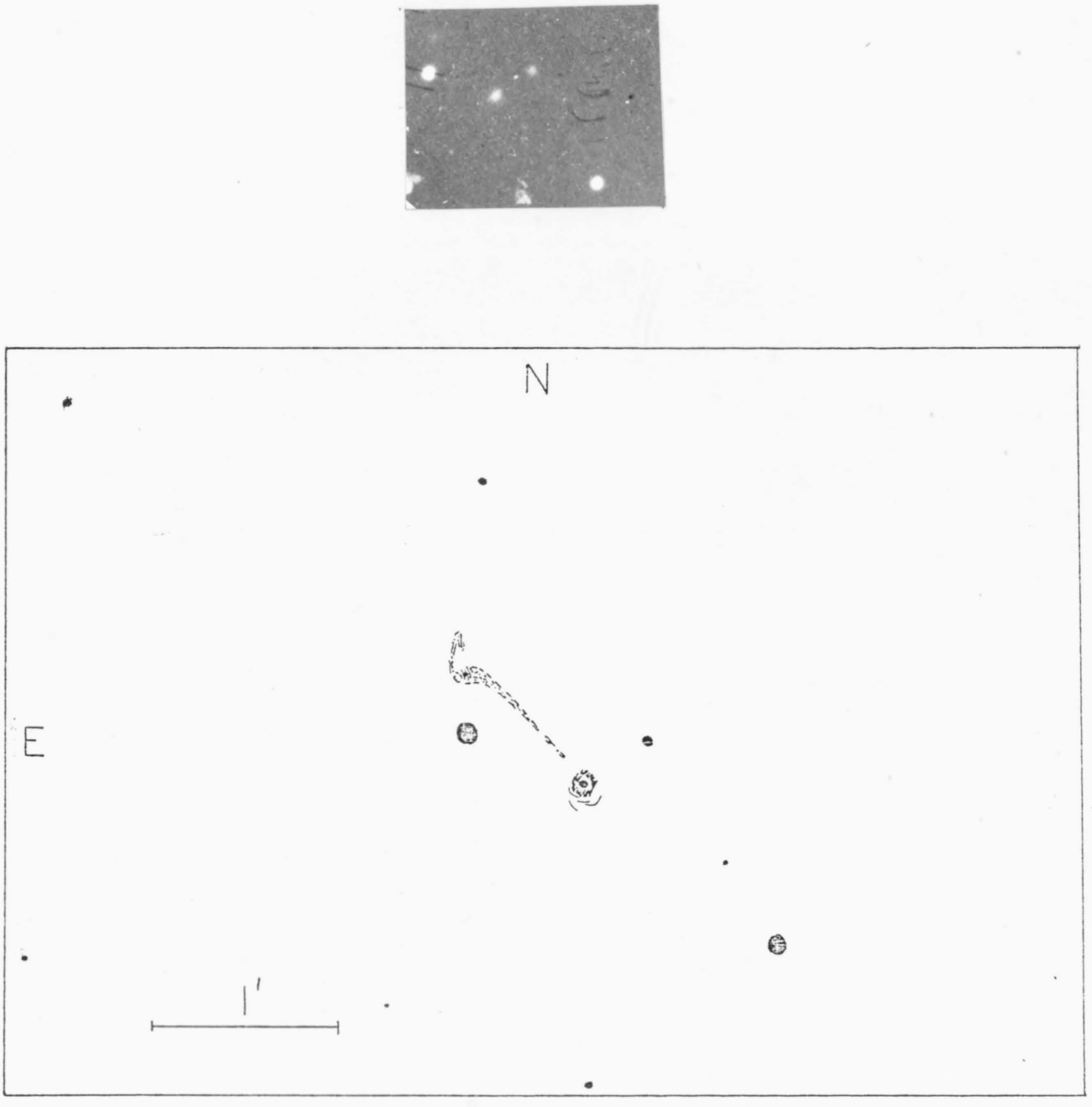

FIGURE 5.1o SKETCH OF FIELD CONTAINING 1ZW92 (ZWICKY, 1966)

The fainter galaxy is 50" (55 kpc) to the north-east of the bright galaxy. It is spherical with spiral arms (Zwicky, 1971). Zwicky (1966 and 1971) measured photographic magnitudes of 16.3 and 17.3 but gave no reasons for this difference. The length of the faint spiral arm shown on the sketch (figure 5.10) is 23" (26 kpc), as projected on a plane normal to the line of sight. This galaxy has no compact part and no usable spectrum has as yet been obtained.

5.4.2 Observations

The electronographs used for this study of 1ZW92 are listed in table 5.13, they were taken at the prime focus of the Isaac Newton Telescope, Herstmonceux. The exposures were taken during astronomical twilight because there was no true dark time in this summer observing session. During the exposures a mist surrounded the dome but the sky appeared clear. The mist increased the sky background level on electronograph I175a (B filter) and electronograph I175c (U filter) was underexposed. The bright stars on electronograph I175b (V filter) were elongated by an effect which has not been repeated (see figure 5.11). This effect probably affected all objects on this electronograph, but it is only apparent as flares on the brighter objects because it is small. The seeing diameter during the observations was estimated as 3 to 4 arc seconds.

Table 5.13 Electronographs of 1ZW92

Date	Telescope	Plate-Scale	Emulsion	Spectracon
19 June 1974	2.5m I.N.T.	$25.65''.mm^{-1}$	L4	AS3

Electronograph	Exposure	Filter
I175a	20 min	B
I175b	15 min	V
I175c	20 min	U

Handscans were made in order to find the principal parameters of the bright component on each electronograph. These parameters are listed in table 5.14. On electronograph I175a, the bright component was too dense for these parameters to be measured.

5.4.3 Morphology

Owing to the effects of the mist, the unusual flares on electronograph I175b, and poor seeing it is not possible to make worthwhile studies of the nucleus of the bright component. However, some studies can still be made of the faint component and any connections between the galaxies. Hence, using the information in table 5.14, it was decided to scan each electronograph with a step-length and aperture equal to 40 μm. As there was a high background density on electronograph I175a, an offset density of 1D was necessary for the scan to be made. This will cause the data on this scan to be noiser than normal.

Maps of the scans are shown in figures 5.11 and 5.12.

Table 5.14 Principal Elements of Handscans of 1ZW92

seeing = 4" = 16 μm

Electronograph	I175a	I175b	I175c
Z	0.3	0.7	>3
Dm	0.4	≏ 3	
G	0.004	0.05	
R	0.3	3.0	
Gs	0.004	0.05	
a_T	20	5	
a_e	70	50	
Δ	5	5	

FIGURE 5.11 ELECTRONOGRAPHS OF 1ZW92

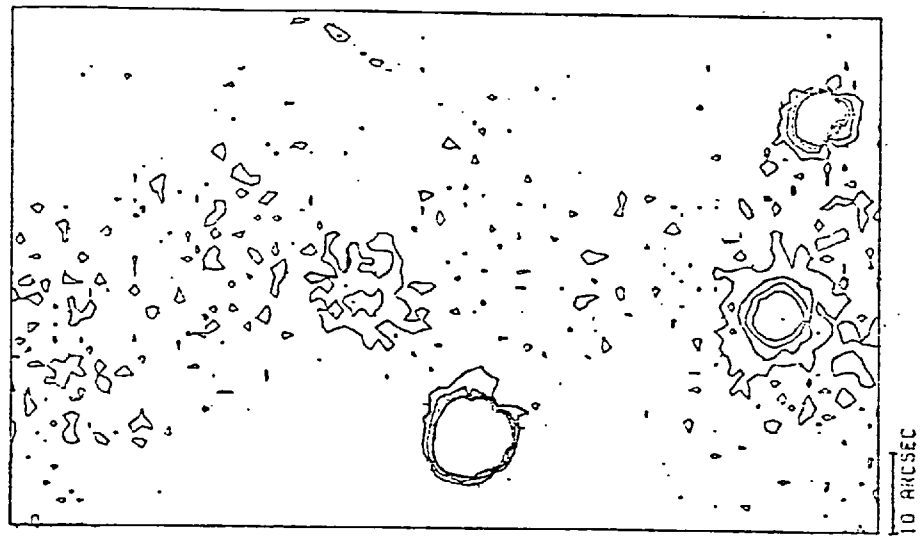

I175a
(B)

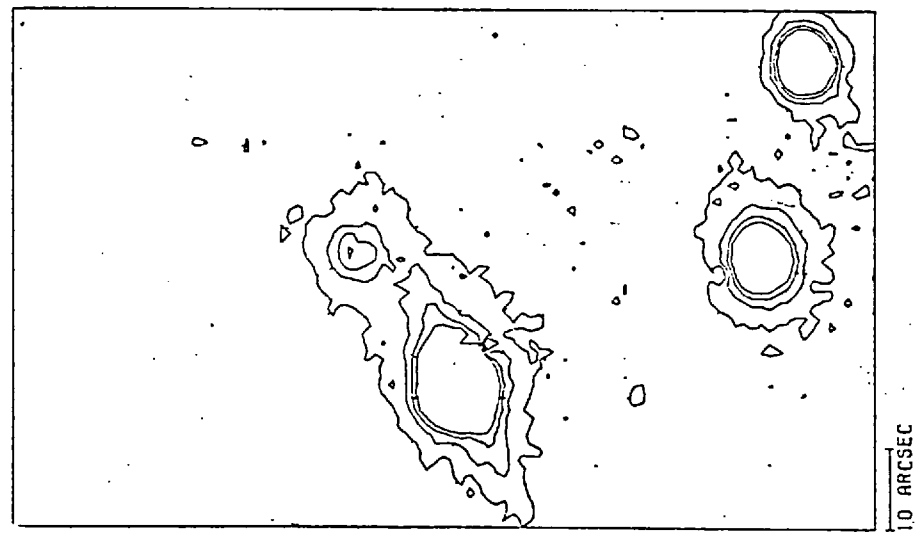

N
E

I175b
(V)

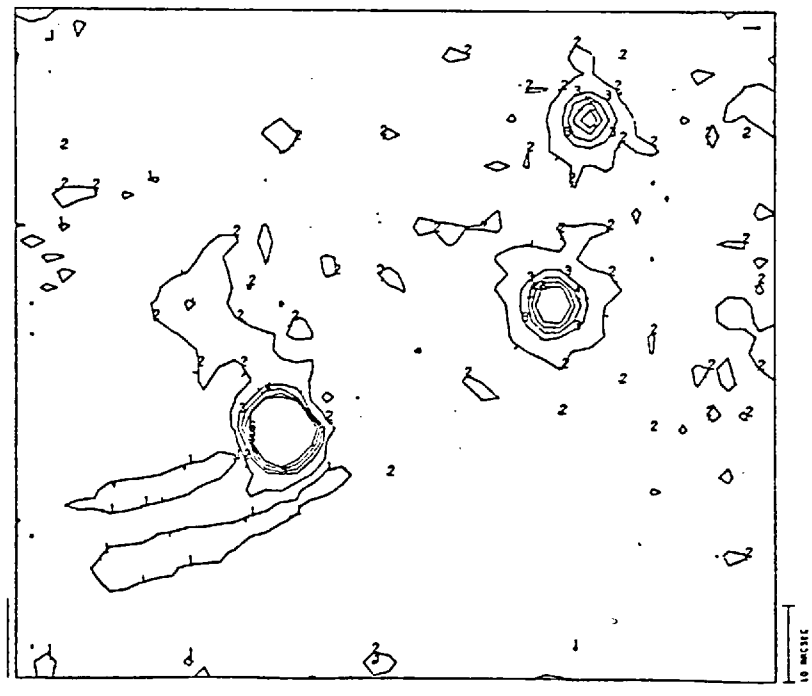

I175c
(U)

FIGURE 5.12 ELECTRONOGRAPHS OF 1ZW92

(Scans are blocked to 120 μm aperture)

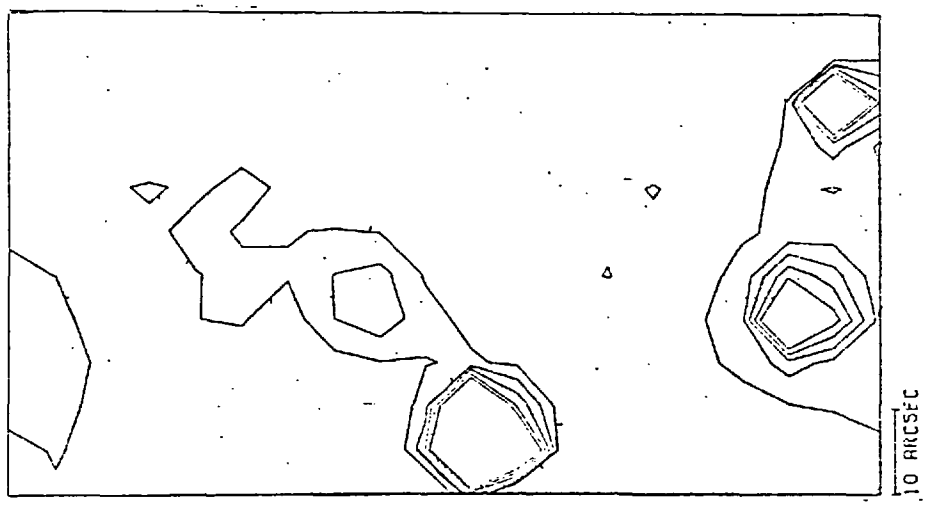

I175a

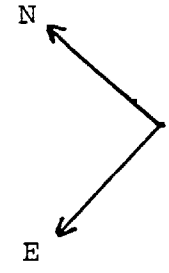

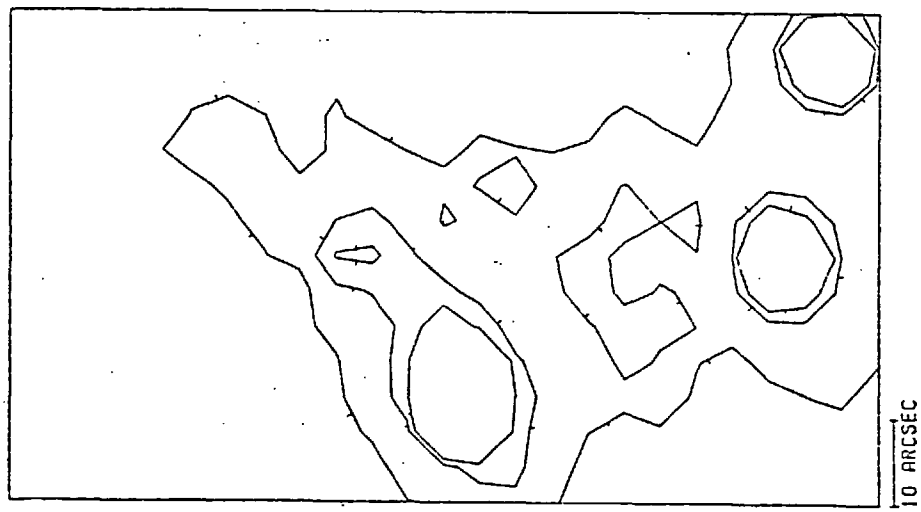

I175b

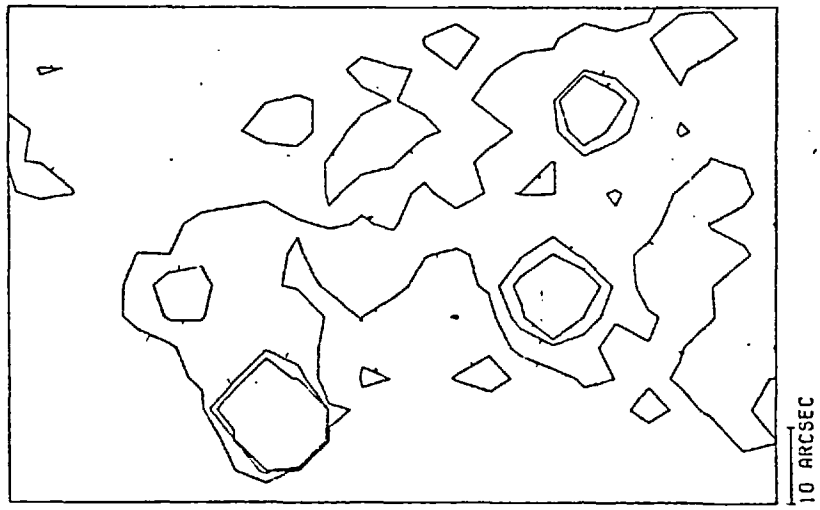

I175c

Figure 5.11 shows the unblocked scans and figure 5.12 shows maps of the scans which were blocked to an analysing aperture of 120 μm in order to reduce the emulsion noise to 1%. Only the contour levels just above the sky background density were drawn on these maps so that the faint galaxy and any flares or extensions might be displayed. A contour level below the sky background level was also drawn on the map of electronograph I157c to show the two scratches through and to the east of the bright star. These scratches do not appear on the blocked map because a contour was not drawn below the background level. The unusual flaring effect is only apparent on the bright star on electronograph I175b.

The unblocked maps show that the distribution of luminosity in the faint component of 1ZW92 is extended and may have circular symmetry. The outer contours show that this galaxy is observed to 10" (11 kpc) in diameter, a similar size to the bright component even though it is about 2 magnitudes fainter (see next section).

The maps in figure 5.12 just show the extension to the north of the faint component. There is evidence of a luminous "knot" in this extension at 20" (22 kpc) to the north of the galaxy. It is not possible to determine whether this extension is connected to the galaxy or if it is a distant line-of-sight object.

Zwicky (1966) observed a bridge between the component, but it is less bright than the extension to the north of the faint component. Since the extension is only just detected, it seemed unlikely that the bridge

would be observed in this study. However, an apparent connection between the galaxies is shown on two of the maps in figure 5.12. This connection is only 1% above the background level, i.e. it is at 25th mag. arcsec^{-2}, but it is in the position which was suggested by Zwicky (1966). It could not have been a result of the effect which caused the flares on the brighter objects because the bridge is at an angle to these flares.

Further observations of these galaxies are necessary in order to

(a) confirm the existence of the bridge,

and (b) study the "extension" from the faint component

These observations will need good seeing (1$\hat{''}$) because the components of 1ZW92 are so small. Short exposures are required for studies of the nucleus of the bright component and long exposures for studies of the faint component, extensions and the "bridge".

5.4.4 Photometry

The weather conditions during the observations of 1ZW92 were poor (see section 5.4.2) and made accurate photometry impossible. However, some photometric parameters of 1ZW92 had not been measured before, so an attempt has been made to measure their approximate values.

The calibration constants were found by comparing the present results with those found by Sandage (1967). Equation III.19 was used to define the calibration constants k_B, k_V, k_U, viz:

$$\left.\begin{aligned} B &= b + k_B \\ V &= v + k_V \\ U &= u + k_U \end{aligned}\right\} \qquad V\text{-}1$$

where B, V and U are the luminosities of the bright component of 1ZW92 measured by Sandage (1967). b, v and u are the instrumental magnitudes which were found in the present study for the same galaxy by integrating within the same aperture as used by Sandage. The calibration constants are listed in table 5.15; they are similar to those calculated in section 4.4 for the same telescope-spectracon combination.

Zwicky (1966) observed the core radius of the bright component as about 1 kpc, whereas the present study measured the core radius as about 3 kpc. The discrepancy might be caused by different definitions of core radius but it is probably due to the poor seeing conditions whilst this study was made. Therefore the compactness of the bright component is likely to be much greater than that given in table 5.15. Zwicky's (1966) measurements indicate that the compactness is probably nearer - 5.0, i.e. it is probably more compact than any other galaxy studied in this thesis.

The results from electronograph I175c (U filter) are more likely to be in error because the selective absorption by the atmosphere had the greatest effect on these results.

The results show that the luminosity of the fainter galaxy is about 1.2 magnitudes below that of the brighter galaxy, but it has a similar colour. A

list of photometric parameters which were measured for the galaxies is given in table 5.15.

Table 5.15 Photometric Parameters of 1ZW92

		Bright	Faint
Integrated magnitude within 20″ diameter	V	14.6	15.8
	B	15.6	16.8
	U	15.5	16.8
Peak Observed Surface Luminosity	V	18.6	20.1
	B	19.6	21.2
	U	19.5	21.2
Maximum detected radius		10″	10″
Bright Component			
V magnitude within 4.2 kpc diameter		16	
K		-36.8	
Core Radius		3 kpc	
Core Magnitude		15.6	
Average Core Luminosity		34.1	
Compactness		-2.7	
Calibration Constants	$k_B = 19.2 \pm 0.2$		
	$k_V = 19.5 \pm 0.2$		
	$k_U = 17.4 \pm 0.3$		

CHAPTER 6

FUTURE WORK

6.1. The Technique of Electronography

The observations made for this thesis showed that the spectracon is a convenient device to use and that electronography has an advantage in speed over traditional photographic techniques. The analysis of the electronographs for the studies in Chapters 4 and 5 confirmed that the properties of electronography (e.g. linearity of the density exposure relationship, constant D.Q.E. with flux) facilitate the data analysis and permit high signal-to-noise ratios.

The studies for this thesis were hampered by several factors, including poor seeing conditions, inappropriate exposure times, drift of telescope focus and poor emulsion. Solutions were indicated, when possible, in the text and, with care, these problems should be reduced in future. The problem most likely to be encountered again is that of poor emulsion. Non-uniformities in emulsion sensitivity thickness can not be calibrated so we must trust the manufacturers to improve their production.

6.2 The Analysis of Electronographs

This thesis, and others (e.g. Coleman, 1974; Worswick, 1975) have shown that the information which is stored in an electronograph can be simply,

accurately and efficiently accessed and displayed by the use of microdensitometers and computers. However, areas for improvement still remain, some of which are outlined below.

The procedure for setting up the microdensitometer is simple, but time consuming. In addition, it can take several hours for the Joyce-Loebl microdensitometer to make a single scan of an electronograph. This period of time is a constraint on users, but during this time the electronics system, which is hardwired on printed circuit boards, occasionally breaks down or introduces errors into the data. The system could be improved by replacing most of the controlling electronics by a microprocessor. Electro-mechanical faults would then be reduced and the setting up procedure could be made more efficient. An alternative solution is to replace the microdensitometer with one which is more sophisticated and faster, but the usage of the machine probably does not justify the high cost that this would involve, unless the costs are shared by several users.

The programs SIMMAP, XSEC and SLARD, which were developed by the author for quick-look displays of the data in a scan, could be easily adopted for use on minicomputers. If this were done, then the analysis of short scans of electronographs could be made immediately, without the time delay involved in using the college computers, and the user would not have to rely on the availability of large computers. This has not been attempted yet because of the cost of transferring the data from the microdensitometer tapes to the computer

discs and insufficient time being available on the minicomputers. However, future upgrades to the system might permit this to be done.

The greatest problem in analysing electronographs is that of displaying all the information that is available from an electronograph in a way that permits the human eye to assimilate the information. This problem was shown specifically in the study of NGC 3521 (see section 4.7) where it was apparent that a contour map is a relatively poor way of displaying information, especially when small gradient changes are present. Tonal colour displays have been shown to be a better way of displaying information (Dainty, 1977) and it is suggested that, should the appropriate equipment be available, these displays be used in future for morphological studies of astronomical objects.

6.3 The Study of Compact Galaxies

The results of Sargent (1970), Kormendy (1977), and Fairall (1978) suggest that compact galaxies may not be a class of galaxies in their own right, but that they are composed of many different types of galaxies. However, their results, and those in this thesis, show that galaxies which have been termed compact do have compact parts, using the definition given in section 4.1. Further studies of compact galaxies are therefore necessary to confirm the exact causes and nature of their compact parts. These studies should measure the size and compactness of the galaxies in addition to examining their spectra and profiles.

This thesis has shown that quantitative measurements of compactness are possible, enabling comparisons of galaxies to be made. Future studies should seek to find answers to the following questions which may indicate some of the properties of compact galaxies.

(1) Is there a maximum absolute surface luminosity?
(2) Is there a minimum core radius?
(3) Is there a maximum compactness?
(4) Do the size and luminosity correlate with redshift?

The number of galaxies studied in this thesis was insufficient to enable these questions to be answered. When sufficient galaxies have been studied, the properties and characteristics of compact galaxies will be known and nearby galaxies of the same type can be studied with greater accuracy.

Research into the value of Hubble's constant has found that the brightest galaxies in all clusters have about the same absolute luminosity (Humason, Mayall and Sandage, 1956). If the most compact galaxies in all clusters have the same absolute compactness, then the value of Hubble's constant might be measured with a greater accuracy. This is because it is easier to measure the compactness of a galaxy in regions of high luminosity (see section 4.1) than to measure the "total" luminosity of a galaxy over a large region of faint luminosity. The apparent compactness of distant galaxies is reduced by the effects of atmospheric "seeing", but techniques (e.g. deconvolution of profiles) should be available to correct for this and

permit the exact compactness of the galaxy to be measured. Alternatively, telescopes beyond the earth's atmosphere may be used for work of this type.

6.4. The Study of Non-Compact Galaxies

All galaxies are difficult to study because they have a high range of luminosities and luminosity gradients. However, the previous sections have shown that electronography can be a convenient and accurate technique for the study of galaxies. It also permits relatively quick and simple analysis of the data, though the display of the results could be improved.

The accuracy of the results and the relatively simple techniques for analysing the data permit the morphology and variations in colour of a galaxy to be easily studied. Future work in this field will probably concentrate on the study of local colour variations of galaxies because few studies of this type have been made and important information about the evolution of galaxies can be found. Although the speed of electronography permits the luminosity of the faint extensions of galaxies to be detected, the variations of its colour index can only be studied in the central brighter regions where the signal to noise ratio is much higher.

APPENDIX A

THE DEVELOPMENT PROCEDURE FOR ELECTRONOGRAPHIC EMULSIONS

(a) Presoaking in water. The characteristic diffusion time for solutions into dry emulsion is 2 minutes for 10 μm emulsion, or ½ minute for 5 μm emulsion. However, when the emulsion is already swollen with water, the diffusion time is reduced about a hundredfold (Barkas, 1963). The use of a short presoak (1 minute for 5 μm emulsion) has, therefore, been introduced to ensure rapid and uniform inward diffusion of developer (and removal of development products). Without the presoak, the diffusion time is comparable with typical development times and is a likely source of non-uniform development even with good agitation.

(b) Development. Uniformity, reproducibility and absence of adjacency effects are important requirements which can only be satisfied by effective agitation. Reproducibility is affected by the previous history of the developer; it was observed that the density obtained on successive development of electronographic plates in 300 ml of Ilford Phen-X developer was 20% lower for the second plate than for the first. This is because of depletion of developing agent, changes of alkalinity, etc. It is, therefore,

advisable to use fresh developer for each plate. Uniformity is attainable only if agitation is sufficient to produce turbulent flow conditions and to make uniform the thickness of the quiescent liquid layer at the film surface (Ives and Jensen, 1943). Methods of agitation have been discussed by Smibert and O'Bern (1955) and Miller (1971). The best methods were by camel-hair brushing and by gaseous burst agitation. Other methods such as tray rocking tend to give rise to standing wave patterns in the developer. The brushing technique cannot be used for electronographs because of their abrasion sensitivity. For this reason, a gaseous burt system has been built and has given excellent results. Nitrogen from a cylinder is released in half second bursts at four second intervals (using a modified commercial controller) into a distributor at the bottom of a perspex developing tank. The gas escapes from about 40 small holes in the base of the tank. At each burst, the solution is violently agitated, and the surface is lifted bodily by about 1.5 cm. Provided that the tank is reasonably level, the bubbles agitate the whole 400 ml volume of developer. Up to four electronographs, mounted vertically in special holders, can be accommodated in the tank. The system, besides its effectiveness, has the additional merits of simplicity and low cost, and needs human intervention only for inserting and withdrawing the plates. Development streaks, which used to mar the quality of electronographs developed in hand-rocked trays, no longer appear when the nitrogen burst system is used.

(c) Stop bath. To stop development precisely, prevent oxidation of developer left in the film, and help to preserve the fixer, it is useful to use an acid stop bath. However, reticulation of the emulsion has been observed with acetic acid concentrations greater than 1%. It is thought that this is caused by the release of CO_2 bubbles when the alkaline developer is neutralised (Hoag and Miller, 1969). The effect is appreciable because a large volume of developer is retained in the thick NT emulsion layer. Provided that the acetic acid concentration is less than ½%, there are no detrimental effects.

(d) Fixing. Undeveloped silver halide is removed using a conventional rapid (ammonium thiosulphate) fixer. Fixing should not be prolonged beyond 1½ times the clearing time; otherwise, severe etching of the very fine image silver may occur. At this stage of the process, the emulsion is under strain as the 50% volume of silver halide is lost; the gelatin matrix must be protected by incorporating a hardener in the fixer.

(e) Washing. To prevent staining, all fixer must be removed by washing. For 5 μm emulsion, it is sufficient to wash for 30 minutes in running (filtered) water.

(f) Drying. It is advantageous to use baths of alcohol solutions of gradually increasing concentration, so that the emulsion dries and shrinks controllably and is not distorted. The gelatin in

high density areas can be tanned by development products (Mees, 1966), and when air-dried, these areas dry more quickly and shrink. The alcohol bath method reduces such effects (Stevens, 1968), gives cleaner plates, and by speeding up drying prevents grain rearrangement and consequent higher granularity (Miller, 1971). Two five minute baths in 50% and 95% alcohol and final air-drying are sufficient for 5 or 10 μm emulsions. The first bath also contains a trace of plasticiser (glycerol) to stop the emulsion becoming brittle and parting from its support.

APPENDIX B - BLOCKING

With reference to figure 2.5.

If the aperture of side a_2 is small compared to the gradients of the image then second-order gradient effects can be ignored. All measurements through the aperture of side a_1 will then have the same error Δ_1 due to the transmission averaging effect, where

$$\Delta_1 = \frac{-19.2 a_1^{\,2} G^2}{Do} \qquad \text{B-1}$$

using equation II-18. When the readings within the area of side a_2 are averaged the result will have an error Δ_2' from the transmission averaging effect, where

$$\Delta_2' = \overline{\Delta_1} \doteq \Delta_1 \qquad \text{B-2}$$

The error Δ_2' is the average of all the individual errors Δ_1 because the transmission averaging effect is a systematic error. The error of a single reading made through a large aperture a_2 will be

$$\Delta_2 = \frac{-19.2 a_2^2 G^2}{Do} = \frac{a_2^2}{a_1^2} \Delta_1 \gg \Delta_1 \qquad \text{B-3}$$

Hence, the error on a single reading is much larger than the error of a result blocked from several readings through a small aperture.

The emulsion noise values δ_1 and δ_2 through the

apertures a_1 and a_2 respectively is given by using equation II-22,

$$\delta_1 = \frac{1}{\sqrt{Ka_1^2D}}$$

$$\delta_2 = \frac{1}{\sqrt{Ka_2^2D}}$$

When all the readings through small aperture a_1 are blocked, the resultant value of emulsion noise is given by

$$\delta'_2 = \frac{1}{n}\sqrt{\sum_1^n \delta_1^2}$$

$$= \frac{1}{n}\sqrt{\sum_1^n \frac{1}{Ka_1^2D}}$$

If the density is large compared to the density difference across the aperture a_2, then

$$\delta'_2 = \frac{1}{n}\sqrt{\sum_1^n \frac{1}{Ka_1^2Do}}$$

$$= \frac{1}{n}\sqrt{n\delta_1{}^2}$$

$$= \frac{\delta_1}{\sqrt{n}}$$

A single measurement through an aperture of side a_2 would have an emulsion noise value of

$$\delta_2 = \frac{1}{\sqrt{Ka_2^2Do}}$$

$$= \frac{a_1}{a_2} \delta_1$$

$$= \frac{\delta_1}{\sqrt{n}}$$

Hence, the emulsion noise is unaffected by blocking.

APPENDIX C

STAR LUMINOSITY PROFILES

A good approximation to the profile of a star is a gaussian profile (Dainty and Scaddan, 1975) . Hence, the profile can be represented by the equation

$$D = Doe^{-kx^2} \qquad C1$$

where D is the density of a point on the image, x is the distance of that point from the peak density Do and K is a constant related to the seeing width S. The seeing width is usually defined as the full width at half the maximum height of a star profile.

$$\therefore \frac{D}{2} = Doe^{-k(S/2)^2}$$

$$\therefore k = \frac{4\ln 2}{S^2} \qquad C2$$

The gradient of the star profile is

$$g = \frac{dD}{dx} = -2kxDoe^{-kx^2} \qquad C3$$

The rate of change of gradient is

$$g' = \frac{d^2D}{dx^2} = 2Doke^{-kx^2}(2kx^2-1) \qquad C4$$

$$\therefore g'' = \frac{d^3D}{dx^3} = 4Dok^2xe^{-kx^2}(3-2kx^2) \qquad C5$$

The maximum gradient (g_m) occurs when g' is zero, this is when

$$x = \sqrt{\frac{1}{2k}} = \frac{S}{\sqrt{8\ln 2}} \qquad C6$$

The maximum gradient is

$$g_m = Do\left(e^{-1/2}\right)\sqrt{2k} = Do\left(e^{-1/2}\right)\left(\frac{\sqrt{8\ln 2}}{S}\right)$$

$$= \frac{1.42\ Do}{S} \qquad C7$$

The maximum rate of change of gradient occurs when g" is zero. Maximums of g" are found when

$$x_1 = 0$$

and when $x_2 = \sqrt{\frac{3}{2k}}$ C8

These give rates of change of gradient of

$$g'_1 = 2Dok$$

$$g'_2 = 6Doke^{-3/2}$$

$$\therefore\ g'_1 > g'_2 \qquad C9$$

Example: Consider a stellar image of density 2D on an electronograph taken on a telescope with a plate-scale of $25\hat{}\,mm^{-1}$, in $2.5\hat{}$ seeing. Substituting in equation C7, the maximum gradient on the image can be calculated:

$$g = \frac{1.42\ Do}{5}$$

$$= \frac{1.42.2}{2.5/25} \quad D.mm^{-1}$$

$$= 0.03\ D.\mu m^{-1}$$

APPENDIX D

COMPUTER PROGRAMS DEVELOPED FOR DATA ANALYSIS

```
C
C                                    PROGRAM MAP
      PROGRAM MAP(INPUT,OUTPUT,SCAN=1200B,SCAN2=1200B,VARN=1200B,VARN2=1
     +200B,TAPE1=SCAN,TAPE2=SCAN2,TAPE3=VARN,TAPE4=VARN2,TAPE5=INPUT,
     +TAPE6=OUTPUT,TAPE27,TAPE62)
C
C     THIS PROGRAM CAN DRAW CONTOUR MAPS ON CALCOMP PAPER OR MICROFILM
C     OF B,V,B-V,B CORRECTED,V CORRECTED,B-V CORRECTED,B CORRN SCAN,
C     V CORRN SCAN IN ANY COMBINATION
C           V ARRAY IS ON TAPE1=SCAN
C           B ARRAY IS ON TAPE2=SCAN2
C           V CORRECTION ARRAY IS ON TAPE3=VARN
C           B CORRECTION ARRAY IS ON TAPE4=VARN2
C     MAGNITUDES OF THE OBJECT WITHIN CONTOURS OR SPECIFIED DIAPHRAGMS
C     CAN BE FOUND AT THE SAME TIME OR SEPERATELY
C
C                                PROGRAM WRITTEN AND DEVELOPED BY D.P.YOULL
C                                                  IMPERIAL COLLEGE 1975
C
      COMMON A(6600),PLDT(8),ASDT(8),SCDT(8),ISCP(4),SCANID(4)
      COMMON /MAGS/ SLPL,APOS(2),ND,DIA(25),ADUM(184)
      COMMON /COORD/ MFST(4),NFST(4),NPX(4),NL(4),NB(8),IREF,REF,REFZRO
      COMMON /NUM/ IBV,NUM1,NUM2,NUM3,NUM4,T(2),CONST(6),F(2)
     +,ZRO(2),RMIN,RMAX,MOOTH,MAG,NCON,AHT(25)
      COMMON /WAY/ CX(4),CY(4),KM1,KM2,SIZE,KKK
C                          SIZEM=MAX WIDTH OF SCAN IN INCHES
C                          NCONT=MAX NUMBER OF CONTOUR LEVELS
C                          KKK IS MEASURE OF NUMBER OF POINTERS DRAWN
      KKK=3 $ SIZEM=8 $ SZ=0.1 $ NCONT=25 $ IFIRST=0
C
C        THE DATA CARDS AREO
C     AO   MICFLM        DEFINES OUTPUT ON PAPER OR MICFILM WITH/WITHOUT
C                          MAGNITUDES
C                        TO USE CALCOMP DRUM PLOTTERO     MICFLM=0
C                          ≡      MICROFILM               MICFLM=1
C                        TO FIND MAGNITUDES               MICFLM=MICFLM+10
C                        TO FIND MAGNITUDES ONLY          MICFLM=100
C     BO   MAPDAT        DEFINES MAP TO BE PLOTTED(B,V,B-V, ETC.)
C          MAPDAT=1,2,3 OR 4 DEPENDING ON WHICH FILE IS TO BE CONTOURED
C          MAPDAT=MAPDAT+10   IF A B-V CONTOUR IS WANTED
C          MAPDAT=MAPDAT+100 CONTOURS TO BE CORRECTED FOR PHOTOCATHODE
C     CO   REFZRO,REF,F(I)     DATA FOR PHOTOCATHODE CORRECTIONS
C     DO   ISCP(I)             SCAN IDS TO BE CHECKED AGAINST TAPE
C     EO   ZRO(I),T(I)           SKY BGD AND EXP. TIME(SECS)   (B-V AND MAGS)
C     FO   (MFST(I),NFST(I)),MLST,NLST,IBLK,STEP,PLSC
C                        CO-ORDS OF AREA TO BE PLOTTED,STEP(MIC),
C                        PLATE SCALE(ARCSEC/MM)
C
C                   MFST,NFST:::::::::MFST,NLST
C                                :     :
C                                :     :
C                                :     :
C                   MLST,NFST:::::::::MLST,NLST
C
C                        CONSIDER DATA TO BE SELECTED AS A BLOCK DEFINED BY
C                        MFST,NFST AND MLST,NLST.IBLK IS  NUMBER OF POINTS
C                        IN A ROW/COLUMN WHICH ARE ADDED TOGETHER TO GIVE
C                          ONE PLOTTING IPOINT IN ARRAY A.
C
C                        M2,N2 IS TRANSLATION VECTOR FROM SCAN TO SCAN2
C                        M3,N3 IS TRANSLATION VECTOR FROM SCAN TO VARN
C                        M4,N4 IS TRANSLATION VECTOR FROM SCAN2 TO VARN2
C     GO   PLDT          ALPHANUMERIC DESCRIPTION OF MAP
C     HO   MOOTH,ICON,NCON,RMIN,RMAX      SMOOTHING,CONTOUR FLAGS,
C                        NCON=NUMBER OF CONTOURS
C                        RMIN,RMAX=MIN AND MAX OF DATA VALUES
C                        FOR EQUALLY SPACED CONTOURS       ICON=0
C                        FOR SPECIFIED HEIGHT CONTOURS     ICON=1
C                        FOR LOG CONTOURS                  ICON=2
C                        FOR SMOOTHING                     MOOTH=1
C     IO   AHT(I)        ARRAY OF CONTOUR HEIGHTS(IF NECCESSARY)
C     JO   CONST(6),APOS(2),ND,DIA(I)   MAGNITUDE DATA(CONSTANTS,CENTRE
C                        NO. OF DIAPHRAGMS,DIAMETERS(ARCSECS)
C               CONSTANTS FOUND FROM THE EQUATIONSO
C                        B-V=C1(BB-VV-C3)+C2
C                        V=(VV-C6)+C4*(B-V)+C5
C
C     CARDS C,E,I,J ARE USED ONLY WHEN NECCESSARY
C     FOR MORE THAN ONE MAP CARDS B TO J ARE REPEATED
C     LAST DATA CARD =MAPDAT= -1
C
      READ,MICFLM
      IF(MICFLM.GT.20)GOTO 12
      MAG=0
```

```
      M=10*(MICFLM/10)
      IF(MICFLM.GT.9)MAG=1
C
CC                          INITIALISE PLOTTING PACKAGE
C
      CALL START(2)
      MICFLM=MICFLM-M
      AMB=1
      IF(MICFLM.EQ.1)AMB=1.8
      CALL FACTOR(AMB)
      GOTO 13
   12 MAG=2
   13 READ,MAPDAT
   14 WRITE(6,1000)
 1000 FORMAT(1H1)
      IBV=1 $ IREF=0 $ SCALE=0
      IF(MAPDAT.GE.100)IREF=1
      M=MAPDAT-(MAPDAT/100)*100
      IF(M.GE.10)IBV=2
      NUM1=M-(M/10)*10
      IF(NUM1.EQ.0)NUM1=1
      NUM2=NUM1+IBV-1
      NUM3=NUM1+2
      NUM4=NUM2+2
C
C*****                      READ FILE DATA AND CHECK SCAN ID
C
      CONST(1)=1.0 $ ZRO(1)=0 $ T(1)=0
      DO100 I=2,6
  100 CONST(I)=0.0
      IF(IREF.EQ.1)READ,REFZRO,REF,(F(I),I=1,IBV)
      JREF=NUM1+2*IREF
      READ,((ISCP(I),I=NN,NN+IBV-1),NN=NUM1,JREF,2)
      DO 17 N=NUM1,JREF,2
      N2=N+IBV-1
      DO 17 I=N,N2
      REWIND I
      READ(I)IUR,ISC,NL(I),NPX(I),ASDT,SCDT
      WRITE(6,1004)ASDT,SCDT
 1004 FORMAT(/,X,4A10,5X,9HEXPOSURE ,A10,5X,7HFILTER ,A10,5X,4HDATE,A10
     +,5X,5HPLATE,A10, //,1X,4A10,5X,5HSTEP ,A10,5X,10HTELESCOPE ,A10,
     +      5X,5HTUBE ,A10,5X,5H FILM ,A10)
      IF(ISCP(I).EQ.ISC) GO TO 17
      WRITE(6,1002)ISC,ISCP(I)
 1002 FORMAT(20H SCAN IDS DONT AGREE,5X,8HTAPE ID=,I9,5X,8HCARD ID=,I9)
      IF(IFIRST.EQ.0)STOP
      GOTO 99
   17 CONTINUE
C
C***** READ IN CARD DATA FOR SUBROUTINE WHICH FORMS PLOTTING ARRAY A
C
      IF(IBV.EQ.2.OR.MAG.GT.0)READ,((ZRO(I),T(I)),I=1,IBV)
      READ,(((MFST(I),NFST(I)),I=N,N+IBV-1),N=NUM1,JREF,2),MLST,
     +NLST          ,IBLK,STEP,PLSC
      READ(5,1006)PLDT
 1006 FORMAT(8A10)
C
C*****                      READ IN CARD DATA FOR INSTRUCTIONS FOR PLOTTING
C
      READ,MOOTH,ICON,NCON,RMIN,RMAX
      IF(NCON.LE.NCONT)GOTO 21
      WRITE(6,1008)
 1008 FORMAT(*YOU CAN ONLY HAVE 25 CONTOUR HEIGHTS IN THIS PROGRAMME)
      STOP
   21 IF(ICON.EQ.1)READ,(AHT(L),L=1,NCON)
      IF(MAG.GT.0)READ,CONST,APOS,ND,(DIA(I),I=1,ND)
      APLSC=0
      IF(PLSC.LT.1000.)GOTO 23
      I=PLSC/100.
      APLSC=FLOAT(I)/100.
C       APLSC=PLATE SCALE OF MAP OUTPUT
      PLSC=PLSC-APLSC*10000.
      KKK=1000
   23 SLPL=STEP*PLSC*1.E-3*FLOAT(IBLK)
      IF(MAG.EQ.2)GOTO 20
      XO=FLOAT(MICFLM)*0.2 $ YOR=MICFLM $ CALL PLOT(XO,YOR,-3)
      CALL PLOT(0.0,0.2,-3)
      IF(IBV.EQ.1)GOTO 18
C
CC                          WRITE ORIGINS ON CALCOMP
C
      Y=-3.*SZ-0.2 $ X=30.*SZ
      CALL SYMBOL(X,Y,0.1,11HB ORIGIN AT  ,0.,11)
      A1=MFST(2)
      CALL NUMBER(X+12.*SZ,Y,0.1,A1,0.0,-1)
```

```
      A1=NFST(2)
      CALL NUMBER(X+17.*SZ,Y,0.1,A1,0.0,-1)
   18 IF(IREF.NE.1)GOTO 20
      Y=-4.*SZ-0.3
      CALL SYMBOL(0.,Y,SZ,22HPHOTOCATHODE ORIGIN AT  ,0.,22)
      A1=MFST(NUM3)
      CALL NUMBER(23.*SZ,Y,SZ,A1,0.0,-1)
      A1=NFST(NUM3)
      CALL NUMBER(28.*SZ,Y,SZ,A1,0.0,-1)
      IF(IBV.EQ.1)GOTO 19
      CALL SYMBOL(32.*SZ,Y,SZ,6HAND AT  ,0.,6)
      A1=MFST(4)
      CALL NUMBER(40.*SZ,Y,SZ,A1,0.0,-1)
      A1=NFST(4)
      CALL NUMBER(45.*SZ,Y,SZ,A1,0.0,-1)
   19 CALL SYMBOL(53.*SZ,Y,SZ,22HREFZRO=      ,REF=       ,0.,22)
      NN=-1
      IF(REFZRO.LT.10.)NN=3
      CALL NUMBER(60.*SZ,Y,SZ,REFZRO,0.0,NN)
      NN=-1
      IF(REF.LT.10.)NN=3
      CALL NUMBER(70.*SZ,Y,SZ,REF,0.0,NN)
      CALL SYMBOL(76.*SZ,Y,SZ,9HFILM BGD= ,0.,9)
      DO 101 I=1,IBV
      NN=-1
      IF(F(I).LT.10.)NN=3
  101 CALL NUMBER((85.+FLOAT(I-NUM1)*6.)*SZ,Y,SZ,F(I),0.,NN)
C
C                          CHECK AREAS TO BE PLOTTED LIE WITHIN SCAN
C
   20 CALL LIMITS(MFST(NUM1),1,NL(NUM1))
      CALL LIMITS(NFST(NUM1),1,NPX(NUM1))
      KDUM=0
      IF(IBV.EQ.2)GOTO 22
      IF(IREF.NE.1)GOTO24
      CALL REORD(MFST(NUM1),MFST(NUM3),KDUM,KDUM)
      CALL REORD(NFST(NUM1),NFST(NUM3),KDUM,KDUM)
      GOTO 24
   22 CALL REORD(MFST(NUM1),MFST(NUM2),KDUM,KDUM)
      CALL REORD(NFST(NUM1),NFST(NUM2),KDUM,KDUM)
      IF(IREF.NE.1)GOTO 24
      CALL REORD(MFST(1),MFST(3),MFST(2),KDUM)
      CALL REORD(NFST(1),NFST(3),NFST(2),KDUM)
      CALL REORD(MFST(2),MFST(4),MFST(1),MFST(3))
      CALL REORD(NFST(2),NFST(4),NFST(1),NFST(3))
   24 DO 103 N=NUM1,JREF,2
      N2=N+IBV-1
      DO 103 I=N,N2
      MM2=NL(I)+MFST(NUM1)-MFST(I)
      NN2=NPX(I)+NFST(NUM1)-NFST(I)
      CALL LIMITS(MLST,1,MM2)
  103 CALL LIMITS(NLST,1,NN2)
   28 WRITE(6,1007)PLDT,MFST(NUM1),NFST(NUM1),MLST,NLST,IBLK
 1007 FORMAT(/,X,8A10,/,X,'AREA',2I8,'TO',2I8,'WITH BLOCKING FACTOR',I5)
      IF(MLST.GT.MFST(NUM1).OR.NLST.GT.NFST(NUM1))GOTO30
      WRITE(6,1018)
 1018 FORMAT(*ERROR IN AREA CO-ORDINATES*)
      STOP1
   30 M=(MLST-MFST(NUM1)+1)/IBLK
      N=(NLST-NFST(NUM1)+1)/IBLK
      ABLK=IBLK
      IF(MAG.GT.0)CALL MAGS(KLST,1,M,N,ABLK)
      IF(SLPL.LE.0.)GOTO 31
      SCALE=1./SLPL
   31 IF(MAG.EQ.2)GOTO 38
      Y=-3.*SZ-0.2
      CALL SYMBOL(0.,Y,0.1,15HAREA     ,     TO  ,0.,15)
      A1=MFST(NUM1)
      CALL NUMBER(0.45,Y,0.1,A1,0.0,-1)
      A1=NFST(NUM1)
      CALL NUMBER(0.95,Y,0.1,A1,0.0,-1)
      A1=MLST
      CALL NUMBER(1.65,Y,0.1,A1,0.0,-1)
      A1=NLST
      CALL NUMBER(2.15,Y,0.1,A1,0.0,-1)
      AM=AMB
      MM=1.25*FLOAT(M)
      IF(MICFLM.EQ.1.OR.MAXO(MM,N).GT.IFIX(SIZEM*10.))AM=AM*(SIZEM*10.)/
     +AMAXO(MM,N)
      IF(APLSC.GT.0.)AM=SLPL/(2.5*APLSC)
C
C*****                   CALCULATE PLOT LENGTH FOR USE IN LABELLING PLOT
C
      SMOOTH=0.0
      IF(MOOTH.EQ.1)SMOOTH=0.2
```

```
      PL=FLOAT(N-1)*0.1-SMOOTH
      RNIK=FLOAT(M-1)/10.-SMOOTH
      TL=80.*SZ
      PL1=PL*AM/AMB
      X2=PL1/2.-4.
      IF(TL.GE.PL1)X2=0.
C
C                          PRINT TITLES
C
      CALL SYMBOL(X2,-2.*SZ-0.1,SZ,PLOT,0.0,80)
      CALL SYMBOL(X2,-SZ,SZ,SCOT,0.0,80)
      CALL SYMBOL(X2,0.1,SZ,ASOT,0.0,80)
      IF(SMOOTH.EQ.1)CALL SYMBOL(3.5,-0.75,0.2,21HCONTOURS ARE SMOOTHED,0
     +.,21)
C
C*****          PLOT SCALE MARSKER 10 ARCSEC LONG AND 10 STEPS LONG
C
      CALL PLOT(0.,0.3,-3)
      CALL FACTOR(AM)
      SIZE=0.07/AM
      X=-0.1/AM
      CALL SYMBOL(2.*X,0.,SIZE*2.,8H10 STEPS,90.,8)
      CALL PLOT(X,1./FLOAT(IBLK),3)
      CALL PLOT(X,0.,2)
      CALL PLOT(0.,0.,3)
      CALL PLOT(PL,0.,2)
      IF(SLPL.LE.0.)GOTO 36
      X=PL+0.15/AM
      CALL PLOT(X-SIZE,0.,3)
      CALL PLOT(X+SIZE,0.,2)
      CALL SYMBOL(X+4.*SIZE,0.,2.*SIZE,9H10 ARCSEC,90.,9)
      CALL PLOT(X+SIZE,SCALE,3)
      CALL PLOT(X-SIZE,SCALE,2)
      CALL PLOT(X,SCALE,3)
      CALL PLOT(X,0.,2)
      SIZE=0.1/AM
C*****
C*****                          DRAW BOX
C*****
      CALL PLOT(PL,0.,3)
   36 CALL PLOT(PL,RNIK,2)
      CALL PLOT(0.,RNIK,2)
      I=8*(1+IBV+IREF+(IBV-1+IREF)/2)
      ENCODE(I,1011,SCANID)((ISCP(J),J=NN,NN+IBV-1),NN=NUM1,JREF,2)
 1011 FORMAT(8HSCAN IDS,4I8)
      CALL SYMBOL(0.,RNIK+SIZE,2.*SIZE,SCANID,0.,I)
      CALL PLOT(0.,RNIK,3)
      CALL PLOT(0.,0.,2)
C
C*****                          PLOT LINEAR OR LOG CONTOURS
C
   38 IF(NCON.GT.0)CALL CONTHT(ICON)
      CALL SECTN(IBLK,M,N)
      IF(MAG.EQ.2)GOTO 97
      IF(NCON.LT.1)GOTO 74
C
C                          WRITE OUT CONTOUR HEIGHTS
C
      CALL FACTOR(AMB)
      YY=SIZE+FLOAT(NCON)*(SZ+SIZE)
      XX=0.65/AM
      CALL PLOT(PL1+XX,YY,-3)
      CALL SYMBOL(0.,0.,SZ,15HCONTOUR  HEIGHT   ,0.,15)
      X=3.5*SZ
      SUB=T(1)*SLPL**2
      DO 74 I=1,NCON
      A1=FLOAT(I)
      Y=-FLOAT(I)*(SZ+SIZE)-SIZE
      CALL NUMBER(X,Y,SZ,A1,0.0,-1)
      CALL NUMBER(X+6.*SZ,Y,SZ,AHT(I),0.0,2)
      IF(IBV.EQ.2.OR.(AHT(I)-ZRO(1)).LE.0.0.OR.
     +SUB.LE.0..OR.MAG.EQ.0)GOTO 74
      A1=(-2.5*ALOG10((AHT(I)-ZRO(1))/SUB)-CONST(6))+CONST(5)
      CALL NUMBER(X+2.5,Y,SZ,A1,0.,2)
   74 CONTINUE
C
C                          FINISH PLOT
C
C*****
C*****                          CENTRE OF OBJECT REFERENCED TO FIRST SCAN
C
      IF(MAG.EQ.0)GOTO 97
      IF(APOS(1).LT.1..OR.APOS(1).GT.FLOAT(M).OR.APOS(2).LT.1..OR.APO
     +S(2).GT.FLOAT(N))GOTO 97
      R1=(FLOAT(M)-APOS(1))/10.0
```

```
      R2=(APOS(2)-1.0)/10.0
      WRITE(6,200)R1,R2
  200 FORMAT(5X,10HCENTRE AT     ,2F10.5)
   97 READ,MAPDAT
      IF(MAPDAT.LT.0)GOTO 99
      IF(MAG.EQ.2)GOTO 14
      IFIRST=IFIRST+1
      IF(MICFLM.EQ.0)GOTO 96
      CALL NEWPAGE
      GOTO 14
   96 IF(MOD(IFIRST,2).EQ.1)GOTO 98
      XL=AMAX1(XL,PL1+XX+30.*SZ)-PL1-XX
      CALL PLOT(XL,-RNIK*AM-YY-2.0,-3)
      GOTO 14
   98 CALL PLOT(-PL1-XX,RNIK*AM-YY+2.0,-3)
      XL=PL1+XX+30.*SZ
      GOTO 14
   99 IF(MAG.EQ.2)STOP
      CALL ENPLOT(30.*SZ)
      STOP
      END
      SUBROUTINE LIMITS(I,J,K)
C      THIS SUBROUTINE CORRECTS CO-ORDS FOR MAX AND MIN
      IF(I.LT.J)I=J
      IF(I.GT.K)I=K
      RETURN
      END
      SUBROUTINE REORD(I,JJ,K,L)
C
C      THIS SUBROUTINE REORDERS CO-ORDS FOR B-V OR CORRECTED MAPS
C
      J=JJ
      IF(I-(1+J))1,2,3
    1 K=K+J-I+1
      L=L+J-I+1
      I=J+1
    2 JJ=1
      RETURN
    3 JJ=I-J
      RETURN
      END
      SUBROUTINE FAULT(A,B)
C      CORRECTION SUBROUTINE WHEN B-V CANT BE CALCULATED
      A=1.0
      B=1.0
      RETURN
      END
      SUBROUTINE SECTN(IB,JS,KS)
C
C***** THIS SUBROUTINE SELECTS AND BLOCKS DATA FROM A FILE
C*****       AND FEEDS IT INTO THE PLOTTING ARRAY A
C
      COMMON A(600,3),B(600,2),ALINE(600,4),AV(600,2)
      COMMON /COORD/ MFST(4),NFST(4),NPX(4),NL(4),NB(4),KL(4),IREF,REF,
     +   REFZRO
      COMMON /NUM/ IBV,NUM1,NUM2,NUM3,NUM4,T(2),CONST(6),F(2)
     +,ZRO(2),RMIN,RMAX,MOOTH,MAG,NCON,AHT(25)
      IBVREF=IBV+2*IREF
      IBLK=IB
      KLST=KS
      JLST=JS
      JI=JLST-2
      KI=KLST-2
      IF(IBV.EQ.2)ISEP=NFST(NUM2)-NFST(NUM1)
      IF(IREF.NE.1)GOTO 10
      REFMAX=REF-REFZRO
      ISEP1=NFST(NUM3)-NFST(NUM1)
      IF(IBV.EQ.2)ISEP2=NFST(4)-NFST(2)
C
C*****                    POSITION SCAN
C
   10 ABLK=IBLK*IBLK
      JREF=NUM1+2*IREF
      DO 104 NN=NUM1,JREF,2
      DO 104 I=NN,NN+IBV-1
      NB(I)=NPX(I)/512
      KL(I)=NPX(I)-NB(I)*512
  104 IF(MFST(I).GT.1)CALL POSIN(MFST(I),NB(I),KL(I),I)
C
C*****                    FOR EACH VALUE OF J
C
      DO 4 J=1,JLST
C
C                         INCREMENT  ARRAYS
C
```

```
      DO103 K=1,KLST
      AV(K,2)=0.0
      A(K,1)=A(K,2)
      B(K,1)=B(K,2)
      A(K,2)=A(K,3)
  108 AV(K,1)=0.0
      DO 116 IZ=1,IBLK
C
C                              READ IN DATA
C
      DO 112 NN=NUM1,JREF,2
      DO 112 I=NN,NN+IBV-1
      CALL REED(NB(I),KL(I),I,ALINE(1,I))
      IF(NN.LT.3.0R.IREF.NE.1)GOTO 112
C
C                              CORRECT REFERENCE ARRAY ROR MAX AND MIN
      DO 110 II=1,NPX(I)
  110 IF(ALINE(II,I).LE.REFZR0.0R.ALINE(II,I).GT.REF)ALINE(II,I)=REF
  112 CONTINUE
      IKI=NFST(NUM1)-1
      DO 114 K=1,KLST
C
C                              BLOCK DATA
      DO 114 IK=1,IBLK
      IKI=IKI+1
      GOTO(16,15,18,17),IBVREF
   15 AV(K,2)=AV(K,2)+ALINE(IKI+ISEP,NUM2)
   16 AV(K,1)=AV(K,1)+ALINE(IKI,NUM1)
      GOTO 114
   17 AV(K,2)=AV(K,2)+(ALINE((IKI+ISEP),2)-F(2))*REFMAX
     +/(ALINE((IKI+ISEP2),4)-REFZR0)+F(2)
   18 AV(K,1)=AV(K,1)+(ALINE(IKI,NUM1)-F(1))*REFMAX/(ALINE((IKI+ISEP1
     +),NUM3)-REFZR0)+F(1)
  114 CONTINUE
  116 CONTINUE
      IF(NCON.LT.1)GOTO 24
C
C                              PUT CONTOURING DATA INTO A(K,3)
      IF(IBV.EQ.2)GOTO 20
      DO 118 K=1,KLST
  118 A(K,3)=AV(K,1)/ABLK
      GOTO 21
   20 DO 119 K=1,KLST
      AL1=AV(K,1)/ABLK-ZR0(1)
      AL2=AV(K,2)/ABLK-ZR0(2)
      IF(AL1.LE.0.0.0R.AL2.LE.0.0)CALL FAULT(AL1,AL2)
  119 A(K,3)=CONST(1)*(2.5*ALOG10(AL1*T(2)/(AL2*T(1)))-CONST(3))+
     +     CONST(2)
   21 IF(MAG.EQ.2)GOTO 24
      IF(MOOTH.NE.1)GOTO 22
      IF(J.LT.3)GOTO 24
C
C                              WHEN SMOOTHING PUT DATA INTO ARRAY B(K,2)
      DO120 K=1,KI
  120 B(K,2)=(A(K,1)+A(K+2,1)+A(K,3)+A(K+2,3))/16.0+(A(K+1,1)+A(K,2)+
     +A((+2,2)+A(K+1,3))/8.0+A(K+1,2)/4.0
C
C**********                    DRAW CONTOURS FOR SET OF POINTS
C
      JIK=J-2
      IF(J.GT.3)CALL CONT(B,JI,KI,JIK)
      GOTO 24
   22 IF(J.GT.1)CALL CONT(A(1,2),JLST,KLST,J)
C
C**********                    SUM READINGS TO GET MAGNITUDE
C
   24 IF(MAG.GT.0)CALL MAGS(KLST,2,J,K,ABLK)
    4 IF(MOD(J,10).EQ.1)WRITE(6,1002)J
 1002 FORMAT(5X,5H LINE,I5)
C
C**********                    OUTPUT MAGNITUDES
C
      IF(MAG.GT.0)CALL MAGS(KLST,3,J,K,ABLK)
      RETURN
      END
      SUBROUTINE MAGS(KLS,IFLAG,J,KK,AB)
C
C      THIS SUBROUTINE FINDS MAGS WITHIN CONTOURS OR DIAPHRAGMS
C         IFLAG=1 O   WRITE DATA AND ZERO ARRAYS
C         IFLAG=2 O   FOR EACH ALINE SUM VALALUES INTOMAGC OR MAGD
C         IFLAG=3 O   CALCULATE MAGNITUDES AND OUTPUT
```

```
C
      COMMON A(600,3),B(600,6),AV(600,2)
      COMMON /COORD/ MFST(4),NFST(4),NPX(4),NL(4),NB(4),KL(4),IREF,REF,
     +    REFZRO
      COMMON /NUM/ IBV,NUM1,NUM2,NUM3,NUM4,T(2),CONST(6),F(2)
     +,ZRO(2),RMIN,RMAX,MOOTH,MAG,NCON,AHT(25)
      COMMON /MAGS/SLPL,APOS(2),ND,DIA(25),BV,BV1,S(4),BB,
     +VV,AMAGC(25,2),AMAGD(25,2),N(25),NC(25),DIS2(25),C5
      KLST=KLS $ K=KK $ ABLK=AB
      GOTO(10,20,30),IFLAG
C*************************IFLAG=1
   10 WRITE(6,1010)CONST,((ZRO(I),T(I)),I=1,IBV)
 1010 FORMAT(1X,2HK=,6F6.2/(5H SKY=,F7.2,11H ,EXP.TIME=  ,F7.0,4HSECS))
      MM=MFST(NUM2)-MFST(NUM1)
      NN=NFST(NUM2)-NFST(NUM1)
      WRITE(6,1012)MM,NN,APOS
 1012 FORMAT(12H B ORIGIN AT ,2I10,5X,10HCENTRE AT  ,2F10.1)
      IF(IREF.NE.1)GOTO 12
      WRITE(6,1014)(MFST(I),NFST(I),I=NUM1,NUM2)
 1014 FORMAT(25H PHOTOCATHODE ORIGINS ARE ,4I10)
      WRITE(6,1016)REFZRO,REF,(F(I),I=NUM1,NUM2)
 1016 FORMAT(8H REFZRO=,F6.1,5X,4HREF=,F6.1,5X,9HFILM BGD=,2F10.1)
   12 APOS(1)=(APOS(1)-FLOAT(MFST(NUM1)))/ABLK+1.0
      APOS(   2)=(APOS(2)-FLOAT(NFST(NUM1)))/ABLK+1.0
      IF(SLPL.LE.0.)STOP10
      S(3)=0 $ S(4)=0 $ S(1)=0 $ S(2)=0
      C5=CONST(5)-5.*ALOG10(SLPL)
      IF(NCON.LT.1)GOTO 11
      DO 100 I=1,NCON
      NC(I)=0
      AMAGC(I,1)=0.0
  100 AMAGC(I,2)=0.0
   11 IF(ND.LT.1)GOTO 14
      SLPL2=SLPL*2.
      DO 104 I=1,ND
      DIS=DIA(I)/SLPL2
      DIS2(I)=DIS**2
      IF(DIS-APOS(1).GT.0..OR.DIS-APOS(2).GT.0.)WRITE(6,1000)I
 1000 FORMAT(1X,32HERROR IN MAGNITUDE FOR DIAPHRAGM  ,I5)
      N(I)=0
      AMAGD(I,1)=0
  104 AMAGD(I,2)=0
   14 RETURN
C*************************IFLAG=2
   20 IF(NCON.LT.1)GOTO 28
      DO 126 K=1,KLST
C
C       FOR MAG WITHIN CONTOUR
C
      DO 122 I=1,NCON
      II=NCON+1-I
  122 IF(A(K,3).GT.AHT(II))GOTO  26
      GOTO 126
   26 IF(A(K,3).LT.-10.)GOTO 126
      DO 124 I=1,II
      NC(I)=NC(I)+1
      DO124 L=1,IBV
  124 AMAGC(I,L)=AMAGC(I,L)+AV(K,L)
  126 CONTINUE
   28 IF(ND.LT.1)RETURN
      AJ2=(FLOAT(J)-APOS(1))**2
C
C                              FOR MAG WITHIN DIAPHRAGM
C
      DO 130 K=1,KLST
      AK2=(FLOAT(K)-APOS(2))**2
      DO 128 I=1,ND
  128 IF(AJ2+AK2.LE.DIS2(I))GOTO 32
      GOTO 130
   32 DO 129 II=I,ND
      N(II)=N(II)+1
      DO 129 L=1,IBV
      IF(AV(K,L).LT.-10.)GOTO 130
  129 AMAGD(II,L)=AMAGD(II,L)+AV(K,L)
  130 CONTINUE
      RETURN
C
C*************     LOWEST CONTOUR LEVEL IS 1
C*************     LARGEST DIAPHRAGM  IS FIRST
C
C                    CALCULATE MAG WITHIN CONTOURS AND OUTPUT
C
   30 IF(NCON.LT.1)GOTO 39
      AK1=2.*SLPL/SQRT(3.14158)
      IF(IBV.EQ.1)GOTO 34
```

```
      WRITE(6,1004)
 1004 FORMAT(////' CONTOUR B-V(INT) B-V(LOC)  V(INT)  SUM/SEC   V(LOC) S
     +UM/SEC/N  B(INT)  SUM/SEC   B(LOC) SUM/SEC/N   N(SUM)  DIA-RAD')
      GOTO 36
   34 WRITE(6,1018)
 1018 FORMAT(////,5X,'CONTOUR  INT.MAG   SUM/SEC  LOC.MAG SUM/SEC/N
     +N(SUM)     DIA-RAD'/)
   36 DO 136 II=1,NCON
      I=NCON+1-II
      CALL MAGS2(AMAGC(I,1),AMAGC(I,2),ABLK,NC(I),NC(I+1),I,NCON)
      DIAM=AK1*SQRT(FLOAT(NC(I)))
      IF(I.NE.NCON)R=AK1*(SQRT(FLOAT(NC(I)))+SQRT(FLOAT(NC(I+1))))/4.
      IF(IBV.EQ.1)GOTO 37
      WRITE(6,1005)I,BV,BV1,AMAGC(I,1),S(1),VV,S(3),AMAGC(I,2),BB,S(4),
     +N(I),DIAM,R
 1005 FORMAT(2X,I9,5F9.2,F9.4,3F9.2,F9.4,I9,2F6.1)
      S(4)=S(2)
      GOTO 38
   37 WRITE(6,1019)I,AMAGC(I,1),S(1),VV,S(3),NC(I),DIAM,R
 1019 FORMAT(2X,I9,3F10.2,F9.4,I9,3X,2F6.1)
   38 IF(MOD(II,5).EQ.0)WRITE(6,1022)
  136 S(3)=S(1)
C
C                    CALCULATE MAG WITHIN DIAPHRAGM AND OUTPUT
C
   39 IF(ND.LT.1)RETURN
      IF(IBV.EQ.1)GOTO 44
      WRITE(6,1020)
 1020 FORMAT(////,5X,9HDIAPHRAGM,X,8HB-V(INT),X,8HB-V(LOC),2X,6HV(INT)
     +,3X,7HSUM/SEC,X,9H V(LOC)   ,9HSUM/SEC/N,9H B(INT)   ,9H SUM/SEC ,
     +9H B(LOC)   ,9HSUM/SEC/N,9H  N(SUM) ,5H     R,/,4X,11HARCSEC/STEP)
      GOTO 45
   44 WRITE(6,1024)
 1024 FORMAT(////,5X,'DIAPHRAGM INT.MAG. SUM/SEC LOC.MAG.  SUM/SEC/N',
     +'    N(SUM)       R'/4X,'ARCSEC/STEP')
   45 DO 140 I=1,ND
      CALL MAGS2(AMAGD(I,1),AMAGD(I,2),ABLK,N(I),N(I-1),I,1)
      D=DIA(I)/SLPL
      IF(I.NE.1)R=(DIA(I)+DIA(I-1))/4.
      IF(IBV.EQ.1)GOTO 46
      WRITE(6,1022)DIA(I),D,BV,BV1,AMAGD(I,1),S(1),VV,S(3),AMAGD(I,2),
     +  S(2),BB,S(4),N(I),R
 1022 FORMAT(X,2(X,F5.1),2F9.2,2(3F9.2,F9.4),I9,F9.2)
      S(4)=S(2)
      GOTO 47
   46 WRITE(6,1026)DIA(I),D,AMAGD(I,1),S(1),VV,S(3),N(I),R
 1026 FORMAT(X,2F6.1,3F9.2,F9.4,I9,F9.2)
   47 IF(MOD(I,5).EQ.0)WRITE(6,1022)
  140 S(3)=S(1)
      RETURN
      END
      SUBROUTINE MAGS2(AM1,AM2,ABLK,NN,NNN,I,II)
      COMMON /MAGS/ABC(29),BV,BV1,S(4),BB,VV,ABC2(175),C5
      COMMON /NUM/ IBV,ABC3(4),T(2),C(6),ABC4(2),Z(2),IABC5(30)
C
C                          THIS SUBROUTINE CALCULATES MAGNITUDES
C
      BB=0 $ VV=0 $ BV=0 $ BV1=0
      S(1)=(AM1/ABLK-Z(1))*FLOAT(NN))/T(1)
      IF(S(1).GT.0.)AM1=(-2.5*ALOG10(S(1))-C(6))+C(4)*BV+C5
      IF(IBV.EQ.1)GOTO 10
      S(2)=(AM2/ABLK-Z(2))*FLOAT(NN))/T(2)
      IF(S(1).LE.0..OR.S(2).LE.0.)GOTO 10
      BV=C(1)*(2.5*ALOG10(S(1)/S(2))-C(3))+C(2)
      AM2=BV+AM1
   10 IF(I.EQ.II)RETURN
      IF(NN.EQ.NNN)RETURN
      AN=NN-NNN
      S(3)=(S(1)-S(3))/AN
      IF(IBV.EQ.1)GOTO 14
      S(4)=(S(2)-S(4))/AN
      IF(S(3).LE.0..OR.S(4).LE.0.)GOTO 14
      BV1=C(1)*(2.5*ALOG10(S(3)/S(4))-C(3))+C(2)
   14 IF(S(3).GT.0.)VV=(-2.5*ALOG10(S(3))-C(6))+C(4)*BV1+C(5)
      BB=BV1+VV
      RETURN
      END

      SUBROUTINE CONT(A,MMM,L,III)
C           A(I,J)      3   A(I,J+1)
C                     *********
C                     *       *
C                     *       *
C                   4 *       * 2
C                     *       *
```

```
C                    *       *
C                    *********
C        A(I+1,J)        1   A(I+1,J+1)
C
C     THIS SUBROUTINE CALLS NINSEC,WAY,FIND
C
      COMMON /NUM/ IABC(21),NN,AHT(25)
      COMMON /WAY/ CX(4),CY(4),KM1,KM2,SIZE,K
      COMMON AA(6600)
      DIMENSION A(600,2),I(4)
      LOGICAL NINSEC
      NIK=L-1 $ M=MMM $ II=III-1 $ X=0 $ Y=0
      AMII=FLOAT(MMM-II)*0.1
      IDIR=-1
      IF(MOD(II,2).EQ.0) IDIR=1
C
C                          MAIN LOOP WITH INITIAL CONDITIONS SET UP
C
      DO 102 J=1,NIK
      JJ=J
      IF(IDIR.EQ.1) JJ=L-JJ
      DO 100 N=1,NN
C
C                           CHECK CONTOUR LEVEL PASSES THRU THIS BOX
C
      IF(AMAX1(A(JJ,1),A(JJ,2),A(JJ+1,2),A(JJ+1,1)).LT.AHT(N)) GOTO 102
      IF(AMIN1(A(JJ,1),A(JJ,2),A(JJ+1,2),A(JJ+1,1)).GT.AHT(N)) GOTO 100
      KOUNT=0
C
C                           CHECK SIDE 3 FOR AN INTERSECTION
C
      IF(NINSEC(A(JJ,1),A(JJ+1,1),AHT(N))) GOTO 10
      KOUNT=KOUNT+1
      I(KOUNT)=3
      CX(3)=FLOAT(JJ)*0.1+DIST(A(JJ,1),A(JJ+1,1),AHT(N))-0.1
      CY(3)=AMII
C
C                           CHECK SIDE 4 FOR AN INTERSECTION
C                           ( IF(IDIR.LT.0)     CHECK SIDE 2 FIRST )
C
   10 IF(IDIR.LT.0) GOTO 16
   12 IF(NINSEC(A(JJ,1),A(JJ,2),AHT(N))) GOTO 14
      KOUNT=KOUNT+1
      I(KOUNT)=4
      CX(4)=FLOAT(JJ)*0.1-0.1
      CY(4)=AMII-DIST(A(JJ,1),A(JJ,2),AHT(N))
   14 IF(IDIR.LT.0) GOTO 20
C
C                           CHECK SIDE 2 FOR AN INTERSECTION
C
   16 IF(NINSEC(A(JJ+1,1),A(JJ+1,2),AHT(N))) GOTO 18
      KOUNT=KOUNT+1
      CX(2)=FLOAT(JJ+1)*0.1-0.1
      CY(2)=AMII-DIST(A(JJ+1,1),A(JJ+1,2),AHT(N))
      I(KOUNT)=2
   18 IF(IDIR.LT.0) GOTO 12
C
C                           IF(KOUNT.EQ.1 OR 3) FIND THE OTHER INTERSECTION
C
   20 IF(KOUNT.NE.2) GOTO 26
   22 IF(X.NE.CX(I(1)).  OR.Y.NE.CY(I(1))) CALL PLOT(CX(I(1)),CY(I(1)),3)
      IJK=N/3
C
C                       IF FIND IS CALLED A POINTER IS DRAWN ON THE CONTOUR
C
      IF(MOD(II,K).EQ.IJK.AND.MOD(JJ,K).EQ.IJK) CALL FIND(A,AHT(N),JJ,CX(
     +I(1))      ,CY(I(1)),CX(I(2)),CY(I(2)),I(2))
      IJ=N/4
      IF(MOD(II,K).NE.IJ.OR.MOD(JJ,K).NE.IJ) GOTO 24
C
C                           NUMBER THE CONTOUR
C
      T=N
      CALL NUMBER(CX(I(1)),CY(I(1)),SIZE,T,0.0,-1)
      CALL PLOT(CX(I(1)),CY(I(1)),3)
   24 CALL PLOT(CX(I(2)),CY(I(2)),2)
      X=CX(I(2))
      Y=CY(I(2))
      GOTO 100
   26 CX(1)=FLOAT(JJ)*0.1+DIST(A(JJ,2),A(JJ+1,2),AHT(N))-0.1
      CY(1)=AMII-0.1
      KOUNT=KOUNT+1
      I(KOUNT)=1
      IF(KOUNT.EQ.2) GOTO22
C
```

```
C       IF ROUTINE REACHES HERE THERE MUST BE 4 INTERSECTIONS ON BOX
C
        CALL WAY
        IF(X.NE.CX(3) .OR.Y.NE.CY(3))CALL PLOT(CX(3),CY(3),3)
        CALL PLOT(CX(KM1),CY(KM1),2)
        CALL PLOT(CX(1),CY(1),3)
        CALL PLOT(CX(KM2),CY(KM2),2)
        X=CX(KM2)
        Y=CY(KM2)
  100   CONTINUE
  102   CONTINUE
        RETURN
        END
        SUBROUTINE FIND(A,VA,JJ,X1,Y1,X,Y,I)
        COMMON /WAY/ CX(4),CY(4),KM1,KM2,SIZE,KKK
        DIMENSION A(600,2)
        COMMON AA(6600)
        INN=I
C
C  ********** DRAW POINTER ( POINTER IS 0.03 INHES LONG)
C
        VAL=VA
        X2=(X1+X)/2.0
        Y2=(Y1+Y)/2.0
        AK=-SIZE/2.
        CALL PLOT(X2,Y2,2)
        IF(Y.EQ.Y1)GOTO 10
        G=((X1-X)/(Y-Y1))
        G2=G**2
        G3=SQRT(1.0/(1.0+G2))
        JJI=JJ
        IF(INN.LT.3)JJI=1+JJ
        JL=1
        IF(INN.EQ.1.OR.INN.EQ.4)JL=2
        IF(A(JJI,JL).GT.VAL)AK=-AK
        IF(INN.GT.2)AK=-AK
        AKK=1.
        IF(G.LT.0..AND.(INN/2)*2.EQ.INN)AKK=-AKK
        YYY=Y2-AK*G*G3
        IF((INN/2)*2.EQ.INN)YYY=Y2-AK*G3
        CALL PLOT(X2-AK*AKK*G3,YYY,2)
        CALL PLOT(X2,Y2,3)
        RETURN
   10   IF(INN.EQ.2)AK=-AK
        CALL PLOT(X2,Y2+AK,2)
        CALL PLOT(X2,Y2,3)
        RETURN
        END
        LOGICAL FUNCTION NINSEC(A,B,V)
C
C  ********** THIS SUBROUTINE FINDS IF CONTOUR CROSSES AN EDGE OF THE BOX *
C
        LOGICAL G
        G=.TRUE.
        IF ( A.GE.V.AND.V.GE.B.OR.A.LE.V.AND.V.LE.B ) G=.FALSE.
        NINSEC=G
        RETURN
        END
        SUBROUTINE WAY
C
C  **********THIS SUBROUTINE FINDS BEST EXIT FOR A CONTOUR PASSING THROUGH
C                SIDE 3 FOR A BOX WITH 3 EXITS **********
C
        COMMON /WAY/ CX(4),CY(4),KM1,KM2,SIZE,K
        KM1=2 $ KM2=4
        DIS1=(CX(2)-CX(3))**2+(CY(2)-CY(3))**2
        DIS2=(CX(4)-CX(3))**2+(CY(4)-CY(3))**2
        IF(DIS1.LT.DIS2)RETURN
        KM1=4 $ KM2=2
        RETURN
        END
        REAL FUNCTION DIST(A,B,VAL)
C
C**********THIS SUBROUTINE FINDS IPOINT OF EXIT ON THE SIDE **********
C
        DIST=(VAL-A)/(B-A)*0.1
        RETURN
        END
        SUBROUTINE CONTHT(IFIK)
        COMMON /NUM/ IBV,NUM1,NUM2,NUM3,NUM4,T(2),CONST(6),F(2)
       +,ZRO(2),RMIN,RMAX,MOOTH,MAG,NCON,AHT(25)
        COMMON /MAGS/SLPL,APOS(2),ND,DIA(25),BV,BV1,S(4),BB,
       +VV,AMAGC(25,2),AMAGD(25,2),N(25),NC(25),DIS2(25),C5
C
C                          THERE ARE NCON CONTOURS.
```

```
C
CC                          CONTOURS AT PRE-DETERMINED HEIGHTS
C
      SUB=T(1)**SLPL**2
      ICON=IFIK+1 & HT=0
      GOTO(13,20,30),ICON
   20 DO100 L=1,NCON
      AHT(L)=AHT(L)-10.E-9
      IF(MAG.EQ.0.0R.SUB.LE.0..0R.(AHT(L)-ZRO(1)).LE.0.)GOTO100
      HT=(-2.5*ALOG10((AHT(L)-ZRO(1))/SUB)-CONST(6))+CONST(5)
  100 WRITE(6,41)L,AHT(L),HT
   41 FORMAT(20H CONTOUR WITH NUMBER, I3,11H HAS HEIGHT, 5X,F9.2
     +,5X,'=',5X,F9.2,5X,'MAG/SEC2')
      RETURN
C
CCC                         EQUALLY SPACED CONTOURS
C     SCALE THE ARRAY
C
   13 SCV=(RMAX-RMIN)/FLOAT(NCON+1)
      DO102 J=1,NCON
      AHT(J)=RMIN+FLOAT(J)*SCV-10.E-9
      IF(MAG.EQ.0.0R.SUB.LE.0..0R.(AHT(J)-ZRO(1)).LE.0.)GOTO102
      HT=(-2.5*ALOG10((AHT(J)-ZRO(1))/SUB)-CONST(6))+CONST(5)
  102 WRITE(6,41)J,AHT(J),HT
      RETURN
C*****                      LOG CONTOURS
C*****
C*****SCALE THE ARRAY
C*****
   30 Z=ZRO(1)
      IF(SLPL.LE.0.)STOP11
      IF(RMIN.LE.Z.OR.RMAX.LE.RMIN)STOP2
      AVAL=NCON+1
      SCALV=2.5*ALOG10((RMIN-Z)/(RMAX-Z))/AVAL
      ZERO=(-2.5*ALOG10((RMIN-Z)/SUB)-CONST(6))+CONST(5)
      DO 104 J=1,NCON
      AJ=FLOAT(J)/AVAL
      AHT(J)=(RMIN-Z)*(1.-AJ)*(RMAX-Z)**AJ
      HT=ZERO+FLOAT(J)*SCALV
  104 WRITE(6,41)J,AHT(J),HT
      RETURN
      END
      SUBROUTINE POSIN(MFST,NB,KL,I)
      MFMI=MFST-1
C
C*****                      READ IN UNUSED ALINES
C
      DO 3 J=1,MFMI
      IF(NB.EQ.0)GOTO 3
      DO 41 NNB=1,NB
   41 READ(I)DATA
    3 IF(KL.GT.0)READ(I)DATA
      RETURN
      END
      SUBROUTINE REED(NB,KL,I,ALINE)
      COMMON AA(6600)
      DIMENSION ALINE(600)
C
C***** NOTE.DATA BLOCK ON STANDARD ARCHIVE TAPE CONSISTS OF
C*****      512 WORDS WHEN FULL
C
      IF(NB.EQ.0)GOTO 48
      DO 47 II=1,NB
      KK=(II-1)*512
   47 READ(I)(ALINE(K+KK),K=1,512)
   48 IF(KL.EQ.0)RETURN
      KK=NB*512
      READ(I)(ALINE(K+KK),K=1,KL)
      ALINE(512)=ALINE(511)
      RETURN
      END
```

```
C                                  PROGRAM CROSS
      PROGRAM CROSS(INPUT=131B,OUTPUT=131B,SCAN=1200B,SCAN2=1200B,VARN=
     +1200B,VARN2=1200B,TAPE27=131B,TAPE62=131B,TAPE1=SCAN,TAPE2=SCAN2
     +,TAPE3=VARN,TAPE4=VARN2,TAPE5=INPUT,TAPE6=OUTPUT,TAPE7=1200B)
C
C     THIS PROGRAM DRAWS CROSS-SECTIONS THROUGH ARRAYS OF DATA
C     ONTO CALCOMP PAPER OR MICROFILM.THE ARRAYS CAN BE B,V,B-V,B CORR-
C     ECTED,V CORRECTED IN ANY COMBINATION.
C           V ARRAY IS ON TAPE1=SCAN
C           B ARRAY IS ON TAPE2=SCAN2
C           V CORRECTION ARRAY IS ON TAPE3=VARN
C           B CORRECTION ARAY IS ON TAPE4=VARN2
C
C                     PROGRAM WRITTEN AND DEVELOPED BY D.P.YOULL
C                                  IMPERIAL COLLEGE 1975
C
      COMMON COL(600,4,3),X(650),Y(650),XX(102),YY(102),DATA(600)
      COMMON /I/IKJ,IKI,MOOTH
      COMMON /REF/ REF,IREF,REFZRO,CONST(6),F(2)
      COMMON NL(4),NPX(4),MFST(4),NB(4),KL
     +(4),ISCP(4),SCANID(4),PLDT(8),SCDT(8),ASDT(8)
      COMMON /NUM/ ISEP(4),NUM1,NUM2,IBV,ZRO(2),T(2)
      COMMON /IBLK/ IBLK,ABLK,NFST(4)
C
C          THE DATA CARDS AREO
C     AO   MICFLM,PLSC,VEL        DEFINES OUTPUT ON PAPER OR MICFILM
C                                 TO USE CALCOMP DRUM PLOTTER      MICFLM=0
C                                   ≡   MICFILM                    MICFLM=1
C                                 PLSC=PLATE SCALE (ARCSECS/MM)
C                                 VEL=RECESSION VELOCITY(KM/SEC) (=0 IF UNKNOWN)
C     BO   MAPDAT                 DEFINES CROSS-SECTION TO BE PLOTTED(B,B-V,ETC)
C     MAPDAT=1,2,3, OR 4 DEPENDING ON WHICH FILE THE XSECTN IS FROM
C     MAPDAT=MAPDAT+10   IF A B-V XSECTN IS TO BE PLOTTED
C     CO   REFZRO,REF,F(I)   DATA FOR PHOTOCATHODE CORRECTIONS
C     DO   ISCP(I)           SCAN IDS TO BE CHECKED AGAINST TAPE
C     EO   ZRO(I),T(I)  SKY BGD AND EXPOSURE TIMES(SECS)  (FOR B-V ONLY)
C     FO   (MFST(I),NFST(I),MLST,NLST,MOOTH,STEP
C                                 CO-ORDS OF AREA TO BE PLOTTED,SMOOTHING FLAG
C                                   AND STEP LENGTH(MICS)
C
C                MFST,NFST:::::::MFST,NLST
C                            :     :
C                            :     :
C                            :     :
C                MLST,NFST:::::::MLST,NLST
C
C                     CONSIDER DATA TO BE SELECTED AS A BLOCK DEFINED
C                     BY MFST,NFST AND MLST,NLST.
C                     M2,N2 IS TRANSLATION VECTOR FROM SCAN TO SCAN2
C                     M3,N3 IS          ≡                  TO VARN
C                     M4,N4 IS          ≡                  SCAN2 TO VARN2
C     GO   PLDT       APLPHANUMERIC DESCRIPTION OF CROSS-SECTION
C     HO   CONST      MAGNITUDE CONSTANTS (SEE PROGRAM MAP)
C
C          CARDS C,E,H ARE USED ONLY WHEN NECCESSARY
C          FOR MORE THAN ONE XSECTN CARDS B TO H ARE REPEATED
C          LAST DATA CARD = MAPDAT = -1
C
C
C     CCL(POINT,SCAN,LINE)
C
      WRITE(6,100)
  100 FORMAT(1H1)
      IBLK=1 $ ABLK=IBLK*IBLK $ ISEP(1)=0 $ SZ=0.1 $ CONST(1)=1
      DO 99 I=2,5
   99 CONST(I)=0.0
      NCOUNT=1
      READ,MICFLM,PLSC,VEL
C
C                          INITIALISE PLOTTING PACKAGE
C
      CALL START(2)
      IF(MICFLM.EQ.1)CALL FACTOR(1.6)
      READ,MAPDAT
   14 MAG=0 $ IREF=0 $ IBV=1 $ ZRO(1)=0 $ ZRO(2)=0
      ISEP(2)=0 $ ISEP(3)=0 $ ISEP(4)=0
      IF(MICFLM.EQ.1)CALL PLOT(1.,1.,-3)
      IF(MAPDAT.GE.1000)MAG=1
      M=MAPDAT-1000*(MAPDAT/1000)
      IF(M.GE.100)IREF=1
      M=M-100*(M/100)
      IF(M.GE.10)IBV=2
      NUM1=M-10*(M/10)
```

```
      IF (NUM1.LT.1) NUM1=1
      NUM2=NUM1+IBV-1
      NUM3=NUM1+2
      NUM4=NUM2+2
      IF (IREF.EQ.1) READ,REFZRO,REF,(F(I),I=1,IBV)
C
C                          READ IN HEADER DATA AND CHECK SCAN IDS
C
      JREF=NUM1+2*IREF
      IBVREF=IBV-1+2*IREF
      READ,((ISCP(I),I=N,N+IBV-1),N=NUM1,JREF,2)
      IF (IBV.EQ.1.OR.MAG.EQ.1) READ,((ZRO(I),T(I)),I=1,IBV)
      DO 102 N=NUM1,JREF,2
      N2=N+IBV-1
      DO 102 I=N,N2
      REWIND I
      READ(I) IUR,ISC,NL(I),NPX(I),ASDT,SCDT
      WRITE(6,1002) ASDT,SCDT
 1002 FORMAT(/,X,4A10,5X,9HEXPOSURE ,A10,5X,7HFILTER ,A10,5X,4HDATE,A10
     +,5X,5HPLATE,A10,//,X,4A10,5X,5HSLIT ,A10,5X,10HTELESCOPE
     +,A10,  5X,5HTUBE ,A10,5X,5H FILM ,A10)
      IF (ISCP(I).EQ.ISC) GOTO 15
      WRITE(6,1004) ISC,ISCP(I)
 1004 FORMAT(20H SCAN IDS DONT AGREE,5X,8HTAPE ID=,I9,5X,8HCARD ID=,I9)
      IF (NCOUNT.EQ.1) STOP
      GOTO 61
   15 NB(I)=NPX(I)/512
  102 KL(I)=NPX(I)-NB(I)*512
      READ,((MFST(I),NFST(I)),I=N,N+IBV-1),N=NUM1,JREF,2),
     +  MLST,NLST,MOOTH,STEP
      READ(5,1006) PLOT
 1006 FORMAT(8A10)
      IF (MAG.EQ.1) READ,CONST
      SC=FLOAT(IBLK)*STEP*PLSC*VEL*4.848/50000.
      IF (VEL.LE.0.) SC=1.
C
C                          PRINT TITLES
C
      Z=0.25
      IF (VEL.LE.0.) GOTO 30
      CALL SYMBOL(0.,0.5,SZ,28HREC.VEL=      ,H=50KM/SEC/MPC  ,0.,28)
      CALL NUMBER(8.5*SZ,0.5,SZ,VEL,0.,-1)
   30 IF (MAG.NE.1.AND.IBV.NE.1) GOTO 31
      DO 108 I=1,IBV
      ZZ=0.35-(I-1)*0.15
      CALL SYMBOL(0.,ZZ,SZ,39HK=       ,SKY=        ,EXP.TIME=     SECS,0.
     +,39)
      CALL NUMBER(2.5*SZ,ZZ,SZ,CONST(5),0.0,2)
      CALL NUMBER(13.5*SZ,ZZ,SZ,ZRO(I),0.,2)
      CALL NUMBER(31.5*SZ,ZZ,SZ,T(I),0.,-1)
  108 IF (T(I).LE.0.) T(I)=1.
      SUB=T(1)*(STEP*PLSC*10.E-3)**2
      IF (SUB.LE.0.) SUB=1.0
   31 IF (IREF.NE.1) GOTO 33
      REFMAX=REF-REFZRO
      CALL SYMBOL(0.,-0.25,SZ,26HCORRECTED FOR PHOTOCATHODE,0.,26)
      CALL SYMBOL(30.*SZ,-0.25,SZ,22HREFZRO=      ,REF=      ,0.,22)
      NN=-1
      IF (REFZRO.LT.10.) NN=3
      CALL NUMBER(38.*SZ,-0.25,SZ,REFZRO,0.,NN)
      NN=-1
      IF (REFZRO.LT.10.) NN=3
      CALL NUMBER(48.*SZ,-0.25,SZ,REF,0.,NN)
      CALL SYMBOL(54.*SZ,-0.25,SZ,9HFILM BGD=,0.,9)
      DO 109 I=1,IBV
  109 CALL NUMBER((64.+FLOAT(I-1)*6.)*SZ,-0.25,SZ,F(I),0.,-1)
   33 IF (IBV.NE.2) GOTO 20
      A2=30.*SZ
      CALL SYMBOL(A2,0.,SZ,11HB ORIGIN AT ,0.,11)
      A1=NFST(NUM2)
      CALL NUMBER(A2+12.*SZ,0.,SZ,A1,0.,-1)
      A1=NFST(NUM2)
      CALL NUMBER(A2+17.*SZ,0.,SZ,A1,0.,-1)
   20 IF (MOOTH.EQ.1) CALL SYMBOL(5.,0.5,SZ,8HSMOOTHED,0.,8)
      CALL SYMBOL(0.,0.,SZ,PLOT,0.,80)
      I=8*(2+IBV-1+IREF+(IBV-1+IREF)/2)
      ENCODE(I,1030,SCANID)((ISCP(J),J=N,N+IBV-1),N=NUM1,JREF,2)
 1030 FORMAT(8HSCAN IDS,4I8)
      CALL SYMBOL(70.*SZ,0.5,SZ,SCANID,0.,I)
      WRITE(6,1008) PLOT,((MFST(I),NFST(I)),I=N,N+IBV-1),N=NUM1,JREF,2),
     +     MLST,NLST,MOOTH
 1008 FORMAT(/,X,8A10/X,11I10)
C
C                          CHECK AREAS TO BE USED LIE WITHIN SCAN
```

```
      IF (MFST(NUM1) .GT. MLST) GOTO 90
      NN1=1+MOOTH
      NN2=NPX(NUM1)-MOOTH
      CALL LIMITS(NFST(NUM1),NN1,NN2)
      CALL LIMITS(NLST,NN1,NN2)
      MM1=1+MOOTH
      MM2=NL(NUM1)-MOOTH
      CALL LIMITS(MFST(NUM1),MM1,MM2)
      CALL LIMITS(MLST,MM1,MM2)
      IF (IBV.NE.2) GOTO 22
      ISEP(NUM2)=-NFST(NUM2)
      CALL REORD(MFST(NUM1),MFST(NUM2),KDUM,KDUM)
      CALL REORD(NFST(NUM1),NFST(NUM2),KDUM,KDUM)
      IF (IREF.NE.1) GOTO 24
      ISEP(NUM3)=-NFST(NUM3)
      CALL REORD(MFST(NUM1),MFST(NUM3),MFST(NUM2),KDUM)
      CALL REORD(NFST(NUM1),NFST(NUM3),NFST(NUM2),KDUM)
      ISEP(4)=-NFST(4)
      CALL REORD(MFST(1),MFST(4),MFST(2),MFST(3))
      CALL REORD(NFST(1),NFST(4),NFST(2),NFST(3))
      GOTO 24
   22 IF (IREF.NE.1) GOTO 24
      ISEP(NUM3)=-NFST(NUM3)
      CALL REORD(MFST(NUM1),MFST(NUM3),KDUM,KDUM)
      CALL REORD(NFST(NUM1),NFST(NUM3),KDUM,KDUM)
   24 DO 113 N=NUM1,JREF,2
      N2=N+IBV-1
      DO 113 I=N,N2
      IF (I.EQ.NUM1) GOTO 113
      NN2=NPX(I)-MOOTH-ISEP(I)
      CALL LIMITS(NLST,NN1,NN2)
      CALL LIMITS(NFST(NUM1),NN1,NN2)
      MM2=NL(I)-MOOTH+MFST(I)-MFST(NUM1)
      CALL LIMITS(MFST(NUM1),MM1,MM2)
      CALL LIMITS(MLST,MFST(NUM1),MM2)
  113 CONTINUE
      WRITE(6,1009) (((MFST(I),NFST(I)),I=N,N+IBV-1),N=NUM1,JREF,2),MLST,
     +    NLST
 1009 FORMAT(X,10I10)
C
C                              POSITION SCANS
C
      DO 110 NN=NUM1,JREF,2
      DO 110 I=NN,NN+IBV-1
      MF=MFST(I)-MOOTH
      IF (MF.GT.1) CALL POSIN(MF,NB(I),KL(I),I)
      IF (MOOTH.NE.1) GOTO 110
      DO 112 J=2,3
  112 CALL READB(I,NB(I),KL(I),COL(1,I,J))
  110 CONTINUE
      A2=40.*SZ
      CALL SYMBOL(A2,Z,SZ,33HXSECTN FROM          TO          ,0.,33)
      A1=MFST(NUM1)
      CALL NUMBER(A2+12.5*SZ,Z,SZ,A1,0.,-1)
      A1=NFST(NUM1)
      CALL NUMBER(A2+17.5*SZ,Z,SZ,A1,0.,-1)
      A1=MLST
      CALL NUMBER(A2+24.5*SZ,Z,SZ,A1,0.,-1)
      A1=NLST
      CALL NUMBER(A2+29.5*SZ,Z,SZ,A1,0.,-1)
      CALL PLOT(0.0,1.0,-3)
C
C                              FIND POINTS ON CROSS-SECTION
C
      IKI=0
      IKJ=1
      NF=1+NFST(NUM1)/IBLK
      IF (IBLK.EQ.1) NF=NF-1
      ML=(MLST-MFST(NUM1)+1)/IBLK
      NL1=(NLST-NFST(NUM1)+1)/IBLK
      IF (ML.GT.1) GRAD=FLOAT(NL1-1)/FLOAT(ML)
      KFST=NF
      KLST=NF+NL1-1
C
C                              FIND POINTS ON EACH LINE
C
      DO 122 J=1,ML
      IF (ML.EQ.1) GOTO 36
      KFST=FLOAT(J-1)*GRAD+FLOAT(NF)
      KLST=FLOAT(J)*GRAD+FLOAT(NF)
      IF (GRAD.GT.0.) GOTO 36
      KDUM=KLST
      KLST=KFST
      KFST=KDUM
   36 DO 114 NN=NUM1,JREF,2
```

```
      DO 114 I=NN,NN+IBV-1
  114 CALL READB(I,NB(I),KL(I),COL(1,I,1))
C
C                        FOR POINTS ON CROSS-SECTION FIND X,Y CO-ORDS.
C
      DO 116 III=KFST,KLST
      II=III
      IF(GRAD.LT.0.0) II=KLST+KFST-III
      IKI=IKI+1
      X(IKI)=SQRT(FLOAT(J-1)**2+FLOAT(II-NF)**2)*SC
      IF(MOOTH.EQ.1)GOTO(42,48),IBV
      GOTO(38,37,40,39),IBVREF
   37 A2=COL(II+ISEP(NUM2),NUM2,1)
   38 A1=COL(II,NUM1,1)
      GOTO 41
   39 IIS2=II+ISEP(2)+ISEP(4)
      IF(COL(IIS2,4,1).GT.REF.OR.COL(IIS2,4,1).LE.REFZRO)COL(IIS2,4,1)
     +   =REF
      A2=(COL(II+ISEP(2),2,1)-F(2))*REFMAX/(COL(IIS2,4,1)-REFZRO)-ZRO(2)
     +   +F(2)
   40 IIS1=II+ISEP(NUM3)
      IF(COL(IIS1,NUM3,1).GT.REF.OR.COL(IIS1,NUM3,1).LE.REFZRO)
     +      COL(IIS1,NUM3,1)=REF
      A1=(COL(II,NUM1,1)-F(1))*REFMAX/(COL(IIS1,NUM3,1)-REFZRO)+F(1)
   41 GOTO(43,44),IBV
   42 CALL AV(A1,II)
   43 Y(IKI)=A1
      IF(MAG.NE.1)GOTO 116
      Y(IKI)=Y(IKI)-ZRO(1)
      IF(Y(IKI).LE.0.0)GOTO 45
      Y(IKI)=(-2.5*ALOG10(Y(IKI)/SJB)-CONST(6))+CONST(5)
      GOTO 116
   45 Y(IKI)=CONST(5)
      YY(IKJ)=Y(IKI)
      XX(IKJ)=X(IKI)
      IKJ=IKJ+1
      GOTO 116
   44 A1=A1-ZRO(1)
      A2=A2-ZRO(2)
   46 IF(A1.LE.0..OR.A2.LE.0.)CALL FAULT(A1,A2)
      Y(IKI)=(A1*T(2))/(A2*T(1))
      Y(IKI)=CONST(1)*(2.5*ALOG10(Y(IKI))-CONST(3))+CONST(2)
      GOTO 50
   48 CALL AV(Y(IKI),II)
   50 IF(Y(IKI).GT.1.4)CALL FLT(1.4)
      IF(Y(IKI).LT.-1.0)CALL FLT(-1.0)
  116 CONTINUE
      IF(MOOTH.NE.1)GOTO 122
      DO 118 NN=NUM1,JREF,2
      DO 118 I=NN,NN+IBV-1
      DO 118 KKJ=1,NPX(I)
      COL(KKJ,I,3)=COL(KKJ,I,2)
  118 COL(KKJ,I,2)=COL(KKJ,I,1)
  122 CONTINUE
      IKJ=IKJ-1
C
C                     DATA IS NOW IN ARRAYS X AND Y,SO SCALE THE ARRAYS
C
      CALL SCALE(X,10.0,IKI,1)
      XAXIS=7HPARSECS  ; YAXIS=7HDENSITY
      IF(IBV.EQ.1)GOTO 56
      INC=1
      IF(MAG.NE.1)GOTO 59
      INC=-1
      YAXIS=10H MAG/SEC2
   59 CALL SCALE(Y,6.0,IKI,INC)
      GOTO 57
   56 YAXIS=10HB-V XSECTN
      Y(IKI+1)=-1.
      Y(IKI+2)=0.4
      IF(IKJ.LT.1)GOTO 57
      XX(IKJ+1)=X(IKI+1)
      XX(IKJ+2)=X(IKI+2)
      YY(IKJ+1)=-1.0
      YY(IKJ+2)=0.4
   57 WRITE(6,302)IKI
  302 FORMAT(5X,I6,29H POINTS USED IN CROSS-SECTION  )
C
C                              DRAW SCALE MARKERS
C
      IF(PLSC.LE.0.)XAXIS=10H
      IF(PLSC.LE.0.)GOTO 64
      AS=2.0*4.848*VEL/(X(IKI+2)*50.0)
      IF(VEL.GT.0.)GOTO 60
      AS=2000./(STEP*PLSC*X(IKI+2))
```

```
      XAXIS=10H
   60 Z=-1.25
      SZZ=80.*SZ
      ASS=10.*SC/X(IKI+2)
      CALL PLOT(SZZ,Z+1.2*SZ,3)
      CALL PLOT(SZZ+ASS,Z+1.2*SZ,2)
      CALL SYMBOL(SZZ,Z,0.1,8H2 ARCSEC,0.0,8)
      CALL PLOT(SZZ,Z-.01,3)
      CALL PLOT(SZZ,Z-.11,2)
      CALL PLOT(SZZ,Z-.06,3)
      CALL PLOT(SZZ+AS,Z-.06,2)
      CALL PLOT(SZZ+AS,Z-.11,3)
      CALL PLOT(SZZ+AS,Z-.01,2)
C
CCC                          DRAW GRAPH
C
   64 CALL AXIS(0.0,0.0,XAXIS,-10,10.0,0.0,X(IKI+1),X(IKI+2))
      CALL AXIS(0.0,0.0,YAXIS,10,6.0,90.0,Y(IKI+1),Y(IKI+2))
      CALL LINE(X,Y,IKI,1,0,4)
      IF(IKJ.GT.0.AND.CONST(1).GT.0.)CALL LINE(XX,YY,IKJ,1,-1,1)
      READ,MAPDAT
      IF(MAPDAT.LT.0)GOTO 61
      NCOUNT=NCOUNT+1
      IF(MICFLM.EQ.1)GOTO 66
      IF(MOD(NCOUNT,3).NE.1)CALL PLOT(0.0,7.0,-3)
      IF(MOD(NCOUNT,3).EQ.1)CALL PLOT(12.0,-17.0,-3)
      GOTO 14
   66 CALL NEWPAGE
      GOTO 14
   90 WRITE(6,1032)
 1032 FORMAT(10HERROR STOP)
   61 CALL ENPLOT(12,0)
      STOP
      END
      SUBROUTINE LIMITS(I,J,K)
      IF(I.LT.J) I=J
      IF(I.GT.K) I=K
      RETURN
      END
      SUBROUTINE FLT(A)
      COMMON C(7200),X(650),Y(650),XX(102),YY(102)
      COMMON /I/ IKJ,IKI,MOOTH
C
CCC            THIS SUBROUTINE CHECKS ARRAYS XX,YY ARE NOT OUT OF RANGE
C
      Y(IKI)=A
      IF(IKJ.GT.100)GOTO 1
      YY(IKJ)=A
      XX(IKJ)=X(IKI)
      IKJ=IKJ+1
      RETURN
    1 WRITE(6,100)
  100 FORMAT(56H DIMENSION OF XX AND YY ARRAYS WILL HAVE TO BE INCREASED
     +      )
      RETURN
      END
      SUBROUTINE FAULT(A,B)
      COMMON C(7200),X(650),Y(650),XX(102),YY(102)
      COMMON /I/ IKJ,IKI,MOOTH
      COMMON /NUM/ ISEP(4),NUM1,NUM2,IBV,ZRO(2),T(2)
      COMMON /REF/ REF,IREF,REFZRO,CONST(6),F(2)
      A=T(1)
      B=T(2)
      IF(IKJ.GT.100)GOTO 1
      XX(IKJ)=X(IKI)
      YY(IKJ)=CONST(2)-CONST(1)*CONST(3)
      IKJ=IKJ+1
      RETURN
    1 WRITE(6,100)
  100 FORMAT(5H OOPS)
      RETURN
      END
      SUBROUTINE AV(RES,M)
      COMMON COL(600,4,3)
      DIMENSION A(9,2),II(4)
      COMMON /REF/ REF,IREF,REFZRO,CONST(6),F(2)
      COMMON /NUM/ ISEP(4),NUM1,NUM2,IBV,ZRO(2),T(2)
C
CCC    THIS SUBROUTINE AVERAGES EACH POINT ON THE XSECTN WITH THE
CCC        SURROUNDING 8 POINTS
C
      II(NUM1)=M
      JREF=NUM1+2*IREF
      DO 100 N=NUM1,JREF,2
      N2=N+IBV-1
```

```
      DO 100 I=N,N2
  100 IF(I.NE.NUM1) II(I)=M+ISEP(I)
      IF(IREF.EQ.1)REFMAX=REF-REFZRO
C
CCCCC  I=SCAN
CCCCC  L=LINE NUMBER
CCCCC  KK=POINT NUMBER
C
      DO 1 I=NUM1,NUM2
      DO 1 L=1,3
      DO 1 KK=1,3
      K=KK-2
      J=KK+3*(L-1)
      IJ=II(I)+K
      III=I-NUM1+1
      IF(IREF.EQ.1)GOTO 6
      A(J,III)=COL(IJ,I,L)
      GOTO 1
    6 I2=I+2
      IIJ=II(I2)+K
      IF(COL(IIJ,I2,L).GT.REF.OR.COL(IIJ,I2,L).LE.REFZRO)COL(IIJ,I2,L)
     +   =REF
      A(J,III)=(COL(IJ,I,L)-F(I))*REFMAX/(COL(IIJ,I2,L)-REFZRO)+F(I)
    1 CONTINUE
      DO 104 I=NUM1,NUM2
      III=I+1-NUM1
      DO 103 J=2,9
  103 A(1,III)=A(1,III)+A(J,III)
  104 A(1,III)=A(1,III)/9.
      IF(IBV.EQ.2)GOTO 14
      RES=A(1,1)
      RETURN
   14 A(1,1)=A(1,1)-ZRO(1)
      A(1,2)=A(1,2)-ZRO(2)
      IF(A(1,1).LE.0..OR.A(1,2).LE.0.)CALL FAULT(A(1,1),A(1,2))
      RES=(A(1,1)**T(2))/(A(1,2)**T(1))
      IF(CONST(1).LE.0.)RETURN
      RES=CONST(1)*(2.5*ALOG10(RES)-CONST(3))+CONST(2)
      RETURN
      END
      SUBROUTINE REORD(I,J,K,L)
      IF(I-(1+J))1,2,3
    1 K=K+J-I+1
      L=L+J-I+1
      I=J+1
    2 J=1
      RETURN
    3 J=I-J
      RETURN
      END
      SUBROUTINE POSIN(MFST,NB,KL,I)
C
CCC                          READ IN UNUSED LINES
C
      MFMI=MFST-1
      DO 3 J=1,MFMI
      IF(NB.EQ.0)GOTO 3
      DO 41 NNB=1,NB
   41 READ(I)DATA
    3 IF(KL.GT.0)READ(I)DATA
      RETURN
      END
      SUBROUTINE REED(I,NB,KL,LINE)
      COMMON AA(9304)
      REAL LINE(600)
C
CCCCCC NOTE.DATA BLOCK ON STANDARD ARCHIVE TAPE CONSISTS OF
CCCCCC       512 WORDS WHEN FULL
C
      IF(NB.EQ.0)GOTO 43
      DO 47 II=1,NB
      KK=512*(II-1)
   47 READ(I)(LINE(KK+K),K=1,512)
   43 KK=NB*512
      IF(KL.GT.0)READ(I)(LINE(KK+K),K=1,KL)
      LINE(512)=LINE(511)
      RETURN
      END
      SUBROUTINE READB(I,NB,KL,LINE)
      COMMON AA(8704),DATA(600)
      COMMON /IBLK/ IBLK,ABLK,NFST(4)
C
CCC                          THIS SUBROUTINE BLOCKS THE DATA
C
      REAL LINE(600)
```

```
      IF(IBLK.EQ.1)GOTO 10
      NP=(NB*512+KL)/IBLK
      DO 100 L=1,NP
  100 LINE(L)=0
      DO 102 L=1,IBLK
      CALL REED(I,NB,KL,DATA)
      IKI=0
      DO 102 LL=1,NP
      DO 102 LJ=1,IBLK
      IKI=IKI+1
  102 LINE(LL)=LINE(LL)+DATA(IKI)/ABLK
      RETURN
   10 CALL REED(I,NB,KL,LINE)
      RETURN
      END
```

```
C
C                          PROGRAM TRANS
C
      PROGRAM TRANS(INPUT,OUTPUT,TAPE5=INPUT,TAPE6=OUTPUT,DATA,TAPE1=
     +DATA,TAPE7)
C
C       THIS PROGRAM TRANSFERS DATA FROM A TAPE TO DISC FOR USE BY
C       THE SIMPLE PROGRAMS SIMMAP,SLARD,XSEC
C       IUR IS MADE NEGATIVE TO DENOTE THAT THERE IS AN EXTRA HEADER RECORD
C       FILES MOST BE COPIED FROM TAPE TO A DISC FILE CALLED DATA
C       THE INFORMATION IS PUT ONTO TAPE7 AND THEN SAVED OR DEFINED
C       SV=S FOR A FILE TO BE SAVED
C       SV=D FOR A FILE TO BE DEFINED DIRECT ACCESS
C       FN=PERMANENT FILE NAME TO BE USED
C       IBLK=-VE IMPLIES THERE IS ANOTHER FILE TO BE PROCESSED
C       AFTER THE PRESENT ONE
C                     PROGRAM DEVELOPED AND WRITTEN BY D.P.YOULL
C                                IMPERIAL COLLEGE 1975
C
      COMMON DATA(1024),PT(256),ASDT(8),SCDT(8)
      REWIND 1
C
C       READ IN HEADER DATA
C
   10 READ(1) IUR,ISC,NL,NPX,ASDT,SCDT
      IUR=-IUR
      READ,ISCP,STEP,PLSC,T,DEL,VEL
      READ,MFST,NFST,MLST,NLST,IBLK
      IFLAG=0
      IF(IBLK.LT.0) IFLAG=1
      IBLK=IABS(IBLK)
      READ(5,1000) SAV,FN
 1000 FORMAT(A1,A7)
      ABLK=IBLK*IBLK
      IF(ISCP.EQ.ISC) GOTO 12
      WRITE(6,1002) ISC,ISCP
 1002 FORMAT('IDS DO NOT AGREE,TAPE=',I10,5X,'CARD ID=',I10)
      STOP1
C
C       POSITION SCAN
C
   12 NB=NPX/512
      IF(MLST.GT.NL) MLST=NL
      IF(NLST.GT.NPX) NLST=NPX
      KL=NLST-NB*512
      IF(MFST.EQ.1) GOTO 14
      MFMI=MFST-1
      DO100 J=1,MFMI
      IF(NB.EQ.0) GOTO100
      DO 102 NNB=1,NB
  102 READ(1) DUM
  100 IF(KL.GT.0) READ(1) DUM
C
C       WRITE NEW HEADER DATA ON TAPE 7
C
   14 STEP=STEP*FLOAT(IBLK)
      NPX=(NLST-NFST+1)/IBLK
      NL=(MLST-MFST+1)/IBLK
      IF(NPX.LT.257) GOTO 15
      PRINT,'ONLY 256 POINTS PER LINE CAN BE TRANSFERRED TO DISC'
      STOP2
   15 REWIND 7
      WRITE(7) IUR,ISC,NL,NPX,ASDT,SCDT
      WRITE(7) STEP,PLSC,T,DEL,VEL
```

```
C
C       READ DATA,BLOCK,AND WRITE ONTO TAPE 7
C
      DO 112 K=1,NL
      DO 104 I=1,NPX
  104 PT(I)=0.0
      DO 110 NUM=1,IBLK
      IF(NB.EQ.0)GOTO 16
      DO 105 II=1,NB
      KK=(II-1)*512
  105 READ(1) (DATA(I+KK),I=1,512)
   16 KK=NB*512
      IF(KL.GT.0)READ(1) (DATA(I+KK),I=1,KL)
      DO 108 I=1,NPX
      JJJ=IBLK*(I-1)+NFST-1
      DO 106 II=1,IBLK
  106 PT(I)=PT(I)+DATA(JJJ+II)/ABLK
  108 CONTINUE
  110 CONTINUE
  112 WRITE(7) (PT(I),I=1,NPX)
C
C       SAVE OR DEFINE TAPE7=FN
C
      IF(SAV.NE.1HD)CALL SAVE(5HTAPE7,FN)
      IF(SAV.EQ.1HD)CALL DEFINE(5HTAPE7,FN)
      WRITE(6,1006)FN
      IF(IFLAG.NE.1)STOP
   18 IF(EOF,1)10,20
   20 READ(1)DUM
      GOTO 18
 1006 FORMAT(5X,A7)
      END
```

```
C                                        PROGRAM SIMMAP
      PROGRAM SIMMAP(INPUT=131B,OUTPUT=131B,TAPE6=131B,TAPE64=131B,TAPE5
     +        =INPUT,DATA=401B,TAPE1=DATA,TAPE61=131B,TAPE66=131B)
C
C     THIS PROGRAM DRAWS CONTOURS OF AN ARRAY OF DATA
C     THE FIRST TWO RECORDS OF THE ARRAY CONTAIN HEADER INFORMATION
C     THE DATA IS IN NL LINES OF NPX POINTS,ONE LINE PER RECORDAND
C     UPTO 256 POINTS PER LINE
C     STEP=STEP LENGTH IN MICRONS
C     PLSC=PLATE SCALE IN ARCSEC PER MM.
C     PRINT,PROMPT,HARDCPY,SWITCH,KXWIRES ARE SIMPLE ROUTINES
C     START,PLOT,SYMBOL ARE STANDARD CALCOMP ROUTINES
C     PROGRAM DEVELOPED AND WRITTEN BY D.P.YOULL
C                                        IMPERIAL COLLEGE 1975
C
      COMMON A(768)
      COMMON ASDT(8),SCDT(8),SCANID(2)
      COMMON /YY/ AM,MFST,NFST,NLST,IBLK,ABLK
      COMMON /WAY/ CX(4),CY(4),KM1,KM2,SIZE,KKK
      COMMON /SETPF/ IPF(4)
C
C                              INITIALISE
C
      ISIZE=180 $ STEP=0 $ PLSC=0 $ KKK=5
      REWIND 6
      CALL START(2)
      CALL SWITCH(9HHARDCPY0N)
      CALL PROMPT('PROGRAM SIMMAP',14)
      GOTO 10
    8 CALL NEWPAGE
C
   10 CALL PROMPT('TYPE FILE NAME CONTAINING DATA ',31)
C
      READ(.ERR.=10,.END.=10,5,1006)D
C
C                              GET OR ATTACH DATA FILE
C
      CALL SETPF(IPF(1))
      CALL GET('TAPE1',D)
      IF(IPF(1).NE.0)GOTO 12
      GOTO 14
   12 CALL SETPF(IPF(1))
      CALL ATTACH('TAPE1',D)
      IF(IPF(1).EQ.0)GOTO 14
      CALL PROMPT('ERROR - CANNOT FIND FILE ',25)
      GOTO 10
C
C                        READ FILE DATA ,SCAN ID AND OUTPUT HEADER DATA
C
   14 REWIND 1
      READ(1)IUR,ISC,NL,NPX,ASDT,SCDT
      WRITE(6,1000)ISC,NL,NPX,ASDT,SCDT
 1000 FORMAT(//,8HSCAN ID=,I6,10X,I6,'LINES OF',I6,' POINTS',//,8A10,
     +     //,8A10)
      IF(IUR.LT.0)READ(1)STEP,PLSC
      WRITE(6,1002)STEP,PLSC
 1002 FORMAT(//,5X,'STEP=',F5.1,5X,'PLATE SCALE=',F5.1///
     +' WHEN THE PROGRAM ASKS FOR A CONTOUR HEIGHT YOU CAN TYPE ANY'/
     +'CONTOUR HEIGHT OR ASK FOR AN OPTION BY TYPING ONE OF THESE NUMBER
     +'S'/
     +'       -11=END PROGRAM AND PROCESS MICROFILM'/
     +'       -12=HARDCOPY PRESENT FRAME'/
     +'       -13=DISPLAY XWIRES(CO-ORDS OF XWIRES WILL BE RETURNED)'/
     +'       -14=CHOOSE NEW AREA FOR PLOTTING(DEFAULT IS WHOLE AREA'/
     +'       -15=MAGNIFY THE PLOT'/
     +'       -16=CHOOSE NEW DATA FILE TO BE CONTOURED'//
     +'THE PROGRAM ASSUMES THE WHOLE SCAN IS TO BE CONTOURED'/
     +'TO CHOOSE A SPECIFIC AREA TYPE  -14'/
     +'IF YOU WISH TO CONTOUR ANOTHER DATA FILE TYPE -16'/
     +'OTHERWISE TYPE GO  ≥    ')
      CALL BUFFEM(-6)
      READ(.ERR.=16,.END.=16,5,)NO
      IF(NO.NE.-14)GOTO 8
      GOTO 40
C
C     DATA FOR SUBROUTINE WHICH FORMS PLOTTING ARRAY A
C
C                    MFST,NFST:::::::::MFST,NLST
C                              :       :
C                              :       :
C                              :       :
C                    NLST,NFST:::::::::NLST,NLST
```

```
C     CONSIDER DATA TO BE SELECTED AS A BLOCK DEFINED BY
C    MFST,NFST AND MLST,NLST. IBLK IS THE NUMBER OF POINTS
C     IN A ROW OR COLUMN WHICH ARE ADDED TOGETHER TO GIVE
C     ONE PLOTTING POINT IN ARRAY A.
C
 1006 FORMAT(A7)
   16 MFST=1
      NFST=1
      MLST=NL
      NLST=NPX
      IBLK=1
C
C                                MAIN LOOP
C
   17 ABLK=IBLK*IBLK
      NCONT=2
      Y=-1.2
      CALL FACTOR(1.)
      IF(MLST.GT.NL)MLST=NL
      IF(NLST.GT.NPX)NLST=NPX
      IF(MFST.LT.1)MFST=1
      IF(NFST.LT.1)NFST=1
      M=(MLST-MFST+1)/IBLK
      N=(NLST-NFST+1)/IBLK
      AM=FLOAT(ISIZE)/AMAX1(FLOAT(2*M),FLOAT(N))
   18 CALL NEWPAGE
C
      CALL PROMPT('-11=END,-12=HARDCPY,-13=XWIRES,-14=NEW AREA,-15=MAGNI
     +FY,-16=NEW DATA',68)
C
C                     CALCULATE PLOT LENGTH FOR USE IN LABELLING PLOT
C
      RNIK=FLOAT(M-1)/10.
      PL=FLOAT(N-1)*0.1
C
C                               PRINT TITLES
C
      CALL PRINT(-1.,0.6,ASDT,72)
      CALL PRINT(-1.,0.2,SCDT,72)
      CALL PRINT(-1.,-0.2,'CONTOUR HEIGHTS',15)
C
C                          PLOT SCALE MARKER 10 ARCSEC LONG
C
      SLPL=STEP*PLSC*FLOAT(IBLK)
      SIZE=0.07/AM
      CALL PLOT(0.,1.1,-3)
      CALL FACTOR(AM)
      CALL PLOT(PL,0.,2)
      IF(SLPL.LE.0.)GOTO  20
      SCALE=1000./SLPL
      X=PL+0.25/AM
      CALL PLOT(X-SIZE,0.,3)
      CALL PLOT(X+SIZE,0.,2)
      CALL SYMBOL(X+4.*SIZE,0.,2.*SIZE,9H10 ARCSEC,90.,9)
      CALL PLOT(X,0.,3)
      CALL PLOT(X,SCALE,2)
      CALL PLOT(X+SIZE,SCALE,3)
      CALL PLOT(X-SIZE,SCALE,2)
C
C                               DRAW BOX
C
      CALL PLOT(PL,0.,3)
   20 CALL PLOT(PL,RNIK,2)
      CALL PLOT(0.,RNIK,2)
      ENCODE(14,1008,SCANID) ISC
 1008 FORMAT('SCAN ID=',I6)
      CALL PRINT(0.,RNIK+SIZE,SCANID,14)
      CALL PLOT(0.,RNIK,3)
      CALL PLOT(0.,0.,2)
      GOTO 26
   22 NCONT=NCONT+2
      CALL FACTOR(1.)
      IFORM=6H(F7.1)
      IF(HT.LT.10.)IFORM=6H(F7.3)
      ENCODE(7,IFORM,CHT)HT
      IF(NCONT.LT.19)GOTO 24
      Y=Y-0.4
      NCONT=4
   24 CALL PRINT(FLOAT(NCONT),Y,CHT,7)
      HT=HT+10.E-9
      CALL FACTOR(AM)
C
C                               DRAW CONTOURS
C
      CALL SECTN(I,N,HT)
```

```
      REWIND 1 $ READ(1)HEAD
      IF(IUR.LT.0)READ(1)HEAD
   26 CALL PROMPT('CONTOUR HEIGHT=',15)
      READ(,END.=26,,ERR.=26,5,)HT
      IF(HT.LT.-16.)GOTO 26
      IF(HT.LT.-9.)GOTO 28
      GOTO 22
   28 IHT=ABS(HT)-10.
      GOTO(30,32,34,38,44,8),IHT
   30 STOP
   32 CALL HARDCPY
      GOTO 26
   34 CALL PROMPT('TYPE 0 TO RETURN XWIRES,OTHERWISE ANYTHING ',42)
   36 CALL KXWIRES(POS1,POS2,I)
      POS1=NFST+(POS1*10.0)*IBLK
      POS2=MFST+(M-(POS2*10.))*IBLK-1
      WRITE(6,1010)POS2,POS1
C
 1010 FORMAT(1X,13HCENTRE AT M=   ,F6.1,3H N=,F6.1)
C
      CALL BUFFEM(-6)
      IF(I.EQ.1HO)GOTO36
      GOTO 26
C
   38 CALL PROMPT(36HDO YOU WANT THE SAME AREA CONTOURED  ,36)
C
      READ(,END.=38,,ERR.=38,5,1006)NO
      IF(NO.EQ.1HY)GOTO 42
C
   40 CALL PROMPT(68HWHAT ARE CO ORDS M,N OF TOP LEFT AND BOTTOM RIGHT O
     +F CONTOURED AREA       ,69)
C
      READ(,END.=40,,ERR.=40,5,)MFST,NFST,MLST,NLST
C
   42 CALL PROMPT(18H BLOCKING FACTOR = ,18)
C
      READ(,END.=42,,ERR.=42,5,)IBLK
      GOTO 17
C
   44 CALL PROMPT(31HWHAT MAGNIFICATION DO YOU WANT   ,31)
C
      READ(,END.=44,,ERR.=44,5,)XMAG
      CALL MAGNIFY(XMAG)
      GOTO 18
      END
      SUBROUTINE SECTN(JL,KL,H)
C
C::::::               THIS SUBROUTINE SELECTS DATA FROM A FILE
C::::::       AND FEEDS IT INTO THE PLOTTING ARRAY A
C
      COMMON A(256,2)
      COMMON /YY/ AM,MFST,NFST,NPX,IBLK,ABLK
      JLST=JL
      KLST=KL
      HT=H
C
C                             POSITION SCAN
C
      IF(MFST.EQ.1)GOTO 4
      MFMI=MFST-1
      DO 2 I=1,MFMI
    2 READ(1)DATA
C
C                             ZERO ARRAY A
C
    4 DO 6 K=1,KLST
    6 A(K,2)=0.0
C
C                             READ AND BLOCK FIRST LINE INTO A(K,2)
C
      CALL READBLK(KLST)
C
C                             FOR EVERY OTHER LINE
C
      DO 14 J=2,JLST
      DO 8 K=1,KLST
      A(K,1)=A(K,2)
    8 A(K,2)=0.0
      CALL READBLK(KLST)
C
C                             PLOT CONTOURS
C
   14 CALL CONT(A,JLST,KLST,J,HT)
      RETURN
      END
```

```
      SUBROUTINE READBLK(KL)
      COMMON A(256,2),ALINE(256)
      COMMON /YY/ AM,MFST,NFST,NPX,IBLK,ABLK
C
C                              THIS SUBROUTINE READS AND BLOCKS DATA
      KLST=KL
      ABLK=IBLK
      DO 12 IZ=1,IBLK
      READ(1)(ALINE(I),I=1,NPX)
      IKI=NFST-1
      DO 12 K=1,KLST
      DO 12 IK=1,IBLK
      IKI=IKI+1
   12 A(K,2)=A(K,2)+ALINE(IKI)/ABLK
      RETURN
      END
      SUBROUTINE CONT(A,MMM,L,III,AMIN)
C          A(J,1)          3    A(J+1,1)
C                    **********
C                    *         *
C                    *         *
C                  4 *         * 2
C                    *         *
C                    *         *
C                    **********
C         A(J,2)               A(J+1,2)
C
C     THIS SUBROUTINE CALLS NINSEC,WAY,FIND
C
      COMMON AA(768)
      DIMENSION A(256,2),I(4)
      COMMON /WAY/ CX(4),CY(4),KM1,KM2,SIZE,K
      LOGICAL NINSEC
      NIK=L-1 $ M=MMM $ II=III-1 $ HT=AMIN $ X=0 $ Y=0
      AMII=FLOAT(MMM-II)*0.1
C
C                    MAIN LOOP WITH INITIAL CONDITIONS SET UP
C
      DO 100 J=1,NIK
      IF(AMAX1(A(J,1),A(J,2),A(J+1,2),A(J+1,1)).LT.HT)GOTO 100
      IF(AMIN1(A(J,1),A(J,2),A(J+1,2),A(J+1,1)).GT.HT)GOTO 100
C
C                     KOUNT=NUMBER OF INTERSECTIONS IN A BOX=0,2,4
C
      KOUNT=0
      IF(NINSEC(A(J,1),A(J+1,1),HT))GOTO 10
      KOUNT=KOUNT+1
      I(KOUNT)=3
      CX(3)=FLOAT(J-1)*0.1+DIST(A(J,1),A(J+1,1),HT)
      CY(3)=AMII
   10 IF(NINSEC(A(J,1),A(J,2),HT))GOTO 12
      KOUNT=KOUNT+1
      I(KOUNT)=4
      CX(4)=FLOAT(J)*0.1-0.1
      CY(4)=AMII-DIST(A(J,1),A(J,2),HT)
   12 IF(NINSEC(A(J+1,1),A(J+1,2),HT))GOTO 14
      KOUNT=KOUNT+1
      CX(2)=FLOAT(J)*0.1
      CY(2)=AMII-DIST(A(J+1,1),A(J+1,2),HT)
      I(KOUNT)=2
   14 IF(KOUNT.EQ.0)GOTO 100
      IF(KOUNT.NE.2)GOTO 18
   16 I1=I(1)
      I2=I(2)
      IF(X.NE.CX(I1).OR.Y.NE.CY(I1))CALL PLOT(CX(I1),CY(I1),3)
      IF(MOD(II,K).EQ.2.AND.MOD(J,K).EQ.2)CALL FIND(A,HT,J,
     +CX(I1),CY(I1),CX(I2),CY(I2),I(2))
      CALL PLOT(CX(I2),CY(I2),2)
      X=CX(I2)
      Y=CY(I2)
      GOTO 100
   18 CX(1)=FLOAT(J-1)*0.1+DIST(A(J,2),A(J+1,2),HT)
      CY(1)=AMII-0.1
      KOUNT=KOUNT+1
      I(KOUNT)=1
      IF(KOUNT.EQ.2)GOTO 16
C
C                     FOR 4 INTERSECTIONS ON A BOX CALL WAY
C
      CALL WAY
      IF(X.NE.CX(3).OR.Y.NE.CY(3))CALL PLOT(CX(3),CY(3),3)
      CALL PLOT(CX(KM1),CY(KM1),2)
      CALL PLOT(CX(1),CY(1),3)
      IT=KM2
```

```
      CALL PLOT(CX(IT),CY(IT),2)
      X=CX(IT)
      Y=CY(IT)
  100 CONTINUE
      RETURN
      END
      SUBROUTINE FIND(A,VA,JII,X1,Y1,X,Y,IN)
      DIMENSION A(256,2)
      COMMON AA(768)
      COMMON /WAY/ CX(4),CY(4),KM1,KM2,SIZE,K
C
CCC    THIS SUBROUTINE DRAWS A POINTER ON A CONTOUR TO MARK
C         THE DIRECTION OF A RISE
C
      INN=IN
      VAL=VA
      X2=(X1+X)/2.0
      Y2=(Y1+Y)/2.0
      CALL PLOT(X2,Y2,2)
      AK=-SIZE/2.
      IF(Y.EQ.Y1)GOTO 10
      G=((X1-X)/(Y-Y1))
      G2=G**2
      G3=SQRT(1.0/(1.0+G2))
      JI=JII
      IF(INN.LT.3)JI=1+JI
      JL=1
      IF(INN.EQ.1.OR.INN.EQ.4)JL=2
      IF(A(JI,JL).GT.VAL)AK=-AK
      IF(INN.GT.2)AK=-AK
      AKK=1.
      IF(G.LT.0..AND.(INN/2)*2.EQ.INN)AKK=-AKK
      YYY=Y2-AK*G*G3
      IF((INN/2)*2.EQ.INN)YYY=Y2-AK*G3
      CALL PLOT(X2-AK*AKK*G3,YYY,2)
      CALL PLOT(X2,Y2,3)
      RETURN
   10 IF(INN.EQ.2)AK=-AK
      CALL PLOT(X2,Y2+AK,2)
      CALL PLOT(X2,Y2,3)
      RETURN
      END
      LOGICAL FUNCTION NINSEC( A, B, V )
C
CC  ********** THIS SUBROUTINE FINDS IF CONTOUR CROSSES AN EDGE OF THE BOX *
C
      LOGICAL G
      G=.TRUE.
      IF ( A.GT.V.AND.V.GT.B.OR.A.LT.V.AND.V.LT.B ) G=.FALSE.
      NINSEC=G
      RETURN
      END
      SUBROUTINE WAY
C
CCC  **********THIS SUBROUTINE FINDS BEST EXIT FOR A CONTOUR PASSING THROUGH
C            SIDE 3 OF A BOX WITH 3 EXITS **********
C
      COMMON /WAY/ CX(4),CY(4),KM1,KM2,SIZE,K
      KM1=2 $ KM2=4
      IF((CX(2)-CX(3))**2+(CY(2)-CY(3))**2.LT.(CX(4)-CX(3))**2+(CY(4)-CY
     +(3))**2)RETURN
      KM1=4 $ KM2=2
      RETURN
      END
      REAL FUNCTION DIST(A,B,VAL)
C
C**********THIS SUBROUTINE FINDS POINT OF EXIT ON THE SIDE **********
C
      DIST=(VAL-A)/(B-A)*0.1
      RETURN
      END
```

```
      MAG=0
   13 CALL PROMPT(54HTYPE D IF YOU WANT A XSECTION IN DENSITY,OTHERWISE
     +M     ,54)
C
      READ(.ERR.=13,.END.=13,5,1004)NO
      IF(NO.EQ.1HM)MAG=1
      IF(MAG.NE.1)GOTO 14
C
   15 CALL PROMPT(50HWHAT IS MAGNITUDE CONSTANT AND BACKGROUND READING
     +,50)
C
      READ(.ERR.=15,.END.=15,5,)DEL,ZRO
C
   14 CALL PROMPT(38HWRITE A DESCRIPTION OF THE X-SECTN,A60  ,38)
C
      READ(.ERR.=14,.END.=14,5,1006)P_DT
 1006 FORMAT(6A10)
C
C      WORK OUT CO-ORDS OF TWO ARRAYS
C
      IF(MFST.LT.1)MFST=1
      IF(NFST.LT.1)NFST=1
      IF(MFST.GT.NL)MFST=NL
      IF(NFST.GT.NPX)NFST=NPX
      IF(MLST.GT.NL)MLST=NL
      IF(NLST.GT.NPX)NLST=NPX
      A(1)=MFST
      A(2)=NFST
      A(3)=MLST
      A(4)=NLST
      CALL NEWPAGE
C
C      PRINT TITLES
C
      CALL PRINT(-1.,0.1,SCDT,72)
      CALL PRINT(-1.,0.5,ASDT,72)
      CALL PRINT(-1.,-0.3,PLDT,60)
      DO 100 J=1,4
      IF(A(J).LT.1.0.OR.A(J).GT.200.)A(J)=0.0
  100 CALL NUMBER((16.0+FLOAT(J-1)*0.7),-0.8,0.2,A(J),0.0,-1)
      ENCODE(54,1008,SCANID)ISC,VEL
 1008 FORMAT('SCAN ID=',I6,'  H=75KM/SEC,RECESSION VELOCITY=',F8.1)
      CALL PRINT(-1.,-0.8,SCANID,54)
      IF(MAG.NE.1)GOTO 16
      ENCODE(20,1010,KZRO)DEL,ZRO
 1010 FORMAT('K=',F5.2,X,'SKY =',F7.2)
      CALL PRINT(16.5,-0.3,KZRO,20)
   16 REWIND 1
      READ(1)HEADER
      READ(1)HEADER
      CALL PLOT(0.0,1.5,-3)
      IF(MFST.EQ.1)GOTO 18
      MFMI=MFST-1
C
C***** READ IN UNUSED SCANS
C
      DO 102 J=1,MFMI
  102 READ(1)DUM
C
C        FIND POINTS ON CROSS-SECTION
C
   18 IKI=0
      GRAD=FLOAT(NLST-NFST)/FLOAT(MLST-MFST+1)
      KFST=NFST
      KLST=NLST
C
C        FIND POINTS ON EACH LINE
C
      DO 106 J=MFST,MLST
      IF(MLST.EQ.MFST)GOTO 20
      KFST=FLOAT(J-MFST)*GRAD+FLOAT(NFST)
      KLST=FLOAT(J+1-MFST)*GRAD+FLOAT(NFST)
      IF(GRAD.GT.0.)GOTO 20
      KDUM=KLST
      KLST=KFST
      KFST=KDUM
   20 READ(1)(COL(K),K=1,NPX)
C
C        FOR POINTS ON CROSS-SECTION FIND X,Y CO-ORDS.
C
      DO 104 III=KFST,KLST
      II=III
      IF(GRAD.LT.0.)II=KFST+KLST-III
      IKI=IKI+1
      X(IKI)=SQRT(FLOAT(J-MFST)**2+FLOAT(II-NFST)**2)*SC
```

```
C
C                              PROGRAM XSEC
C
      PROGRAM XSECTN(INPUT=1318,OUTPUT=1318,TAPE5=INPUT,TAPE6=1318,
     +DATA=4018,TAPE1=DATA,TAPE61=1318,TAPE64=1318,TAPE66=1318)
C          THIS PROGRAM DRAWS A XSECTN THRU AN ARRAY OF DATA
C          WHEN AN ORIGIN AND AN END POINT ARE DEFINED BY THE USER
C          THE PROGRAM WAS DESIGNED FOR USE BY THE ASTRONOMY GROUP
C          SO THE X-AXIS MAY BE IN PARSECS AND A SEEING MARKER IS DRAWN
C          A MAG/SEC2 PLOT MAY BE DRAWN USING THE FORMULA
C                          M=K-2.5*LOG(R-Z)
C          Z=BACKGROUND(SKY) READING
C          R=DATA VALUE
C          K=CONSTANT TO BE FOUND BY USER FROM STUDIES OF A STANDARD STAR
C          THE PROGRAM IS TO BE USED USING 'SIMPLE' ON A GRAPHICS TERMINAL
C          AT IMPERIAL COLLEGE
C           A LINE OF DATA IS READ INTO THE ARRAY COL AND POINTS IN THAT
C           LINE FOR THE XSECTN ARE PUT INTO THE X,Y ARRAYS
C                STEP=STEP LENGTH IN MICRONS
C                PLSC=PLATE SCALE IN ARCSEC/MM
C                T=EXPOSURE TIME IN SECS
C                VEL=RECCESSION VELOCITY IN KM/SEC
C                MFST,NFST=Y,X CO-ORDS OF UPPER END POINT OF XSECTN
C                MLST,NLST=Y,X     "       "  LOWER END POINT  "    "
C          SUBROUTINES PROMPT,BUFFEM,HARDCPY,SITCH,KXWIRES ARE =SIMPLE= SUBS
C          ALL OTHERS ARE CALCOMP SUBS
C               DEVELOPED AND WRITTEN BY D.P.YOULL
C                                    IMPERIAL COLLEGE 1975
C
      COMMON COL(256),X(220),Y(220)
      COMMON PLDT(6),KZRO(2),SCANID(6),A(4),SCDT(8),ASDT(8)
      COMMON /SETPF/ IPF(4)
      DATA XAXIS,YAXIS/7HPARSECS,7HDENSITY/
      STEP=0 $ PLSC=0 $ T=1 $ DEL=0 $ VEL=0
      CALL START(2)
      CALL SWITCH(9HHARDCPYON)
      CALL PROMPT('PROGRAM XSEC',12)
      GOTO 2
    1 CALL NEWPAGE
    2 CALL PROMPT('TYPE FILE NAME CONTAINING DATA ',31)
      READ(.ERR.=2,.END.=2,5,1004)D
      CALL SETPF(IPF(1))
      CALL GET('TAPE1',D)
      IF(IPF(1).NE.0)GOTO 4
      GOTO 6
    4 CALL SETPFF(IPF(1))
      CALL ATTACH('TAPE1',D)
      IF(IPF(1).EQ.0)GOTO 6
      CALL PROMPT('ERROR - CANNOT FIND FILE ',25)
      GOTO 1
    6 REWIND 1
C
C          READ IN HEADER DATA
C
      READ(1)IUR,ISC,NL,NPX,ASDT,SCDT
      WRITE(6,1000)ISC,NL,NPX,ASDT,SCDT
 1000 FORMAT(/,/,8HSCAN ID=,I6,10X,I6,9H LINES OF,I6,7H POINTS,/,/,8A10
     +,/,8A10)
      IF(IUR.LT.0)READ(1)STEP,PLSC,T,DEL,VEL
      WRITE(6,1002)STEP,PLSC,T,DEL,VEL
 1002 FORMAT(//X,5HSTEP=,F5.1,5X,12HPLATE SCALE=,F5.1,5X,
     +15HEXPOSURE TIME= ,F6.1,5X,6HCONST=,F6.2/5X,20HRECESSION VELOCITY:
     + ,F7.0)
      CALL BUFFEM(-6)
      IF(T.LE.0.)T=1.0
      IF(VEL.GT.0.0)GOTO 10
C
    8 CALL PROMPT(49HRECESSION VELOCITY NOT READ FROM TAPE,WHAT IS IT
     +,49)
C
      READ(.ERR.=8,.END.=9,5,)VEL
C
C          SET DATA VALUES
C
   10 SC=STEP*PLSC*4.848*VEL/75000.0
      IF(VEL.GT.0.)GOTO 12
      SC=1.
      XAXIS=10H
C
   12 CALL PROMPT(54HWHAT IS THE ORIGIN M,N AND END M,N OF THE CROSS-SEC
     +TN          ,54)
C
      READ(.ERR.=12,.END.=12,5,)MFST,NFST,MLST,NLST
 1004 FORMAT(A7)
C
```

```
      Y(IKI)=COL(II)
      IF(MAG.NE.1)GOTO 104
      Y(IKI)=COL(II)-ZRO
C
CC    WORK OUT MAG/SEC2
C
      IF(Y(IKI).LE.0.)GOTO 24
      Y(IKI)=DEL-2.5*ALOG10(Y(IKI)/T)
      GOTO 104
   24 Y(IKI)=DEL
  104 CONTINUE
  106 CONTINUE
      CALL SCALE(X,12.5,IKI,1)
      INC=1
      IF(MAG.EQ.1)INC=-1
      CALL SCALE(Y,8.,IKI,INC)
      IF(MAG.EQ.1)YAXIS=10H MAG/SEC2
C
CC     PLOT GRAPH
C
      CALL FACTOR(1.6)
      CALL AXIS(0.,0.,XAXIS,-10,12.5,0.,X(IKI+1),X(IKI+2))
      CALL AXIS(0.,0.,YAXIS,10,8.,90.,Y(IKI+1),Y(IKI+2))
      CALL LINE(X,Y,IKI,1,0,4)
      CALL FACTOR(1.)
      IF(STEP.LE.0..OR.PLSC.LE.0.)GOTO 26
      AS=2.0*4.848*VEL/(X(IKI+2)*75.0)
      IF(VEL.LE.0.)AS=2000./(STEP*PLSC*X(IKI+2))
      AS=AS*1.6
      AT=-1.8
      AK=14.
C
CC     PLOT SEEING MARKER
C
      CALL PRINT(AK-2.5,AT,8H2 ARCSEC,8)
      CALL PLOT(AK,AT,3)
      CALL PLOT(AK,AT+0.1,2)
      CALL PLOT(AK,AT+0.05,3)
      CALL PLOT(AK+AS,AT+0.05,2)
      CALL PLOT(AK+AS,AT+0.1,3)
      CALL PLOT(AK+AS,AT,2)
C
   26 CALL PROMPT('OPTIONS..1=END,2=HARDCOPY,3=XWIRES,4=AGAIN,5=NEW DATA
     +',53)
C
      READ(.ERR.=26,.END.=26,5,)NO
      IF(NO.GT.5.OR.NO.LT.1)GOTO 26
      GOTO(34,32,28,12,1),NO
   28 CALL FACTOR(1.6)
      CALL PROMPT('WHEN RETURNING THE XWIRES TYPE 0 TO REPEAT ',46)
   30 CALL KXWIRES(X1,Y1,K)
      X1=X(IKI+1)+X1*X(IKI+2)
      Y1=Y(IKI+1)+Y1*Y(IKI+2)
      WRITE(6,1012)X1,Y1
 1012 FORMAT('XWIRE POSITION AT X=',F10.2,10X,'Y=',F10.2)
      CALL BUFFEM(-6)
      IF(K.EQ.1HO)GOTO 30
      CALL FACTOR(1.0)
      GOTO 26
   32 CALL HARDCPY
      GOTO 26
   34 STOP
      END
```

```
C
C                                   PROGRAM SLARD
C
      PROGRAM SLARD(INPUT=130B,OUTPUT=130B,TAPE6=130B,TAPE64=131B,TAPE5
     +=INPUT,DATA=401B,TAPE1=DATA,TAPE61=130B,TAPE66=130,TAPE4=401B)
C
C       THIS PROGRAM DRAWS A LINE CONNECTING DATA POINTS IN A LINE
C       FOR EACH LINE OF THE ARRAY.THE PROGRAM IS QUICK AND EASY TO RUN
C       WRITTEN FOR USE ON A TEKTRONIX TERMINAL AT IMPERIAL COLLEGE
C       USING =SIMPLE ROUTINES AND CALCOMP ROUTINES
C       A LINE OF DATA IS READ INTO ARRAY LINE AND BLOCKED INTO ARRAY
C       PBUF READY FOR PLOTTING
C       FIRST TWO RECORDS ARE HEADER INFORMATION
C       EVERY LINE IS IN A NEW RECORD
C       THERE IS AN EASY ROUTINE TO REMOVE NOISY SIGNALS FOR A BETTER
C       DISPLAY
C
C       PROGRAM DEVELOPED BY C.L.STEPHENS AND REWRITTEN FOR TEKTRONIX
C       USE BY D.P.YOULL . HIDE ROUTINE BY M.A.R.HARDWICK.
C                               IMPERIAL COLLEGE 1975
C
      COMMON ALINE(256),PBUF(256),ASDT(8),SCDT(8),SCANID(2)
      COMMON /SETPF/ IPF(4)
C
C:::::: INITIALISE
C
      STEP=0 $ PLSC=0
      CALL START(2)
      CALL SWITCH(9HHARDCPYON)
      CALL PROMPT('PROGRAM SLARD',13)
      GOTO 50
   52 CALL NEWPAGE
   50 CALL PROMPT('TYPE FILE NAME CONTAINING DATA ',31)
      READ(,ERR.=50,.END.=50,5,1002)D
      CALL SETPF(IPF(1))
      CALL GET('TAPE1',D)
      IF(IPF(1).NE.0)GOTO54
      GOTO56
   54 CALL SETPFF(IPF(1))
      CALL ATTACH('TAPE1',D)
      IF(IPF(1).EQ.0)GOTO56
      CALL PROMPT('ERROR - CANNOT FIND FILE ',25)
      GOTO 50
   56 REWIND 1
      REWIND 4
C
C:::::: READ HEADER DATA AND CHECK SCAN ID
C
      READ(1)IUR,ISC,NL,NPX,ASDT,SCDT
C
      IF(IUR.LT.0)READ(1)STEP,PLSC
      WRITE(6,1000)ISC,NL,NPX,ASDT,SCDT,STEP,PLSC
 1000 FORMAT(//,'SCAN ID=',I6,10X,I6,' LINES OF',I6,' POINTS',//8A10
     +//8A10//10X,'STEP=',F5.1,5X,'PLATE SCALE=',F5.1)
      CALL BUFFEM(-6)
C:::::: READ IN CARD DATA TO SELECT AREA OF SCAN REQUIRED
C
C                 MFST,MFST:::::::::MFST,NLST
C                           :     :
C                           :     :
C                 MLST,NFST:::::::::MLST,NLST
C:::::: CONSIDER SCAN AS AN ARRAY WITH M ROWS AND N COLUMNS
    2 MFST=1
      NFST=1
      MLST=NL
      NLST=NPX
      IBLK=1
      IHID=1
C
    4 CALL PROMPT('DO YOU WANT A DISPLAY OF THE FULL SCAN ',39)
C
      READ(,ERR.=4,.END.=8,5,1002)NO
      IF(NO.EQ.1HY)GOTO 8
      IHID=0
C
    6 CALL PROMPT(58HCO-ORDS OF TOP LEFT AND BOTTOM RIGHT CORNERS AND IB
     +LK ARE          ,58)
C
      READ(,ERR.=6,.END.=6,5,)MFST,NFST,MLST,NLST,IBLK
 1002 FORMAT(A7)
C
C:::::: CHECK THAT AREA FOR PLOTTING LIES WITHIN SCAN
C:::::: AND CALCULATE SIZE OF PLOTTING ARRAY
C
    8 IF(MLST.GT.NL)MLST=NL
```

```
      IF(NLST.GT.NPX)NLST=NPX
      JLST=(NLST-NFST+1)/IBLK
      KLST=(NLST-NFST+1)/IBLK
C
C***** POSITION SCAN
C
      IF(NFST.EQ.1)GO TO 10
      NFMI=NFST-1
C
C***** READ IN UNUSED SCANS
C
      DO 100  J=1,NFMI
C
  100 READ(1)DUM
C
C***** FOR EACH VALUE OF J
C
   10 DO 110 J=1,JLST
C
C***** ZERO THE PLOTTING ARRAY
C
C
      DO102 K=1,KLST
  102 PBUF(K)=0.0
C
C***** REDUCE IN J DIRECTION
C
      DO104  I=1,IBLK
      READ(1)(ALINE(K),K=1,NPX)
      IKI=NFST-1
      DO 104 K=1,KLST
C
C***** REDUCE IN K DIRECTION
C
      DO 104 IK=1,IBLK
      IKI=IKI+1
  104 PBUF(K)=PBUF(K)+ALINE(IKI)
C
C***** INITIAL VALUE OF LIMITS
C
      IF (J.GT.1) GO TO14
      XMAX=PBUF(1)
      XMIN=XMAX
C
C***** FIND XMAX-XMIN
C
   14 DO 108 K=1,KLST
      IF(PBUF(K).GT.XMAX)XMAX=PBUF(K)
  108 IF(PBUF(K).LT.XMIN)XMIN=PBUF(K)
  110 WRITE(4)(PBUF(IQ),IQ=1,KLST)
C
C***** PLOTTING CONSTANTS, HIGH IS DISTANCE IN INCHES
C*****             CORRESPONDING TO XMAX-XMIN
C
      HIGH=8.0
      SCALE=(XMAX-XMIN)/HIGH
      DIST=(13.0-HIGH)/AMAX0(JLST,KLST)
C
C***** PLOT HEADER UNDER MAIN PLOT
C
      IF(IHID.EQ.1)GOTO 18
      IHID=0
C
   16 CALL PROMPT(40HDO YOU WANT TO REMOVE BACKGROUND LINES     ,40)
C
      READ(.ERR.=16,.END.=16,5,1002)NO
      IF(NO.EQ.1HY)IHID=1
   18 CALL NEWPAGE
      WRITE(6,1007)XMIN,XMAX
 1007 FORMAT(21HDATA VALUES VARY FROM  ,F6.1,3H TO ,F6.1)
      CALL BUFFEM(-6)
C
C      PRINT HEADER DATA
C
      CALL PRINT(-1.,0.1,SCDT,72)
      CALL PRINT(-1.,-.4,ASDT,72)
 1008 FORMAT(8HSCAN ID=,I6)
      ENCODE(14,1008,SCANID)ISC
      CALL PRINT(-1.,0.5,SCANID,14)
      CALL PLOT(0.0,1.2,-3)
      Y=DIST*FLOAT(JLST)
      X=0.0
      XINC=DIST
      IFST=1
      INC=1
```

```
      ILST=KLST
C
CC     GOTO 7001 IF HIDDEN ALINES ARE TO BE REMOVED
C
      IF(IHID.EQ.1)GOTO 7001
      REWIND 4
C
C***** PLOT ARRAY LINE BY LINE
C
      DO 112 J=1,JLST
      READ (4) (PBUF(IQ),IQ=1,KLST)
      CALL PLOT (X,Y+(PBUF(IFST)-XMIN)/SCALE,3)
      I=IFST
   22 I=I+INC
      X=X+XINC
      CALL PLOT (X,Y+(PBUF(I)-XMIN)/SCALE,2)
      IF(I.NE.ILST) GO TO 22
      IST=ILST
      ILST=IFST
      IFST=IST
      INC=-INC
      XINC=-XINC
  112 Y=Y-DIST
C
C***** PLOT SCALE INDICATOR 10 ARCSECS LONG
C
 6666 DUMMY=1.0
      IF(STEP.LE.0..OR.PLSC.LE.0.)GOTO 24
      X=1000.0/(STEP*PLSC*FLOAT(IBLK))
      X=X*DIST/0.1
      Y=DIST*FLOAT(KLST+2)
      CALL SYMBOL(Y+0.3,0.0,0.07,9H10 ARCSEC,90.0,9)
      CALL PLOT(Y+0.1,0.0,3)
      CALL PLOT(Y,0.0,2)
      CALL PLOT(Y+0.05,0.0,3)
      CALL PLOT(Y+0.05,X,2)
      CALL PLOT(Y+0.1,X,3)
      CALL PLOT(Y,X,2)
C
   24 CALL PROMPT('OPTIONS..1=END,2=HARDCOPY,3=AGAIN,4=NEW DATA ',44)
C
      READ(.ERR.=24,.END.=24,5,)NO
      IF(NO.LT.1.OR.NO.GT.4)GOTO 24
      GOTO(30,26,28,52),NO
   26 CALL HARDCPY
      GOTO 24
   28 REWIND 1
      REWIND 4
      READ(1)HEAD
      READ(1)HEAD
      GOTO 2
   30 STOP
C
CC     SECTION TO REMOVE HIDDEN LINES
C
 7001 Y=0.0
C
CC     DRAW FIRST LINE BACKSPACE ONE OR TWO
C
      BACKSPACE 4
      READ(4) (PBUF(IQ),IQ=1,KLST)
      CALL PLOT(X,(PBUF(1)-XMIN)/SCALE,3)
      DO 7002 I=2,KLST
      X=X+XINC
 7002 CALL PLOT(X,(PBUF(I)-XMIN)/SCALE,2)
C
CCC    SET ALINE WITH VALUES OF PBUF
C
      DO 7003 II=1,KLST
 7003 ALINE(II)=(PBUF(II)-XMIN)/SCALE
C
CCC    DRAW ALL OTHER ALINES
C
      X=0.0
 7004 JLST=JLST-1 $ IF(JLST.EQ.0)GOTO 6666
      Y=Y+DIST
      NW=2
      DO 567 ITAP=1,2
  567 BACKSPACE 4
      READ(4) (PBUF(IQ),IQ=1,KLST)
      I=IFST $ PBUF(IFST)=Y+(PBUF(IFST)-XMIN)/SCALE
      CALL PLOT(X,PBUF(IFST),3)
      IF(ALINE(IFST).GT.PBUF(IFST))NW=3
      IF(NW.EQ.2)ALINE(IFST)=PBUF(IFST)
```

```
7005  I=I+INC
      IF(I.LT.1.OR.I.GT.KLST)GOTO 7007
      X=X+XINC
      PBUF(I)=(PBUF(I)-XMIN)/SCALE+Y
      IF(PBUF(I).LT.ALINE(I))  GO TO (7005,7006,7005) NW
      ALINE(I)=PBUF(I)  $ CALL PLOT(X,PBUF(I),NW)  $ NW=2 $ GO TO 7005
7006  NW=3  $ GO TO 7005
7007  IST=ILST  $ ILST=IFST $ IFST=IST $ INC=-INC $ XINC=-XINC
      GOTO 7004
      END
```

```
C
C                                   PROGRAM VOL
C
      PROGRAM VOL(INPUT,OUTPUT,DATA,TAPE5=INPUT,TAPE6=OUTPUT,TAPE1=DATA)
C
C      THIS PROGRAM FINDS THE VOLUME OF A STAR BY THE SIGMA METHOD
C
      COMMON A(256),ASDT(8),SCDT(8)
C
C                 GET FILE,INITIALISE AND OUTPUT HEADER DATA
C
    8 PRINT,'FILE NAME'
      READ(5,1010)D
      IF(D.EQ.4HSTOP)STOP
 1010 FORMAT(A10)
      CALL GET(4HDATA,D)
      REWIND 1
      READ(1)IUR,ISC,NL,NPX,ASDT,SCDT
      IF(IUR.LT.0)READ(1)DUM
      WRITE(6,1000)ISC,NL,NPX,ASDT,SCDT
 1000 FORMAT(' SCAN ID=',I7,I7,' LINES OF ',I5,' POINTS'/X8A10/X8A10
     +    //' CENTRE M,N= ')
      READ,MM,NN
      PRINT,'    N        SUMAV          SUMSD       ZROAV       ZROSD
     +MAG          MAGF'
      NMAX=MINO(MM,NN,NL-MM,NPX-NN)*2+1
      N2=NMAX-36
      IF(N2.LT.1)N2=1
C
      DO 110 NDUM=N2,NMAX,2
      N=NMAX+N2-NDUM
      ZROA=0 $ ZROB=0 $ SUMA=0 $ SUMB=0
      REWIND 1 $ READ(1)DUM $ IF(IUR.LT.0)READ(1)DUM
      N1=(N-1)/2
      MF=MM-N1-1
      DO 100 M=1,MF
  100 READ(1)DUM
C                                          SUM READINGS
      DO 108 M=1,N
      READ(1)(A(K),K=1,NPX)
      DO 102 K=NN-N1+1,NN+N1-1
      IF(A(K).LT.-1.)WRITE(6,1002)
  102 SUMA=SUMA+A(K)
      ZROA=A(NN-N1)+A(NN+N1)+ZROA
      IF(M.EQ.1.OR.M.EQ.N)GOTO 10
      DO 104 K=NN-N1,NN+N1
  104 SUMB=SUMB+A(K)
      GOTO 108
   10 DO 106 K=NN-N1,NN+N1
  106 ZROB=ZROB+A(K)
  108 CONTINUE
C                                          CALCULATE AND OUTPUT RESULTS
      ZROA=ZROA/(2*N)
      ZROB=ZROB/(2*N)
      SUMSD=ABS(SUMA-SUMB)
      SUMAV=(SUMA+SUMB)/2.
      ZROSD=ABS(ZROA-ZROB)
      ZROAV=(ZROA+ZROB)/2.
      AMAG=SUMAV-ZROAV*FLOAT(N*(N-2))
      IF(N.EQ.NMAX)GOTO 12
      AMAGF=SUMAV-ZRO1*FLOAT(N*(N-2))
      GOTO 110
   12 ZRO1=ZROAV
  110 WRITE(6,1002)N,SUMAV,SUMSD,ZROAV,ZROSD,AMAG,AMAGF
 1002 FORMAT(I5,4X,8F11.1)
      GOTO 8
      END
```

```
C
C                                  PROGRAM DIA
C
      PROGRAM DIA(INPUT=131B,OUTPUT=131B,TAPE5=INPUT,TAPE6=131B,TAPE
     +64=131B,TAPE61=131B ,          TAPE66=131B)
      COMMON ERROR(408),DIAM(408),NUM(4)
      CALL START(2)
      CALL SWITCH(9HHARDCPYON)
C
C      FOR A DIAPHRAGM OF RADIUS UPTO 25 IN STEPS OF 0.25
C
      DO 4 K=1,100
      IF(MOD(K,10).EQ.1)CALL PROMPT('G+1  ',2)
      AMAG=0.0 $ BMAG=0.0 $ CMAG=0.0 $ DMAG=0.0
      RAD2=K*K
      RAD2=RAD2/16.0
C
C      FOR TOP LEFT HAND CORNER OF 50*50 ARRAY
C
      DO 2 I=1,24
      A=(I-25)*(I-25)
      IF(A.GT.RAD2)GOTO 2
      DO 3 J=1,25
      DIS2=FLOAT((J-25)**2)+A
      IF(DIS2.LT.RAD2)GOTO 32
      GOTO 33
   32 AMAG=AMAG+1.0
      CMAG=CMAG+EXP(-DIS2)
   33 IF(DIS2.LE.RAD2)GOTO 34
      GOTO 3
   34 BMAG=BMAG+1.0
      DMAG=DMAG+EXP(-DIS2)
    3 CONTINUE
    2 CONTINUE
C
C      EQUATE TO WHOLE ARRAY
C
      AMAG=4.*AMAG+1.
      BMAG=4.*BMAG+1.
      CMAG=4.*CMAG+1.
      DMAG=4.*DMAG+1.
C
C      CALCULATE TRUE AREA AND VOLUME AND ERRORS
C
      AREA=3.14158*RAD2
      VOL=3.14158*(1.0-EXP(-RAD2))
      DIAM(K)=FLOAT(K)/2. $ DIAM(K+102)=DIAM(K) $ DIAM(K+204)=DIAM(K)
      DIAM(K+306)=DIAM(K)
      ERROR(K)=ABS((AREA-AMAG)*100./AREA) $ ERROR(K+102)=ABS((AREA-
     +BMAG)*100./AREA)
      ERROR(K+204)=ABS((VOL-CMAG)*100./VOL) $ ERROR(K+306)=ABS((VOL-
     +DMAG)*100./VOL)
    4 CONTINUE
      NUM(1)=100 $ NUM(2)=100 $ NUM(3)=100 $ NUM(4)=100
      SC=10.
      CALL FACTOR(1.7)
    6 CALL NEWPAGE
C
C      DRAW GRAPHS
C
      CALL AXIS(0.,0.,'DIAMETER',-8,10.,0.,0.,5.)
      CALL AXIS(0.,0.,'ERROR(PERCENTAGE)',17,6.,90.,0.,SC)
      DO 10 I=1,4
      DIAM(I*102-1)=0.
      DIAM(I*102)=5.
      ERROR(I*102-1)=0.
      ERROR(I*102)=SC
      J=(I-1)*102+1
   10 CALL LINE(DIAM(J),ERROR(J),100,1,-1,I)
      CALL HARDCPY
      IF(SC.LT.5.)STOP
      SC=2.
      GOTO 6
      END
```

```
C
C                              PROGRAM APTUR
C
      PROGRAM APTUR(INPUT,OUTPUT,TAPE5=INPUT,TAPE6,TAPE64=131B,TAPE61
     +          =131B,TAPE66=131B)
      COMMON AA(202),ERRADT(202),ERRCDT(202),ERRCDD(202),BINTEG(2),
     + AAA(202),       NUM(2),DINTEG(2)
      REAL K,K1
C
C       THERE ARE M DATA POINTS ON THE GRAPH
C          APERTURE IS CENTRED AT X=Y=ORIGIN
C
      ORIGIN=0
      M=50
      CALL START(2)
      NUM(1)=M & NUM(2)=M
      N=11
      AN22=2**N
      AN2=N**N
      B=N-1
      K1=ALOG(2.)
      K=ALOG(10.)
C
C       TEST FOR APERTURE SIDE UPTO SEEING/2=1 UNIT
C            IN STEPS OF 1/M
C
      DO 200 I=1,M
      A=FLOAT(I)/FLOAT(M)
      A2N=A/AN22
      DO 150 II=1,2
      ORIGIN=FLOAT(II-1)*(-A/2.)
      BINT=0.
      DINT=0.
      AA(I+(II-1)*M)=A/2.
      AAA(I+(II-1)*M)=A/2.
      DO 100 J=1,N
      X=ORIGIN+A*FLOAT(J-1)/B+A2N
      DO 100 L=1,N
      Y=ORIGIN+A*FLOAT(L-1)/B+A2N
      D=EXP(-K1*(X*X+Y*Y))
      T=EXP(-K*D)
      DINT=DINT+D
  100 BINT=BINT+T
      DINTEG(II)=DINT/AN2
  150 BINTEG(II)=-ALOG10(BINT/AN2)
C
C       BINTEG=AVERAGE DENSITY
C       DINTEG=AVERAGE TRANSMISSION DENSITY
C
      SUM=EXP(-K1*A**2/2.)
C
C       CALCULATE ERROR DUE TO TRANSMISSION
C
      ERRADT(I)=100.*ABS(DINTEG(1)-BINTEG(1))/DINTEG(1)
      ERRADT(I+M)=100.*ABS(DINTEG(2)-BINTEG(2))/DINTEG(2)
C
C       CALCULATE ERROR DUE TO BLOCKING
C
      ERRCDD(I)=100.*ABS(SUM-DINTEG(1))/SUM
  200 ERRCDD(I+M)=100.*ABS(1.-DINTEG(2))
      CALL SWITCH(9HHARDCPYON)
C
C       DRAW GRAPHS
C
      CALL PLOT(2.,2.,-3)
      CALL FACTOR(1.8)
      CALL GRAF(AA,ERRADT,NUM,2,1,'APERTURE(FWHM) ',14,'ERROR(PERCENT) '
     +    ,14,10.,6.)
      CALL PRINT(1.5,-1.,'ERROR IN AVERAGE DENSITY BY TRANSMISSION EFFEC
     +T    ',47)
      DO 250 I=1,M
      AA(I)=AAA(I)
  250 AA(I+M)=AAA(I+M)
      CALL PROMPT('TYPE 1 FOR HARDCOPY',19)
      READ,N
      IF(N.EQ.1)CALL HARDCPY
      CALL GRAF(AA,ERRCDD,NUM,2,1,'APERTURE(FWHM) ',14,'ERROR(PERCENT) '
     +    ,14,10.,6.)
      CALL PRINT(1.5,-1.,'ERROR IN CENTRAL DENSITY DUE TO BLOCKING',40)
      CALL PROMPT('TYPE 1 FOR HARDCOPY',19)
      READ,N
      IF(N.EQ.1)CALL HARDCPY
      STOP
      END
```

REFERENCES

Ables, H.D., 1971, P.U.S.N.O., Vol XX-Part IV

Ables, H.D. and Ables, P.G., 1972a, An.J., 77, 642

Ables, H.D. and Ables, P.G., 1972b, A.A.S. Photobulletin, 2,8

Bacik, H, 1973, Thesis, University of London

Bacik, H., Coleman, C.I., Cullum, M.I., Morgan, B.L., Ring, J., Stephens, C.L., 1972, A.E.E.P., 33B, 747

Barkas, W.H., 1963, Nuclear Research Emulsions, Vol.1., Academic Press

Baum, W.A., 1976, private communication

Beaver, E.A., Harms, R.J., Tifft, W.G., Sargent, T.A., 1974, P.A.S.P. 86, 639

Beddoes, D.R., et al, 1976, private communication

Bigay, J.H., 1951, Ann.d'Ap., 14, 319

Bird, G.R., Jones, R.C., Ames, A.E., 1969, App.Opt.8, 2389

Chincarini,G.L. and Heckathorn, H.M., 1974, Electronography and Astronomical Techniques, McDonald Obs., 343

Chincarini, G.L., Rood, H.J., 1974, Ap.J., 194, 21

Cohen, M., 1972, Thesis, University of London

Cohen, M., Kahan, E., 1972, A.E.E.P., 33A, 53

Coleman, C.I., 1974, Thesis, University of London

Coleman, C.I., 1975, Journal of Photographic Science, 23, 50

Cullum, M.J., 1973, Thesis, University of London

Cullum, M.J., 1973, private communication

Cullum, M.J., Stephens, C.L., 1972, A.E.E.P., 33B, 757

Dainty, J.C., 1977, private communication

Dainty, J.C., Scadden, R.J., 1975, Mon.Not.R.A.S., 170, 519

Fairall, A.P., 1978, Observatory, 98, 1

Gull, T.R., 1974, Electronography and Astronomical Techniques, McDonald Observatory, 273

Hardie, R.H., 1962, Astronomical Techniques, Ed.Hiltner, Chapter 8

Hardwick, M.A.R., Morgan, B.L., 1976, Procs. of IAU.Coll. No.40, Paris

Hewitt, A.V., 1969, Pub.A.S.P., 81, 541

Hoag, A.A., Miller, W.C., 1969, Appl.Opt., 8, 2417

Holmberg, E., 1931, A Study of Double and Multiple Galaxies, Lund.Obs.Ann., 6

Holmberg, E., 1958, Meddelande Lund, Ast.Obs., II, Nr.,136

van Houters, C.J., 1961, Bulletin of the Astro.Inst. of the Netherlands, 16, 1

Hubble, E., 1930, Ap.J., 71, 231

Humason, M.L., 1936, Ap.J., 83, 10

Humason, M.L., Mayall, N.U., Sandage, A.R., A.J., 61, 97

Ives, G.E., Jensen, E.W., 1943, J.Soc.Mot.Pict.Engrs., 40, 107

Johnson, H.L., Morgan, W.W., 1953, Ap.J., 117, 313

Kahan, E., Cohen, M., 1969, A.E.E.P., 28B, 725

Kiepenheur, K.O., 1934, Die Sterne, 9, 190

Kormendy, J., 1977, Ap.J., 214, 359

Kron, G.E., Ables, H.D., Hewitt, A.V., 1969, A.E.E.P., 28A, 1

Lallemand, A., 1936, C.R.Acad.Sci.Paris, 203, 243 and 990

Lallemand, A., 1966, A.E.E.P., 22A, 1

McGee, J.D., 1973, Vistas in Astronomy, 15, 61

McGee, J.D., Phillips, E.G., 1974, Electronography and Astronomical Techniques, McDonald Observatory, 69

McGee, J.D., Khogali, A., Ganson, A., 1966, A.E.E.P., 22A, 31

McGee, J.D., McMullan, D., Bacik, H., Oliver, M., 1969, A.E.E.P., 28A, 61

McGee, J.D., Bacik, H., Coleman, C.I., Morgan, B.L., 1972, A.E.E.P., 33A, 13

McMullan, D., Powell, J.R., Curtis, N.A., 1972, A.E.E.P., 33A, 37

Mees, C.E.K., 1966, Theory of the Photographic Process, 3rd Ed., McMillan

Merkilijn, J.K., Wall, J.V., 1970, Aust. J. Phys., 23, 575

Miller, R.H., Prendergast, K.H., 1962, Ap.J., 136, 713

Miller, W.C., 1971, Amer.Astron.Soc.Photobulletin, (No.2), 3

Newell, E.B., O'Neill, E.J., 1974, Electronography and Astronomical Applications

Pettit, E., 1954, Ap.J., 120, 413

Pilkington, J.D.H., 1972, Interim Report on the Requirements of Measuring Machines, RGO

Priser, J.B., 1974, Pub.USNO, 20, Pt 7

Purgathofer, A.Th., 1974, Electronography and Astronomical Applications, McDonald Observatory, 199

Reay, N.K., 1976, private communication

Redman, R.O., 1936, Mon.Not.R.A.S., 96, 588

Reynolds, J.H., 1913, Mon.Not.R.A.S., 74, 132

Reynolds, J.H., 1920, Mon.Not.R.A.S., 80, 746

Ring, J., Worswick, S.P., 1975, A.E.E.P., 408, 679

Rood, H.J., Baum, W.A., 1967, Astron.J., 72, 398

Sandage, A., 1961, Hubble Atlas of Galaxies,
Washington: Carnegie Inst.of Washington
Sandage, A, 1967, Ap.J., 150, L177
Sargent, W.L.W., 1970, Ap.J., 160, 405
Silverstein, L., Trivelli, A.P.H., 1938, J.Opt.Soc.Am., 28, 441
Smibert, J.A., O'Bern, M., 1955, in "Science and
Applications of Photography", Royal Ast.Society
Stebbins, J., Whitford, A.E., 1937, Ap.J., 86, 247
Stevens, G.W.W., 1968, "Microphotography", 2nd edition:
Chapman and Hall
Stephens, C.L., 1974, private communication
Sulentic, J.W., Tifft, A.J., 1973, RNGC, Univ. of Arizona
Press

Takada, M., Kodaira, K., 1972, Pub.Astron.Soc.Japan, 24, 525
Tifft, A.J., 1969, A.J., 74, 354

Varontsov - Velyaminov, B.A., 1962, Trudy Shternberg State
Astr.Inst., Vol 32
de Vaucouleurs, G., 1948a, J.des Observ. 31, 113
de Vaucouleurs, G., 1948b, Ann.D'Ap., 11, 247
de Vaucouleurs, G., 1961, Ap.J.Supp., 5, 233
de Vaucouleurs, G., de Vaucouleurs, A., 1964, Reference
Catalogue of Bright Galaxies, U. of Texas Press, Austin.
de Vaucouleurs, G., 1971, private communication
(see Ables & Ables, 72)

Walker, M.F., 1970, Ap.J., 161, 835
Walker, M.F., Kron, G.E., 1967, Pub.A.S.P., 79, 551
Weedman, D.W., 1976, Ap.J., 203, 6
Wlerick, G., Michet, D., Labeyrie, C., 1974, Electronography
and Astronomical Applications, McDonald Observatory, 177

Worswick, S.P., 1975, Thesis, Univ. of London

Worswick, S.P., 1976, private communication

Zinn, R.J., Newell, E.B., 1972, A.A.S. Photobulletin, 2, 6

Zwicky, F., 1966, Ap.J., 143, 192

Zwicky, F., 1971, Catalogue of Selected Compact Galaxies and of Selected Post-Eruptive Galaxies - Guenligen : F. Zwicky